





Universitatea POLITEHNICA din București
Facultatea Ingineria și Managementul Sistemelor
Tehnologice



Journal of Industrial Engineering and Robotics

2022, Volume 6, Issue 3

Comitetul Științific al Revistei de Inginerie Industrială

Prof.dr.ing.	AMZA Catalin
Conf.dr.ing.	BACIU Florin
Conf.dr.ing.	CATANA Madalin-Gabriel
S.l.dr.ing.	DIJMARESCU Manuela-Roxana
S.l.dr.ing.	NICULAE Elisabeta
Conf.dr.ing.	POPA Laurentiu
S.l.dr.ing.	POPESCU Adrian
Prof.dr.ing.	SEVERIN Irina
S.l.dr.ing.	TUDOSE Daniela Ioana
Conf.dr.ing.	UNGUREANU Liviu Marian

Comitetul de Redacție al Revistei de Inginerie Industrială

Prof.dr.ing.	DUMITRESCU Andrei
S.l.dr.ing.	PARPALA Radu
S.l.dr.ing.	RADU Constantin
S.l.dr.ing.	ROTARU Alexandra
S.l.dr.ing.	TUDOSE Virgil

Editori

Prof.dr.ing.ec.	DOICIN Cristian
Conf.dr.ing.	VLĂSCLEANU Daniel
As.dr.ing.	CIOLCĂ Miruna

Cuprins

Research on data acquisition for a moving point. ENACHE Adrian-Daniel, Roman MURZAC	1
Modeling and simulation of wedm process for increase precision and machine surface quality. BOGOSLOV Vasile-Ionut, NECȘULESCU Oliver-Andrei, GHICULESCU Liviu Daniel	7
Modeling and simulation by laser and plasma cutting of some steels and polymeric materials. NIȚĂ Liviu-Florinel, POP József, RUSU Andrei-Cosmin, GHICULESCU Liviu Daniel	13
A cyber security application for reporting malicious attacks on IOT networks that use the MQTT protocol. CUCURUZAC Andrei-Traian, ABAZA Bogdan Felician	19
Research on the designing and manufacturing of an experimental robotic arm model for drilling rods handling. BRĂNESCU Teodora – Elena, TARBĂ Ioan – Cristian	25
LabVIEW application for the moment of inertia calculus. CIOCONEA Adina-Mariana, SPÂNU Paulina	31
Development of a web platform application for the administration of bachelor’s degree final projects. CHIRIAC Nicu – Manuel, TARBĂ Ioan – Cristian	37
LabVIEW application for calculating stress in a steel bar. IVANCU Iilca, SPÂNU Paulina	43
Research on designing and developing an experimental model of device for slicing products in the food industry. SIMION Maria Mihaela, TARBĂ Ioan – Cristian, ENCIU Cornel – Cristian	47
Research on the designing of an algorithm and creating a software application for a security system based on IoT and RFID. DOBRE Mihaela Cosmina Daiana, TARBĂ Ioan – Cristian	53
Building a CNC polystyrene cutting machine. BIRDA Gabriel, BÎRLEANU Adrian-Florin, DUGĂEȘESCU Ileana	58
Development of an automatic guided chassis. BANU George-Sebastian, PĂUN Andreea-Alina, DRĂGAN Silviu-Daniel, POPONETE Ștefan-Mădalin, ABAZA Bogdan Felician, SPIROIU Marius Adrian, DIJMARESCU Manuela-Roxana	66
Development of a system for assessing the posture of the human body. MIERLITĂ Iulia-Sorina, BĂCIOIU Mihaela-Roxana, CIOCOIU Daniela-Adriana, UȚICĂ Nicoleta-Georgiana, VOINEA Costin-Bogdan, ZAHARIA Ștefania, DIJMĂRESCU Manuela-Roxana, ABAZA Bogdan Felician, SPIROIU Marius Adrian	74
Microfluidic device for blood analysis. CÎRSTINA Maria-Mihaela, BOERESCU Vlad, IONESCU Robert-Ionuț, MATEI Eduard Florentin, GHICULESCU Daniel	82
Topological optimization and generative design of components that are part of electric motors. JOIȚA Cristian-Gabriel, DAVIDOIU Alexandra, VĂLU Maria-Cătălina, ANDREI Bianca Nicoleta, CHIRCIOAGĂ Ioana-Bianca, LĂCĂTUȘ Elena	90
Detailed design of the operating temperature optimization system for electronic devices. GRĂMADĂ Victor, ȘERBAN Mihail-Răducu, IONESCU Nicolae	98

Development of a smart wallet. MARIA Geni, CHISELEFF Alexandru-Nicolae, CREȚA Gheorghe-Cosmin, PĂUN Ionuț-Alexandru, PAȘAVEL Sînzian-Albert, POPA Bianca-Alexandra, SPIROIU Marius Adrian, ABAZA Bogdan Felician, DIJMARESCU Manuela-Roxana	105
Li-ion auto battery temperature monitoring device. VĂLIMĂREANU Beniamin, SAVCA Stelian, BUGHIANU George, VĂDUVA Rareș, GRIGORE Dănuț, OPRAN Constantin Gheorghe, ILIE Cristian	113
Research on fixturing small parts in machining systems. BARBU Ana-Maria, MUȘAT Miruna-Diana, FLEACĂ Cristina-Mihaela, GHEORGHE Marian, POLOVȚEV Nicolae Onorel, GANNAM Nasim, MANOLACHE Daniel-Silviu	120
Research on the design and development of a smart knee orthosis. BORCAN Maria Alexandra, NEACȘU Angela-Miruna, VLAD Mihaela-Marilena, ULMEANU Mihaela-Elena, DUGĂEȘESCU Ileana	126
Research concerning machining some alloys of Co, Cr and Ti by milling and electrical discharge machining. DINCĂ Cristian-Daniel, FRANCISC Petre, GHICULESCU Liviu Daniel	132
Influence of hollow glass microspheres and multi walled carbon nanotubes on the water absorption in polyamides. ENE Elena, FLEACĂ Cristina-Mihaela, PÂRVU Gabriela-Marina, PERDUM Andrei-Ionuț	138
Research on analysis, simulation and programming of picking systems. MILOIU Andrei Nicolae, GHEORGHE Marian, MANOLACHE Daniel-Silviu	143
Research on dividing schemes and devices with numerical control. GHITĂ Nicoleta-Sorina, FĂTU Andrei-Marian, DUCMAN Dorina-Denisa, GHEORGHE Marian, POPAN Gheorghe, GANNAM Nasim, PÂRVU Corneliu	149
Thermoforming technology of hybrid sandwich structures. DĂNICIUC Marius, OPRAN Constantin Gheorghe, DRĂGHICI Cătălin	155
Research on designing-simulation and 4D printing of a product. VLADMihaela-Marilena, DOICIN Cristian	160
Design and implementation of an experimental patruped robot model. SIMA Mihai, SIMA Gabriel, SAVU Tom	166
Monitoring and remote control, by IoT, of a hydraulic press. SPĂTARU Andrei, SAVU Tom	172
Designing an algorithm and making an informatic application for implementing MQTT specific actions. TUREAC Marius, SAVU Tom	177
Monitoring and remote control, by IoT, of a pneumatic press. ANTON Andrei-Sebastian, SAVU Tom, DUGĂEȘESCU Ileana	182
Design of an algorithm and development of an online application for managing the structure of products. PINTILIE Dănuț-Sebastian, GHEORGHITĂ Vlad	187

RESEARCH ON DATA ACQUISITION FOR A MOVING POINT

ENACHE Adrian-Daniel¹, Roman MURZAC²

¹Faculty of Industrial Engineering and Robotics, Study program: Economic Industrial Engineering,
Academic year: IV, e-mail: enacheadriandaniel@gmail.com

²Faculty of Industrial Engineering and Robotics, Manufacturing Engineering Department, University
POLITEHNICA of Bucharest

ABSTRACT: The study presents research on determining the real-time position of a moving object. An HC-SR04 ultrasonic sensor, configured on an Arduino development board, was used to determine its position. In the first application, the sensor was used to count parts or products that pass through a drive belt in a production unit. In the second application, the sensor was used to measure the level of filling in a pool. The sensor was mounted above the pool. The fill percentage was displayed in the Serial Monitor window of the Arduino software. The results of the study aimed to identify a solution for monitoring an object / point in real time at a low cost.

KEYWORDS: movement, sensor, ultrasounds, infrared.

1. Introduction

The term of sensor has become more frequently used with the development of robots, as well as complex measurement / monitoring systems. These are devices that convert a physical quantity into an information signal that can be mechanical, optical or electrical. The next step after conversion is to enter the information into a computer or microprocessor to be processed, analyzed, and, if necessary, displayed or sent as a control signal for other circuits. [1].

Systems using sensors can be divided into [1]:

- measurement systems - where a quantity or property is measured and its value is displayed;
- control systems - information is used to meet certain criteria.

Motion sensors are electrical devices that detect nearby movements. These devices are usually integrated as a component of a system that performs tasks automatically or provides signals to a user in a particular area. They are an important component for security systems, automatic lighting systems, home control, energy efficiency and other useful systems.

Motion sensors have a wide range of uses and the most common are those used in anti-burglary systems. Motion sensors help maintain the quality of life for people with disabilities, being used in applications such as door openers, also motion sensors ensure the security of properties by detecting movement [2].

Two types of sensors are used to control lighting installations. These sensors for intelligent home lighting control are [2]:

- radar motion sensor (high frequency);
- passive infrared motion sensor (PIR);
- microwave sensor;
- ultrasonic sensor;
- tomographic motion sensor;
- photodetectors.

A passive infrared sensor is an electronic device that measures infrared radiation from objects in its field of vision. Motion is detected when a body with a certain temperature passes in front of the infrared source with a different temperature, such as a wall. This means that the sensor detects heat from

passing an object through the sensor's field of action, and that object breaks the field that the sensor previously determined to be "normal." Any object, even one of the same temperature as the surrounding objects will activate the PIR sensor if the body moves in the visual field of the sensor [3].

All bodies emit energy in the form of radiation. Infrared radiation is invisible to the human eye, but can be detected by electronic devices designed for this purpose [4].

Ultrasound is a mechanical vibration with frequencies higher than 20,000 Hz. They are usually of low intensity. High intensity ultrasound is obtained by electromechanical processes that are based on the piezoelectric phenomenon and / or the magnetostriction phenomenon [5].

The so-called radar motion sensors, also called ultrasonic sensors or high frequency sensors, work by transmitting high frequency sound waves, which scan the surrounding objects and transmit environmental information to the sensor. The motion detected in the sensor's field of action disturbs the pattern of the reflected waves and activates the sensor. The ultrasonic motion sensor emits high frequency sound waves not perceptible to human hearing [4].

2. The current stage

The biggest advantage of the high frequency motion sensor is also the biggest disadvantage. HF sensors are sensitive to any movement, not just human movements, and can therefore create false alarms. When HF sensors are used for light control, the lights may turn on even if no one is in the field of view of the sensor.

HF sensors have similar coverage to infrared motion (PIR) sensors. HF sensors have a range of 3 meters in height and 8 meters in length [4].

HF sensors can have built-in dual technology, meaning that in addition to the HF sensor, a PIR sensor is included. Dual technology sensors use the PIR sensor which has a moderate sensitivity over long distances and the HF sensor which has a high sensitivity over short distances. Together the HF and PIR sensors improve the overall detection capability [4].

Another advantage / disadvantage of the HF sensor is that it detects motion through solid objects (glass, wall). In areas where there is no direct view, the sensor can detect movement. In this case, the fact that the sensor detects motion through solid objects is an advantage. If the HF sensor detects movement from an adjacent populated area, the sensor will trigger light from the unpopulated area, creating false alarms [4].

The correct choice and installation of the sensor leads to a viable option for light control in both residential and industrial / commercial areas [4].

3. Principles of operation

Ultrasonic transducers and ultrasonic sensors are devices that generate or detect ultrasonic energy. These can be divided into three broad categories: transmitters, receivers, and transceivers. Transmitters convert electrical signals into ultrasound, receivers convert ultrasound into electrical signals, and transceivers can transmit and receive ultrasound at the same time [6].

Ultrasound can be used to measure the speed and direction of the wind (anemometer), the level of liquid in the tank or channel and the speed through air or water. To measure speed or direction, a device uses multiple detectors and calculates the speed from distances relative to particles in the air or water. To measure the level of the liquid in the tank or channel and also the sea level (tide gauge), the sensor measures the distance in the range to the surface of the fluid. Other applications include: humidifiers, sonar, medical ultrasonography, burglar alarms, non-destructive testing, etc. [6].

The distance to the target is calculated by measuring the duration using equation [9]:

$$d = c * t / 2 \tag{1}$$

where d = distance [m];

c = sound speed [m / s];

t = duration [s].

The systems usually use a transducer that generates sound waves in the ultrasonic field, over 18 kHz, converting the electrical energy into sound, then, upon receiving the echo, transforms the sound waves into electrical energy that can be measured and displayed. Infrared motion sensor (PIR) technology illuminates when a person passes through the sensor's field of view, and the sensor will not turn on the light if a person remains motionless within the sensor's range [3].

Infrared motion sensors are more sensitive on cool days than on hot days. This is due to the fact that the temperature difference between the ambient air and the human body is larger on cold days, the sensor easily noticing the temperature difference. This has its disadvantages, if the sensor is too sensitive, the sensor will also detect the movement of small animals creating false alarms, unnecessary lighting. The optimum operating temperature of the motion sensor for luminaires is between 15°-20° C. At temperatures above 30° C, the sensitivity of the sensor will decrease and infrared emissions will be more difficult to detect [3].

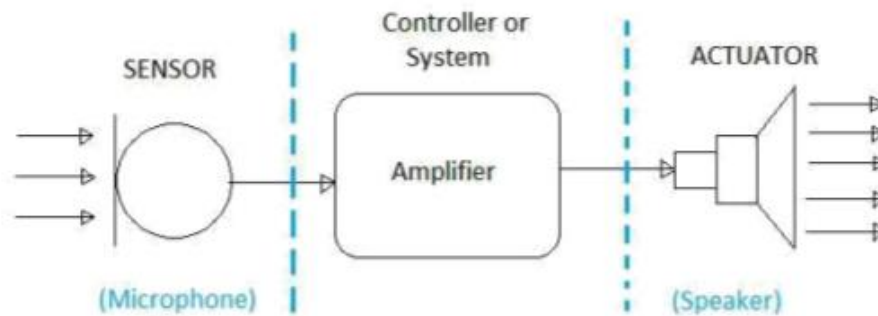


Fig. 1. Principle of operation of a sensor system [7]

4. Using the ultrasonic sensor to measure batches of parts

The sensor systems assist the production of cars with innovative technology and high quality standards. Temperature, pressure, fill level and flow sensors reliably monitor process environments. Optical barriers, optical safety curtains and inductive safety sensors guarantee the safety of machines and people, for example in the presses, robot cells and mounting stations. The positions of the machine components are accurately detected by inductive, capacitive, optoelectronic and cylinder sensors. Vibration monitoring systems are available for state-of-the-art machine tool maintenance [9]. The ultrasonic sensor will count the parts that will pass on a conveyor belt. For this application we used an ultrasonic sensor HC-SR04. Table 1 shows the sensor's specifications.

Tabel 1. Specifications of HC-SR04 ultrasonic [8]

Supply voltage [V]	Electricity consumed [mA]	Operating distance [cm]	Operating frequency [KHz]	Measurement angle	Error [mm]	Input signal duration [μs]	Dimensions [mm]
5	15	2-400	40	15°	±3mm	10μs	45x20x15



Fig. 2. HC-SR04 ultrasonic distance [8]

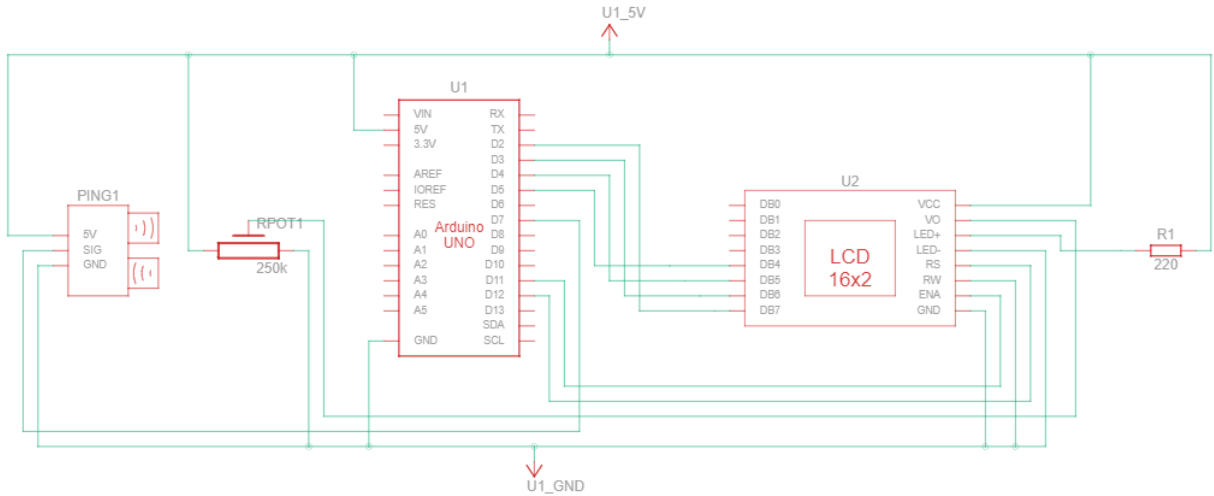


Fig. 3. Wiring diagram of the application

This system can be used for production lines where the drive belt through which the parts or products pass has a width of up to 3.5m. The sensor will be positioned sideways facing the drive belt and will be able to transmit a signal for each part that passes in front of it regardless of shape, color or material. This number can be displayed either on an LCD screen connected to the Arduino board or in its Serial Monitor window.

```

sketch_may10a $
// C++ code
//
int inches = 0;
int cm = 0;
int currentState = 0;
int previousState = 0;
int counter = 0;
long readUltrasonicDistance(int triggerPin, int echoPin)
{
  pinMode(triggerPin, OUTPUT); // eliberam transmitatorul
  digitalWrite(triggerPin, LOW);
  delayMicroseconds(2);
  digitalWrite(triggerPin, HIGH);
  delayMicroseconds(10);
  digitalWrite(triggerPin, LOW);
  pinMode(echoPin, INPUT);
  return pulseIn(echoPin, HIGH);
}
void setup()
{
  Serial.begin(9600);
}

void loop()
{
  // transformam timpul de reactie in centimetri
  cm = 0.01723 * readUltrasonicDistance(2, 3);

  if (cm <= 20) {
    currentState=1;
  }
  else {
    currentState=0;
  }
  if(currentState != previousState) {
    if(currentState == 1){
      counter = counter + 1;
      Serial.println(counter);
    }
  }
  delay(1000);
}
Done uploading.

```

Fig. 4. Code sequence used

5. Non-contact and continuous measurement of filling level

Important applications of ultrasonic sensors include measuring the level of filling in tanks or silos. Whether it is a vessel containing liquids or bulk products, these measurements are always reliable and accurate. Particularly aggressive agents and vapors encountered in certain applications can be a major challenge for many sensors [9].

The ultrasonic signaling device is non-contact and wireless, so it can be used even in aggressive and explosive environments. After the initial configuration, such a sensor does not require any specialized maintenance, and the absence of moving parts significantly prolongs the life [10].

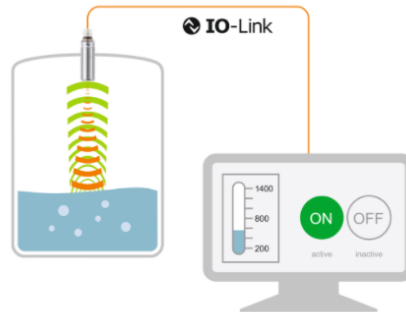


Fig. 5. Filling level measurement system [9]

The same sensor was used for this application as in the previous application. The ultrasonic sensor will be positioned at the top of the container and the waves will be reflected from its contents. To avoid errors, different adapters can be attached to the sensor depending on the shape and size of the container.

```

sketch_may10a $
// C++ code
//
int inches = 0;
int cm = 0;
long readUltrasonicDistance(int triggerPin, int echoPin)
{
    pinMode(triggerPin, OUTPUT); // eliberam transmitator
    digitalWrite(triggerPin, LOW);
    delayMicroseconds(2);
    digitalWrite(triggerPin, HIGH);
    delayMicroseconds(10);
    digitalWrite(triggerPin, LOW);
    pinMode(echoPin, INPUT);
    return pulseIn(echoPin, HIGH);
}
void setup()
{
    Serial.begin(9600);
}

void loop()
{
    // transformam timpul de reactie in centimetri
    cm = 0.01723 * readUltrasonicDistance(2, 3);

    if (cm<16){
        Serial.println("100%");
    }
    else if (cm<17){
        Serial.println("75%");
    }
    else if (cm<18){
        Serial.println("50%");
    }
    else if (cm<19){
        Serial.println("25%");
    }
    else {
        Serial.println("0%");
    }
    delay(100); // Wait for 100 millisecond(s)
}

```

Fig. 6. Code sequence used

6. Conclusions

Ultrasonic sensors can detect the movement of targets and can measure the distance to them in many automated factories and processing plants, which makes the choice of these types of sensors feasible for various industrial applications.

Although some ultrasonic sensors are widely used in the automotive industry as parking sensors, they are being tested for a number of other uses in the automotive field and beyond.

Because ultrasonic sensors use sound rather than light for detection, they work in applications where photoelectric sensors cannot operate. Ultrasound is an excellent solution for detecting clear objects and measuring liquid levels, applications that photoelectricians struggle with due to the transparency of the target. Also, the target color or reflectivity does not affect the ultrasonic sensors, which can operate reliably in high brightness environments [11]. These features give an advantage to these types of sensors for use in detecting a moving object. Passive ultrasonic sensors can also be used to detect high pressure gas or liquid leaks or other hazardous conditions that generate ultrasonic sounds.

7. Bibliography

- [1]. Wikipedia, Motion Sensor, available at: https://ro.wikipedia.org/wiki/Senzor_de_mișcare, accessed on: 22.04.2022;
- [2]. Parede, What are motion sensors and how they work, available at: <https://ro.jf-parede.pt/what-are-motion-sensors>, accessed on: 22.04.2022;
- [3]. Wikipedia, Pasive-infrared sensor, available at: https://ro.wikipedia.org/wiki/Senzor_infraroșu_pasiv, accessed on: 22.04.2022;
- [5]. Wikipedia, Ultrasound, available at: <https://ro.wikipedia.org/wiki/Ultrasunet>, accessed on: 24.04.2022;
- [4]. Wikipedia, Radar motion sensor, available at: https://ro.wikipedia.org/wiki/Senzor_de_mișcare_radar, accessed on: 24.04.2022;
- [6]. Wiki, Ultrasound transducer, available at: https://hmn.wiki/ro/Ultrasound_transducer, accessed on: 27.04.2022;
- [7]. Orner, R., Grünbacher, E., Guger, C., „State of the Art in Sensors, Signals and Signal Processing”, in GmbH/Guger Technologies OG, 2009;
- [8]. eMAG, HC-SR04 ultrasonic sensor, available at: <https://www.emag.ro/senzor-ultrasonic-hc-sr04-cl03/pd/D15ZTFBBM/>, accessed on: 27.04.2022;
- [9]. IFM, Ultrasonic sensors – Applications, available at: <https://www.ifm.com/ro/ro/shared/technologien/senzori-cu-ultrasunete/aplicații>, accessed on: 6.05.2022;
- [10]. Tigerdoor, Determining the water level in the tank. All about water level sensors, available at: <https://tigerdoor.ru/ro/the-ceiling/opredelenie-urovnya-vody-v-bake-vs-o-datchikah-urovnya-vody-kontrol-urovnya/>, accessed on: 6.05.2022.

8. Notations

The following symbols are used in the paper:

HF = High frequency;

PIR = Passive infrared;

LCD = Liquid Crystal Display;

Hz = Hertz;

UAV = Unmanned aerial vehicle.

MODELING AND SIMULATION OF WEDM PROCESS FOR INCREASE PRECISION AND MACHINE SURFACE QUALITY

BOGOSLOV Vasile-Ionut¹, NECȘULESCU Oliver-Andrei¹, Liviu Daniel GHICULESCU²

¹Faculty of Industrial Engineering and Robotics, Study program: Machine Building Technology,
Year of study: IV, e-mail: bogoslovionut@yahoo.com

²Faculty of Industrial Engineering and Robotics, Manufacturing Engineering Department, University
POLITEHNICA of Bucharest

ABSTRACT: The paper deals with modeling and simulation of Wire Electrical Discharge Machining (WEDM) process using Mastercam and Comsol Multiphysics to assure precision and surface quality of machined surfaces. Two items were approached: right and inclined cutting of interior contours and lead-in and lead-out tool paths as well as corner generation of exterior contour. Some solutions to increase the precision and surface quality for the problems were presented.

KEYWORDS: modelling, simulation, WEDM, precision, quality.

1. Introduction

Wire discharge electrode processing is currently one of the best known electrothermal processing.

Wire electrode erosion processing is a process of electrothermal processing by which the material is removed due to electrical discharges, which occur between the wire electrode and the part. The waste resulting from the electric arc area is removed by the circulation of the dielectric liquid. [1].

The plasma channel generated between the cathode and the anode converts electricity into thermal energy.

The tool used is a wire-shaped electrode which in processing is carried from one coil to another to eliminate the influence of the loss of wire material on the processing accuracy [2].

The wire electrode is guided by two conical bores which are positioned above and below the machined part. The movement of the upper guide on the Z axis ensures the possibility of adjusting the distance between the two guides. The cutting of the semi-finished product is done with an advance movement 's' in relation to the wire, coordinated by the computer, in two directions X, Y. The current software allows the development of CNC programs by non-specialized personnel [3].

2. Literature review

Through the initial WEDM version, simple contour plate parts were machined. The advantages of EDM are: efficient production capacity, burr-free cutting, excellent finishes [4].

The wire electrode was vertically tensioned by two guide subsystems. The speed of movement between the electrode and the workpiece was 2-6 mm/min. The movement of the upper guide support horizontally allowed the processing of conical surfaces [5].

The diameter of the wire electrode was 0.01-0.3 mm, with a length between 7-12 Km, so as not to interrupt the processing. Its conditions were flexibility and resistance to traction and bending. [6]. With the help of a multi-roller system, the machining precision is achieved by rolling and tensioning the thread (fig.1). Figure 2 shows the WEDM processing.

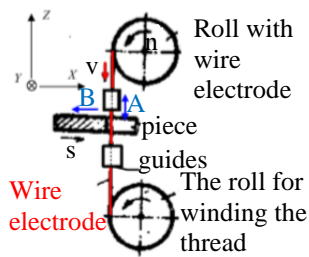


Fig. 1 WEDM kinematics

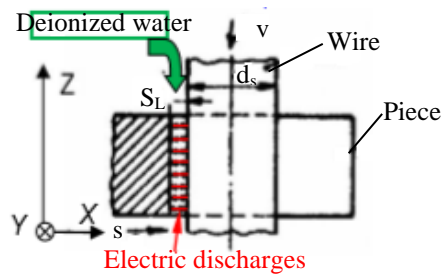


Fig. 2 WEDM processing

The preferred working fluid is deionized water, which by its fluidity removes detached particles. A disadvantage is the appearance of electrolysis, which could cause the wire to break [7].

The mechanical part of the WEDM process is described by the computer-controlled workpiece and a mechanism for driving the wire electrode through the workpiece with a mechanical tension. The speed of movement of the wire electrode is very high, in order to avoid its thinning during the process. The rectilinearity is ensured by the action of forces of 0.04-0.7 daN. The spark generator allows various forms of electrical pulses depending on the working conditions. The improvement of the pulse generator focused on the variation of the characteristics of the processing pulse. Another goal was environmental protection. Electrostatic induction feeding methods have been investigated to eliminate its parasitic capacity.

The place of passage, from one thickness to another of the piece, represents an area of instability of the process. In this sense, a subsystem has been developed that uses the information during the process and modifies it. Spark frequency information, variable gap error, abnormal spark ratio during a sampling period were used [8].

The performance of the WEDM process is achieved by the introduction of powder particles, which modify the removal mechanism of the material. The arrangement of particles in form of a chain facilitates the early generation of electrical discharges. The resulting effects relate to improved material removal rate and improved roughness. These materials are tungsten carbide, cobalt.

WEDM enhancement can be defined by combining it with other unconventional processes, such as ultrasonic field vibration assistance, electrochemical discharge, or abrasive electrode processing.

The WEDM system is defined by input factors and output parameters. Input factors are related to the workpiece or WEDM machine devices. In recent years, the efforts of researchers have been directed towards improving the process of wire EDM for the processing of superalloys. These specific materials can be: nickel alloys, titanium alloys, shape memory metal materials, nickel-titanium alloys [9].

3. Simulating the WEDM process using Mastercam

The simulation of the WEDM process will be performed in the Mastercam program. The first step is to make the piece with the inner contours. Draw the contours and extrude with the help of 'Extrude' (fig.3). The semi-finished product is defined using the Bounding Box command.

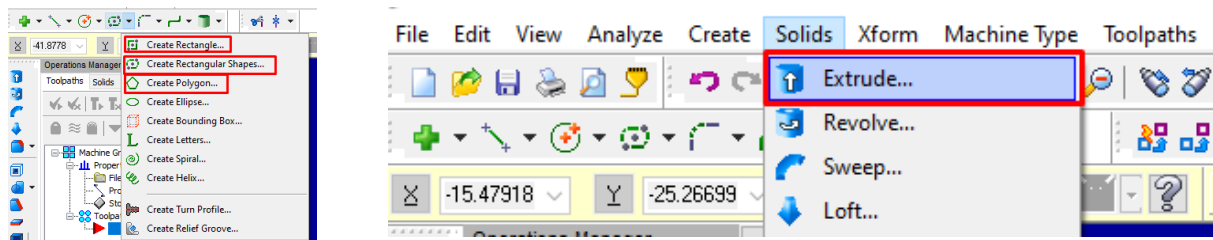


Fig. 3. Creating the semi-finished product

The outer contour parameters change. To do this, move the thread point three mm out of the lead distance menu. Set the input and output path to be a 0.5 mm radius arc, entering the lead menu and selecting 'Line

and arc' and 'Arc and line'. When obtaining overlap, three mm are noted, so as not to leave through the entry point, which increases the accuracy (fig.4). The second step is to define the threading points. (Thread Point). Define a point on the outside of the contour and a point on the inside of each inner contour (fig.5).

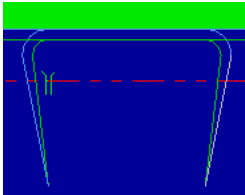


Fig.4 Input trajectory

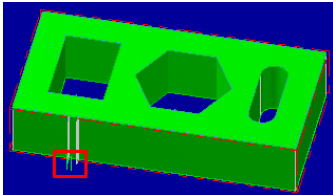


Fig. 5 The piece with the inner contours

The first time the inner contour is processed, from which we will help to catch the piece with the help of some flanges, in order to process the outer contour.

From the Toolpath→Contour menu, define the first inner contour, by clicking on the threading point and on the contour. The processing settings menu opens. A wire with a diameter of 0.3 mm is used, the processing gap being 0.05 mm. The other contours are also selected. Improved accuracy is achieved by approximating the two guides in the Taper menu.

When processing the inner contours, a bridge must be placed, at which point the processing stops and the cut part is caught. This is done from Parameters→Cut parameters→Tab. Choose the value of the 4 mm bridge and check the 'skin cuts' after tab to finish the surface.

From the Parameters window of the outer contour, the fish tail type and a radius of 0.5 mm are chosen in the corner submenu. The trajectory of the wire on the corner of the outer contour is selected as a fish tail for an increase in accuracy. This fish tail trajectory involves an exit from the contour, a complete circular motion and a entry into the next contour. (fig.6). To avoid breaking the thread, use a dot, which is set from the cut parameters menu, by checking the tab option (fig.7).

In the Parameters menu, the slash is made by selecting the Taper option and choosing a specific angle. Figure 8 shows the sloping cut.

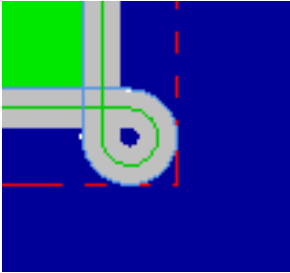


Fig. 6 Fish tail

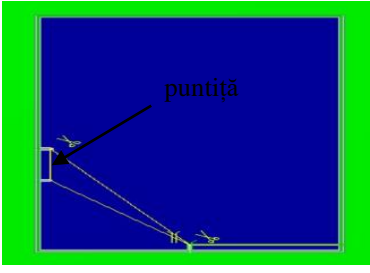


Fig. 7 The location of the deck

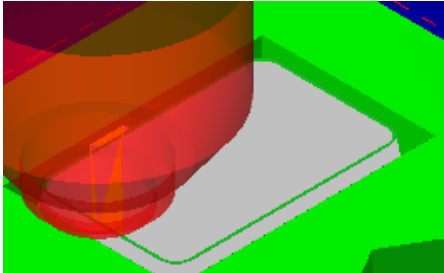


Fig. 8 Inclined cutting

4. Comsol Multiphysics modeling and simulation of the WEDM process

Figure 9 shows the parameters of the straight cut model. Figure 10 creates the necessary geometry for the simulated models, consisting of geometric elements such as rectangle, ellipse, point.

Name	Expression	Value	Description
hp	10	10	Grosimea piesei
ds	0.3	0.3	Diametrul sculei
sl	0.05	0.05	Interstitiul lateral
unghi	0	0	Unghi inclinare
unghirad	$\pi \cdot \text{unghi} / 180$	0	Unghi inclinare radiani
lp	4	4	Lungimea piesei
dcr	$17e-3$	0.017	Diametrul crater de descarcare initiala
Ra	$0.8e-3$	$8.0E-4$	Rugozitate initiala a suprafetei
xp	0	0	Coordonata x a pct. de descarcare
yp	5	5	Coordonata y a pct. de descarcare
rbg	0.1	0.1	Raza bula gaz
ti	$0.8e-6$	$8.0E-7$	Timpul de impuls

Fig. 9 Model parameters

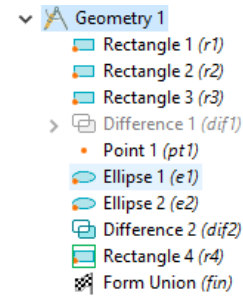


Fig. 10 Creating geometry

The material allocated for the workpiece is C120, a hardened steel with more than 60 HRC, used for the active surfaces of the punching machines. The boundary conditions for straight cutting are described in the figures 11, 12 and 13. The boundary conditions for inclined cutting are described in the figures 14, 15 and 16.

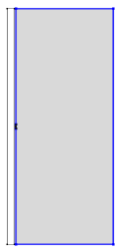


Fig. 11 Convective cooling in dielectric liquid

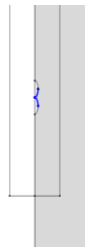


Fig. 12 Temperature on the EDM spot



Fig. 13 Thermal insulation of the gas bubble

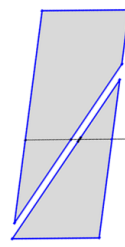


Fig. 14 Convective cooling in dielectric liquid

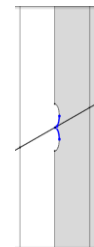


Fig. 15 Temperature on the EDM spot

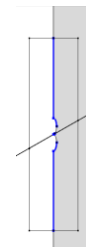


Fig. 16 Thermal insulation of the gas bubble

The temperature in the plasma channel area consists of the boiling point of the material and the overheating above the boiling point, shown in figure 17. Choose the heat transfer coefficient for convective cooling in dielectric liquid $h=10 \text{ W/m}^2 \cdot \text{K}$ [10]. Figure 18 shows the setting of the time-dependent model parameters where 'ti' is the discharge time.

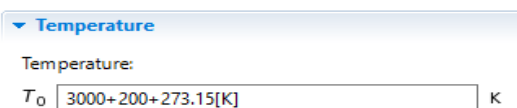


Fig. 17 Discharge temperature

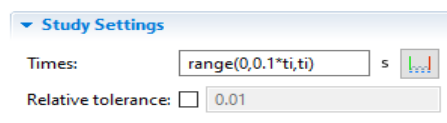


Fig. 18 Time-dependent study settings

Figures 19 and 20 show the discretizations of the models for straight and inclined cutting, and the generation of a corner with a 90° angle.

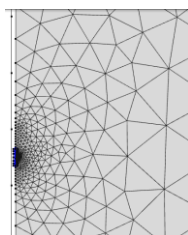


Fig. 19 Discretization of the model with free triangular elements for straight and inclined cutting

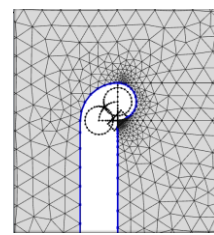


Fig. 20 Discretization of the model with free triangular elements for cutting a corner at 90° angle

Figures 21, 22, 23 and 24 show the creation of the geometry in front view to generate an outer contour with a 90° angle. In figure 28 the contour is generated by moving the center of the tool along an arc of a circle with the center of rotation in the corner of the profile cut by WEDM. Figure 29 creates the geometry after two previous discharges positioned near the corner. Figure 30 shows the geometry for generating the corner in the form of a living edge using a path with a loop (fish tail). Figure 31 shows the microgeometry of the surface after a discharge produced near the corner.

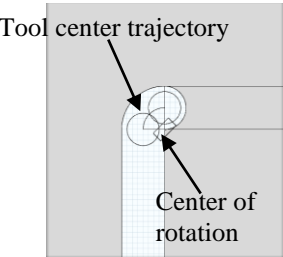


Fig.21 Generating the outer contour after an arc of a circle

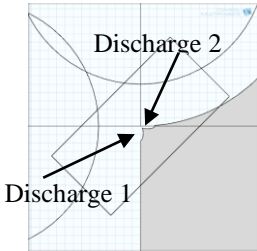


Fig.22 Microgeometry after two discharges

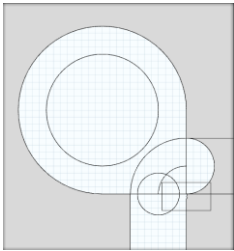


Fig.23 Generate living edge corner using fish tail

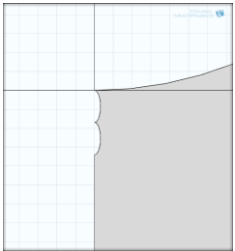


Fig.24 Microgeometry after a discharge

The boundary conditions for corner cutting with a circular arc are described in the figures 25, 26 si 27. The boundary conditions for cutting fish tail fangs are described in the figures 28, 29 si 30.

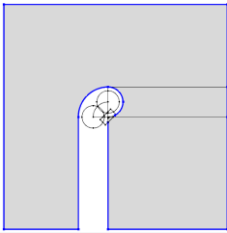


Fig. 25 Convective cooling in dielectric liquid

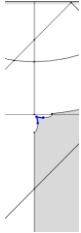


Fig.26 Temperature on the EDM spot

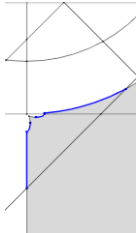


Fig.27 Thermal insulation of the gas bubble

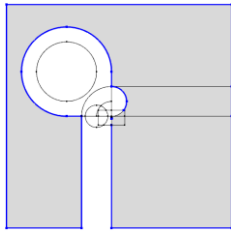


Fig.28 Convective cooling in dielectric liquid

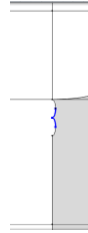


Fig.29 Temperature on the EDM spot

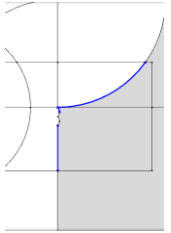


Fig.30 Thermal insulation of the gas bubble

The results from the modeling and simulation of the 90° corner generation are shown in the figures 31 and 32. In the first case, due to a very low feed rate, the probability of locating a discharge in the corner of the profile is very high. The corner is rounded due to the sample material shown in the figure 31. In the second case, when using the fishtail loop, the feed rate is high and the probability of locating the discharge in the corner of the profile is low (fig.32). In this case a sharp edge is obtained.

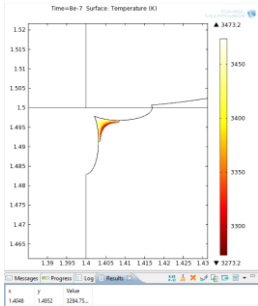


Fig. 31 Material removed at a single discharge produced in the corner of the profile

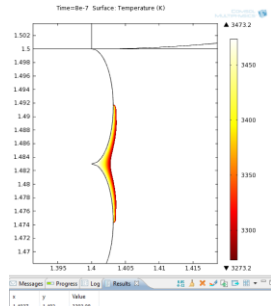


Fig. 32 Material removed at a single discharge produced near the corner of the profile

It is observed that on the right cut the depth of the crater produced by a single discharge is less than on the inclined cut. After simulating a similar discharge, 2.5 microns of the piece material is removed in

the right cut, (fig. 33), and in the case of inclined wire cutting, 2.7 microns of the piece material is removed (fig. 34).

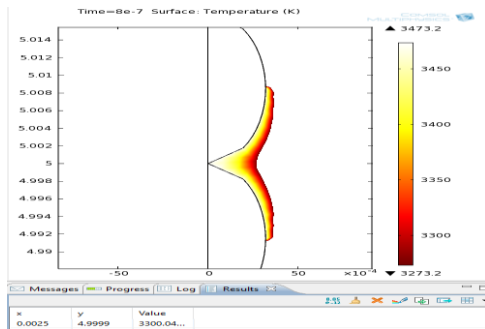


Fig. 33 Material removed for a single discharge in case of straight cutting

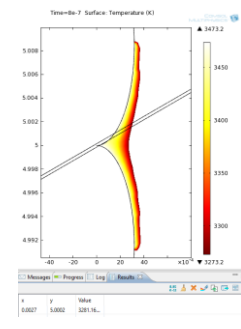


Fig. 34 Material removed in a single discharge in the case of inclined cutting

5. Conclusions

1. Straight and inclined cutting was modeled and simulated by WEDM, using Mastercam and Comsol Multiphysics, with the aim of increasing the precision and quality of the surface processed when cutting interior contours. Measures have been taken to introduce bridges that prevent the wire from breaking when the contours are closed, minimizing the distance between the guides to ensure the necessary accuracy. Finite element modeling has shown a lower depth of craters in straight cutting compares to inclined cutting and a better quality of the machined surface.

2. To increase the accuracy and quality of the machined surface, the input trajectories were used on an outer contour in the form of a circular arc, the generation of corners at 90° in the form of sharp edges with the help of the trajectory in the form of a loop (fish tail) in Mastercam. Finite element modeling in Comsol Multiphysics has shown the ability to achieve sharp edges by reducing the likelihood of producing discharges located on the corner of the profile as a result of maintaining a relatively high wire feed rate.

6. References

- [1]. Balan, A.S.S.; Giridharan, A. A progress review in wire electrical discharge machining process. *Int. J. Autom. Mech. Eng.* 2017, 14, 4097–4124.
- [2] G. Boothroyd, A.K. Winston, *Nonconventional machining processes, Fundamentals of Machinig*, Marcel Dekker, Inc, 1989, pp. 491.
- [3] Vala, U.H.; Sama, M.R. A review on different effects on flushing of dielectric fluid in WEDM. *Int. J. Adv. Res. Sci. Eng.* 2017, 6, 37–44.
- [4] Ghiculescu, L. D. (2021), *Curs de tehnologii neconventionale*, Disponibil: <https://curs.upb.ro/2021/my/>, Accesat la: 2.05.2022
- [5] G.F. Benedict, *Electrical discharge machinig (EDM), Non-Traditional Manufacturing Processes*, Marcel Dekker, Inc, New York & Basel, 1987, pp. 231-232.
- [6] Kumar, S.; Mitra, B.; Dhanabalan, S. The state of Art: Revolutionary 5-Axis CNC Wire EDM & its recent developments. *Int. J. Manag. IT Eng.* 2018, 8, 328–353.
- [7] Meena, K.I.; Manna, A.; Banwait, S.S. Effect of wire feed rate and wire tension during machining of PR-AL-SiC-MMC's by WEDM. *Eur. J. Eng. Technol.* 2013, 1, 7–13.
- [8] Okada, A.; Uno, Y.; Onoda, S.; Habib, S. Computational fluid dynamics analysis of working fluid flow and debris movement in wire EDMed kerf. *CIRP Ann.* 2009, 58, 209–212.
- [9] Okada, A.; Uno, Y.; Nakazawa, M.; Yamauchi, T. Evaluation of spark distribution and wire vibration in wire EDM by high-speed observation. *CIRP Ann. Manuf. Technol.* 2010, 59, 231–234.
- [10] *** Comsol Multiphysics, Library, Disponibil: <http://www.comsol.com>, Accesat la: 9.05.2022

MODELING AND SIMULATION BY LASER AND PLASMA CUTTING OF SOME STEELS AND POLYMERIC MATERIALS

NIȚĂ Liviu-Florinel, POP József¹, RUSU Andrei-Cosmin¹, Liviu Daniel GHICULESCU²

¹Faculty: Industrial Engineering and Robotics, specialization: Machine building Technology, year of study: 2021-2022, e-mail: pop.jozsef99@gmail.com

²Faculty of Industrial Engineering and Robotics, Manufacturing Engineering Department, University POLITEHNICA of Bucharest

ABSTRACT: The following work aims to model and simulate laser and plasma cutting of some steel and polymer materials. These types of machining are increasingly used to obtain complex, costly and difficult contours to obtain with current conventional technologies. The Comsol Multiphysics program was used to model with finite elements and to simulate the laser and plasma cutting process of the established materials. After the introduction of the parameters in Comsol Multiphysics and their optimization, experiments were carried out to obtain an optimal cut and some practical tests on the machines specific to each type of materials: stainless steel, steel C45, PVC and plexiglas. These samples were analyzed in terms of cutting quality and implicitly the roughness obtained

KEYWORDS: Laser, plasma, steel, polymeric material, cutting, simulation, optimization

1. Introduction

The process of “light amplification by stimulating emission of radiation” (LASER) is framed in unconventional thermal technologies, but due to its countless applications: electrotechnics, machine building, fine mechanics, aeronautics and due to the reduction of the costs of laser installations, the process tends to become classic. [1]

Laser cutting process is a thermal process in which the laser beam is focused and used to melt the semi-finished material. A coaxial gas jet is used to remove the molten material [2]. In CO₂ laser cutting we have a gas mixture that includes carbon dioxide [3].

Plasma cutting is a process in which an inert gas (compressed air) is blown at high speed from a nozzle, at the same time an electric arc is formed by a copper electrode at the nozzle level, converting part of the gas into plasma. Plasma is the fourth state of matter, a gas-like substance being a mixture of electrons, positive ions, and neutral particles (atoms or molecules) that are in continuous and disordered motion. The concentrations of electrons and ions are approximately equal, so macroscopically the plasma is electrically neutral. [4]

In the cutting process, the plasma arc locally melts the material and removes it at high speed, realizing the cutting purpose. The high degree of energy concentration and the high temperature of the arc make it possible to cut metal and metal alloys, high alloy steels, aluminum, copper, titanium.

2. State of the art

Laser cutting is a contact-free thermal processing process with high automation. High dimensional accuracy and low roughness of the processed surface can be obtained.

The high-power density beam when focused on a small, point-sized surface melts and vaporizes the material in a fraction of a second and is removed by a jet of coaxial gas. [5]

In Figure 3. above, 1 is the resonant cavity, 2 is the prism of deflection of the laser beam toward the desired direction; 3 - focus lens (made of NaCl, Ge, CdTe, etc.); 4 – the semi-finished material moving at the speed of v .

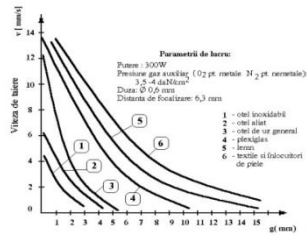


Fig. 1 Working parameters on laser cutting [2]

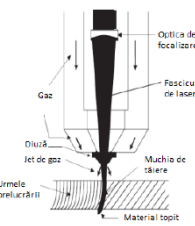


Fig. 2 Laser cutting principle scheme [5]

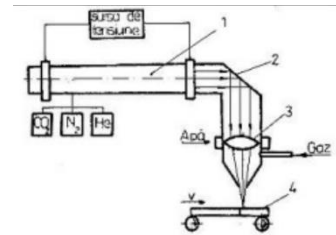


Fig. 3. Components of laser cutting equipment [1]

The laser and plasma cutting process is achieved by automation with CAD/CAM systems, they control either 3-axis flat beds or 6-axis robots for three-dimensional cutting. [5]

From an environmental point of view, it is recommended that laser cutting machines be operated at maximum power and processing speed possible, and from a resource point of view, it is necessary to optimize the cut in order to save raw material, processing time and reduce machine wear. [6]

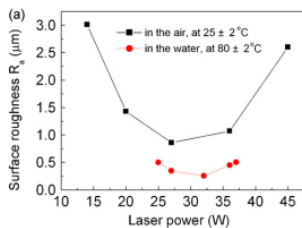


Fig. 4 Roughness according to laser power [11]

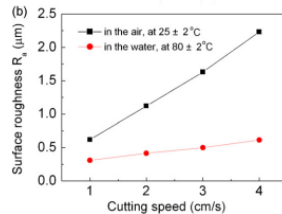


Fig. 5 Roughness according to cutting speed [11]

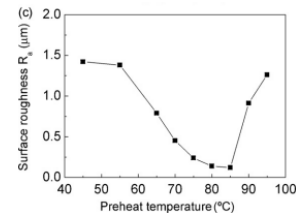


Fig. 6 Influence of material preheating on roughness [11]

Figures 4 and 5 show that it is insufficient to change only certain parameters in order to achieve the best possible roughness. In the case of plexiglass, the lower the cutting speed, the more qualitative the cut is, and therefore the roughness is better.

Table 1. Results obtained when laser cutting of polymeric materials

The material	Laser beam output power, P [kW]	Cutting thickness, h [mm]	Cutting speed, vt [m/min]
Polyvinyl chloride	0.3	3.2	3.6
Plexiglas	0.3	9	2.5

From Table 1 we can see that the parameters used for cutting vary depending on the material. The cutting speed varies depending on the thickness of the material and its characteristics.

In the case of plasma generators using direct current generation, the electric arc is maintained either between the tungsten electrode as cathode and the copper nozzle as anode, or between the electrode and an anode outside the plasma generator (the part).

The plasma cutting nozzle performs the function of creating a high-speed plasma flow. The geometric configuration of the nozzle determines the speed and power of the plasma cutter, as well as the quality of the cut edge obtained. The required pressure is provided by the air compressor. [7]

The cutting speed is inversely proportional to the nozzle diameter. To form a high-quality plasma arc, an air vortex compressed air source is used. [8]

The possibilities of increasing the cutting speed are as follows: increase the intensity of the spring; increase arc tension by using biatomic gases (H₂, N₂, O₂, etc.) [4]

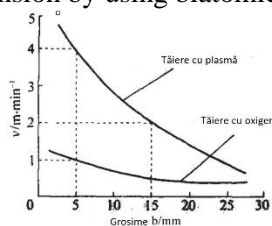


Fig. 8 Variation of plasma velocity according to thickness [10]

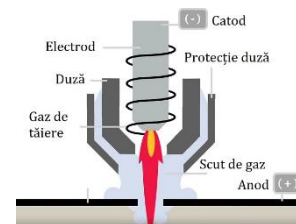


Fig. 9 Plasma cutting principle scheme [9]

3. Experiments

Table 2. Characteristics of the laser cutting machines Bodor i7 1kW and NOVA51

Characteristics	Bodor i7 1kW	NOVA51
Laser source power [W]	1000	100-130
Mode of operation	Continuous/modulated	Continuous/modulated
Wavelength [nm]	1080±10	1080±10
Laser beam quality	≤1.5mm x mrad (50µm QBH)	-
Frequency [kHz]	≤20	≤5
Diameter of optical fiber [µm]	50, doped with ytterbium	-
Laser spot diameter [mm]	Focalization depending on thickness	Focalization depending on thickness
Maximum thickness [mm]	12 (steel)	10 (polymeric materials)



Normal parameters
v=80 mm/s
P=1000 W



Low power
v=80 mm/s
P=800 W



Increased speed
v=90 mm/s
P=1000 W



Low speed
v=70 mm/s
P=1000 W

Fig. 10 Results obtained when laser cutting C45 material according to parameters



Normal parameters
v=70 mm/s
P=1000 W



Low power
v=70 mm/s
P=800 W



Increased speed
v=80 mm/s
P=1000 W



Low speed
v=60 mm/s
P=1000 W

Fig. 11 Results obtained when cutting stainless steel type 304 material according to parameters



Normal parameters
v=15 mm/s
P=78 W



Low power
v=15 mm/s
P=65 W



Low speed
v=10 mm/s
P=78 W



Increased speed
v=17 mm/s
P=78 W

Fig. 12 Results obtained when cutting the plexiglass material according to parameters



Normal parameters
v=15 mm/s
P=78 W



Low power
v=15 mm/s
P=65 W



Low speed
v=10 mm/s
P=78 W



Increased speed
v=17 mm/s
P=78 W

Fig. 13 Results obtained when cutting PVC material according to parameters

Table 4. Features of the Powermax105 SYNC Plasma cutting machine plasma generator

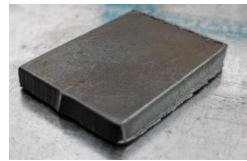
Generator power [kW]	Maximum 30 kW for 105A current
Voltage [V]	380
Current intensity	35 - 105
Gas supply	Clean, dry air, no oil or oxygen
Optimum intake gas pressure [bar]	7.6-8.3 bar (110-120 psi)
Minimum inlet gas pressure [bar]	4.6 bar (58 psi)
Type of power supply	IGBT Inverter (Bipolar Transistor with isolated deck)



Inox 2mm
 $v = 4350 \text{ mm/min}$
 $p = 5 \text{ bar}$
 $I=35A (P = 13.3 \text{ kW})$



Inox 4mm
 $v = 3500 \text{ mm/min}$
 $p = 5.6 \text{ bar}$
 $I=45A (P = 17.1 \text{ kW})$



C45 4mm
 $v = 3500 \text{ mm/min}$
 $p = 5.6 \text{ bar}$
 $I=45A (P = 17.1 \text{ kW})$



C45 2mm
 $v = 4350 \text{ mm/min}$
 $p = 5 \text{ bar}$
 $I=35A (P = 13.3 \text{ kW})$

Fig. 14 Cutting results for Inox and C45 according to the parameters specific to each thickness.

4. Modeling and simulation

Figure 15 shows the parameterization of the three models.

Name	Expression	Value	Description
Wp	$1 \times 10^6 / \text{lambda}^2$	1818 W/m ²	Densitatea de putere [W/m ²]
Wp	$P / (100 \times \text{lambda}^2)$	8.5734812 W	Densitatea de putere [W/m ²]
wcon	S	5	unghi con de focalizare [grd]
dspotrim	S*lambda	5.46E-6	diametrul spotului minim (teoretic)
lambda	1000e-9	1.000E-6	lungimea de unda [m]
wconrad	$(2.14 \times 100) / \text{wcon}$	0.087022	unghi con de focalizare [rad]
dspot	$98.4 \text{ m} / \text{wcon}$	98.4 m	diametrul spotului laser [um]
gsp	[2mm]	0.002 m	grosimea piesei
speed	70 [mm/s]	0.07 m/s	vitaza de avans [m/s]
ttop	$(1 - 2) \times \text{gsp} / \text{speed}$	0.085714 s	temp. de productie [s]
l1	10 [mm]	0.01 m	latimea piesei
l2	20 [mm]	0.02 m	lungimea piesei
l3	20 [mm]	0.02 m	raza spot laser
Temp304	1400-273.15	1073.2	temperatura de topire inox 304
P	1400 [W]	1400 W	Puterea laser
sigma	0.9	0.9	coeficient de reflectie de la centrul spotului laser
sigma	0.9	0.9	coeficient de absorbtie in otel
emi	0.9	0.9	coeficient de emisivitate
h1	$10 \text{ W} / (\text{m}^2 \cdot \text{K})$	10 W/(m ² K)	coeficient de transfer termic
Ed	$P / (\text{pi} \times \text{dspot}^2)$	1.3791813 W/m ²	Densitatea de putere pe spotul laser
sr	$\text{wcon} \times \text{speed} / \text{tp}$	0.002 m	punctul de referinta mobil
tp	[6s]	6 s	tempul de productie

Laser: steels

Name	Expression	Value	Description
Wp	$1 \times 10^6 / \text{lambda}^2$	1818 W/m ²	Densitatea de putere [W/m ²]
Wp	$P / (100 \times \text{lambda}^2)$	2.2282 W	Densitatea de putere [W/m ²]
wcon	S	5	unghi con de focalizare [grd]
dspotrim	S*lambda	5.18E-5	diametrul spotului minim (teoretic)
lambda	100e-9	1.00E-6	lungimea de unda [m]
wconrad	$(2.14 \times 100) / \text{wcon}$	0.087022	unghi con de focalizare [rad]
dspot	$(3.14 \text{ mm}) / \text{wcon}$	0.002 m	diametrul spotului laser [um]
gsp	[2mm]	0.002 m	grosimea piesei
speed	1.500 [mm/s]	0.0015 m/s	vitaza de avans [m/s]
ttop	$(1 - 2) \times \text{gsp} / \text{speed}$	6 s	temp. de productie [s]
l1	10 [mm]	0.01 m	latimea piesei
l2	10 [mm]	0.01 m	lungimea piesei
l3	10 [mm]	0.01 m	raza spot laser
TempPVC	175-273.15-20	58.4 m	temperatura de topire PVC
P	175 [W]	175 W	Puterea laser
sigma	0.9	0.9	coeficient de reflectie de la centrul spotului laser
sigma	0.9	0.9	coeficient de absorbtie in plastic
emi	0.9	0.9	coeficient de emisivitate
h1	$10 \text{ W} / (\text{m}^2 \cdot \text{K})$	10 W/(m ² K)	coeficient de transfer termic
Ed	$P / (\text{pi} \times \text{dspot}^2)$	1.62482 W/m ²	Densitatea de putere pe spotul laser
sr	$\text{wcon} \times \text{speed} / \text{tp}$	0.4 m	punctul de referinta mobil
tp	[6s]	6 s	tempul de productie

Laser: polymer materials

Name	Expression	Value	Description
Wp	$1 \times 10^6 / \text{lambda}^2$	1818 W/m ²	Densitatea de putere [W/m ²]
Wp	$P / (100 \times \text{lambda}^2)$	1.200914 W	Densitatea de putere [W/m ²]
wcon	S	5	unghi con de focalizare [grd]
dspotrim	S*lambda	5.46E-6	diametrul spotului minim (teoretic)
lambda	1000e-9	1.000E-6	lungimea de unda [m]
wconrad	$(2.14 \times 100) / \text{wcon}$	0.087022	unghi con de focalizare [rad]
dspot	$(3.14 \text{ mm}) / \text{wcon}$	0.002 m	diametrul spotului laser [um]
gsp	[2mm]	0.002 m	grosimea piesei
speed	50 [mm/s]	0.050000 m/s	vitaza de avans [m/s]
ttop	$(1 - 2) \times \text{gsp} / \text{speed}$	0.1194 s	temp. de productie [s]
l1	10 [mm]	0.01 m	latimea piesei
l2	20 [mm]	0.02 m	lungimea piesei
l3	20 [mm]	0.02 m	raza spot laser
Temp304	1400-273.15	1073.2	temperatura de topire inox 304
P	1400 [W]	1400 W	Puterea laser
sigma	0.9	0.9	coeficient de reflectie de la centrul spotului laser
sigma	0.9	0.9	coeficient de absorbtie in otel
emi	0.9	0.9	coeficient de emisivitate
h1	$10 \text{ W} / (\text{m}^2 \cdot \text{K})$	10 W/(m ² K)	coeficient de transfer termic
Ed	$P / (\text{pi} \times \text{dspot}^2)$	1.155511 W/m ²	Densitatea de putere pe spotul laser
sr	$\text{wcon} \times \text{speed} / \text{tp}$	0.25 m	punctul de referinta mobil
tp	[6s]	6 s	tempul de productie
lmpa	[0.1mm]	0.1 m	nuaj minime sac.zilavne

Plasma: steels

Fig. 15 Parameters used in modeling and simulation

Figure 16 shows how the variables were set, they are common to the three models. The distribution of energy on the laser spot and plasma follows Gauss's curve.

Name	Expression	Unit	Description
G_space	$\exp(-(x-x1)^2 / (2 \times \text{sigma}^2))$		
Plaser	A1*Ed	W/m ²	
LHS	Plaser*G_space	W/m ²	

Fig. 16 Definition of variables

Figure 18 shows the characteristics of the materials used

Property	Variable	Value	Unit
Thermal conductivity	$k_{iso}; k_{ii} = k_{iso}, k_{ij} = 0$	16.2	W/(m·K)
Density	rho	8000	kg/m ³
Heat capacity at constant pressure	Cp	502	J/(kg·K)

304 Stainless steel

Property	Variable	Value	Unit
Density	rho	1760 [kg/m ³]	kg/m ³
Thermal conductivity	$k_{iso}; k_{ii} = k_{iso}, k_{ij} = 0$	0.1 [W/(m·K)]	W/(m·K)
Heat capacity at constant pressure	Cp	880	J/(kg·K)

PVC

Property	Variable	Value	Unit
Heat capacity at constant pressure	Cp	475 J/(kg·K)	J/(kg·K)
Density	rho	7850 [kg/m ³]	kg/m ³
Thermal conductivity	$k_{iso}; k_{ii} = k_{iso}, k_{ij} = 0$	44.5 [W/(m·K)]	W/(m·K)

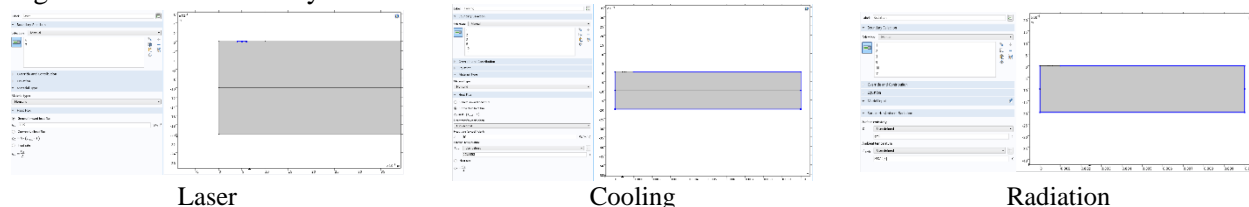
Steel C45

Property	Variable	Value	Unit
Density	rho	1180 [kg/m ³]	kg/m ³
Thermal conductivity	$k_{iso}; k_{ii} = k_{iso}, k_{ij} = 0$	0.18 [W/(m·K)]	W/(m·K)
Heat capacity at constant pressure	Cp	1700	J/(kg·K)

Plexiglas

Fig. 18 Material characteristics

Figure 19 shows boundary conditions



Laser

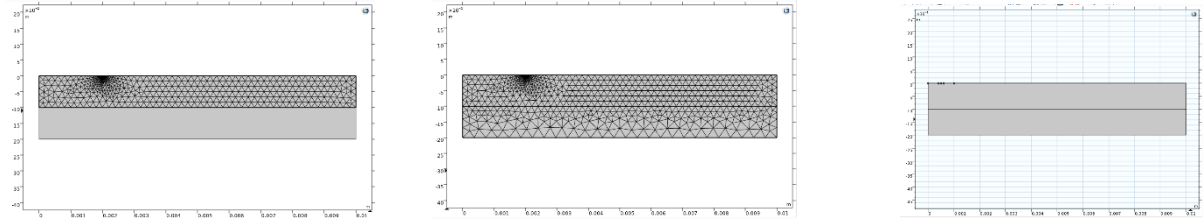
Cooling

Radiation

Fig. 19 conditions at the limit

The mesh consists of forming a network of triangles, and the calculation of the temperature distribution is obtained based on the approximation with the values in the peaks of each triangle. The smaller the triangles (fine) the better the accuracy. The exception to this step is the model developed for polymeric materials,

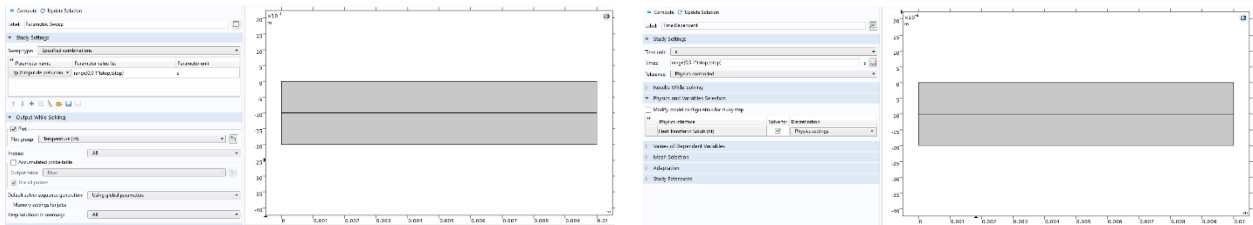
because it is very sensitive to changing parameters and implicitly to obtaining optimal results, it was considered a solution to create an extra-fine mesh on all surfaces that will give us a better result. The two layers (Figure 20 c) are created in order to help in future steps, namely in creating the mesh. Thus on the upper section will be a finer mesh (extra fine), and on the lower section a less fine mesh.



A) creating the network on the top section B) creating the network on the lower section c) creation of layers

Fig. 20 Creation of the mesh

In order to simulate the movement of the laser/plasma spot on the surface of the blank, the parametric sweep option (figure 21 a) was used with the sweep processing time (t_p) parameter. The time-dependent parameter was also set as the final processing time, t_{stop} (Figure 21 b)

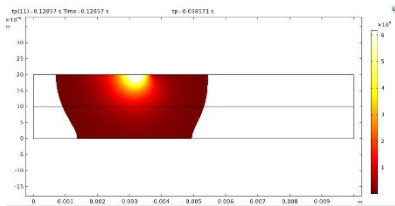


a) Parametric Sweep b) Time dependent

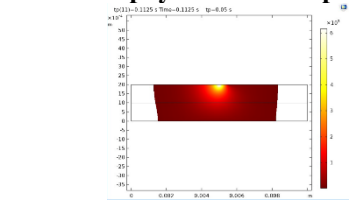
Fig. 21 Settings for performing the study

Table 11 shows the results obtained when simulating cuts by varying the speed, spot diameter and laser power (when cutting polymeric materials) achieving three situations: Moderate heating (low roughness), overheating (high roughness) and low heating (high roughness with the appearance of striations).

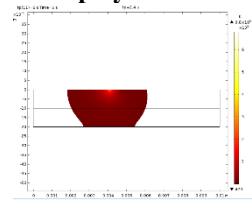
Table 11. Results obtained in Comsol Multiphysics for laser/plasma cutting of steel and polymeric materials



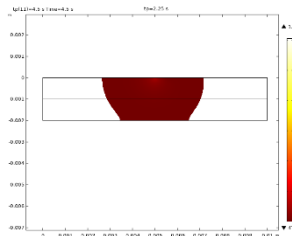
Optimal laser cutting: Stainless steel
spot diameter=0,015 mm
cutting speed=70 mm/s



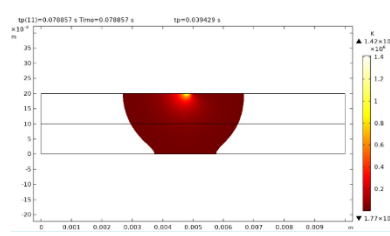
Optimal laser cutting: C45
spot diameter=0,012 mm
cutting speed=90 mm/s



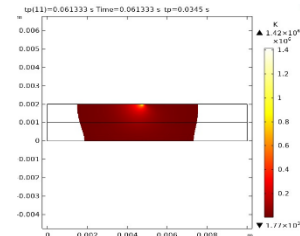
Optimal laser cutting: PVC
spot diameter=0.14 mm
cutting speed=1.5 mm/s
Power = 25 W



Optimal laser cutting: Plexiglas
spot diameter=0.2 mm
cutting speed=2 mm/s
Power=30 W



Optimal plasma cutting: Stainless steel
spot diameter=0,2 mm
cutting speed=7000mm/min.



Optimal plasma cutting: C45
spot diameter=0,1 mm
cutting speed=9000mm/min.

5. Conclusions

Finite element modeling and simulations of laser and plasma cutting processes of stainless steel 304, C45 steel, as well as laser cutting of PVC and plexiglass polymer materials were made. The models created are dynamic by scenting the processing time to simulate the speed of advance of the laser/plasma spot. The contribution to the heating of the material (temperature distribution within the semi-finished) of the following technological parameters was highlighted, aiming to reduce the roughness of the processed surface, increasing the quality of the surface layer. The analyzed technological parameters were: Laser/plasma spot diameter, advance speed and power distributed on the laser/plasma spot. An optimization was achieved in terms of material heating by correlating the three parameters mentioned. Experiments were also carried out on laser and plasma cutting of the mentioned materials, which confirmed the influence of the mentioned technological parameters on the quality of the processed surfaces.

6. Bibliography

- [1]. Ghiculescu, D. (2020), Curs Tehnologii Neconvenționale, București.
- [2]. Marinescu, N.I., Ghiculescu, D. (2017), *Procese tehnologice cu fascicule, oscilații și jeturi*, editura Printech, București
- [3]. Landry, J. (2020, 26 november), „FIBER LASERS: EVERYTHING YOU NEED TO KNOW”. Available at: <https://www.laserax.com/blog/fiber-laser> . Accessed: 25.04.2022
- [4]. Amza, Gh. (2009),– *Tehnologia Materialelor si produselor*, vol 3, editura Printech, Bucuresti.
- [5]. V.Senthil Kumar and Dr.G.Jayaprakash (2017), “State of Art of Laser Cutting Process”, *International Journal for Modern Trends in Science and Technology*.
- [6]. M. Radovanovic and P. Dasic (2006), “Research on surface roughness by laser cut, ”*The Annals of University Dunarea de Jos of Galati Fascicule VIII, Tribology*
- [7]. K. Küpfmüller, W. Fathis und A. Reibiger (2013), *Theoretische Elektrotechnik: Eine Einführung*, Springer
- [8]. H. Zohm (2013), *Plasmaphysik*, LMU München, München
- [9] ***Hypertherm, „Plasma cutter technology”. Available at: <https://www.hypertherm.com/learn/cutting-education/plasma-technology/> . Accessed: 02.05.2022
- [10] „Huafei” (2020, 19 november), „oxy-fuel flame cutting VS plasma cutting”. Available at: <https://thebestcnc.com/oxy-fuel-cutting-vs-plasma-cutting/> . Accessed: 02.05.2022
- [11] Yongguang H., Shibing L., (2009), “Surface roughness analysis and improvement of PMMA-based microfluidic chip chambers by CO₂ laser cutting”. Available at: https://www.sciencedirect.com/science/article/pii/S0169433209013993?casa_token=AWDY3vreYlMAAAAA:MgwjcfndeVx6yri3hOVIR3L-8DxIyYHmgkUbFX1iKnzmVrrtXiQx9UXTxjkUI-PBRsBqQLBmpeo . Accessed: 04.05.2022

A CYBER SECURITY APPLICATION FOR REPORTING MALICIOUS ATTACKS ON IOT NETWORKS THAT USE THE MQTT PROTOCOL

CUCURUZAC Andrei-Traian¹, ABAZA Bogdan Felician²

¹Faculty of Industrial Engineering and Robotics, Specialization: Applied Computer Science in Industrial Engineering, Year of study: 4, e-mail: andreicucuruzac99@gmail.com

² Faculty of Industrial Engineering and Robotics, Manufacturing Engineering Department, University POLITEHNICA of Bucharest

ABSTRACT: It is known that information and communication technology has advanced a lot in recent decades and with it, the risk of malicious attacks increased. New and abstract concepts have emerged that have improved and continue to improve human life. Whether we are talking about cities, factories, universities or even households, the need to automate and monitor the various processes that take place within them has increased, paving way for IoT networks. Unfortunately, in many cases this accelerated development forgot about securing devices that transmit valuable information. Thus, the data transmitted in the networks became an easy target for malicious people. This paper focuses on the creation of an IoT network on which we will simulate a set of possible attacks that shows us where and what these malicious people could hit.

KEYWORDS: Internet of Things, MQTT Protocol, Cyber Security, Network Attacks

1. Introduction

The rapid development of information and communication technology has made people's lives easier in many ways. But with the digitization of information has also come the danger that information can be stolen or obstructed, leading to economic loss or even loss of life. *"Every American depends - directly or indirectly - on our system of information networks. They are increasingly the backbone of our economy and our infrastructure, our national security and our personal well-being. But it's no secret that terrorists could use our computer networks to deal us a crippling blow ... As President, I'll make cyber security the top priority that it should be in the 21st century."* - Barack Obama, 44th President of the U.S., "Summit on Confronting New Threats", Purdue University, 16 July 2008.

The present work entitled "Cybersecurity application for reporting malicious attacks in IoT networks running on the MQTT protocol" aims at securing MQTT servers in IoT architectures, which are known within the protocol as brokers, by generating a report that can help detect certain vulnerabilities and propose possible suggestions in their remediation.

The Internet of Things, or IoT for short, is a concept that involves the use of the Internet in interconnecting various devices, sensors, software or automated systems to form a network of objects that aims to provide various services easily accessible to humans [1]. With the appearance of IoT, other innovative concepts such as smart industry, smart city or smart home have emerged, all of which improve everyday human life. Smart industry or Industry 4.0 has led to the restructuring of factories thus increasing production while managing to decrease the number of employees, smart city has led to efficient air quality monitoring or smart traffic management, and smart home has in some cases even led to the disappearance of the common light switch, homeowners using only their voice to operate light bulbs or other devices. This is even more useful in the case of people with mobility problems. [2-5].

2. Architecture of IoT Networks running on the MQTT protocol

Accelerated progress in information and communications technology has forced the IoT concept to rapidly take shape and adopt certain types of architectures. Although there are several types of architectures, the main ones used are: three-layer architecture, service-based architecture and middleware-based architecture. At the core of this work is the service-based architecture, which in turn is divided into

four layers: the perception layer, the network layer, the service layer and the application layer. For the last-mentioned layer, although there is currently no standardization, protocols for low bandwidth environments are used, for example: MQTT, CoAP, XMPP, DDS, AMQP [6].

The protocol used in this paper is MQTT or Message Queuing Telemetry Transport. This is a simple protocol that has been designed for limited networks that operates with devices with poor processing capabilities and high latencies. It is on layer seven of the OSI (Open Systems Interconnection) stack and on layer four in the service-based architecture (Fig.2.). On the main layer, the perception layer, are the sensors. They allow the conversion of information from the environment into digital information. Further on the next layer are the technologies for transmitting sensor data. In this paper, data will be transmitted via WIFI and Bluetooth.[7]

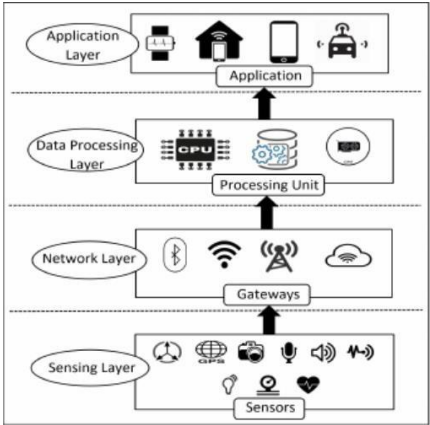


Fig. 2. Service-based architecture. [7]



Fig.3. Architecture applied in this paper.

A difference can be seen on the service layer, also called the data processing layer. Where, the processing is not done directly by a physical computer but by a virtual machine with the HomeAssistant operating system, which is based on Docker containers. On the last layer, the application layer, there is the MQTT broker, Mosquitto, which makes it possible for clients to connect and transmit data. (Fig.3.)

MQTT is used today in different types of industries such as consumer goods manufacturing, the automotive industry or the oil industry. The protocol works on the principle of transmitting data through a publish-subscribe system where, as suggested by the name, IoT network devices send data to an MQTT broker to which they have subscribed [8] (Fig.4.).

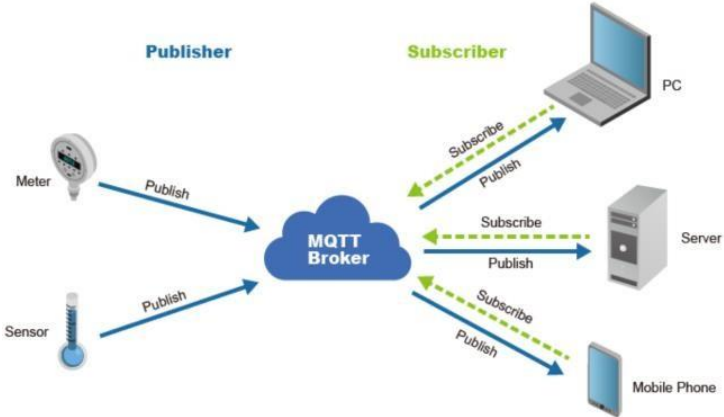


Fig.4. Principle of data transmission via MQTT. [9]

In order to carry out the present work and for a better understanding of the infrastructure of an IoT network, it was necessary to create a test environment as similar as possible to a real case, in which we can connect different sensors, transmit via MQTT, visualize and store in a database the information received from them. The final objective being to test the created environment and understand the vulnerabilities to which the IoT network is exposed.

3. Defining the IoT network test environment

The test environment is currently fully and actively set up in one of the university rooms, collecting data from April 18, 2022 to present. Following the service based IoT architecture and considering what sensors can be found in industrial environments, but at the same time taking into account the components accessible on the market, the environment created is divided as follows:

- Perception layer (Sensor layer)
 - a) PM 2.5 particle sensor.
 - b) Bluetooth humidity and temperature sensor
 - c) Humidity and temperature sensor
- Network layer
 - a) ESP32 – Microcontroller responsible for taking data from sensors and transmitting them using the WIFI standard via MQTT.
- Service layer (Data processing layer)
 - b) Home Assistant OS - Operating system that embeds containerization services via Docker to install applications in a controlled and secure environment.
- Application layer
 - c) Mosquitto broker - Application responsible for retrieving data transmitted via MQTT.
 - d) Graph - The application responsible for the graphical representation of data.
 - e) Influx DB - Database.
 - f) Home Assistant Core - Module present in the operating system that allows automation based on intercepted data.

The PM 2.5 sensor used is a commercial ready-to-use sensor that is powered from the socket using a USB-C cable. To make the design as practical as possible, it had to be modified (Fig. 6). Thus, the modification of the sensor consists of powering the ESP32 microcontroller and the DHT22 sensor from its motherboard and collecting data from the two sensors in serial mode by the microcontroller. At the same time the ESP board will receive temperature and humidity information via Bluetooth from two other nearby sensors.

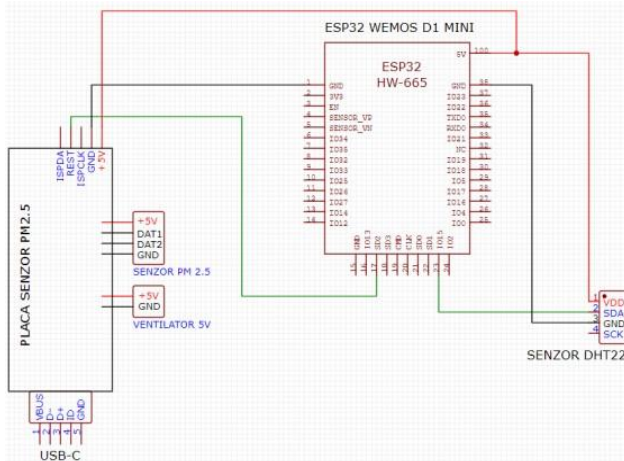


Fig. 5. Wiring diagram



Fig. 6. Soldering components

In the case of the two Bluetooth sensors, a modification was also made by changing the firmware pre-installed by the manufacturer with a custom firmware already available on the internet [10]. This was necessary to make it possible to transmit parameters to the microcontroller via Bluetooth.

The ESP-Home environment was used to program the microcontroller, which is based on a YAML file translator. After translation, the program compiles a firmware based on the configurations made later in the file to be uploaded to the ESP board. The process proceeds as follows:

- Configure the YAML file with the name of the microcontroller and its type.

- Activate the Bluetooth module and set the WIFI credentials that will allow the microcontroller to access the internet.
- Sensor configuration. This part involves choosing the pins over which serial communication will be done and setting the MAC addresses for the Bluetooth sensors.
- Configure the MQTT client that will transmit to the server. This involves setting the IP and port of the broker, as well as setting the username and password that were set when configuring the server.
- Generate firmware and install it on the ESP via USB

After programming the microcontroller, the MQTT is configured on the Home Assistant OS server. The broker available for this OS is Mosquitto, a broker supporting the latest version of the MQTT protocol. As the chosen OS works on docker containers, the configuration only involved setting the authentication credentials and setting the port through which the data exchange will be performed.

Thus, with simple software that subscribes to the broker topic, [11] it is possible to visualize the first data transmitted by the sensors. In the following picture, four topics are shown that have been selected to demonstrate data transmission via MQTT (Fig.7).

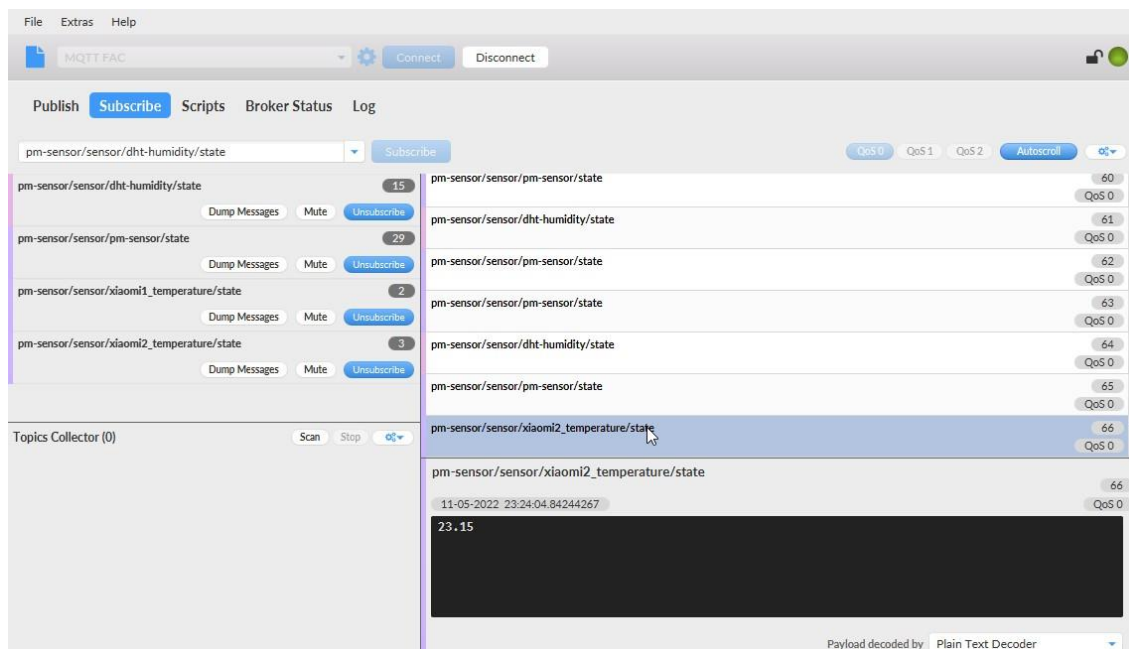


Fig.7. Sensor data captured with the MQTT.fx program [11]

Once the necessary settings have been made, the storage of all the values sent on the protocols intercepted by Home Assistant will begin. The data will be kept on the server for 365 days in the database called "data_1". The following figure shows the temperature data from one of the two installed Bluetooth sensors. The data shown is stored from the time of installation on 18 April 2022 until the day this paper was created (Fig.8.).



Fig.8. Querying the database

Finally, for data visualization we configured the main panel of Home Assistant so that the parameters were delimited by zones, according to how the sensors were placed in the room (Fig.9.).



Fig. 9. Monitoring panel

Thus, a system was created based on an existing architecture, which takes temperature and humidity parameters both via Bluetooth and serial mode, as well as air quality parameters, to be transmitted by the MQTT client, via WIFI, using the ESP32 microcontroller to the virtual machine with Home Assistant OS, where the data is taken, processed and stored.

4. Security simulation and analysis

Like most WAN (Wide Area Network) connected networks, MQTT-based IoT networks can also be vulnerable to cyber-attacks. A retrospective analysis by Cloudflare Inc. shows that in 2016 the "Mirai" malware managed to infect 65,000 IoT devices on the first day of its release peaking in November 2016 when it reached 600,000 infections. Internet service provider Deutsche Telekom suffered massive signal disruptions and the compromise of hundreds of thousands of routers because of the "DoS" attack carried out by the IoT botnet created after the infections [12].

With the help of libraries for the Python programming environment and tools available on the Internet [13], a series of attacks were attempted. These attacks aim to load the MQTT broker with fake clients. As a result of the attack parameters such as CPU utilization, RAM utilization and system temperature were influenced. The biggest differences can be seen in the processor utilization parameters where the values increased from 5% normally to 63% during the attack (Fig.10.).

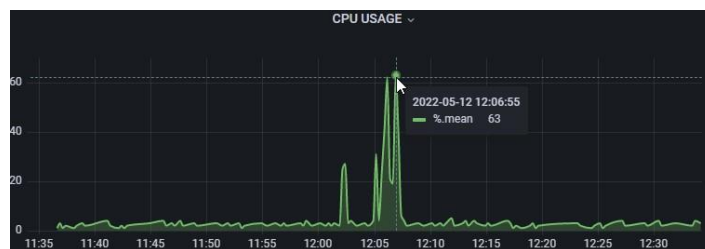


Fig. 10. Processor usage parameters

It must be mentioned that the attack was carried out from an old computer with a dual-core processor and 8 GB RAM. The higher the performance of the computer on which the attack is carried out, the greater the damage can be. In this case, the damage is not considerable, but only a slowdown of the system. However, if routine updates by the system operator are added to this scenario, concomitant with the attack, there is a possibility that the usage parameters may reach higher levels, leading to the broker's inability to function.

This test was carried out without encrypting the data, in the future it is intended to set up a server that will encrypt the data and the connection using known protocols such as TLS or SSL. The current security settings that have been made on the test environment relate to blocking other data ports on the network that communicate with the outside and using only those that are strictly necessary for remote system operation and actuation.

This is where the issue of studying the security of microcontroller update management came into play. Since other ports were blocked for security reasons, it made it inaccessible to send updates wirelessly to ESP. With any firmware update it is necessary to disassemble the sensor and connect via USB to the computer from where the action will be performed. As a result, ways to send these updates via MQTT, where port 1882 is available for external communication, have been investigated. An unfriendly but possible way is to compile the firmware and transmit it in small bit packets. But an unstable WIFI connection can lead to a data packet being lost *en route*, so there is the possibility of corrupting the ESP's memory and making it unusable.

5. Conclusions

In conclusion, it is easy to see that technology has advanced and at the same time the risks to users have increased, which is why a thorough analysis of the vulnerabilities of all information systems is necessary.

The system was developed from the desire to create and secure a functional IoT network in real scenarios, in this case monitoring temperature, humidity and air quality in a classroom according to an existing architecture. Following the service based IoT architecture, it was possible to capture sensor data using the ESP32 microcontroller, connect it to a network via WIFI, transmit the retrieved data to a server via MQTT, store and visualize the data. At the same time, a type of MQTT attack has been carried out which has been shown to slow down the processing capacity of a server, and in other scenarios may even render it unusable.

6. Bibliography

- [1]. Samuel Greengard (2015), The Internet of Things, The MIT Press, ISBN 978-0-262- 52773-6, Massachusetts.
- [2]. Marcelo Tsuguio Okano (2017), IOT and Industry 4.0: The Industrial New Revolution, International Conference on Management and Information Systems, Chitkara University in association with AIMS-International and INFOMS, Bangkok, 25-26 September 2017.
- [3]. Ashraf Tahat, Ruba Aburub, Aseel Al-Zyoude and Chamseddine Talhi (2018), A Smart City Environmental Monitoring Network and Analysis Relying on Big Data Techniques, ICSIM2018: Proceedings of the 2018 International Conference on Software Engineering and Information Management, January 2018.
- [4] Yamuna Kaluarachchi (2022), Implementing Data-Driven Smart City Applications for Future Cities, MDPI Smart Cities, 30 March 2022.
- [5]. Soojung Chang and Kyeongsook Nam(2021), Smart Home Adoption: The Impact of User Characteristics and Differences in Perception of Benefits, MDPI Buildings, 3 September 2021.
- [6]. Marco Lombardi, Francesco Pascale and Domenico Santaniello (2021), Internet of Things: A General Overview between Architectures, Protocols and Applications, MDPI Information, 19 February 2021.
- [7]. Sikder, Amit Kumar & Petracca, Giuseppe & Aksu, Hidayet & Jaeger, Trent & Uluagac, Selcuk. (2018) A Survey on Sensor-based Threats to Internet-of-Things (IoT) Devices and Applications.
- [8]. MQTT - The Standard for IoT Messaging, 2022 - <https://mqtt.org/>
- [9]. Image source - <https://oringnet.com/en-global/tech/detail/93>
- [10]. Custom firmware for the Xiaomi Thermometers and Telink Flasher via USB to Serialconverter - https://github.com/pvxx/ATC_MiThermometer
- [11]. MQTT.fx - <https://mqttfx.jensd.de/>
- [12]. Cloudflare, Inside the infamous Mirai IoT Botnet: A Retrospective Analysis, 12/14/2017 - <https://blog.cloudflare.com/inside-mirai-the-infamous-iot-botnet-a-retrospective-analysis/>
- [13]. Stfbk (2019), Github, MQTTSA, <https://github.com/stfbk/mqttsa>

RESEARCH ON THE DESIGNING AND MANUFACTURING OF AN EXPERIMENTAL ROBOTIC ARM MODEL FOR DRILLING RODS HANDLING.

BRĂNESCU Teodora – Elena¹, TARBĂ Ioan – Cristian²

¹Faculty of Industrial Engineering and Robotics, Study program: Applied Informatics in Industrial Engineering, Academic year: 4, e-mail teodora.branescu1405@gmail.com

²Faculty of Industrial Engineering and Robotics, Manufacturing Engineering Department, University POLITEHNICA of Bucharest

ABSTRACT: There are a few problems on the drilling market regarding the handling of the drilling rods by the technical operative. There are a few rods loaders on the market at this point, but they are only accessories of the drilling rigs and can be used only as machinery equipment. The idea of a custom rods loader, who can work with any drilling rigs, has the purpose to create an automated system who can transport, pick and handle the drilling rods to the drilling point, without manually intervention by the operative.

KEYWORDS: holder, pipe, motors, hydraulic, cylinder

1. Introduction

Drill pipes are necessary elements in the geotechnical drilling process and are made of steel or aluminium (see Fig. 1). They are used on drilling rigs and are necessary for auxiliary sampling, such as mechanical coring and layering samples. They are hollow on the inside because they must ensure that the drilling fluid is pumped through the borehole [1].

In the working environment, they are centred in the drill head and screwed to it. Their lengths can be 3000 mm or 6000 mm and the diameter varies depending on the requirements of the working environment. The most commonly used drill rods are 101.6 mm in diameter. For a length of 3000 mm, they reach a weight of about 60 kg [2].



Fig.1. Drilling pipes

At the moment, in most jobs, the pipes are handled manually by the operators. The weight of the pipes can cause health problems for them over time and at the same time manual handling is a disadvantage in terms of flexibility in the working environment. There are several drilling machines on the market that have attached loading equipment for drill pipes. The purpose of this equipment is to create an automatic process of loading and handling drill pipes (Fig. 2.). They are also divided into two categories: the tracked ones for shorter length pipes and the long ones for longer length pipes.

There are a number of disadvantages in using these fixed loader designs:

- a. They are fixed elements that have a capacity of a limited number of pipes.
- b. They are used only for the machines for which they are constructed and cannot be used outside of them.
- c. Involve a larger gauge than that originally used for drilling machinery. The soil and environment do not allow the use of very heavy drilling machine sometimes.
- d. The addition of such equipment changes the gauge dimensions of a drilling machine and a too large gauge size can create problems during transport.



Fig.2. The loading equipment for drill rods.

2. State of the art

This machine has a capacity of 49 drill rods (Fig. 4.), each 3000 mm long. The holder in which the pipes are loaded is interchangeable. An advantage is that when the last drill rod is used at the drilling point, this holder can be replaced by an identical one containing 49 more drill rods. The whole system is electrically and hydraulically controlled. The hydraulic pump unit helps to drive the hydraulic cylinders that set certain systems in motion.

The solution is to implement a prototype of an individual loading machine, which has the ability to transport, hold, load and handle rods. This machine is positioned next to the drilling machine and automatically loads and positions the pipes in the rotating head of the drilling machine (Fig. 3.).

The purpose of implementing such a prototype is to create an automatic drilling process using drill pipes.



Fig.3. The 3D model of the drilling pipes machine



Fig. 4. The 3D loaded model of the drilling pipes machine

The assembly is divided in a few mechanical sub-systems. These sub-systems are:

- 2.1. The holder for drilling pipes (Fig. 5. and Fig. 6.)
- 2.2. The bridge crane (Fig. 7.)
- 2.3. The robotic arm (Fig. 8.)

2.1. Holder of the Drilling Pipes

It is a holder in which pipes are loaded and stored. It has a capacity of 49 pieces of 3000 mm length, aligned vertically and horizontally in 7 rows (Fig. 8. and Fig. 9.). The rack weighs 490 kg and the pipes weigh 2900 kg.

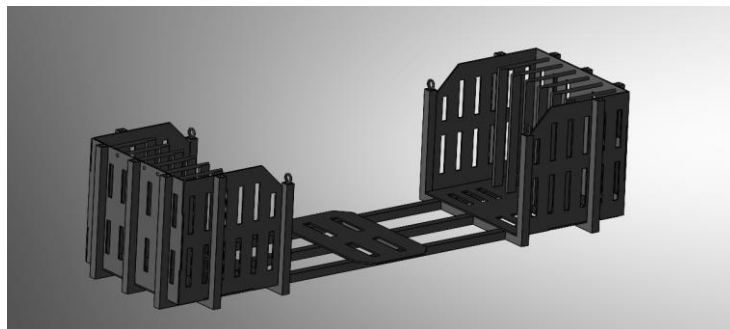


Fig. 5. The holder for drilling pipes

Also, there are 4 rings for the clamp (Fig. 6.) which can be used to lift the holder and replace it with another. The operator can change this holder with another one.

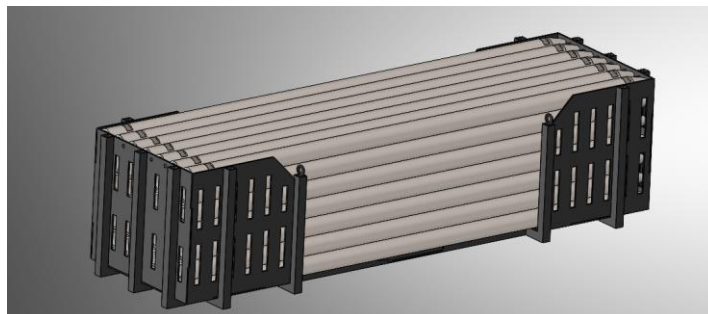


Fig. 6. The loaded holder for drilling pipes

2.2. Bridge Crane

It moves over the 7 rows of the rack by means of linear guides (Fig. 10) and contains a hydraulic shear system that lowers itself to the gripping point of the pole. The gripper is hydraulically operated.



Fig. 7. The 3D model of the bridge crane

2.3. Robotic Arm

Its purpose is to take the pole from the crane gripper and bring it to the drilling point (Fig. 11) and the other way around. It approaches the gripper to grab the pipe which it picks up from the overhead crane via a stepper motor on linear guides. It moves away from the scraper towards the edge of the chassis. The lower boom extends from the bracket outside the machine approx. 1500 mm. The upper arm moves from horizontal to vertical position by means of a hydraulic cylinder. The upper link is based on a joint driven by a stepper motor which will rotate the upper link approx. $\pm 30^\circ$ from the fixed point.



Fig.8. The 3D model of the robotic arm

The movement and functionality of the bridge crane

Movement is achieved by two stepper motors moving symmetrically at the two ends of the bridge. The whole system moves by means of two linear bearings for each bridge base. The bearings move on a linear guide. The gripper descends and ascends by means of a hydraulically operated shear system. The movement of the gripper to tighten the pole is hydraulically operated. During the functional process we encountered a number of problems such as:

- a. The bridge crane must constantly maintain a position perfectly parallel to the rows of the fence in order to be able to grab the pipe. Its length is 3620 mm, and at such a size such

problems can arise much more easily if the two motors do not move symmetrically at the same time.

- b. The gripper must fix the pipe correctly so that it does not cause accidents in the working environment that may affect the machine and operators.

The solution to these problems is to implement an algorithm that ensures the correct functionality of the whole system. This uses two microswitches placed on the inside faces of the gripper that signal that the pipe has been fixed in the gripper when they are pressed against its walls. If this is the case, the hydraulic cylinder will lift the pole through the shear system. When the pipe is at the upper transport point, the bridge crane will start moving. The two stepper motors will start driving the bridge crane at the same time. To check that the movement is symmetrical, the distances of both ends from the starting point are measured and if they are equal the movement is symmetrical. This is measured using two ultrasonic sensors.

3. The solution using LABVIEW

An Arduino Mega board, two 28BYJ-48 stepper motors, two HC-SR04 ultrasonic sensors and two SS-5GL microswitches were chosen for the command and control system.

The user interface (Fig. 9.) contains: a selection area to choose the connection port, two LEDs, which will light up to confirm when the two microswitches are pressed, indicators showing the distance measured by each sensor in centimetres, a control button that operates the two stepper motors and a switch that changes the direction in which the spindle rotates.

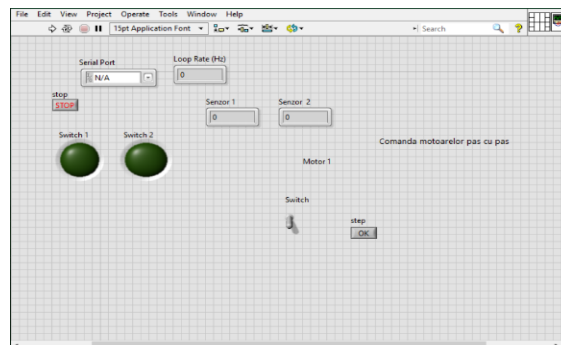


Fig. 9. LABVIEW interface

In the control diagram of the program, when the two switches send a digital signal to the Arduino board, the two sensors will start taking measurements and the two motors will be able to move the crane (Fig. 10.).

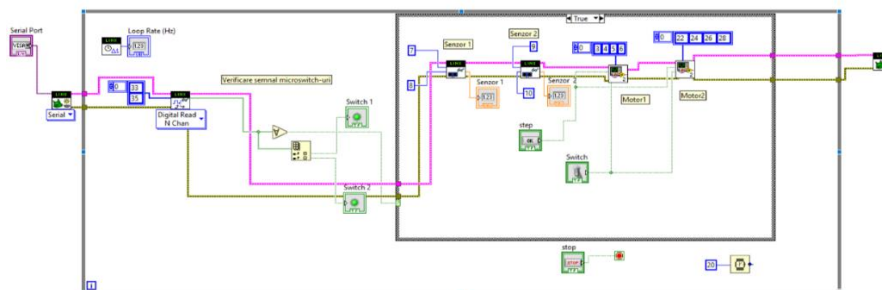


Fig. 10. The algorithm in Labview

A separate program was developed for the motor drives, which was later integrated into the main program as SUBVI for each motor (Fig. 11.). Element 1 of the Case structure will contain the Boolean values for the counter clockwise rotational motion, while element 3 will contain Boolean values opposite to the original ones for the clockwise motion of the motor shaft. In element 0 all Boolean values are False. Since the initial mechanical action of the Step button performs a single step for one press, it changes to Switch when pressed for a continuous movement over a certain period of time indicated in the main VI [3].

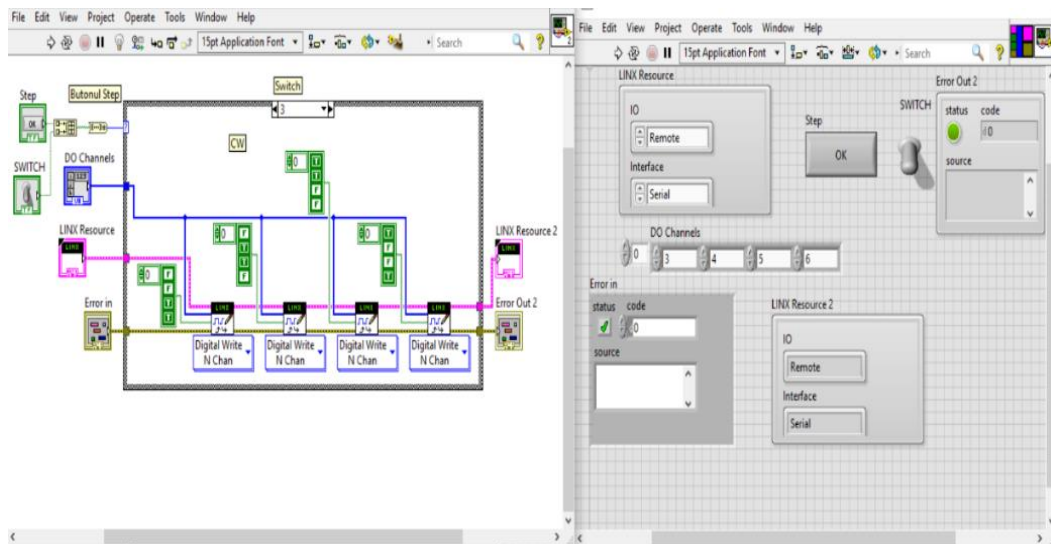


Fig. 11. The algorithm used for the motor drives

4. Conclusions

The own contribution to the implemented system consists both in the adaptation of a model of an overhead travelling crane, used in industrial halls, to create a customized mechanical system on tracks, which aims at automating the processes of handling, loading and transport of drill rods and for the shearing system, which ensures stability in the process of handling the drill rods. Future research consists in the development of an algorithm that ensures good functionality of the robotic arm and an algorithm that ensures correct positioning of the designed prototype in relation to the drilling machines when performing geotechnical drilling.

5. Bibliography

- [1] I. C. Oleg, in *Fabricarea de material tubular petrolier destinat forajului adânc*, București, INSTITUTUL GENERAL DE DOCUMENTARE TEHNICĂ, 1967.
- [2] Gloria Mocuta, *Mașini și utilaje de foraj*, București, 1973.
- [3] https://www.youtube.com/watch?v=qwvP2AzoB_M&ab_channel=SINC.

LABVIEW APPLICATION FOR THE MOMENT OF INERTIA CALCULUS

CIOCONEA Adina-Mariana¹ and SPÂNU Paulina²

¹Faculty of Industrial Engineering and Robotics, Specialty: Industrial Engineering, 1st year,
e-mail: adina.cioconea@stud.fiir.upb.ro

²Faculty of Industrial Engineering and Robotics, Manufacturing Engineering Department,
University POLITEHNICA of Bucharest

ABSTRACT: The moment of inertia is an essential quantity, needed in many engineering areas and also studied, especially on the mechanical and engineering educational institutes. The following LabVIEW Virtual Instrument (VI) is able to compute the moment of inertia, the center of mass and also the area of a specific complex 2D figure with variable dimensions. The VI algorithm uses classical theorems in order to determinate the previous mentioned quantities.

KEYWORDS: LabVIEW, center of mass, moment of inertia, area

1. Introduction

The determination of the moment of inertia (MOI) is of fundamental importance in various engineering domains. It represents a quantity that determines the torque needed for a desired angular acceleration about a rotational axis, akin to how mass determines the force needed for a desired acceleration. The ability to precisely determine the moment of inertia allows the engineer to properly size their components while achieving the high-performance demands, e.g., in the aerospace and defense industries. In other cases, the measurement of MOI can be used to verify that manufacturing and assembly tolerances and processes goals are nominal. In this paper the author conceived a program in LabVIEW software capable to calculate the moment of inertia of a specific complex 2D figure with various dimensions, along with its center of mass and the area. The conception process of the application presented in the following required a fundamental understanding of the algorithm that implies breaking the formulas from a simple, general figure to a composed one.

2. Understanding the problem requirements

The given problem requires the moment of inertia of a 2D figure, with given dimensions. The figure is an irregular one, formed by various basic forms (rectangle, triangle).

The calculus of the moment of inertia requires the center of mass and the area of each individual component of the figure, therefore it is necessary to establish the basic figure components of the main figure and if the basic figure is added or subtracted.

The main figure contain: one rectangle (added), one smaller rectangle(subtracted), two triangles (subtracted)

3. Establishing the inputs and outputs

Resulting by the analyzation of the problem the following inputs are established (see figure 1), followed by their insertion in the VI in the form of a numeric controller (see figure 2):

- Height
- Gap height
- Gap width
- Base gap

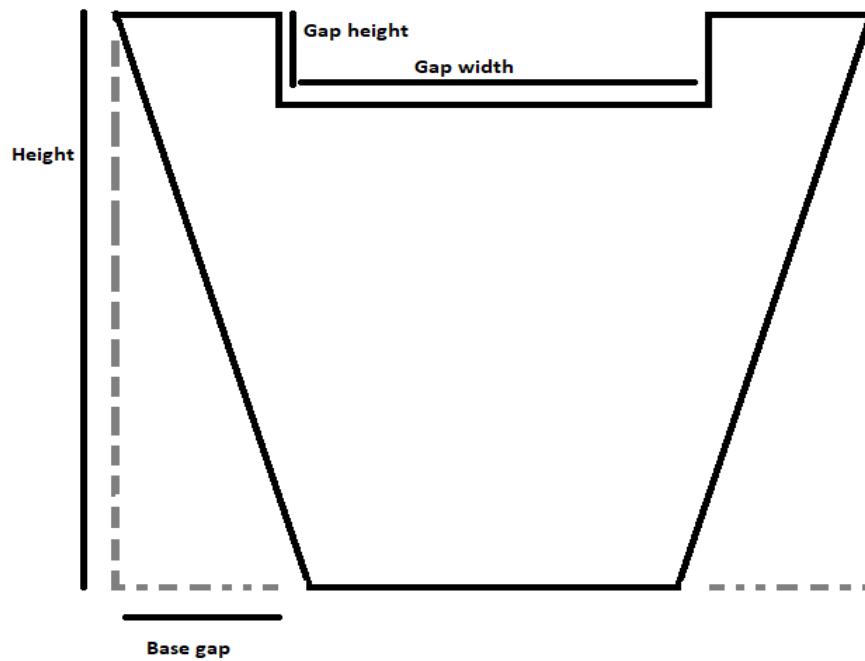


Fig. 1. 2D Figure (inputs notation)

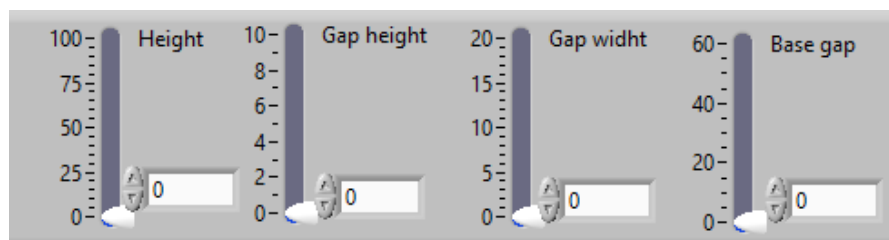


Fig. 2. Inputs in form of numeric controllers

Also, from the requirements of the problem we can detect the main output moment of inertia, but also the intermediary outputs (table 1), and represented as numeric indicators in the VI (see figure 3):

Table 1. Outputs

Figure name	Area	Center of gravity
2D figure	Total area	Center of gravity
Big rectangle	Area rectangle	CGV rectangle
Gap rectangle	Area top-gap	CGV top-gap
Side triangle	Area side-gap	CGV side-gap



Fig. 3. Outputs in form of numeric indicators

4. Equations and algorithm applied in the VI

The necessary formulas to determine the moment of inertia are [1] :

- Center of gravity (1)
- Steiner's formula for moment of inertia (2)

$$Z_c = \frac{\sum A_i Z_i}{\sum A_i} \quad (1)$$

Z_c = center of gravity for the entire figure [mm];

Z_i = center of gravity for one basic figure [mm];

A_i =The area of one basic figure [mm²]

$$I_c = \sum I_i + \sum (Z_i - Z_c)^2 A_i \quad (2)$$

I_c = moment of inertia for the entire figure [mm⁴];

I_i = moment of inertia for one basic figure [mm⁴];

The algorithm of the VI implies the following steps:

1. Breaking down the figure in basic figures: one big rectangle and one small rectangle and two triangles that will be subtracted from the big rectangle.
2. Computing the Center of gravity
 - a. Areas for each figure
 - b. Center of gravity for each figure
3. Computing the moment of inertia

The LabVIEW permits different ways of implementation, one of them is the one using the basic mathematical functions of the LabVIEW (see figure 4), but considering the amount of work and the difficulty on debugging, a more optimal implementation was provided, using Formula Node (see figure 5)

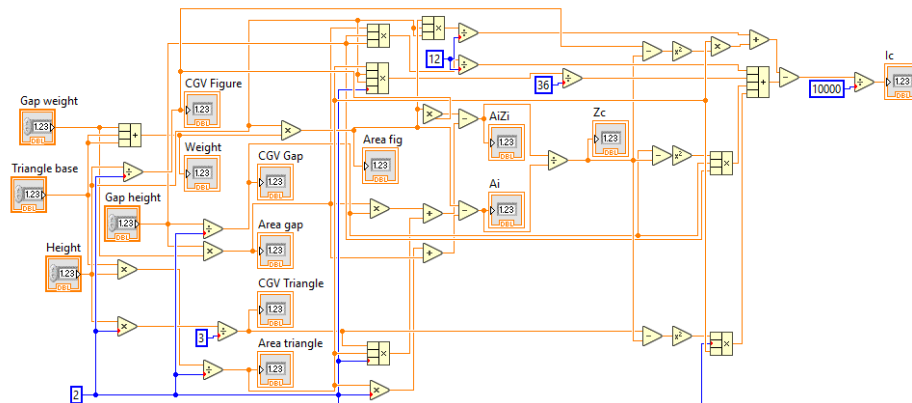


Fig. 4. Formulas implementation using the basic numerical functions



Fig. 5. Formulas implementation using Formula Node

5. Converting and displaying the result

The moment of inertia is calculated in mm^4 by default, but the in order to change the measurement unit another controller was added.

The results are presented in a table, created by a two-dimensional array, including the moment of inertia with the required unit and the center of gravity in mm (see figure 6), the array contain $t=\text{data of type string}$.

The table was created by converting the results from the numeric form in a formatted string concatenated to another given string adjusted to the unit required and adding the specific values to the array in the respective form (see figure 7)

Results array	
0	Moment of inertia
0	Gravity center
84.76190476 cm^4	31.42857mm

Fig. 6. Results table

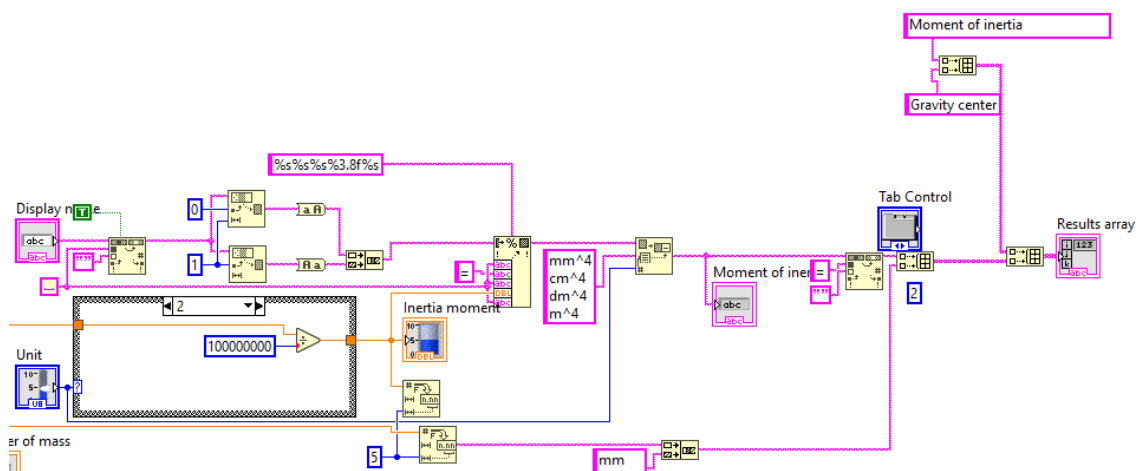


Fig. 7. Converting and formatting the results

6. Designing the figure using 2D picture and XY Graph

LabVIEW perming the visual representation in multiple ways. For this project were used 2 methos of visual representation:

- a) 2D image, that also permit a more dynamic approach for the visualization (see figure 8)

The process of constructing this image implies:

- Calculating the coordinates of each point
- Grouping each point coordinates by the Bundle function
- All point were transmitted to the image using the function Build Array

Also, the center of gravity was added together with the text and in order to give dynamic to the image, there were used a While loop structure, that was the center of migrates from the top of the image to its place

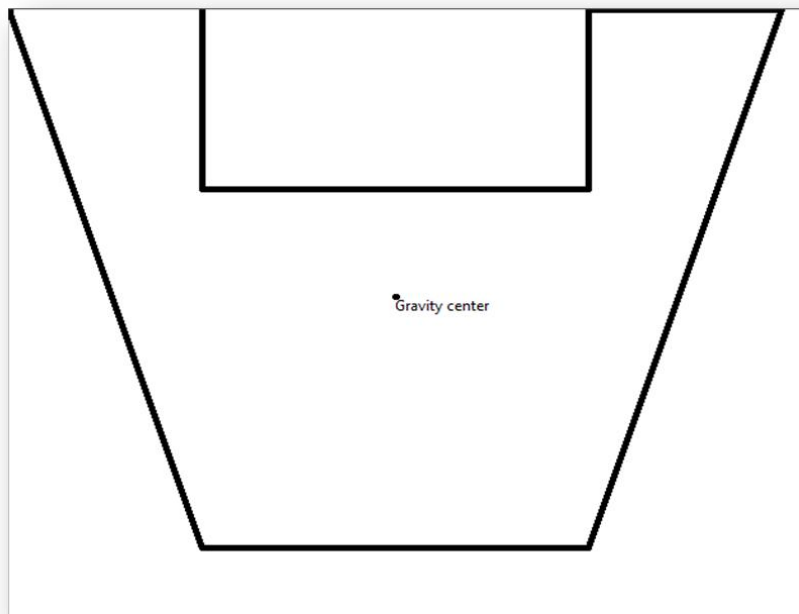


Fig. 8. 2D Image representation

- b) a XY Graph representation, that permits the visualization of the system of axis and the scaling (see figure 9)

The process of constructing this graph implies:

- Computing all x coordinates for each point and grouping them in an array, using the function Build Array
- The same procedure for the y coordinates
- The coordinates were transmitted to the XY Graph using the Bundle function

Also, the arrows for the graph were added using a SubVI.

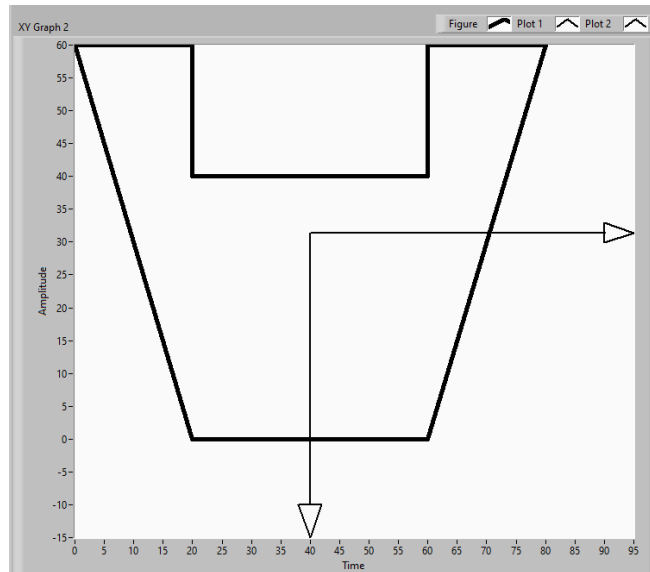


Fig. 9. XY Graph representation

7. Current state

In the present the application has the following characteristics:

- Receiving the data from the user, representing the dimensions of the respective figure
- Computing the moment of inertia, along with the intermediary necessary quantities as: areas of the individual parts of the figure, the general area, the center of mass of each individual parts of the figure, the general center of gravity on the Z axis
- Displaying the moment of inertia in the required unit measure and in a specific format.
- Displaying the figure in a XOY Graph along with the center of mass, along with the scale for each axis according with the dimension provided by the user.
- Displaying the figure in a 2D image form and mobile center of mass according with the dimension provided by the user.

8. Conclusion

In conclusion the presented VI represents a tool that compute mainly the moment of inertia and consequently, the area and the center of mass of a specific complex figure. Also, it permits visualization of the figure in two different forms using the dimensions given by the user.

As future resolutions it is intended to add the function to export the results into a text file in a specific folder and to read the inputs from a text file.

9. Bibliography

- [1]. Jiga, G.(2014) Strength of Materials,Volume 1, Ed. PRINTECH, București, ISBN 978-606-23-0168-2
- [2]. Savu T., Spânu P., Abaza B.(2014), Reprezentări grafice – îndrumar de laborator, Ed. PRINTECH, București , ISBN 978-606-23-0230-6
- [3]. Savu T., Spânu P., Abaza B.(2014), Algoritmi – îndrumar de laborator, Ed. PRINTECH, București , ISBN 978-606-23-0229-0
- [4]. Savu T., Spânu P., Abaza B.(2018)Bilingual Laboratory Guide (Romanian -English)Computer Programming, Ed. Printech Bucuresti , ISBN 978-606-23-0819-3

DEVELOPMENT OF A WEB PLATFORM APPLICATION FOR THE ADMINISTRATION OF BACHELOR'S DEGREE FINAL PROJECTS

CHIRIAC Nicu – Manuel¹, TARBĂ Ioan – Cristian²

¹Faculty of Industrial Engineering and Robotics, Study program: Applied Informatics in Industrial Engineering, Academic year: 4, e-mail nicu.chiriac99@yahoo.com

²Faculty of Industrial Engineering and Robotics, Manufacturing Engineering Department, University POLITEHNICA of Bucharest

ABSTRACT: The purpose of the developed application is to facilitate the way in which the projects of the students of final years are managed by the department management. The application must keep track of the students, the coordinating teachers, the assigned topics and the files that contribute to the final grade. Files can be text, 2D drawings, tables, etc. The platform administrator can monitor and approve the whole process of assigning homework, uploading files on time, approving students for the final exam, etc. The application uses web-specific technologies to ensure a consistent process from assigning the diploma topic to taking the bachelor's thesis final exam.

KEY WORDS: client, server, database, communication, authentication

1. Introduction

Efficient data management is a key point in the conduct of any process involving a data flow. A web application that integrates the data management part becomes necessary when multiple users from different locations need to access and / or modify certain records stored in a database. The application aims to achieve this goal, giving teachers the opportunity to view, insert, assign topics or extract information / files about the students in the years III and IV from Manufacturing Engineering Department. Within the platform, the administrator / director of the department / or the approved staff of the faculty can register students, teachers, homework assignments, assign them, creating the relationship between student - bachelor's thesis - coordinating teacher, upload various documents / files necessary for the student to be able to participate in the final exam. Also, the Admin of the platform (user with full access and rights) will be able to confirm the correctness of the data, give students access to the final verification after all their main data / files are validated, will be able to edit fields or delete records. The application will integrate all the necessary data for the bachelor's degree administration process.

2. Application structure and technologies

The project is divided into two distinct parts: Front-end and Back-end.

The Front-end is the user interface, also known as the client-side. Here are important the design elements (graphics display), their intuitiveness in use, adaptability to different types of displays, fast response. It is the interactive area of the platform, as this is where the requests are made - the exchange of data between the client and the server.

The Back-end (server) is the area where the logic needed to run the application is performed. Various endpoints (routes) are called here, which are in fact often asynchronous functions, which are built to serve, as the case may be, the needs of the user, which he can trigger (make requests) at any time he wishes to get data from the server or even transmit it. The back-end in this case is complemented by another extremely important component - the database.

The database serves to maintain the coherence of all the data that is saved / stored. With a strong emphasis on the idea of management, the platform uses a relational model database, separating the data

into tables specific to the type of records: students, teachers, topics, files, users. Using specific SQL methods, the attributes can be combined, forming new entities necessary for the case type.

The technologies used will be presented and defined as follows:

- **HTML** (HyperText Markup Language) is a descriptive language that creates the basic structure of a site, consisting of tags, elements and attributes.
- **CSS** (Cascading Style Sheets) represents the language used for editing / styling the layout and for formatting all the elements we see on the site.
- **JavaScript** is a client-side scripting language that is interpreted by the web browser. JavaScript scripts are used to increase the interactivity of web pages, giving users the power to take action within the web page. In the early stages of the Web, most sites were static, only in presentation format, meaning they displayed static elements, and there was no interaction between the page and the user.
- **React** is one of the open source JavaScript libraries. It is used to build interactive user interfaces. It is an efficient, declarative and flexible library. It deals with the component V in the Model-View-Controller Architecture (MVC). It's not a whole framework, it's just a front-end library. It allows the creation of complex user interfaces using isolated and small pieces of code known as components. The major advantage of the components is that the change to any other component does not affect the entire application. It was developed by the software engineer Jordan Walke, who works at Facebook. Facebook deployed it in their newsfeed and used it to improve its user interface. It was made public in May 2013. [1]
- **Node.js** is an open-source JavaScript execution environment, that runs on the Google Chrome V8 engine and can run JavaScript code outside of a web browser [2]. It is mainly used on the back-end (server) programming side.
- **Express.js** is one of the most used frameworks for Node.js. It makes the creation of HTTP routes and content parsing very easy for the application.
- **PostgreSQL** is a relational database management system (RDBMS) that uses Structured Query Language (SQL) as the main query language. [3]

2.1. Database

The database is a central landmark of the application. Most of the functionality is around it, as the platform exists for this purpose - to store and process data. The design of the database followed a number of well-established steps: organizing the necessary information, dividing the information into tables, transforming the information elements into columns (each element becomes a field in a table column), specifying the primary keys (unique way of identifying each row - ID), configuration of the relationships in the table, testing and application of normalization rules (checking the coherent structure to reduce redundant data).

Thus, the database was structured in 4 linked tables: „studenti” (students), „teme” (topics or homeworks), „profesori” (teachers) and „fisiere” (files). An additional table called "users" was created to store user authentication data (id, email, password), but that is standalone, having no direct connection to the rest of the tables. Fig. 1 shows the Entity Relationship Diagram (ERD), where the tables are presented with: table header - table name, primary key (PK), foreign key (FK) and the relationships (associations) between entities. In order to be able to make the diagram, it is necessary to know the cardinality between the tables; these were shown separately in Fig.2.

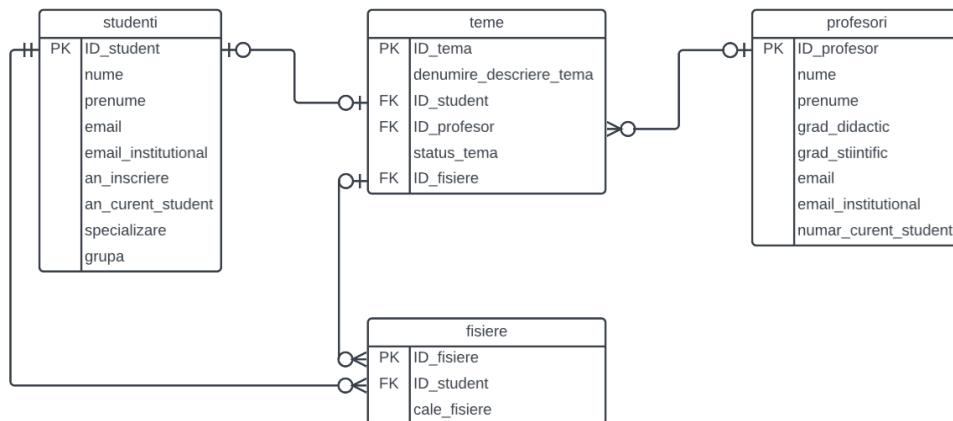


Fig. 1 – Entity Relationship Diagram (ERD)

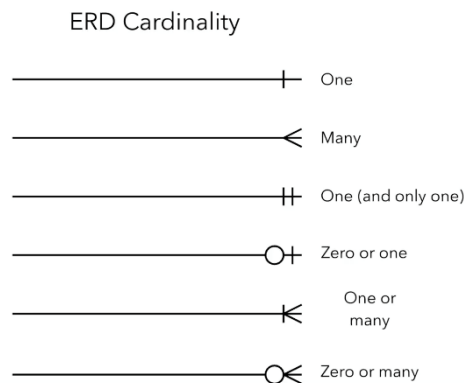


Fig. 2 – ERD Cardinality[4]

2.2. Server and routes

The construction of the server is facilitated by the use of two technologies: Node.js and Express.js. The first of these became very popular in web development, as it unified the use of a single language for both the frontend and the backend - JavaScript. Previously, it was necessary to know at least two languages in order to work in both areas of an application structure. The second (Express.js) is a framework (a library from which you can directly extract predefined / improved functionality) that complements the utility needs that a programmer / web developer may encounter. Among the advantages of using Express.js are: fast definition of Hypertext Transfer Protocol (HTTP) method-based routes; it includes various middleware modules that can perform additional tasks on client-server requests and responses; allows for quick setup when connecting to a database. A simplified case of creating a server in Node.js using Express.js and making a request between the client and the database will be presented (Fig.3).

```

const { PORT, CLIENT_URL } = require("../src/constants");
const express = require("express");
const app = express();
app.use(express.json());
const port = PORT || 3002;
//app start
const appStart = () => {
  try {
    app.listen(port, () => {
      console.log(`The server is running at http://localhost:${port}`)
    })
  } catch (error) {
    console.log(`Error:${error.message}`)
  }
}

appStart()

exports.getStudentList = async (req, res) => {
  try {
    const results = await db.query("SELECT * FROM studenti ORDER BY nume asc");

    res.status(200).json({
      status: "succes",
      results: results.rows.length,
      data: {
        studenti: results.rows,
      },
    });
  } catch (err) {
    console.log(err);
  }
};

router.get("/studentlist", userAuth, getStudentList )

```

Fig. 3 - 1)creating the simplest server structure using Express.js;
2)the syntax of a server request to the database.

In Fig.3, in the area marked with 1, it can be seen that in order to create and start a server the following parameters were required: importing the express library, defining a constant running express, defining a port and using the “listen” method, integrated in a function, respectively in a “try-catch” block (a structure that knows how to manage the occurrence of errors). The “listen” method has in this case set 2 arguments: the port and a callback function (a function that runs / is “called” only after completing the function whose argument it is in). In the area numbered 2 there is an example of an asynchronous function (which allows the execution of the following lines of code, without blocking / delaying other procedures in case the response can be long-lasting), which queries the database by a query of type SELECT * FROM which returns all records in a table. The response is converted by the .json () method (which is based on the JSON.stringify () method) to a JavaScript Object Notation (JSON) object, because the server needs a data type that it can interpret. . Further processing is done on the object to return only the data of interest - the columns with students. Also, in zone 2 is presented the form of a route (endpoint) that uses the HTTP method of GET type, “/ studentlist”, which can be called later by the front-end to get the desired set of results. Why is it necessary to use asynchronous functions in these cases? Because it does not block the server if it doesn’t return the answer (which is known as promise) - the application continues to execute other requests even if a function fails to return.

2.3. Client and interface

The client (front-end) and the interface are the bridge between a user and the rest of the application. The key features that define the success of an application, beyond the result it offers, is the way in which it manages to mediate the communication between man and machine. In making this component, details are needed in advance about the operating points that want to be interfaced. Traditionally, websites were based on HTML, CSS and JavaScript (in its unaltered form, without the addition of other frameworks or libraries). Due to performance reasons, coding time optimization, and structuring of complex projects, different libraries (based on JavaScript) have appeared to fill the gaps of the classic model.

The React library was chosen for this project. The reasons for this were chosen as follows: 1) the structuring of the project into individual parts called components, which can exist independently of each other, and can be reused, for example: a button is built, stylized and with the functionality implemented; it can be imported into any other component without having to rebuild it. This results in a high degree of application development speed and flexibility; 2) high performance, as the core of the React lies in the existence of a Virtual Document Object Model (Virtual DOM).

The DOM is a cross-platform, language-independent application programming interface that treats an HTML, XHTML, or XML document as a tree structure in which each node is an object that is a part of

the document. Objects can be handled on a scheduled basis, and any visible changes may be reflected in the document display. [5]

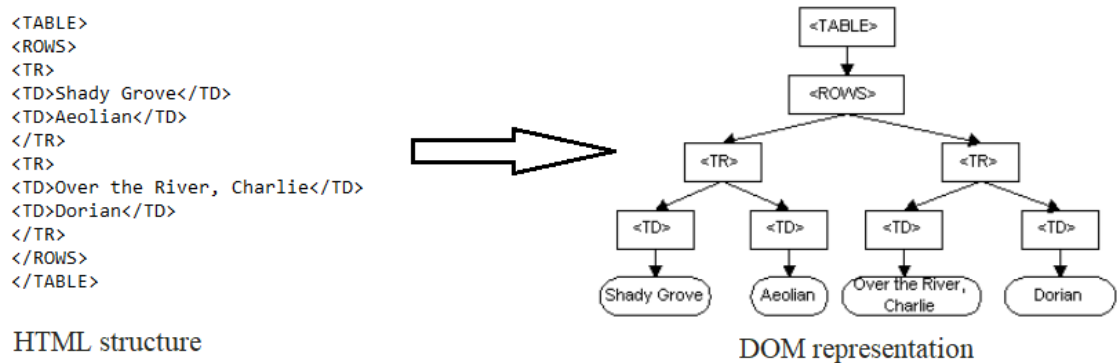


Fig. 4 – Representation of the tree structure in DOM[6]

In essence, the DOM interprets and graphically renders / displays the structure of a document, in this case HTML. The important idea behind the Virtual DOM that React has as a basis for its functionality is that it acts as a comparator with the original DOM, making the minimum number of changes (down to the lowest level), respectively the re-rendering of a component, only if it has been modified. In Fig. 5 is the differentiated rendering of components, a major factor in improving the performance of an application.

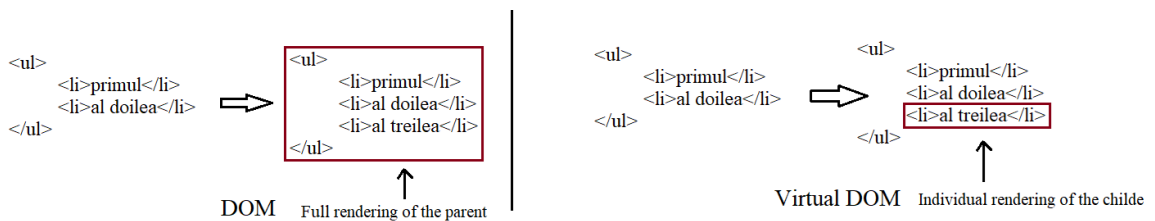


Fig. 5 – DOM vs. Virtual DOM

2.4. Authentication

The authentication process provides the security of the platform. Existing and established methods of authorizing user access were used in its creation. First, in the registration stage, an encryption method called bcrypt was used, which uses the Blowfish block cipher cryptomatic algorithm. The use of this algorithm ensures the storage of passwords in the database in an encrypted form, its reinterpretation being possible only by its decryption by the server. At the same time, JSON Web Token (JWT) was used to validate the user's identity. It consists of a header that contains the encryption method, a payload that contains information about the user trying to authenticate and a signature that contains the secret key of the server. The token will be stored in the Cookie Storage of the platform and only based on its existence the users can perform actions within the platform. A JWT is shaped like:

eyJhbGciOiJIUzI1NiJ9.(HEADER)eyJudm9udGVzIjoiSm91IENvZGVyIn0.(PAYLOAD)5dlp7GmziL2QS06sZgK4mtaqv0_xX4oFUuTDh1zHK4U(SIGNATURE)

Fig.6 shows the flow chart of the user authentication process

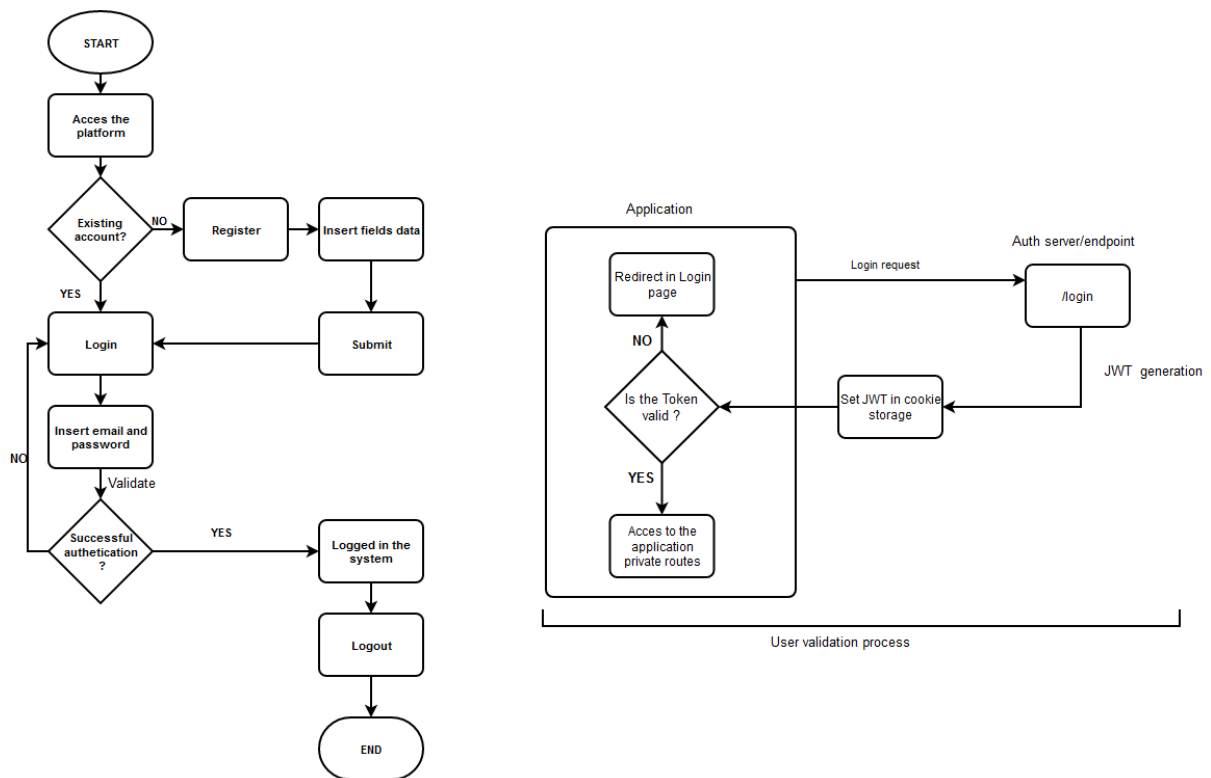


Fig. 6 - Authentication process flowchart

3. Future developments

The future directions for the application development will include methods for storing files on the server, adding rights for users (improvements to the current form of authentication) and scalability of the platform on any device, either desktop browser or mobile.

4. Conclusions

The Internet is an indispensable tool now, every field that operates on a large scale requires a means of transition / migration in the online area through one or more applications, which expose the data and processes to a wider audience, users or customers. The application aims to make the work of teachers easier, to eliminate working with multi-files (.txt, .csv, Google Docs, etc.) to keep track of data, unifying sources into a monolithic structure from which data can be entered or extracted at any time from the diploma work process.

5. Bibliography

- [1]. <https://ro.education-wiki.com/9050114-what-is-react> [accessed on : 15.04.2022]
- [2]. <https://ro.wikipedia.org/wiki/Node.js> [accessed on : 29.03.2022]
- [3]. <https://ro.education-wiki.com/5154595-what-is-postgresql> [accessed on : 3.04.2022]
- [4]. <https://stackoverflow.com/questions/54544859/er-diagram-are-the-relations-and-cardinalities-correct> [accessed on : 25.04.2022]
- [5] https://ro.wikipedia.org/wiki/Document_Object_Model [accessed on : 5.05.2022]
- [6] <https://www.w3.org/TR/WD-DOM/introduction.html> [accessed on : 5.05.2022]

LABVIEW APPLICATION FOR CALCULATING STRESS IN A STEEL BAR

IVANCU Ilinca¹ and SPÂNU Paulina²

¹Faculty of Industrial Engineering and Robotics,, Specialization: Industrial Engineering, Year: I,
e-mail: ilinca.ivancu@stud.fiir.upb.ro

²Faculty of Industrial Engineering and Robotics, Manufacturing Engineering Department,
University POLITEHNICA of Bucharest

ABSTRACT: The designed LabView application calculates and displays the stress in a steel bar with two simple supports on each side, the bar itself having two different dimensions. Using 2 main equations for deformation and stress, the VI calculates how the bars will behave under temperature changes. The program uses a formula node to do most of the exercise, then using string functions displays the resulting sigmas (stresses) in an easy-to-read format on the front panel. The program also has a slider to choose the unit of measurement between Pa and MPa, using case functions to change between them.

1. Introduction

Upon temperature change, deformation starts to occur in most materials. For metals, such as steel, temperature differences can alter the material quite fast. This is an effect that happens in real cases with weather, so any engineer needs to be able to tell how materials behave in such conditions. Using a formula node, the program calculates sigma (stress) in the steel bars and all the elements needed until it reaches the stress formula. Then, using string functions and arrays, it displays the values obtained for each sigma, the unit of measurement and the names of the variables. The program also has a slider to choose which unit to show the results in (Pa or MPa), using a case function to either multiply or divide the value obtained to have it in the right unit.

2. Translating the exercise into basic computations in a VI

Laboratory 1 – Elementary functions for numeric values; Understanding the problem and doing basic calculations using numeric functions. We use the equations to calculate stress, but we do it in a simple drag-drop-link manner. Very rudimentary start.

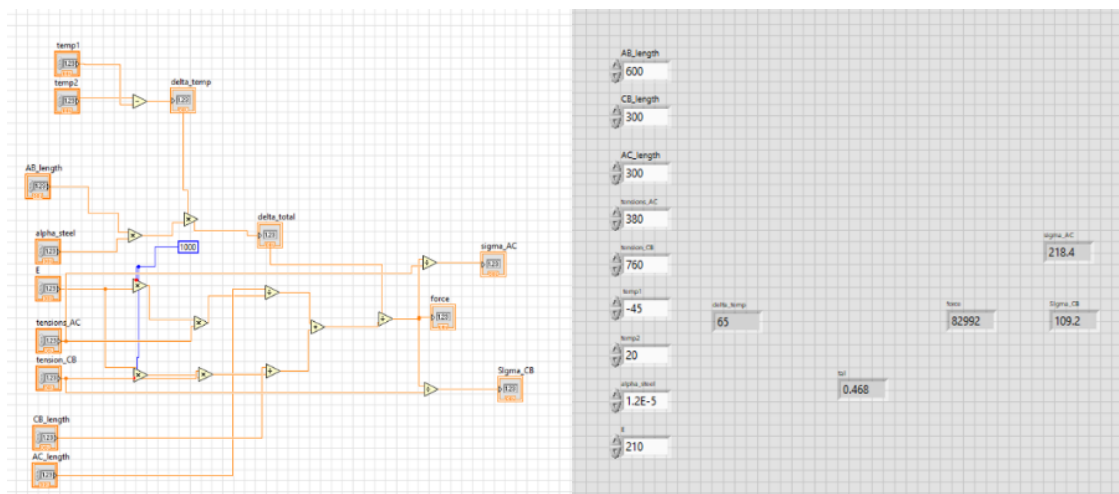


Fig. 1. First VI with simple computations

3. Organizing the VI with Formula Nodes

Laboratory 2 – Generating random numeric values; Using formula nodes to clean up the block diagram. Linking all the variables to the formula node and using the equations to calculate everything. The front panel stays the same as before.

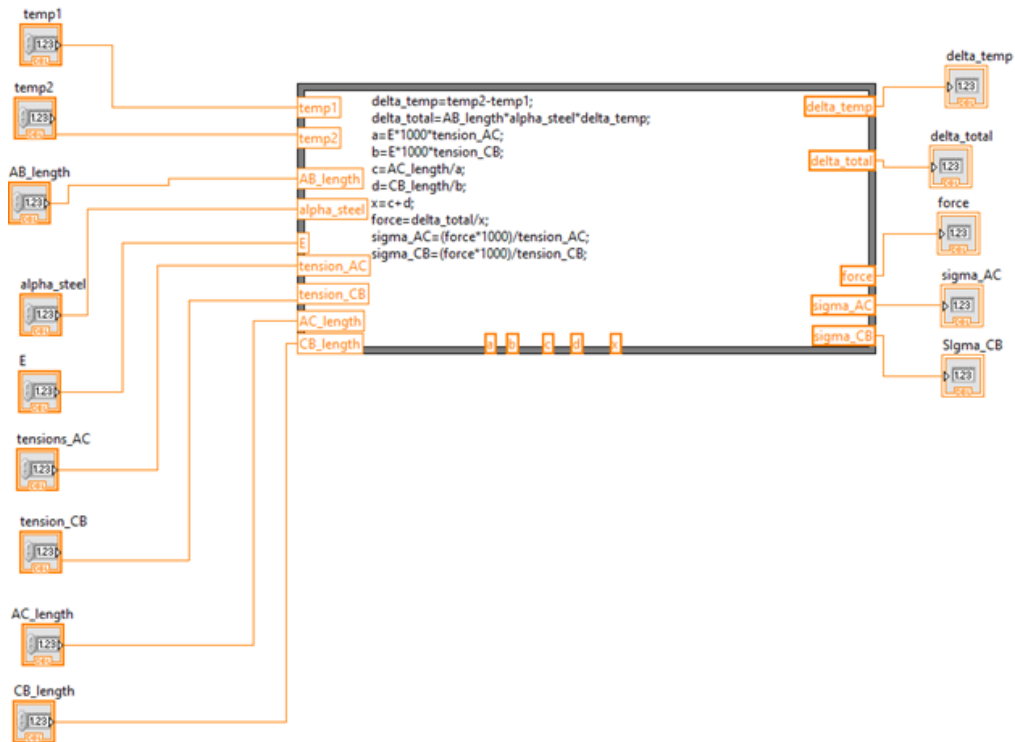


Fig. 2. Formula node containing all equations

4. Adding string elements to display the results

Laboratory 3 – Using the functions for the string data; Using string functions to display the results in a simple-to-read manner, adding a slider to choose between Pa and MPa. We achieve this by using a case function to multiply or divide by 100 for each unit of measure. The program changes the result as the user selects.

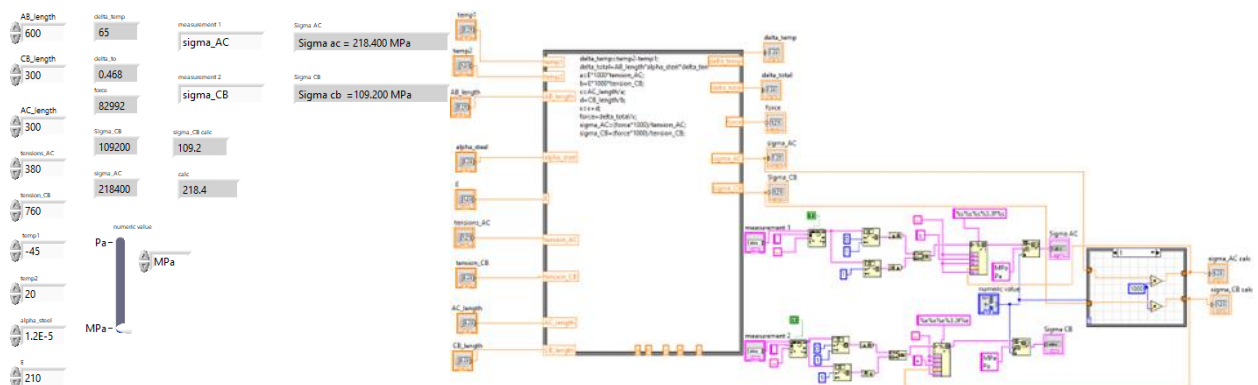


Fig. 3. Organized VI with string type results and case function

5. Using arrays to display the results in a table

Laboratory 4 – Array functions; Using arrays to arrange the values and their names in a simple table. With only two, the table for my problem is small, but the concept is very important for larger scale projects.

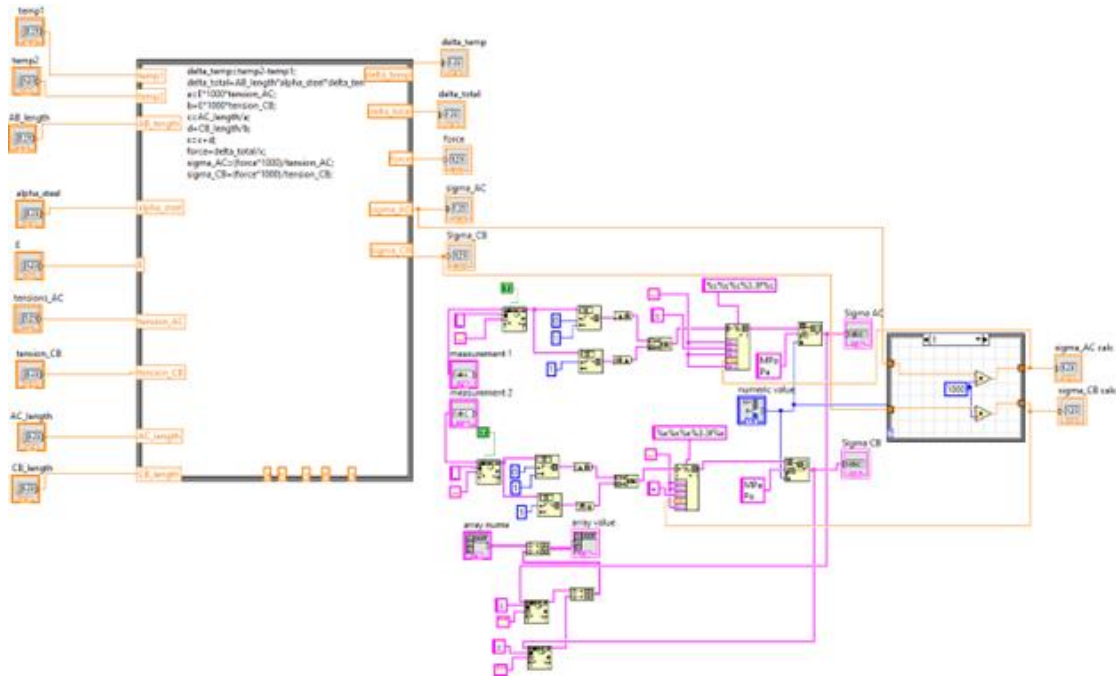


Fig. 4. Current VI with arrays

6. Current state

Finally, we achieve a program able to help us calculate the stresses in steel bars, and display all the results in a neat and clean manner. As for future updates, I plan to add a graph and pictogram of the scheme for the exercise. The graph will be able to plot the drawing using subVIs.

7. Equations

$$\Delta t = T_2 - T_1 \quad (1)$$

$$\delta_T = \sum L_i \alpha_i \Delta t \quad (2)$$

$$-\frac{F \times 300}{210 \times 1000 \times 380} - \frac{F \times 300}{210 \times 1000 \times 760} + 0,468 = 0 \quad (3)$$

$$\sigma_{AC} = \frac{F}{T_{AC}}; \sigma_{CB} = \frac{F}{T_{CB}} \quad (4)$$

Where: (1) Δt is the difference in temperature between T_1 and T_2 ;

(2) δ_T is the total deformation, which is calculated with the sum of lengths, α of steel and Δt ;

(3) F is a sum of forces F_A and F_B , applied at their respective supports;

(4) σ_{AC} is the stress on portion AC, while σ_{CB} is on portion CB; T is the tension on each section;

8. Figures

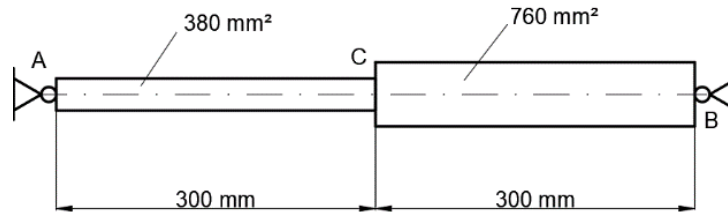


Fig. 5. Steel bar

9. Conclusion

The program aids with calculations of a steel bar similar to the one in the figure, only requiring input of a few values. Such programs can help engineers check buildings for issues.

My program uses formula nodes, string and array functions and a case function to complete a physics exercise in which we have to calculate stresses in two conjoined steel bars, affixed at each end with a simple support.

10. Bibliography

- [1]. Jiga, G.(2014) Strength of Materials, Volume 1, Ed. PRINTECH, București, ISBN 978-606-23-0168-2
- [2]. Savu T., Spânu P., Abaza B.(2014), Reprezentări grafice – îndrumar de laborator, Ed. PRINTECH, București , ISBN 978-606-23-0230-6
- [3]. Savu T., Spânu P., Abaza B.(2014), Algoritmi – îndrumar de laborator, Ed. PRINTECH, București , ISBN 978-606-23-0229-0
- [4]. Savu T., Spânu P., Abaza B.(2018) Bilingual Laboratory Guide (Romanian - English) Computer Programming, Ed. Printech Bucuresti , ISBN 978-606-23-0819-3

RESEARCH ON DESIGNING AND DEVELOPING AN EXPERIMENTAL MODEL OF DEVICE FOR SLICING PRODUCTS IN THE FOOD INDUSTRY

SIMION Maria Mihaela¹, TARBĂ Ioan – Cristian², ENCIU Cornel – Cristian²

¹Faculty of Industrial Engineering and Robotics, Study program: Applied Informatics in Industrial Engineering, Academic year: 4, e-mail mihaela.1899@gmail.com

²Faculty of Industrial Engineering and Robotics, Manufacturing Engineering Department, University POLITEHNICA of Bucharest

ABSTRACT: This scientific paper focuses on developing a device/machine for cutting wheels of cheese. It contains information about some of the existing types of cheese cutting machines, the working principle and the solutions that will be implemented. The machine has to cut cheese wheels in slices with required weight and can be placed in stores, supermarkets and restaurants. Two cameras send the acquired images to a program in which data is collected and the calculations are made. In order to do this the cameras will read the actual diameter and height of the cheese wheel that is placed on the table. Next, the program will determine the volume of the wheel and, knowing the weight that is required, the table will rotate with the angle needed to cut the desired slice.

Keywords: image processing, food industry, slicing

1. Introduction

The subject of this paper is represented by designing and programming of a preferential slicing device of cheese wheels. Currently, the applications used in the food industry field are machines which cut the products only at standard dimensions [1].

The pursued goals are the presentation of the working principle and the development of the algorithm used for the determining the piece which will be sliced and also of the elements that will be improved with future research, starting with the initial obtained results.

In order to develop the product, and the programme that will coordinate the components, Catia V5 R21, and the processing image module of Python were used.



Fig. 1. Cheese slicer RS [2]

Table 1. Actual stadium/stage



Fig. 2. Hard Cheese slicer Rock 13 [3]



Fig. 3. Hendi Profi Line 300 [4]



Fig. 4. Hard Cheese slicer Rock 20 [5]



Fig. 5. Cheese slicer EC14 [6]

2. Working principle

2.1. Logical scheme of the working principle

The series of steps that the product uses is shown in figure 6, as it follows:

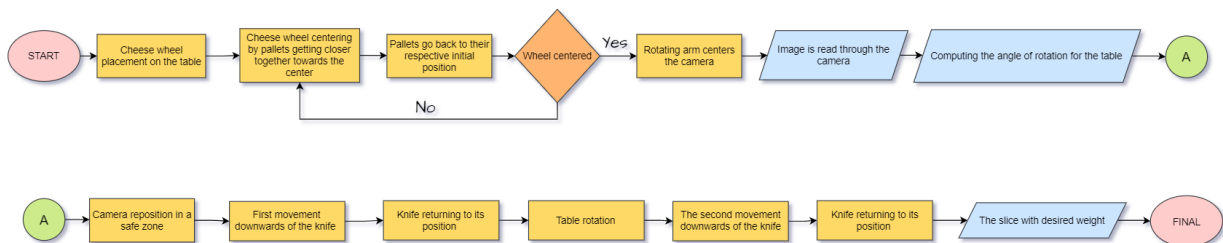


Fig 6. Logical scheme of the operating principle

2.2. The components of the designed device

The equipment has two cameras, the one mounted on the upper cover which will transmit information about the diameter; the other one is placed on the side, therefore will collect images of the wheel profile. After image acquisition, the programme will determine the volume. As the desired quantity is known, the angle of rotation of the table can be computed, such that the final slice will be at the specified weight.

The block diagram of the equipment is presented in figure 7, as follows:

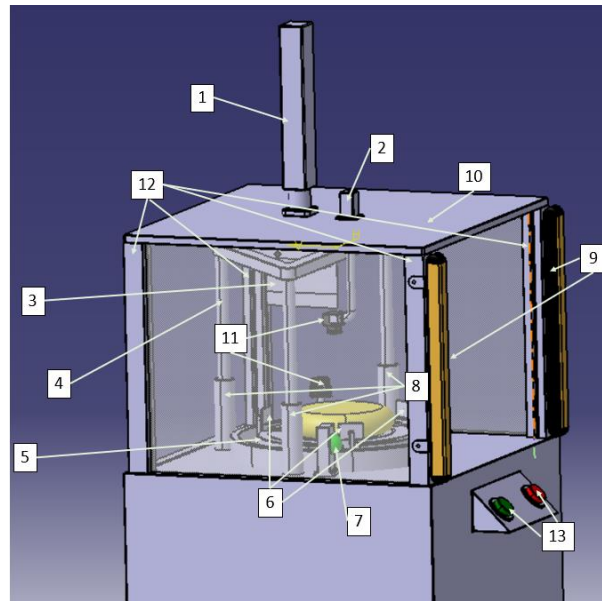


Fig. 7. Block diagram of the equipment

The device components are as follows:

- 1 - Actuator
- 2 - Motor
- 3 - Knife
- 4 - Knife subassembly
- 5 - Rotating table
- 6 - Pallets
- 7 - Led
- 8 - Guiding nuts
- 9 - Protection barriers
- 10 - Lid/Cover
- 11 - Cameras
- 12 - Support bars
- 13 - Start/Stop buttons

3. Identified problems

3.1. The position of the cameras

The cameras must be centred and placed perpendicular to the surface of the cheese wheel in order to determine with precision its dimensions. To ensure this functionality I assembled the cameras on a mobile support. The upper camera is placed on a support controlled by a stepper motor, which has only rotational motion, whereas the other camera is placed on a stand that only has translation motion on the vertical axis, in order to always be positioned in the middle of the distance between the table and the maximum height of the wheel. Because it was necessary that both the camera and the knife to be in the middle, it was chosen a support that has a 90° angle, which is larger than the overall dimension of the knife subassembly, in order to read the diameter of the cheese wheel, without interrupting the image acquisition.

3.2. The calculation of the geometrical parameters

After image acquisition stage, in which the programme reads the effective dimensions, the density of the individual cheese wheel is inputted, followed by the determination of the total volume by computational means. After the volume was found, the operator enters the weight of the desired slice. With these two values, the programme defines the angle where the table should rotate so that at the end of the knife movements, it results the slice with the desired weight. In figure 8, are represented the steps for the volume determination. Initially are represented the views of a cheese wheel (A1 from the side, A2 from the top).

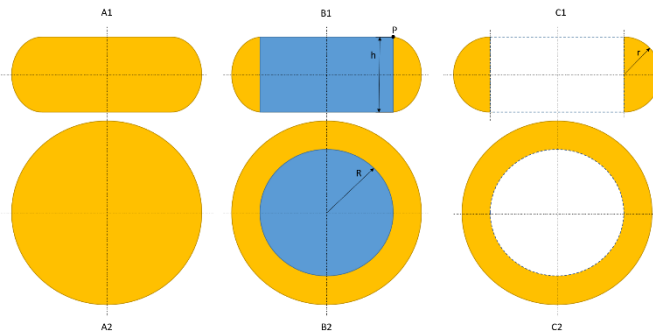


Fig. 8. Steps for the volume determination

In order to determine the volume of a cheese wheel, it can be separated in two volumes easier to calculate: the blue cylinder and half of a torus represented in views C1 and C2 with the colour yellow.

Firstly the volume of the blue cylinder can be calculated with the following formula:

$$V_C = \pi * R^2 * h \quad (1)$$

In figure 9 it is demonstrated the fact that when a torus is unfolded, it is exactly a cylinder. In this case, the height of the cylinder is identical to the length of the circle of diameter R, represented in figure 8.

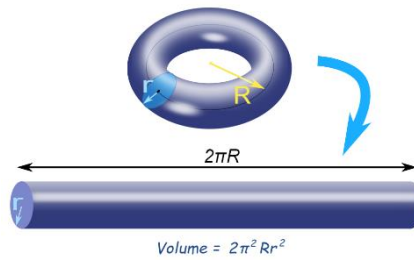


Fig. 9. Volume of a torus [6]

To determine the volume of a torus the following formula is used [7]:

$$V_T = 2 * \pi^2 * R * r^2 \quad (2)$$

For the computation of the zone represented in yellow in figure 8, C1 and C2 views, the volume of the torus will be used and divided in half. Because the volume of the figure that must be identified is half of a cylinder.

$$V_{T/2} = \pi^2 * R * r^2 \quad (3)$$

Finally, to determine the volume of the cheese wheel we need to add the 2 formulas (1) and (3).

$$V_{Total} = \pi * R^2 * h + \pi^2 * R * r^2 \quad (4)$$

3.3. Software development

In order to read the dimensions of the wheel of cheese it is necessary a programme written in Python and integrate them in the formulas earlier mentioned in order to determine the volume.

The logical scheme on which the programme is based is represented in figure 10.

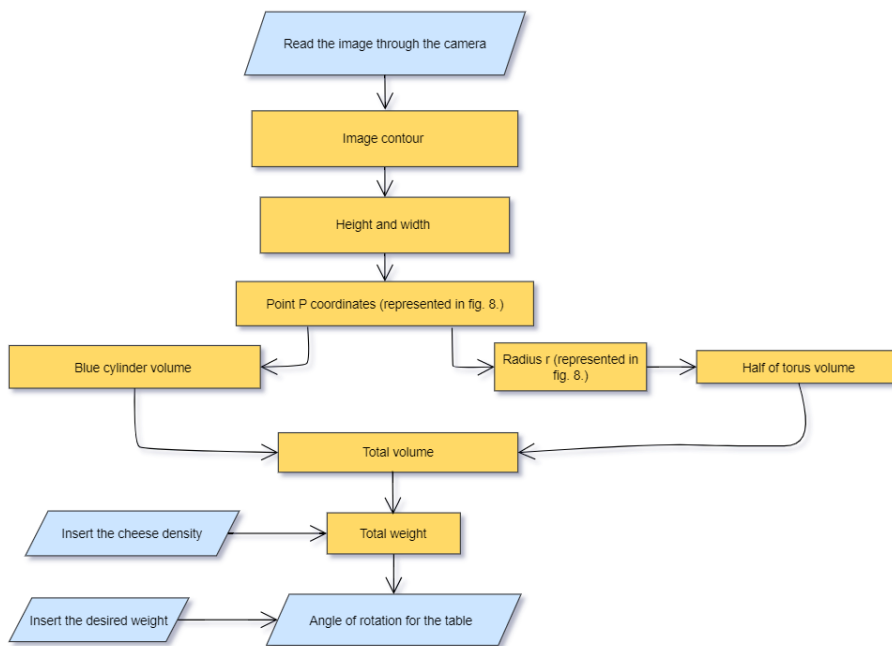


Fig. 10. The logical scheme of the written programme

3.4. The position of the cheese wheel

In order to complete this task, a number of three pallets are needed, which will be actioned by three actuators. These are located in some existing canals in the table support, so that the translation motion be possible. Also, these have the role of centring the cheese wheel, therefore they should be placed equidistantly, at 120°. They have a pressure sensor which determinates the moment when they can start retiring to their initial position.

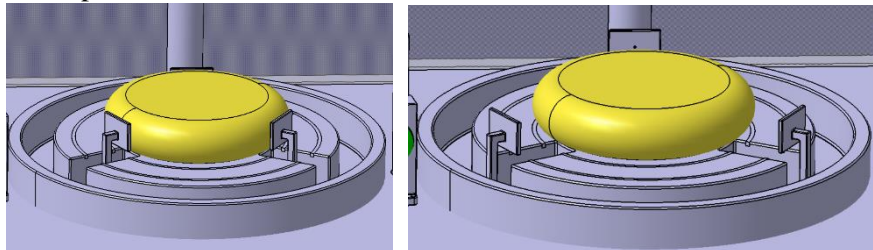


Fig. 11. Centering the cheese wheel

4. Conclusions

Original contributions are represented by the designing the product and having a few optimisation solutions such as cameras positioning or the movement of the knife.

Future research is represented by equipment optimisation so that it can slice a variety of products with different dimensions.

5. Bibliography

- [1]. <https://www.sciencedirect.com/science/article/abs/pii/S0260877419303796> (accessed at date 11.05.2022)
- [2]. <https://www.plevnik.eu/product/cheese-cutting-device-rs/> (accessed at date 21.12.2021)
- [3]. <https://www.directindustry.com/prod/caseartecnica-bartoli/product-86193-1474071.html> (accessed at date 21.12.2021)
- [4]. https://www.emag.ro/feliator-hendi-profi-line-300-420-w-grosime-reglabila-diametru-max-200mm-argintiu210017/pd/D4RS19BBM/?ref=ps&emag_click_id=950d285b2ce9b28a6613ec8c740ddf48&utm_source=bucatariaioanei.ro_affiliate_QSXB&utm_medium=profitshare&utm_campaign=profitshare_QSXB&utm_content=link (accessed at date 21.12.2021)
- [5]. <https://www.directindustry.com/prod/caseartecnica-bartoli/product-86193-1474057.html> (accessed at date 21.12.2021)
- [6]. <https://www.directindustry.com/prod/marchant-schmidt-inc/product-193983-2112539.html> (accessed at date 21.12.2021)
- [7]. <https://www.mathsisfun.com/geometry/torus.html> (accessed at date 07.05.2022)

6. Notations

The following symbols were used in this paper

V_C = volume of the cylinder [mm^3];

V_T = volume of the torus [mm^3]

$V_{T/2}$ = half the volume of the torus [mm^3]

RESEARCH ON THE DESIGNING OF AN ALGORITHM AND CREATING A SOFTWARE APPLICATION FOR A SECURITY SYSTEM BASED ON IOT AND RFID

DOBRE Mihaela Cosmina Daiana¹, TARBĂ Ioan – Cristian²

¹Faculty of Industrial Engineering and Robotics, Study program: Applied Informatics in Industrial Engineering, Academic year: 4, e-mail mihaela.dobre20@yahoo.com

²Faculty of Industrial Engineering and Robotics, Manufacturing Engineering Department, University POLITEHNICA of Bucharest

ABSTRACT: The purpose of the paper is to develop a software application for simulating and testing IoT and RFID systems. The subject studied aims to develop an application with database access to authenticate the users to protect the facility by implementing different security policies. In this paper we have exemplified some ideas about architectures, communication protocols and IoT technologies, designed a smart factory, in which we have connected several IoT devices, which can be remotely controlled using a smartphone or personal computer.

KEYWORDS: IoT, RFID, Firebase, Java, Android Studio.

1. Introduction

The purpose of this work is to develop a software application, a database and an experimental model of access control, the communication being carried out through the Internet. The objective of system is to have access and to monitor the records of the personnel entering or leaving an area where access is intended to be controlled. The way this system is wanted to work is by creating a software application and an experimental model that represents the physical access control system, all of which interact with a database developed specifically through the Firebase utility, a platform developed by Google for creating mobile and web applications.

For the realization of the software application, the Java language will be used in the Android Studio development environment, and for the experimental layout, an ESP32 device will be used, programmed via the Arduino IDE in C++, together with an RFID RC522 card reader.

2. State of art

RFID is one of the main technologies available that has made the Internet of Things (IoT) come to life. It is a wireless technology for automatic identification and data capture. The RFID technology shown in Figure 2 is a booming communication technology in IoT applications. It is based on a wireless technology in which a label is attached to an object, using contactless communication with a radio frequency reading device through a radio link. [1]

RFID is a system in which this object is uniquely identified by transmitting its identity (unique ID) through radio waves to a middleware responsible for data handling. Free of human error, it guarantees the quick and easy collection of information about a product, time, transaction or place. As a wireless communication protocol for active RFID operating in the Industrial Scientific Medical (ISM) tape is DASH7, which is available at world wide level and is suitable for IoT requirements. DASH7 (DA7) is standardized by ISO 18000-7. [2]

3. IoT architectures, communication protocols, and technologies

Objects that we use in everyday life are interconnected, from here we can understand the importance of the Internet of Things (IoT). Given this importance, a flexible architecture for IoT systems needs to be defined. With the advent of IoT, which will connect numerous objects to the Internet, traffic will increase substantially and higher data storage requirements will arise. Such a large network also leads to security and privacy issues [5]. Therefore, the proposed IoT architecture must address various factors such as reliability, quality of service, and scalability.

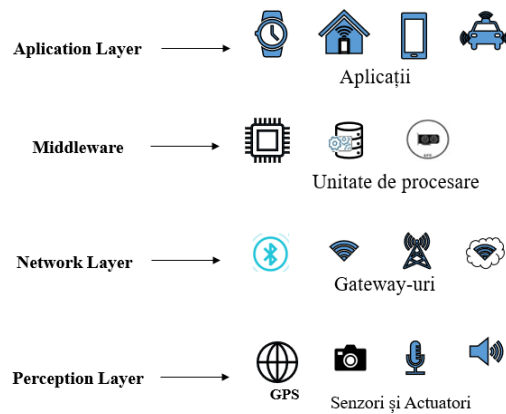


Figure 1 – IoT Architecture

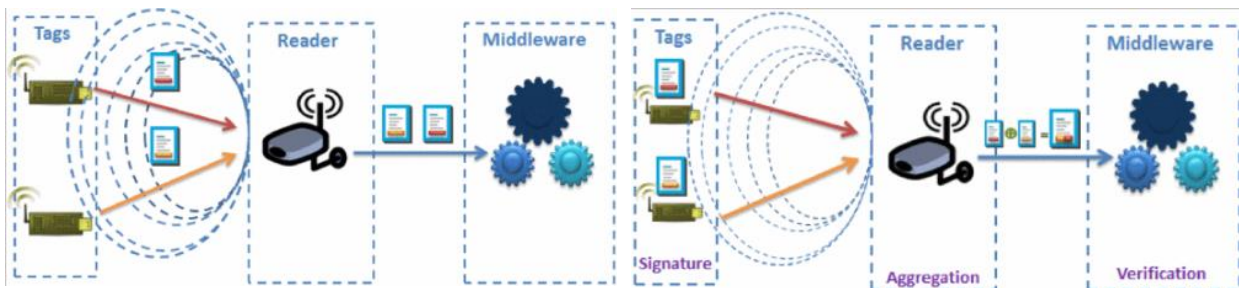


Figure 2 – RFID Architecture [1]

Figure 3 – Secure RFID architecture [1]

Achieving device interconnection requires a communication environment. For example, if a sensor is part of an IoT network, it needs a wired or wireless environment, such as Bluetooth or others, to transmit the data it collects. When it comes to IoT technology, wireless communication is the main focus, and many communication technologies and protocols can be used to connect smart devices, such as Internet Protocol version 6 (IPv6), through low-consumption personal area wireless networks such as: (6LoWPAN), DASH7 (ISO 18000–7 standard), ZigBee, Bluetooth and near field communication (NFC).

- DASH7

The DASH7 Alliance protocol (D7A) is an open standard for two-way, sub-GHz, medium-range wireless communications, adapted for sensor-actuator applications using private networks. The D7A comes from ISO 18000-7 for active RFID and operates in sub-GHz ISM bands. The protocol specification is free to use without any patent or license requirement. [2]

- Radio Frequency Identification (RFID)

As the name Radio Frequency Identification suggests, it is a technique that uniquely identifies objects using radio waves. An RFID system has a label, an antenna, and a reader. Using the antenna, the reader sends a signal to the label to get the unique data, and the label responds with its unique data. The label can be attached to objects, this allows them to be uniquely identified and be part of the IoT network, in this way they can communicate on the network. There are two types of RF tags in the label system, the active label and the passive label. [4]

- ZigBee

ZigBee is a technology that has been created to be able to improve the operation and use of wireless sensor networks (WSN). ZigBee Alliance has been in charge of developing this technology, designed in 1998, standardized in 2003 and revised in 2006. This technology works at frequencies of 868 MHz, 902-928 MHz and 2.4 GHz, has a low cost, is reliable and scalable. It has a low data transmission speed, which can be used within a range of up to 200 meters and can even use 128-bit AES encryption. ZigBee is developed on the IEEE 802.15.4 standard that obtained approval in 2003. The protocol allows devices to communicate in a variety of network topologies with low power consumption, which helps to increase the autonomy of equipment using the technology. This protocol is used in areas such as industrial automation, home automation, smart metering and metering, etc. [3]



Figure 4 – ZigBee Protocol Stack

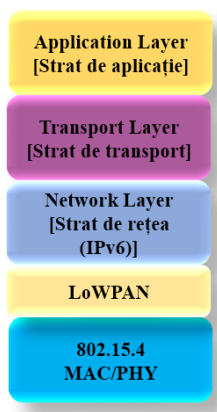


Figure 5 – 6LoWPAN Protocol Stack

- 6LoWPAN

6LoWPAN is the first and most commonly used standard in IoT communication protocols because it is a standard IP-based interconnection protocol. It can be connected directly to another IP network without intermediate entities such as translation gateways or proxy. This standard was created by the Internet Engineering Task Force (IETF), a standard Internet protocol (IP) communication over low-power

IEEE802.15.4 wireless networks that use IPv6. This is aimed at accepting addresses (IPv6) of different lengths. It is also a low cost, a low energy consumption with bandwidth. 6LoWPAN supports different types of topologies, such as mesh and star topology. 6LoWPAN proposes an adaptation layer between the MAC and network level (IPv6) to manage the interoperability between IEEE 802.15.4 and IPv6. The most competitive alternative to 6LoWPAN is ZigBee, as seen in Figure 4 . Both use the same IEEE 802.15.4 protocol at the physical level.

4. Designing a smart factory using IoT and Wi-Fi technologies

IoT and Wireless Sensor Network (WSN) technologies can be used to deploy a smart home over Wi-Fi. Through IoT, all home devices can be connected to the Internet via Wi-Fi, so they can be monitored remotely. Sensor and device grouping technology in WSN technology detects and collects data from different parts of the smart factory, and this information is sent to a central location. In this section of the article, a simulation is designed using the software "Cisco Packet Tracer 8.0" that simulates various devices and sensors to implement security and control functions of a smart factory. Cisco Packet Tracer is a visual simulation tool designed by Cisco Systems that allows users to create network topologies and imitate modern computer networks. [6] The proposed system can control and monitor various devices and devices using a "Smartphone" or a personal computer. Cisco Packet Tracer offers a variety of smart devices and objects that can be configured and programmed. The personal wireless gateway router has been used to connect all devices and components over the Wi-Fi network using the IEEE 802.11 standard. The devices were registered on the network by assigning an IP address. On the router, encryption protocols can be configured to protect the wireless connection such as Wired Equivalent Privacy (WEP), Wi-Fi Protect Access – Pre-Shared-Key (WPA – PSK), WPA2, as we can see in Figure.6.

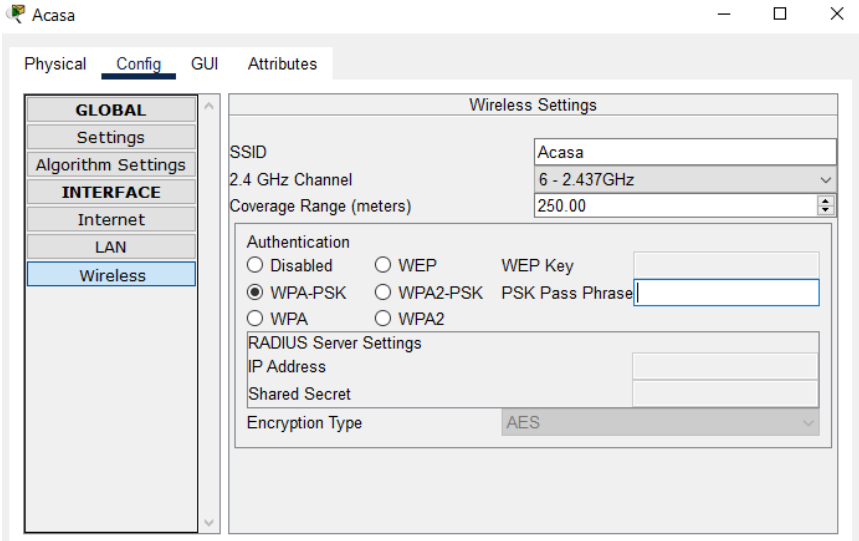


Figure 6 – Home router configuration page.

Figure 7 shows the components and the sensor. The router is connected to the devices via wireless and wired network connection. Different devices can be controlled and monitored, connecting them to the same wireless network. A laptop, an alarm, 2 cameras, a fan, a gas sensor, 5 doors and an RFID reader are connected to the gateway router.

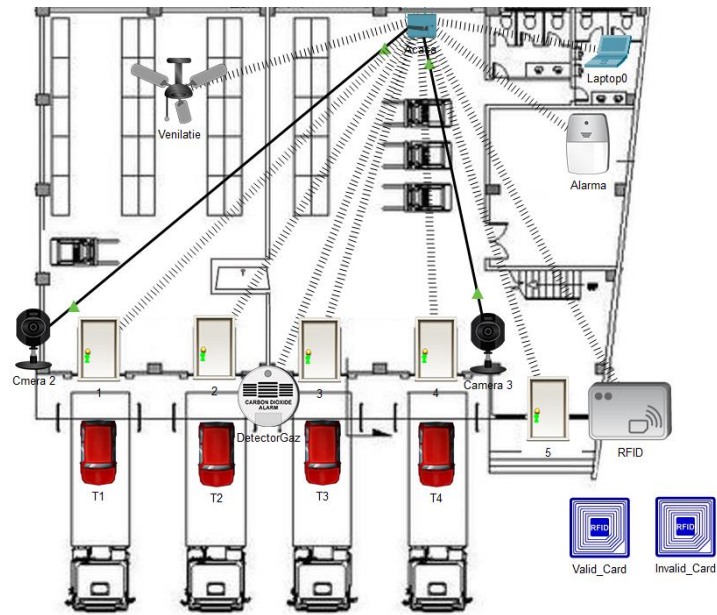


Figure 7 – "Smart" components connected to the home gateway

5. Conclusions

In this paper, the concept of the "Internet of Things (IoT) was generally presented, which contains architectures, existing technologies, their usefulness, as well as the main challenges of the IoT field. A simulation of the security of a smart factory was conducted in the Cisco Packet Tracer program to understand IoT concepts and how they work. In terms of future development directions, I want to address the technological and social issues that prohibit RFID technology from enabling IoT and meeting ubiquitous computing expectations. With the EPC standard, an adaptive and scalable security scheme will be created that offers new cryptographic suites, while wanting to implement certain security policies. I consider a technical security solution that can present a promising solution for RFID-based IoT applications.

6. Bibliography

- [1] Marwa Chamekh and Mohamed Hamdi and Sadok El Asmi and Tai-Hoon Kim (2018) "Security of RFID Based Internet of Things Applications: Requirements and Open Issues", IEEE Publishing House, Conference name "2018 15th International Multi-Conference on Systems, Signals & Devices (SSD)", Oraş Yasmine Hammamet, Tunisia, Date 19-22 March 2018, ISBN 978-1-5386-5305-0. URL:<https://ieeexplore-ieee-org.am.e-information.ro/document/8570558/figures#figures>
- [2] <https://www.dash7-alliance.org/>
- [3] [https://en.wikipedia.org/wiki/Zigbee#Zigbee Alliance](https://en.wikipedia.org/wiki/Zigbee#Zigbee_Alliance)
- [4] Muhammad Junaid, Munam Ali Shah, Imran Abbas Satti "A survey of internet of things, enabling technologies and protocols", 2017 23rd International Conference on Automation and Computing (ICAC), 26 October 2016, ISBN: 978-0-7017-0260-1 at URL:<https://ieeexplore.ieee.org/document/8082058>; I PUT IT AT 5
- [5] Eleonora Borgia, Danielo G. Gomes, Brent Lagesse, Rodger Lea, Daniele Puccinelli, "Editorial Special Issue on Internet of Things: Research challenges and Solutions", Computer Communications, Volumes 89–90, 1 September 2016;
- [6] Kriti Chopra, Kunal Gupta, Annu Lambora "Future Internet: The Internet of Things- A Literature Review", 10 October 2019, ISBN: 978-1-7281-0211-5;

BUILDING A CNC POLYSTYRENE CUTTING MACHINE

Gabriel BIRDA¹, Adrian-Florin BÎRLEANU¹ and Ileana DUGĂEȘESCU²

¹Faculty of Industrial Engineering and Robotics, Specialization: Industrial Engineering,
Year of study: II-Master, e-mail: gabriel.birda@stud.fiir.upb.ro

²Faculty of Industrial Engineering and Robotics, Manufacturing Engineering Department, University
POLITEHNICA of Bucharest

ABSTRACT: Cutting polystyrene shapes using a heated wire, is a method widely used in making mounds, volumetric letter cut-outs or 3D shapes. In order to reach a very good quality and precision of the cut in polystyrene, it is necessary to take into account parameters that can vary depending on the cutting speed, working environment, amperage introduced in the heated wire.

This paper shows how to build a CNC machine that cuts with nickel wire. This machine has 4 working axes (two vertical axes and two longitudinal axes). The aim of the research is to build an automatic and autonomous polystyrene cutting machine.

The machine control system uses an Arduino mega 2560 microcontroller. The cutting process is performed by sending the G code file through a serial USB or by loading the code on a SD card, the machine has the autonomy to work without the use of a computer. After sending the code by the microcontroller, it activates the stepper motors.

1. Introduction

Thermal cutting of polystyrene is the process of removing material by following a path dictated by a drawing or code, it is often used in modeling or sculpting by bringing polystyrene to desired shapes and sizes. Passing a current through a wire or a metal surface generates heat. The width of the cut and the finish of a surface are determined by the feed rate, the electrical power assigned to the heated wire, and the characteristics and properties of the material to be cut. Cutting with heated wire is aimed at making any cut to almost any length with low cutting forces and high cutting speeds. This type of cutting can also be used in 3D polystyrene carving, as the flexibility of the wire is high.

Cutting with heated wire improves the process as well as the cutting techniques, thus reducing manufacturing costs and time.

The use of heated wire can be found in a variety of fields such as construction, aerospace, medical, artistic.

The objectives of this research include:

-Constructing/calibrating/testing a CNC to put cutting into practice.

The following sections are mainly aimed at familiarizing the reader with the design processes, 3D printing using a 3D printer as well as mechanical assembly of elements.

Also, in this research will be found calculations about the current used to control the stepper motor drivers, calculations for the current in the nickel wire.

Identifying and controlling the cutting parameters are considered as the main factors affecting the product quality. The controlling should be precisely done to move the hot wire in the correct path. [1]

2. Current status

This research work has reached the stage of mechanical assembly and calibration of the axes, in the pictures below you can see the design using the specialized Solidworks software as well as the implementation of the design.

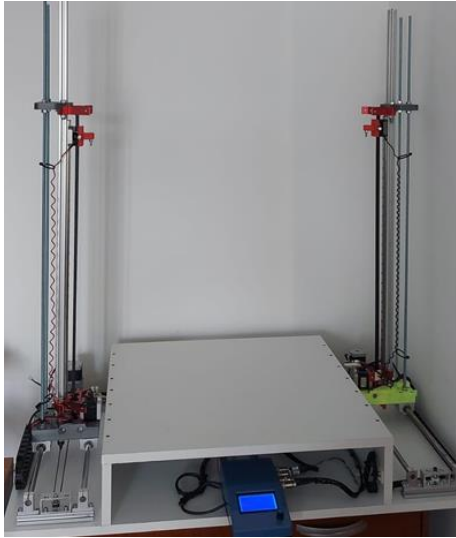


Fig.1 Current state of prototyping

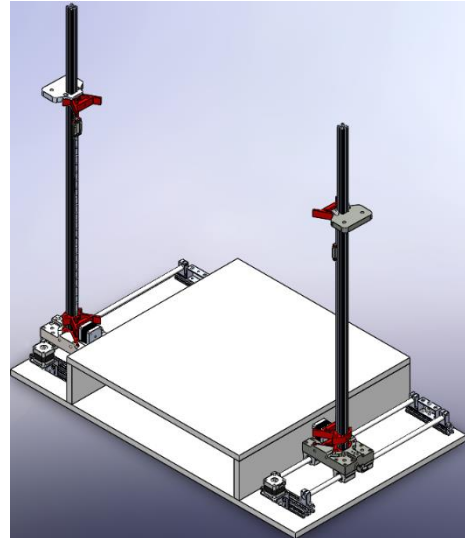


Fig.2 Current design status

The prototype is ready to move both vertically and horizontally.

In the following chapters I will detail how to design, 3D print, assemble, and program the prototype.

2.1 Design of the CNC foam

The picture below shows the cnc design, detailing of component parts is done during the research process

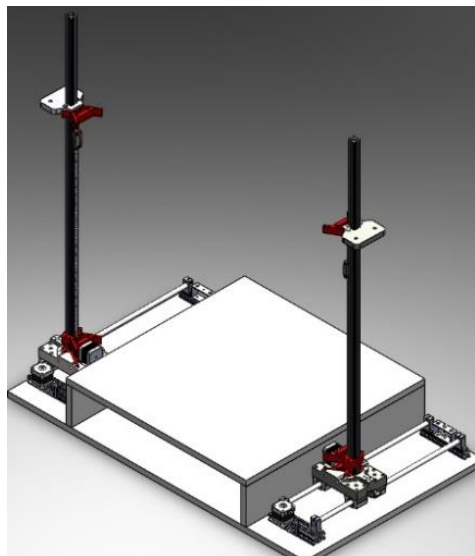


Fig.3 CNC Foam Design Assembly

2.2 Mechanical Design

The designed elements are shown in the figures below:

The parts were designed in Solidworks, their prototyping was done by 3D printing.

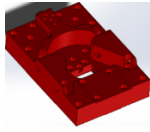


Fig.4 Movement support

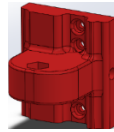


Fig.5 Nickel wire support

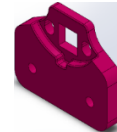


Fig.6 Structure reinforcement support

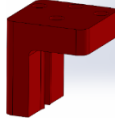


Fig.7 Belt fixing piece

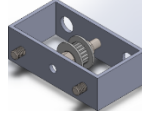


Fig.8 Flares assembly

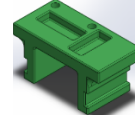


Fig.9 Stroke limiter support

2.3 3D printing and Parameterization

The figures below show the printed elements and a number of parameters used.

In table 1 you can see the parts generated in the Cura program as well as the parts printed using the Delta 3D printer, the material used is PLA.

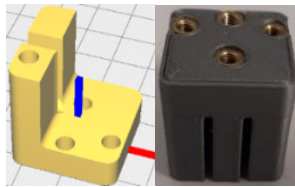


Fig.10 Belt fixing piece

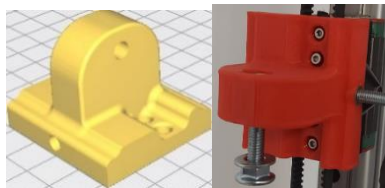


Fig. 11 Wire clamp

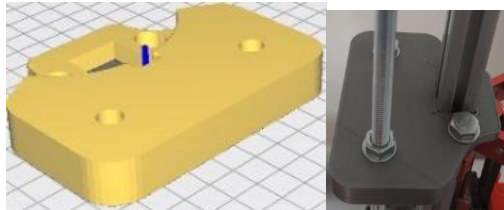


Fig.12 Reinforcement element

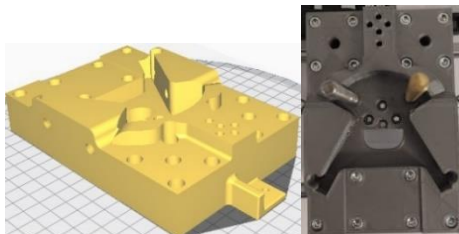


Fig.14 Elements of Cure and Print 3D

Table 1

Profile	Normal 0.2
Layer Height	0.2
Wall Thickness	2
Infill Density	80%
Infill Pattern	Octet
Printing Temperature	200
Print Speed	70
Support pattern	Triangles
Estimated print time	1h
Material usage	11g/3,68m
Profile	Normal 0.2
Layer Height	0.2
Wall Thickness	2
Infill Density	80%
Infill Pattern	Octet
Printing Temperature	200
Print Speed	70
Support pattern	Triangles
Estimated print time	2h
Material usage	21g/7m
Profile	Extra Fast 0.3
Layer Height	0.2
Wall Thickness	1
Infill Density	75%
Infill Pattern	Cross 3D
Printing Temperature	200
Print Speed	80
Support pattern	Triangles
Estimated print time	6h
Material usage	68g/23m
Profile	Extra Fast 0.3
Layer Height	0.3
Wall Thickness	1
Infill Density	75%
Infill Pattern	Cross 3D
Printing Temperature	200
Print Speed	80
Support pattern	Triangles
Estimated print time	16h
Material usage	281g/100m

3. Assembly and design optimization

In the pictures below you can see 2 sets of prototypes, below is the explanation:



Fig. 15 First prototyping

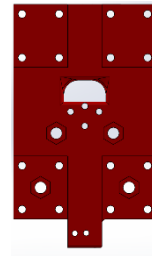


Fig.16 Optimizing design

Explanation

In fig.15 you can see the first prototyping attempt, we encountered the following problems :

-After assembly, on each longitudinal guide there was only one slide, the assembly being in translational motion, was in a constant unbalance, because the 2020 profile is high and forms the arm of the force that is applied in the 2 longitudinal bearings.

In fig. 16 you can see an improvement of the construction, I chose to mount 2 bearings on each longitudinal guide, as well as reinforcing the structure by inserting 2 M8 threaded rods which are meant to support and dampen shocks and vibrations.

For assembly we followed the following steps

Step 1: Assembly Stand

The prototyping station is made of sheet metal, its assembly is done using screws.

In the picture below you can see the designed stand as well as the necessary parts.



Fig.17 Designed stand

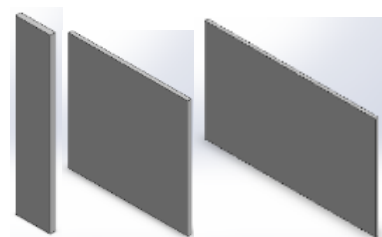


Fig.18 Elements for the stand

Step 2: Making the practical stand

The stand made of Pal is in the picture below:

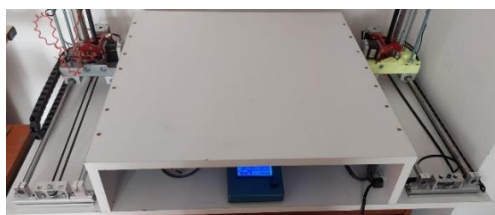


Fig.19 The stand made of PAL

Step 3: Toothed wheel bearing brackets

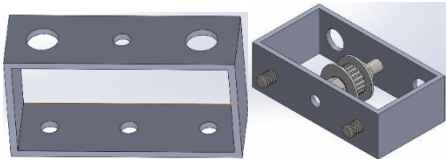


Fig.20 Toothed wheel support

The bracket is used for mounting and securing the Gt2

It is made of aluminum and has an M5 thread for threading the screw.

Step 4: Making a movement sled



Fig.21 Sled carcass order

The mobile sled aims at easing the control of the machine, it executes a movement similar to a drawer, and allows accessibility to the lcd.

Step 5: Mechanical assembly

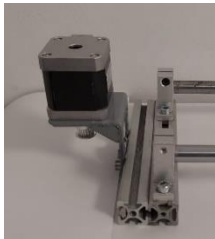


Fig.22 Assembling the motor to the bracket

The motor mount has been designed in steel; it has an internal clearance to allow the belt to move easily.

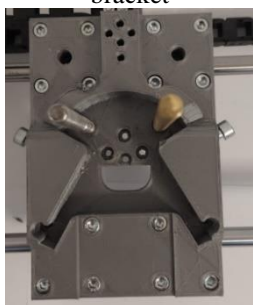


Fig.23 Movement support

The support for longitudinal movement is 3D printed and is designed to support the runners, the 2020 profile and to allow a movement of the Mgn12H linear guide moving vertical parts.

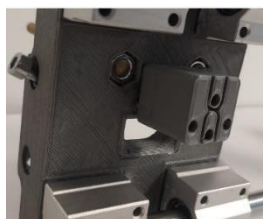


Fig.24 Belt fastening

The belt fastener is 3D printed it has M4 threaded inserts attached which are hot inserted

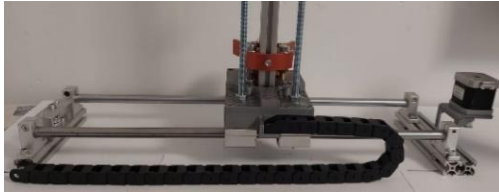


Fig.25 Final assembly

The final assembly is detailed in the picture below, it has a cable carrier chain, linear guides, the parts listed above as well as 2020 profiles that serve as legs.

Vertical and horizontal movement is provided by Gt2 belts.

The assembly of the elements is done manually

4. Driver calibration

For accuracy and safety in use, the following calibration steps are used:

Step 1

Resistance check

Drv8825 uses a resistance of 0.068Ω



Fig.26 Ramps 1.4

Step 2

Identify parameters:

Rated motor current: 1.68 A

Minimum operating voltage: 8 V

Internal resistance (R_{sense}): 0.05Ω

Operation in a 10% safety zone

$V_{ref} = 0.6$

$$V_{ref} = \text{rated}_{current} * \text{Minimum}_{voltage} * \text{Internal}_{resistance} \quad (1)$$

The calculation shown for driver calibration is below:

$$V_{ref} = 1.68 * 8 * 0.05 = 0.672V \quad (2)$$

Step 3

Measure the voltage value using a multimeter.

Set the multimeter to the DC voltage measurement scale (Vcc).

Check if the Ramps 1.4 board is powered from an external current source.



Fig.27 DC voltage measurement

Step 4

Set the potentiometer to the value of $V_{ref} = 0.6$

A value higher than 0.6V will cause the Drv8825 driver to heat up.

The motor may heat up and the motor torque decreases

Potentiometer adjustment is done by turning the potentiometer trigonometrically, the value of the V_{REF} voltage will decrease, and by turning the potentiometer clockwise, the value of the V_{REF} voltage will increase.

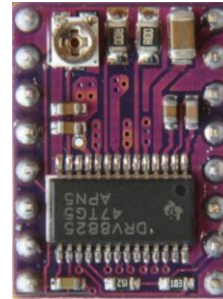


Fig.28 Driver Drv8825

4.1 Useful calculations:

$$Axle_{spur\ wheel} = \frac{Number\ of\ teeth * steps}{2 * \pi} \quad (3)$$

The number of teeth used for the gearwheel is 20 teeth. The pitch is the distance between 2 teeth, this distance is 2 mm for the GT2 gearwheel.



Fig.29 GT2 Pulley

Detailing and calculating relationships

$$Axle_{spur\ wheel} = \frac{20 * 2}{2 * \pi} = 6.36\ mm \quad (4)$$

Formula for complete rotation:

$$Complete_{Ratio} = Number\ of\ teeth * steps \quad (5)$$

Calculated ratio:

$$Complete_{Ratio} = 20 * 2\ mm = 40\ mm \quad (6)$$

4.2 Elements used, making the control housing

Below are detailed the elements used in the construction of the CNC:



Fig.30 Case

The casing is recovered from an older printer, it has undergone some modifications such as: Hole punching for the insertion of couplers, interior modifications, as well as adaptation for the



Fig.31 Control elements

Arduino mega 2560 programming board.

The component parts for programming are:

- Arduino mega 2560
- Ramps 1.4
- Driver Drv8825
- Lcd



Fig.32 Stepper motor NEMA 17

A stepper motor is a common component in the construction of cnc 3d printers, lasers or cnc routers.

An important criterium in choosing a stepper motor is the motor torque.

Torque = force x distance

5. Conclusions and further objectives

Design and physical execution are synchronized.

3D printing was a defining factor in this work as most of the parts were made using this process.

The research is ongoing, cutting polystyrene with heated wire is a way of prototyping and executing different shapes from polystyrene.

So far, the research has reached the assembly and calibration plan, below you can see the further goals I want to go through

- CNC parameterization and programming
- Testing
- Temperature variation in current
- Temperature variation during cutting
- Temperature variation in relation to wire length
- Temperature variation as a function of cutting distance
- Variation of cutting width in relation to feed speed

6. Bibliography

[1]. https://www.researchgate.net/publication/303688329_Development_of_a_numerically_controlled_hot_wire_foam_cutting_machine_for_wing_mould_construction.

[2] Isermann, R.: Information Processing for Mechatronic Systems, Robotics and Autonomous Systems, 19 (1996), pp.117-134

[3] https://ro.wikipedia.org/wiki/Programarea_mașinilor-unelte_cu_comandă_numerică

[4] Patrick M., Friction and Lubrication in Metal Rolling, Ph. D. Thesis, Cambridge university,

[5] Linear Guideway, AMT Precision Motion Industries Inc., Taiwan, 2005, p. 6;

DEVELOPMENT OF AN AUTOMATIC GUIDED CHASSIS

BANU George-Sebastian¹, PĂUN Andreea-Alina¹, DRĂGAN Silviu-Daniel¹,
POPONETE Ștefan-Mădalin¹, ABAZA Bogdan Felician²,
SPIROIU Marius Adrian³ and DIJMARESCU Manuela-Roxana²

¹Faculty: Industrial Engineering and Robotics, Study program: Engineering and Management of Complex Projects,
Year of study: 2, e-mail: banu_george25@yahoo.com

²Faculty of Industrial Engineering and Robotics, Manufacturing Engineering Department

³Faculty of Transports, Railway Vehicles Department, University POLITEHNICA of Bucharest

ABSTRACT: Studying and implementing the latest technologies on the market is a priority for many companies, given the benefits that new technologies offer. The current trend of flexibly automating the production process comes in direct response to market demand. to be able to offer a wide range of products, manufactured in different time regimes, in different batches, with different particularities. Most of the time, the time and quality of the production process study of feasibility to be able to identify its degree of applicability.

KEYWORDS: Industry 4.0, automation, robots

1. Introduction

Industry 4.0 is constantly evolving, so the goal of this research is to automate the transportation process with the help of an AGV robot. The development direction of the research is the development of a chassis with optimal control, which will minimize costs and be able to withstand high demands and withstand the external environment. The flexibility of automatically guided robots is their ability to move in certain directions at certain speeds. A very important aspect in the operation of these robots is not only the actual transport of materials but also the way they transfer and pick up transported objects. The loading and unloading of the robot with materials is done automatically, while the operator can handle the processing of parts on production lines.

Taking all this into account, we can see that the automation of a process requires attention special analysis, an analysis of the current situation in which automation is desired and then, data analysis, identifying how automation can or cannot be implemented.

2. Business strategy

In order to understand what the customer wants and how these desires are reflected in the characteristics / functions of the new product, research was conducted on the analysis of the needs. For this, a questionnaire was applied for a sample of 50 companies with various fields of activity. The reference data in the following table have

Table 1. Need analysis

Willingness expressed	Parameter	Value
I want it to be resilient	Material	Aluminium
I want it to have great battery life	Autonomy	12V-40Ah
I want it to charge quickly and easily.	Charging time	2-3 h
I want it to have a preset route	Number of routs	2-3
I want to be able to order it from my phone	Planificare traseu	1-2 min
I want to increase my work speed	Speed	2 m/s
Identifying and circumventing obstacles	Device with sensor	2 m
To have a small overall size	L x l	max.608 x 312 mm

Once the user's expectations of the product were set, a clear picture of the market in which the product was to be launched followed. This was done by studying the range of AGVs currently on the market, by the manufacturers of AGVs and by defining the target customer for our product presented below [5-7]:

1. Field of activity: Storage companies, sorting of components and products, consumer goods
2. Possibly interested markets: EMAG, UNILEVER, NESTLE, FAN COURIER, DECHATLON, IKEA
3. Number of employees in charge of transport: 1-5
4. Decision makers price, product quality, credibility, service.
5. Desires: adaptable product, from fragile load to Heavy-duty,
6. The reason why you buy to increase productivity and reduce costs;
7. Possible purchase objections: maximum load.

3. Functional analysis

Through the functional analysis, a research was carried out on the functions that must be performed fulfill the product. These were characterized and subsequently ranked according to the degree of importance.

- FPI-To support and transport objects,
- FCO-Self-guided,
- FCI-To adapt to various work surfaces. external,
- FC2-To be resistant to the environment
- FC3-To be esthetic
- FC4-To allow storage in confined spaces,
- FCS-To abide by the rules and regulations.
- FC6-To adapt to the charging source,
- FC7-To be harmless with objects

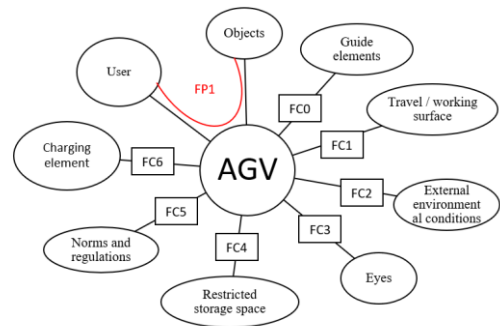


Fig. 1. The relationship of the system with the environmental elements

Based on the interactions of the system with the elements of the external environment for the life phase it was realized functional analysis presented in table 1, where one can observe a main function and seven functions constraints for which the target level and their flexibility were analyzed [14].

Tabel 1. Functional analysis

Function	Targetlevel	Flexibility
FP1	Max 100 kg	Imperativ
FC0	Independent	Imperativ
FC1	Adaptable	Impertiv
FC2	To be airtight	Mandatory
FC3	Product shape	Intermediate
FC4	Product size	Mandatory
FC5	100%	Imperativ
FC6	Adaptable	Mandatory
FC7	Seating surface	Imperativ

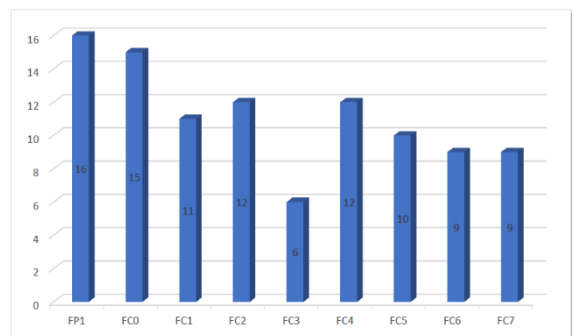


Fig. 2 Diagram

The functional analysis functions have been defined to be implemented on the new concept. The functions of "supporting and transporting objects" "and guiding oneself" turned out to be the most important. Analyzing the period of time that the product spends on the market, a life cycle for the proposed product was made and all the use scenarios that it has been analyzed.

Analyzing the time period that the product spends on the market a life cycle was achieved for the proposed product and all possible usage scenarios have been analyzed.

4. Concept development

To ensure the loading and unloading of loads that the AGV carries were developed more concepts. Only 2 of the 7 developed concepts are presented in this research [6].

The first concept in Fig. 2 is the use of roller transfer devices. For this purpose, the vehicle and the fixed structure of the unloading loading station shall provide roller horses. When unloading, the rollers are actuated on the vehicle. The friction force between the blade and the rollers pushes the blade on the roller track of the fixed station. When loading, proceed in reverse, operating the rollers of the horse in the fixed position. It must therefore be possible to operate both the rollers on the vehicle and those on the fixed station.

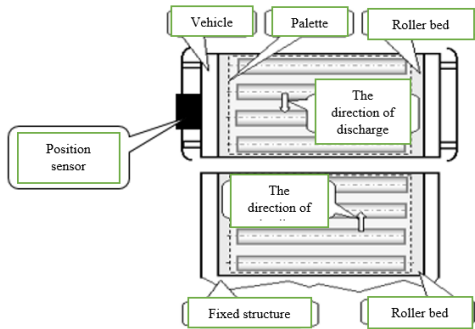


Fig. 3 Roller platform

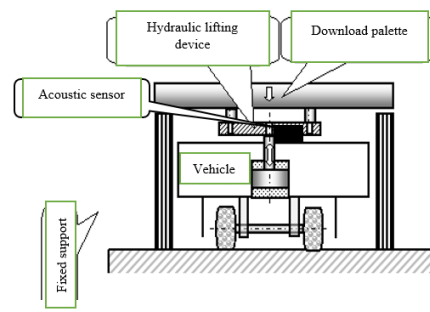


Fig. 4 Lifting platform

The following concept in Fig. 4. is equipped with a self-actuating lifting device. The load is supported by the support pads of the lifting device. After stopping the vehicle in the unloading-loading station, the lifting device lowers the load on the support of the fixed structure, after which the unloaded vehicle leaves the station. When loading the empty vehicle stops in the station, the buffers of the lifting device skip the load, then the loaded vehicle leaves the station. In this chapter two concepts have been specified. These were made taking into account the functions of the functional analysis and the customer's need expressed by the product request, identified in the chapter previous The concept to be developed in the following chapters is the lifting platform because they meet the required criteria, namely the cost and the workload.

5. Development of technical solution and prototyping

The developed product was designed to meet the functional analysis required for the development of technical solutions. It is divided into three subsystems, namely, the mechanical, electrical and software subsystem. They are represented in the following figures in the order of the constructive evolution of the product and in figure 5 is presented the unloading-loading position. [1], [2]. [3]

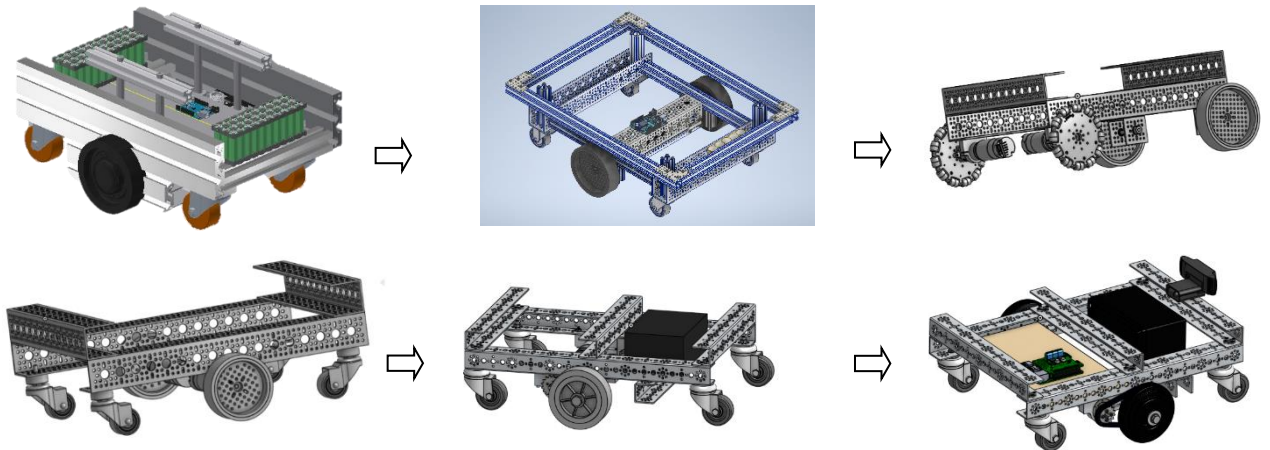


Fig. 5. The soft design developing of AGV prototype iterations

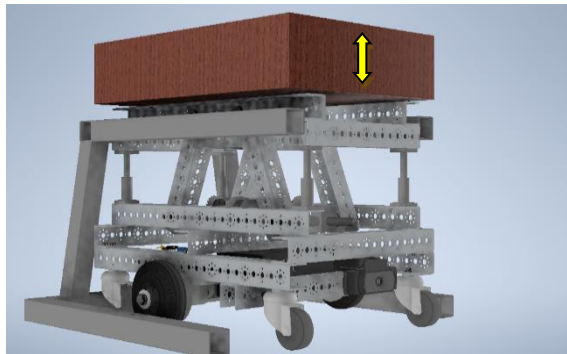


Fig. 6 AGV prototype with lifting and unloading mechanism with electric and mechanical actuation on the U platform

The first stage was the construction of the metal shaft: For a low weight but also a good resistance to the demands of the chassis, it was decided to use U-type profiles that have the dimensions of 32 x 32 mm and the thickness of the material of 2 mm of aluminum. therefore, the redesign of the chassis was necessary to be able to carry a mass of maximum 100 Kg. The new design being more compact and easier to assemble.



Fig. 7 Switching from wheel locations directly on the drive shaft to the use of a gear and chain gear

The power supply for the motors and electronic components is given by a 12 V NiMh type battery and 3000 mAh initially located in the back of the AGV.

The solution by which the maximum load mass of 100 Kg will be reached during transport according to the product specifications, is by using a wheel axle with a diameter larger than the original one of 6 mm. need and use of flange bearing bearings The bearing was obtained by printing with PLA and a density of 100% for a very good resistance to compression and pressing of bearings in bores

For the drive of the wheels was introduced as a whole a sprocket with z-14 driven by an electric motor with a torque of 2.47 Nm. The torque given by the motor is amplified by the reduction created with the second sprocket which has z-32. Thus, moving with a higher mass load will be more efficient. Along with the use of drive wheels with a diameter of 100 mm, the pivoting wheels that can be required up to 50 Kgf each have also been replaced. The diameter of the rollers is 50 mm. The location of the wheel pivot has been shifted so that the radius of rotation of the roller does not protrude beyond the chassis to avoid accidents during use. The location of the battery in the central part of the chassis for a better agility in corners was necessary. This positioning had the advantages of smaller connectors but that came with another problem, namely how it will be powered or how it will change since it is under the chassy in the central part. The solution is to recharge it through a connector.

Another component that is important in product development and helps with functionality is the program through which the robot operates. It is written in the memory of the raspberry pi 4 8 GB card from component of the machine, using the Baleno program and is in the form of Python code.

Also, the module Pololu engine control is installed on the board. The subsystem located at the top has the function of loading and unloading products. By operating the electric motors and rotating the threaded shafts the 4 connecting rods change their angle, so the mechanism produces the translation of the platform on the axis za of the structure. During the unloading of the products the mechanism is raised so that it can enter the unloading area and by lowering the product will result in a placement on the flat surface of the U-type platform, the loading being the opposite of this operation.

After the physical realization of the chassis, a deformation analysis was performed by using the 3D Inventor professional design software and more precisely the analysis menu (Analysis) had as first step the updating of the 3D drawing in its last form. have a structural role in the analysis by placing a weight in the upper part of the chassis being the loading area. The rest of the electronic components and support of the electric motor, including the motor, were extracted from the analysis drawing in order to simplify both visually and in terms of processing the results, finally obtaining a shorter charging time. To this simplification I later added pin type contacts in the places where the fixing is done with screws for the same reasons. 10 kgf Thus we obtained on the one hand a confirmation of the appropriate location of the contacts and constraints but also a result of the analysis in which it can be seen that the aluminum profiles were not subjected to cold plastic deformation confirmed by safety coefficient with higher scale value [7]. [10]

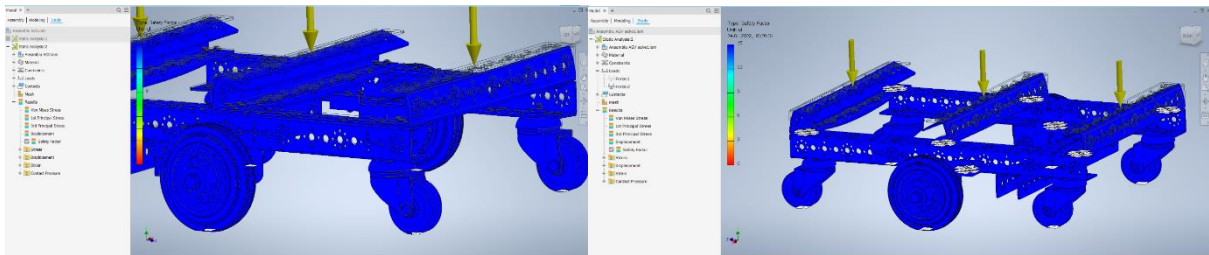


Fig. 8 Selection of parameters and surfaces to be subjected to deformation analysis

In the following test a higher value close to the one proposed in the specifications of the AGV type robot was used, namely 90 Kgf. After obtaining the results, it was found that in this variant the safety factor is somewhere on the scale of number 2, so deformations appear at the level of the profiles, the bottom contact surface pushed inwards.

Logically, this situation is not the real one because the assembly does not contain the loading surface represented in reality by a sheet metal strip of a certain thickness. This would have a greater influence on the deformation of the profiles being a factor that increases the rigidity of the assembly. In order to verify this hypothesis, the component that represents the loading surface but at a considerably smaller thickness was introduced in the analysis, as it is represented by a plan. Thus, the analysis of the structure became more plausible by the fact that the respective sheet raised the safety coefficient in the evening to a value of over 3.74 and the profiles did not deform excessively inwards. The most deformed line is the one that joins the centers of the profile bores.

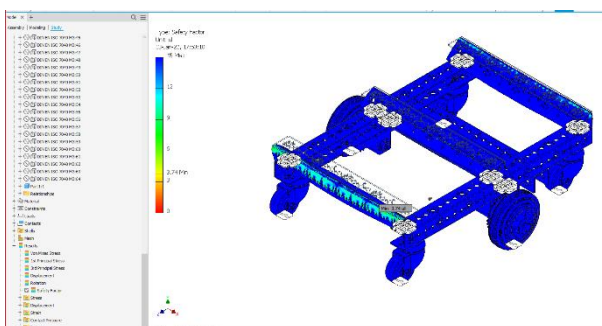


Fig. 9 The result of the deformation analysis and the representation of the required points

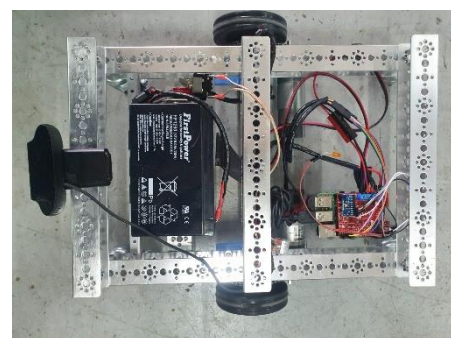


Fig. 10 AGV prototype with Raspberry Pi control board Pololu motor control module MAP sensor

Following the assembly of the hardware components and the installation of the software codes of the AGV type robot, much better results were obtained compared to the first prototype. For all criteria except battery life where a solution has been implemented by using a larger and rechargeable battery, but which is economically advantageous. The new battery can store 3 on more electricity with a capacity of 12 V with 9000 mAh Autonomy in working mode reaching the initial specifications set out in the product data sheet. A first step in the operation of the AGV was to test the engine, chassis, battery system. To perform

this step, they were temporarily mounted and connected to the chassis engines, the battery and a pleasant wi-fi capable of being able to transmit commands to the engines for moving in two directions, forward or backward.

To test the product, we connected to the wi fi board (Raspberry Pi) via a phone through its wi fi function, in the phone we connected a joystick controller.

From the first test it was observed that the engines are capable of performing the transport function, different weights were placed on the chassis to observe both its mode and behavior and the Rejes engine and weaknesses such as the fact that the battery is not suitable, the motor shaft takes up a very large part of the weight of the load.

Another step was to make the left / right turn, for this we used the engine encoders, when you want to turn left the engine on the right keeps its speed and the one on the left decreases speed, the same thing happens for the right turn, but the engine that keeps its speed is the one on the left and the one that decreases its speed is the one on the right. In the improvement of the autonomous robot cartre, we replaced its control, the control is done now through online platforms. Correction of space travel of traction losses through the addition of engine rotations will be done with the help of the MAP-9250 accelerometer sensor and the camera web video located on the front [3]. [11]

A simulation was performed in the Tecnomatix Plant Simulation program: In this simulation it is presented a well-defined workspace consisting of the next route to be completed by AGV

The AGV starts from the first working point (CNC LABCENTER 260), point where it was loaded with the necessary parts for transport to the second point (DRILLING MACHINE MG 16), the parts transported by AGV are unloaded at this point following that it is move to the third point (LOADING STATION) until the next tasks are transmitted to it. At this moment the second simulation is performed in proportion of 60%, the AGV starting from the rest point (charging station) to point A (CNC LABCENTER 260) where it takes over the parts transport to point B (DRILLING MACHINE) is required, transport to be carried out later. At this moment in the simulation there is no return of the AGV in point C, loading point, following in the future through several interactions and changes of constancy in the program overcoming this problem and performing a complete simulation.

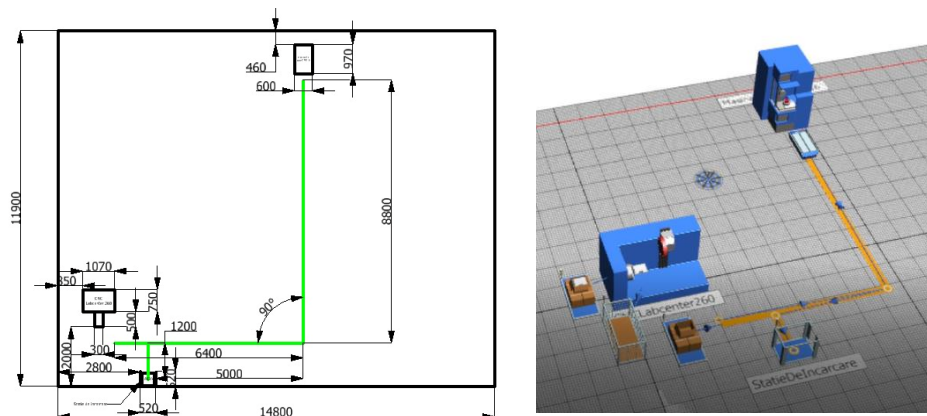


Fig. 11 Numbering and simulation of the AGV route in the laboratory

In the case of an autonomous robot, it works according to a well-defined route, a route that is possible make in the next figure.

The route was defined both physically within the faculty lab and numerically through the Autodesk Inventor design program. The projected sketch is made on a scale of 1.1. the sketch data coincides with the dimensions of the work front followed by the robot. Various transport cycles between the 2 stations (CNC Labcenter 260- Drilling Machine MG 16) and loading station will be further simulated, taking into account various parameters specific to the route between the 2 workstations that will help to dimension the parameters. odometry and navigation of the robot.

6. Economics analysis

The cost of production is the cost of purchasing materials and consumables, processing costs of raw materials for processing into a finished product.

The Table 2 shows the selling price of the AGV product for which the expenses related to the jobs, the salary expenses, the maintenance expenses, the expenses with the necessary materials and others were taken into account [12,13].

Table 2. Costs

	Value	Measure unit
Annual fixed costs	2364932	lei/year
Variable unit costs	970	lei/unit
Total unit costs	2862	lei/unit
Selling price	4000	lei
Sale price with TVA	4768	lei

The break-even point is the point at which the proceeds from the sale of the production fully cover the variable costs of that production and the fixed costs, so that the enterprise derives neither profit nor loss.

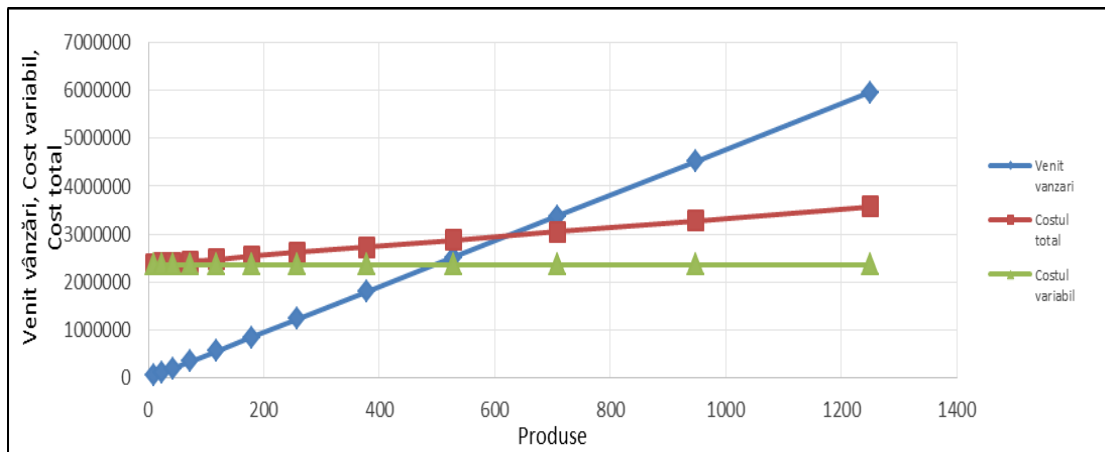


Fig. 12. Calculation and arrangement of results to determine the break-even point.

Following the calculations made it can be seen in Fig 12 that after the sale of 623 products from the reaches the break-even point After about 10 months of production, the break-even point is reached, which means that at the end of October we will make a profit.

7. Conclusions

Today's robotic applications are becoming more numerous, and all have as their main goal the reduction of the operational costs related to the industry. Also, the current trend is to replace the people who perform these operations, in order to obtain constant results. A criterion analysis was performed for each product. The needs expressed on based on a questionnaire applied to a sample of 50 enterprises and the new characteristics for choosing a concept were defined.

Through the newcomer analysis, a research was carried out for the development of the product in order to understand what the customer wants and how these desires are reflected in the characteristics / functions of the new product. By segmenting the market and choosing the target segment, the customer profile was created. Through the functional analysis, the functions to be implemented on the new concept were defined.

Functions "support and transport objects and take objects and transport them from the storage space" they turned out to be the most important. Analyzing the time, the product spends on the market a

life cycle for the proposed product has been completed and all usage scenarios have been analyzed which we may have.

Two concepts have been developed. These were made taking into account the functions of the functional analysis and the customer's need expressed by the product request, identified in the previous chapter. These chassis concepts have different characteristics based on some criteria; a hierarchy was made to observe the degree of importance of chassis. Thus, with each new prototype, improvements have been made at the construction level, so that the demands arising from a transport of 90 Kgf do not affect essential components such as engines in terms of premature wear.

One more performance has been added by using a high-capacity battery but also by programming the engine speeds for low speed and efficient travel. Regarding the deformations of the resistance structure, namely the set of U-type profiles fixed with screws, we obtained from the analysis at software level values that did not allow the definition of the loading limits of the AGV type robot, namely 90-100kg All components were analyzed and depending on the cost, so as to result in a price as low as possible with the raw materials for a total cost of the reduced product

8. References

- [1] Abaza B., „Logistica, note de curs, UPB, 2019-2020
- [2] Abaza B. „Managementul proiectelor 1 ”, note de curs, UPB, 2020-2021
- [3] Abaza B. „Managementul proiectelor 2 ”, note de curs, UPB, 2021-2022
- [4] Anirudha S., „A Study of Free Ranging Automated Guided Vehicle Systems”, 1990
- [5] Dijmărescu M. „Proiecte de dezvoltare 1”, note de curs, UPB, 2020-2021
- [6] Dijmărescu M. „Proiecte de dezvoltare 2”, note de curs, UPB, 2020-2021
- [7] Dijmărescu M. „Proiecte de dezvoltare 3”, note de curs, UPB, 2021-2022
- [8] Enrique S. , „Preliminary Design of an Automatic Guided Vehicle (AGV) System”, 2018
- [9] Gheorghe M. „Fabricarea produselor”, note de curs, UPB , 2020-2021
- [10] Parausanu I. „Modelarea și calculul structurilor”, note de curs, UPB, 2020-2021
- [11] Panea I. „Robotica”, UPB , 2020-2021
- [12] Stanciu C. „Dezvoltare de produse și servicii inovative 1”, note de curs, UPB, 2020-2021
- [13] Stanciu C. „Dezvoltare de produse și servicii inovative 2”, note de curs, UPB, 2021-2022
- [14] Spiroiu M. „Analiza valorii ”, note de curs, UPB , 2021-2022
- [15]:*** <https://www.tente.com/ro-ro/termeni-tehnici/agv-uri-sisteme-de-transport>,(accesat la 29.10.2020)
- [16]:***, <https://trans.info/ro/logistica-4-0-integrarea-agv-urilor-in-fluxul-operational-94132>, (accesat la 29.10.2020)
- [17]:*** <https://antreprenoriat101.ro/segmentarea-pietei-definitie-tipuri-exemple/> (accesat la 25.04.2021)
- [18]:*** <https://www.mdpi.com/2227-9717/9/11/1955> (accesat la 05.09.2021)
- [19]:*** <https://www.mdpi.com/2076-3417/11/24/11808> (accesat la 03.01.2022)
- [20]:*** <https://www.mdpi.com/2076-3417/12/7/3397> (accesat la 01.04.2022)
- [21]:*** <https://www.mdpi.com/2218-6581/10/2/55> (accesat la 01.04.2022)

Acknowledgement

The authors would like to thank to Associate prof. Camelia STANCIU from Thermotechnics, Thermal engines, Energy and Refrigeration Equipment Department, Faculty of Mechanical Engineering and Mechatronics, for the support and guidance in completing this research.

DEVELOPMENT OF A SYSTEM FOR ASSESSING THE POSTURE OF THE HUMAN BODY

MIERLITĂ Iulia-Sorina¹, BĂCIOIU Mihaela-Roxana¹, CIOCOIU Daniela-Adriana¹, UȚICĂ Nicoleta-Georgiana¹, VOINEA Costin-Bogdan¹, ZAHARIA Ștefania¹, DIJMĂRESCU Manuela-Roxana², ABAZA Bogdan Felician², SPIROIU Marius Adrian³

¹Faculty: Industrial Engineering and Robotics, Study program: Engineering and Management of Complex Projects, Year of study: 2, e-mail: sorina.iulia98@yahoo.com

²Faculty of Industrial Engineering and Robotics, Manufacturing Engineering Department

³Faculty of Transports, Railway Vehicles Department, University POLITEHNICA of Bucharest

ABSTRACT: The present study is based on the analysis of the proposed need for follow-up and focuses on the development of a technical solution, as well the performing of tests to build a prototype. It addresses the issue of the link between user awareness of the problem and action to address it. Thus, by applying the sensors in key positions, it is desired to develop a device with which the user is alerted and can correct the position of the back. Performing the experimental tests there are determined the key positions that will lead to the realization of the prototype.

KEY WORDS: human body posture, device, sensor, tests, measurements.

1. Introduction

The need that led to the development of this paper is the incorrect position of the back.

The device for warning of the incorrect posture of the back has the role of helping us to have a correct posture of the body, especially during the state on the chair.

The general objective of this work is to develop an innovative product that will alert the user to every incorrect position of the back. All data collected by the sensors will lead to the transposition of the information received by the sensors into graphs and diagrams to inform the user interactively about the position approached during the use of the device.

2. Need analysis

One of the fundamental steps in the development and prototyping of a device is the identification, understanding and characterization of the need. So, we compiled a list of the experienced need that we parameterized and capitalized on.

A characterization of the expressed needs / requirements is presented in Table 2.1.

Table 2.1. Expressed need

Need expressed	Parameter	Value
I want it to be quickly adjusted	Time	3-4 sec
I want it to be easy to adjust	Force	Some N
I want it to be resilient	Supported weight	Max. 130 kg
I want it to be easy	Weight/ Material	Max. 800 g
I want it to be easy to store	Volum	Max. 100 x 60 x 20 mm ³
I want it to be stable	Stable center of gravity	Depending on body position
I want to be warned about the correctness of the posture	Vibration / sound	Hz/ dB

Need expressed	Parameter	Value
I want to have access to the data collected on my phone	Dedicated device application	Bluetooth connection
I want it to have an attractive design	-	Varied design, wide range of colors

2.1. Functional need analysis

Environmental elements and the interfaces of these elements with the device for keeping the back straight, are shown in Fig. 2.1.

When defining the functions of the system, the relations of the system with the environmental elements are followed [1].

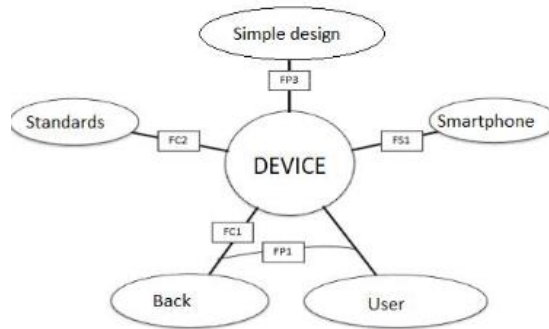


Fig.2.1. Relationships of the system environmental elements

The functions of the product are defined as:

FP1 – the device warns of the incorrect position of the user's back;

FC1 – the device adapts to the shape of the user's back;

FC2 – the device complies with the rules and regulations;

FC3 – the device must be easy to use;

FS1 – the smartphone provides data about the user's position;

The analysis shows that the first function is the most important. In order to achieve the concepts related to this project, this function was respected as a priority.

2.2. Research and evaluation of the posture of the human body

Posture is defined as the attitude assumed by the body either with support during muscle activity or as a result of coordinated action by a group of muscles working to maintain stability [5].

There are two types of posture: dynamic posture and static posture.

The spine has three natural curves at the level - cervical, thoracic and lumbar. The correct posture should keep these curves in a neutral position, without increasing or decreasing the angles.

In order to define the user's positions while using the developed product, an analysis of the anatomically and / or medically described posture types was required. The most common types of posture are shown in Fig. 2.2.



Fig. 2.2. Posture types

Were analyzed articles that debate the idea of the posture of the human body, with the aim of centralizing and creating a system for assessing posture.

3. Concurrent concepts

3.1. Existing products that meet the need

Following a rigorous documentation, two competing products were selected, as shown in Fig.3.1, 3.2:

Corset for correction and straightening column and shoulders with smart sensor



Fig. 3.1 [2]

Trainer posture Upright



Fig. 3.2 [3]

3.2. The competition's analysis

A comparative analysis between competing products and the product proposed for development is presented in Table 3.1.

Table 3.1. Compare specifications

Specifications				
Nr. crt	Product	Warning device of the incorrect posture of the user's back	Corset for correction and straightening column and shoulders with smart sensor	Trainer posture Upright
1	Adjustment time	3 – 4 sec	-	-
2	Type of grip	Velcro closure	-	-
3	Supported Weight / Size	Max. 130 kg	Universal	-
4	Weight / Material	Max. 800 g	Textil, antialergenic, nylon-elastic	-
5	Volum	Max. 100 x 60 x 20 mm³	-	48mm ³
6	Stable center of gravity	Depending on body position	-	-
7	Warning type	Vibration	-	Vibration
8	Data accessibility	Bluetooth connection - phone application	-	-
9	Colour	Wide range	White or black	-
10	Charging time	Aprox. 1,3 h	Aprox. 1,5h	30 h
11	Charger	USB C	Universal with included micro USB	-
12	Charging voltage	-	DC5V	-
13	Charging current	1200mA	500mA	-
14	Battery specifications	3,7 V/ 1000mAh	400mA/ 3,7V	-
15	Upload interface	USB C	Mini-USB	-

As can be seen (Table 3.1), the product proposed for development has several characteristics that could place it in an important place in the market. The wide range of colors, the type of charger, the battery with its specifications, etc., are some of these advantages that it could have compared to other competing products [2, 3].

4. Business strategy

4.1. Possible market segments and their evaluation

For market segmentation, an analysis was performed for the product developed from a geographical, demographic and economic-social point of view.

The criteria on the basis of which the market is segmented are the following: age, occupation, gender, type of customer, etc.

From a geographical point of view, the product can be distributed both nationally and internationally, and the areas where, initially, the market of the product takes place are the counties of Ilfov, Prahova, Argeş and Neamţ. This is due to the fact that they are the countries of origin of the team members, and this would influence when the product will be launched, put to use.

Demographically, according to a global study [4] on the incidence of back pain, it was found that 88% of people in the countries participating in the study suffer from this problem. People between the ages of 35 and 65 are among those most at risk. The activity carried out by the people on whom the study was carried out is mainly office work, with a minimum of 8 hours / day. The device is intended for both males and females, and can be adjusted according to the height of the user. The type of customer who would purchase such a device can be: individual, medical office or a recovery center.

From an economic and social point of view, the income that a user must have differs depending on various factors, among which: the country of origin, the place where he carries out his activity, the salary package, etc.

4.2. Choice of target segment

The development of the device will take into account the segmentation from the demographic point of view, and the criteria on which this segmentation is based are age, gender, respectively occupation.

Table 4.1. Choice of target segment

Age	Gender	Occupation	Ability to straighten the spine	Client category
< 18 years	- feminin - masculin	-pupil	high	individual
18- 30 years		- student - office work - field work - mixt work	high	- individual - medical office - recovery center
> 30 years		- office work - field work - mixt work	medium	

4.3. Target customer profile

Following the above analysis, the profile of the target customer can be outlined, namely: in particular, people aged 18-30 years, regardless of gender and geographical position, who spend a lot of time sitting on seat.

5. Development of technical and prototyping solution

5.1. Conceptual variants

The idea that was chosen for development led to the generation of five conceptual variants, as shown in Fig. 5.1 - 5.5, with different types of drives: mechanical; mechanical-electronic; made up of different types of components and materials.

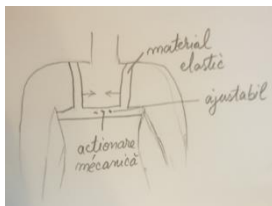


Fig. 5.1

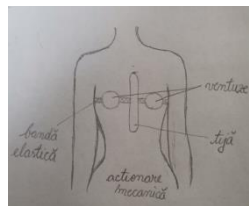


Fig. 5.2

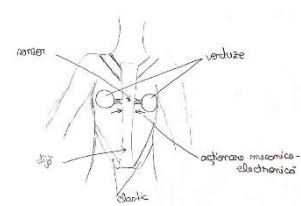


Fig.5.3

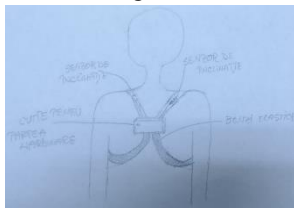


Fig. 5.4

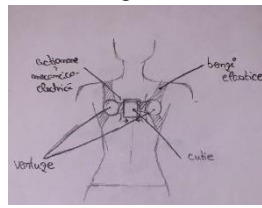


Fig. 5.5

5.2. Analysis and choice of two concepts

For the choice of two concepts, which will be further developed, an analysis was performed based on the following criteria: Sistem de prindere ușor de utilizat;

1. -Presence of sensors for immediate detection of incorrect position;
2. -Mechanical-electronic drive;
3. -Simple design.

It is found that there are two concepts that are closest to meeting the need. The most important and defining point in choosing the two concepts was how to measure and detect the incorrect position. This involves measuring angles and, when the reference points exceed the preset range, a vibration will be triggered [6].

5.3. Development of the proposed concept for prototyping

The present concept was chosen following an analysis, based on certain criteria, from a list of concepts, it having the highest score. Therefore, the high score he obtained leads to the idea that it will satisfy to high standards the need that we set out to satisfy.

The mode of operation of this concept is as follows: the user "dresses" the device as if he were wearing an item of clothing. When the user's position exceeds the preset angle when setting the device, it starts to vibrate until the user corrects its position so that it is within the preset angle range. One of the three sensors will be placed in the housing of the device for recording the coordinates of the chosen point as the main reference. The other two sensors will be placed on the deltoid muscles, which will also record the coordinates of the points. When the angle between the sensor in the housing and the other sensors exceeds the set tolerance range, the device will start vibrating [7]. All data collected by the sensors will be recorded and processed to provide the user with graphs and charts to illustrate the progress they are making using this device. The 3D realization of the future prototype in a 3D design software marks the evolution of the project and outlines the prototype we want to obtain. From the point of view of the demands that may arise on the device, there are no elements that

interfere with its smooth operation. The total mass of the product is in the order of hundreds of grams, so the user will not be adversely affected.

The accepted technical solution involved a simulation of the angle of inclination and the allocation of an orthogonal system of axes. Thus, all this approach led to the establishment of points on the user's back where the sensors can be placed.

The 3D model of the concept is shown in Fig. 5.6 - 5.11.

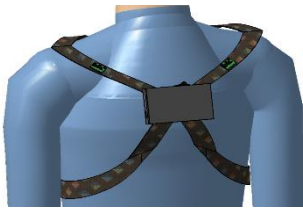


Fig. 5.6. Isometric view 1



Fig. 5.7. Isometric view 2

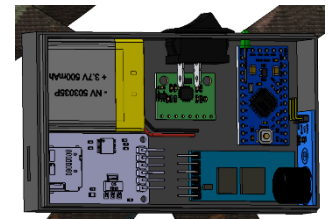


Fig. 5.8. Detail 1



Fig. 5.9. Detail 2

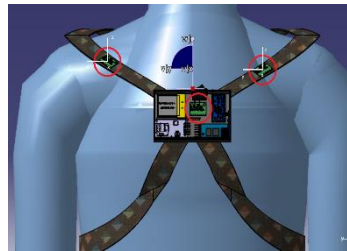


Fig. 5.10. Measure points

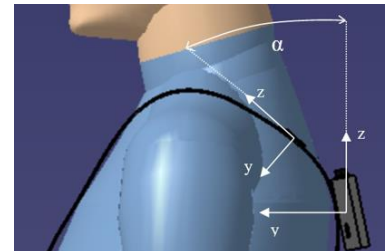


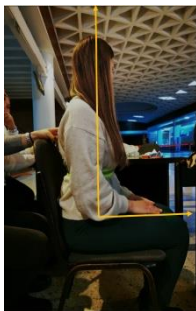
Fig. 5.11. Measurement principle

Experimentally, connections were made between the Arduino Pro Mini board and the MPU6050 sensor, and the case and cover were 3D printed in the faculty lab [8].

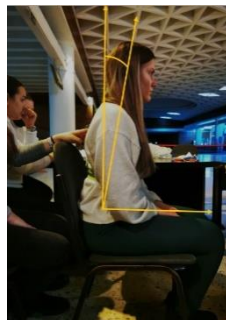
The usage scenario marks the route of the steps the device will go through during use. Closely related to this, the product life cycle also appears.

After assembling the components, it was possible to read the data recorded by the sensor. Thus, five body positions were determined. The first position was recorded as the reference position (the correct one), and the next four positions represent incorrect body positions. The data recorded by the sensor was collected for their interpretation.

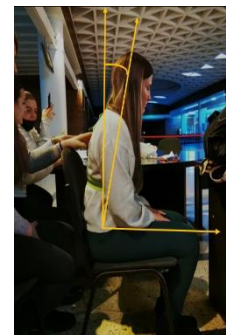
Position 0 – Reference

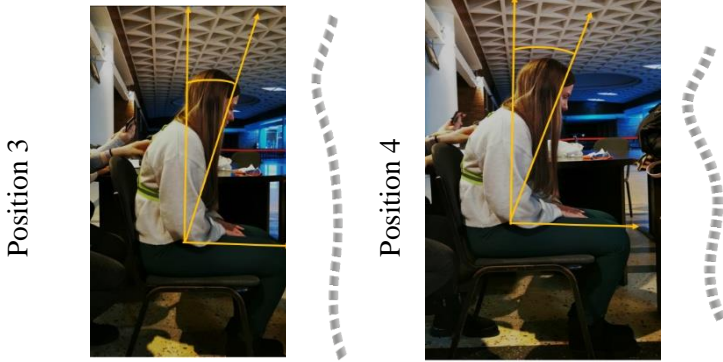


Position 1



Position 2





5.4. Data measurement, monitoring, transmission and analysis subsystem

Experimentally, for measurement, connections were made between the ESP8266 NodeMCU board and the MPU6050 sensor.

The MPU-6050 module consists of a digital motion that performs all complex processing, calculations and provides sensor data to other MCUs via I2C communication. It communicates with other microcontrollers and sensors via I2C communication. The architecture of the ESP8266 NodeMCU measuring subsystem with MPU-6050 is shown in Fig.5.12.

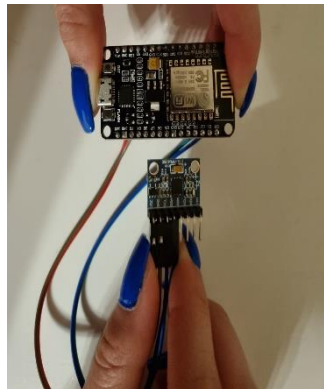


Fig.5.12. Measurement subsystem architecture

The data is transmitted via WiFi, through protocols to be tested (I2C) and tested.

6. Economic analysis

Following the calculations performed, it was established that, at an annual quantity of 5000 pieces sold, with a selling price of 670 lei, the break-even point will be reached at the beginning of September. This is justified by the fact that in the first year the investment is the largest, being necessary the acquisition of both the raw material, the production system and the place where the activity will take place. Starting in the second year, the recovery of losses will begin.

7. Conclusions

The idea for this paper was obtained after a brainstorming session. The realization of the project consisted in using the numerous methods of analysis to outline the profile of the target customer, to know the competition, but also to identify the risks that may arise. The functional analysis, followed by the elaboration and development of several concepts outlined the technical solution with which we continued the study to try to obtain a prototype. Economic analyzes were also performed to ensure that the project is reliable and to ensure a fair cost for both the developer and the end customer.

Analyzing the objectives that were proposed in the introduction of the paper, they differ from the results obtained. Thus, the current stage of the project is an intermediate one. The main components have been assembled. Several experimental measurements were performed, which led us to five positions, including the reference position (the one considered correct). By collecting all the data from the sensor, but also the photography of the stations, we obtained the necessary parameters to perform an analysis, which will be the basis of the programming code of the device. In the following educational cycles, this study can be completed and a fully functional prototype obtained.

8. References

- [1] Stanciu C., *Dezvoltare de produs și servicii inovative I*, Note de curs, UPB, 2021.
- [2] ***, Emag, <https://www.emag.ro/corector-de-postura-inteligent-cu-senzor-de-vibratie-pentru-indreptare-spate-umeri-si-coloana-tenxcor-gri-marime-universala-tnx002/pd/DFN402MBM/>
- [3] ***, UPRIGHT, https://store.uprightpose.com/products/upright-go2?_ga=2.6868656.344934286.1605198642-975295177.1605198642
- [4] ***, <https://www.multivu.com/players/English/7542151-survey-uk-tops-the-bodypain-charts/document/5bf96f02-21c7-47d1-abea-dd15ea786119.pdf>
- [5] ***, <https://www.medlife.ro/articole-medicale/durerile-de-spate-sunt-principalacauza-a-incapacitatii-de-munca-la-scara-mondiala-studii.html>
- [6] Vitalyi Epishev, *Chair posture detection with force platform*, Advances in Health Sciences Research, volume 17, 4th International Conference on Innovations in Sports, Tourism and Instructional Science 2019 (ICISTIS 2019).
- [7] Jian Wang, Xue Hua Liu, *Human Posture Recognition Method Based On Skeleton Vector With Depth Sensor*, IOP Conference Series: Materials Science and Engineering, Volume 806, International Conference on AI and Big Data Application 2019 (AIBDA 2019), 20-22 December 2019, Guangzhou, China.
- [8] Dijmărescu M., *Proiecte de dezvoltare 1, 2*, Note de curs, UPB, 2020-2021.

Acknowledgement

The authors would like to thank to Prof. Marian GHEORGHE from Manufacturing Engineering Department, Faculty of Industrial Engineering and Robotics and to Associate prof. Camelia STANCIU from Thermotechnics, Thermal engines, Energy and Refrigeration Equipment Department, Faculty of Mechanical Engineering and Mechatronics, for their support and guidance in completing this research.

MICROFLUIDIC DEVICE FOR BLOOD ANALYSIS

CÎRSTINA Maria-Mihaela¹, BOERESCU Vlad¹, IONESCU Robert-Ionuț¹,
MATEI Eduard Florentin¹ and GHICULESCU Daniel²

¹ Faculty of Industrial Engineering and Robotics, Specialty: INPN; DIPI; IAAC, Year of study: II,
e-mail: cirstinamihaela97@gmail.com

² Faculty of Industrial Engineering and Robotics, Manufacturing Engineering Department,
University POLITEHNICA of Bucharest

ABSTRACT: The scientific work presents aspects regarding the functioning and modeling of a lab-on-a-chip microfluidic device used for blood tests where the leukocyte count is followed, which informs us about the state of the immune system. Aspects regarding the stage of development of lab-on-a-chip devices are presented, extremely useful in the current conditions of the pandemic due to the rapidity of providing analysis results and the opportunity to perform certain determinations, impossible with current conventional equipment. AutoDesk INVENTOR Professional software was used to model the device and COMSOL Multiphysics software was used to simulate the finite element operation of a circuit variant, as well as its geometric optimization. Research has been carried out on the components of the device, such as the pressure system and the counting system. The conditions for the execution of the device on a millimeter silicon wafer were created using photochemical microtechnologies.

KEY WORDS: leukocytes, microfluids, photochemical microtechnologies.

1. Introduction

The abbreviation for Micro Electro Mechanical System is "MEMS" (Micro Electro Mechanical System), which was officially adopted by Dr. Albert P. Pisano in 1989. He used the term "MEMS" to describe the resonant structure made as a frequency stabilizer. [1]. In the early 1990s, a micro-analytical system, also known as a "chip laboratory", was proposed. Due to the micro-scale, the fluid flow in the microfluidic device has different characteristics, ranging from 0.1 μm to 1 mm [2].

In this study, we analyzed the realization of the flow circuit on a silicon plate, to obtain a MEMS type microfluidic device used to determine the number of leukocytes in a blood sample, which are an indicator in determining the state of the immune system.

2. The product strategic marketing

Table 1. Restrictions for fabrication the product prototyping

Restrictions for fabrication the product prototyping	
<i>R 1: To be a product which has the smaller dimensions than the classics products</i>	<i>R 5: To have the lowest cost.</i>
<i>R 2: To have a simple constructive form;</i>	<i>R6 : To be able to be reused</i>
<i>R3: <u>Be able to quickly interpret the results collected</u></i>	<i>R7 : To have easy maintenance</i>
<i>R 4: To have a large market sales;</i>	<i>R8 : To choose the optimal circuit</i>

Data collected from potential customers

The issue of the analysis time of the microfluidic device was analyzed again and it was necessary to update and resend the previous questionnaire to the respondents. The following questions have been added to the existing questionnaire:

What would be the maximum waiting time for interpreting the results?

What do you think is the most important parameter that influences the reaction time of the device?

Also, in order to have a correctly interpreted answer and to help completed the device as well as possible, a new market segment was introduced in the selection matrix and more exactly the companies that deal with the manufacture of medical equipment.

Data collected from potential customers

The questionnaire used for the market research in the case of marketing the “Microfluidic Device” was made exclusively online. The questions added above have been interpreted in the figures below.

What would be the maximum waiting time for the result interpretation?
13 answers

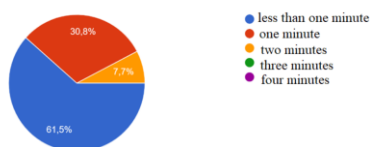


Fig.1 Graph waiting time

Which do you think it's the most important parameter which influences the reaction time of the device?
13 answers

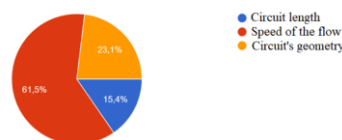


Fig. 2 Graph response time

The questionnaire guide together with the two interpreted requirements are presented in Table 2.

Table 2. Interview guide

No. crt	Question	Customers statement	Need interpreted
1	What would be the maximum waiting time for interpreting the results?	<ul style="list-style-type: none"> ○ In less than a minute ○ One minute ○ Two minutes ○ Three minutes ○ Four minutes 	<ul style="list-style-type: none"> ○ The need for as little analysis time as possible
2	What do you think is the most important parameter that influences the reaction time of the device?	<ul style="list-style-type: none"> ○ Circuit length ○ Flow rate ○ Establishing relative importance Circuit geometry 	<ul style="list-style-type: none"> ○ The need to choose the most concrete parameter that best influences the analysis time of the device.

Hierarchy and relative importance

Following the study of the answers and the interpretation of the clients' needs, a grouping of the main needs was made, and then their relative importance will be established. Table 3 shows the relative importance, giving the grades 1 to 5 depending on the importance considered.

Table 3. Establishing relative importance

Client requests	Relative importance
The microfluidic device for the analysis of leukocytes in the blood is portable and easy to store	5
The microfluidic device for the analysis of leukocytes in the blood is reusable	5
The microfluidic device for the analysis of leukocytes in the blood is easy to use	4
<u>Microfluidic device for blood leukocyte analysis has a prompt response in interpreting the results</u>	5
Microfluidic device for blood leukocyte analysis provides precision in the analysis of collected samples	5
The microfluidic device for the analysis of blood leukocytes can be used in the medical industry	4
The microfluidic device for the analysis of blood leukocytes can be used in any environment being independent of the workplace	5
The microfluidic device for the analysis of leukocytes in the blood has affordable price for the current medical market	3

3. Product approval

- the overall dimensions of the microchip - it is checked if they allow the assembly with the display device and the pressure pumps. Depending on the geometry of the microchip, the sample has certain flow velocities during the analysis, pressures on the path traversed by the sample and a certain pressure in the capture chamber;
- the structure, size and hardness coefficient of the support plate, which helps to stabilize and protect the geometry of the microfluidic chip;
- use of the outer plate, which helps to protect the silicon microchip and its stability and fixation on the support plate;
- use of a counting sensor for the purpose of counting leukocytes in the blood sample inserted into the silicon microchip circuit.
- checking the volume of blood needed to analyze and number the blood sample;
- testing the density and kinematic viscosity characteristics of the lysis liquid used;

4. Internal organization for marketing

The delivery sector - one of the most important departments, given that the activity carried out by it, ensures the connection between the manufacturer and customers, is the interface with the beneficiaries, it's efficiency depending on customer satisfaction and consequently turnover. In view to determine the efficiency of the product delivery activity, the cost involved in the delivery to a sample of 10 medical laboratories located at various distances from the point of sale was analyzed.

The analyzed parameters were the delivery destinations, the distances to the delivery place, the delivery times, the quantity to be delivered versus the capacity of the transport machine (weight and volume to be transported), the delivery hours taking into account the traffic on the selected routes.

Hypotheses:

No. customers =10; No. ordered devices =95; Transport capacity information:

Table 4. Transport capacity information

Device weight	7 kg
Transport machine capacity (kg)	1000 kg
No. pcs. maximum that can be transported depending on the maximum weight	142 pcs.
Device volume 277 x 276 x 270 mm	0.02064 m3
Transport machine capacity (volume)	2 m3
Nr. pcs. maximums that can be transported depending on the volume	pcs.

Two delivery options were analyzed:

1. Delivery according to the ranking of the orders versus optimized delivery of all orders received / day
2. Delivery with own transport versus rented transport.

4.1. Analysis presentation: Delivery according to the ranking of the orders - the transport of the order is carried out punctually, with the main purpose of obtaining customer satisfaction through the short delivery time, on the principle of "first come, first served"

Table.5 Customer distances

No. crt	Customer	Route (round - trip)	Quantity ordered	Distance (km)	Time (min)
1	Sante Clinic	University Politehnica of Bucharest- > Sante Clinic	10	2.6	7
2	Synevo	University Politehnica of Bucharest- > Synevo	20	2.8	11
3	Sfânta Maria Clinic	University Politehnica of Bucharest- > Sfânta Maria Clinic	10	2.6	18
4	Regina Maria Hospital	University Politehnica of Bucharest- > Regina Maria Hospital	5	3	11
5	Medlife Clinic	University Politehnica of Bucharest- > Medlife Clinic	10	4.2	18
6	OneLife Clinic	University Politehnica of Bucharest- > OneLife Clinic	5	3.2	9

No. crt	Customer	Route (round - trip)	Quantity ordered	Distance (km)	Time (min)
7	Cris Medical Clinic	University Politehnica of Bucharest- > Cris Medical Clinic	5	3.6	13
8	Sanador Hospital	University Politehnica of Bucharest- > Sanador Hospital	10	3.4	16
9	Apaca Polyclinic	University Politehnica of Bucharest- > Apaca Polyclinic	5	1	7
10	Emergency hospital of Bucharest	University Politehnica of Bucharest - > Emergency hospital of Bucharest	15	3.6	10
Total			95	30	120

The transport routes are presented below:

-Optimized delivery of orders- the aim is to streamline costs while meeting customer expectations, respectively the delivery time communicated to them (24 hours from the date of the order).

Table 6. Optimized order delivery

No. crt	Customer	Route (round - trip)	Quantity ordered	Distance (km)	Time (min)
1	Synevo	University Politehnica of Bucharest- > Synevo	20	2.2	6
2	Sfânta Maria Clinic	Synevo - > Sfânta Maria Clinic	10	0.35	2
3	Regina Maria Hospital	Sfânta Maria Clinic - > Regina Maria Hospital	5	0.45	2
4	Medlife Clinic	Regina Maria Hospital - > Medlife Clinic	10	0.9	3
5	Sante Clinic	Medlife Clinic - > Sante Clinic	10	0.85	3
6	Cris Medical Clinic	Sante Clinic - > Cris Medical Clinic	5	7.1	16
7	Onelife Clinic	Cris Medical Clinic - > OneLife Clinic	5	1.2	4
8	Sanador Hospital	OneLife Clinic - > Sanador Hospital	10	1.1	4
9	Emergency hospital of Bucharest	Sanador Hospital - > Emergency hospital of Bucharest	15	1.1	3
10	Apaca Polyclinic	University Politehnica of Bucharest- > Apaca Polyclinic	5	1.8	7
Total			95	17.05	50

1. Delivery with own transport versus rented transport.

In calculating the costs, the driver's salary, fuel and other expenses related to the transport car (depreciation, tax, insurance, repairs) were taken into account. The expenses of the car represent a percentage of 3% in total salary and fuel expenses.

Table 7. Own transport costs

Costs of company transport	
Wage	3000 lei wage + employer taxes/160 hours = 18.75 lei/hour * 2 hour = 37.5 lei
Fuel	7 lei/liter * 15 km* 10 liters consumption/100 km = 10.5 lei
Car expenses	(3000 wage + 10.5 lei/day *20days)* 3/100=96.3 lei/month/20 days = 4.815 lei/day
Total internal transport costs / day	52.815 lei/day

In the calculation of the expenses with a rented car, a cost of 1.5 lei / km and 2 lei / stop was taken into account.

$$\text{Extern transport costs/day} = 1.5\text{lei/km} * 15 + 2 \text{ lei/stop} * 10 \text{ customers} = 42.5 \text{ lei/day} \quad (1)$$

5. Computer modeling and simulation of microfluidic flow in the micro-electro-mechanical device

Computer simulation has become an essential part of science and engineering, it is the technique that verifies the correctness of selected materials in the construction of new parts / devices, as well as production / manufacturing technologies. Thus, the dedicated Comsol Multiphysic finite element modeling software was used and then successively the working modules were selected: Fluid Flow, Single Phase Flow and Laminar Flow for modeling and simulating the flow of substances used in the microfluidic device. The input data are presented in Table 8.

Table 8. Input data for microfluidic modeling and simulation

Flow proportions	
Blood	50 $\mu\text{m}/\text{min}$
Lysis solution	1600 $\mu\text{l}/\text{min}$
Lysis stop solution	265 $\mu\text{l}/\text{min}$

The simulation of the flow rate of the fluid mixture is presented in Fig. 3

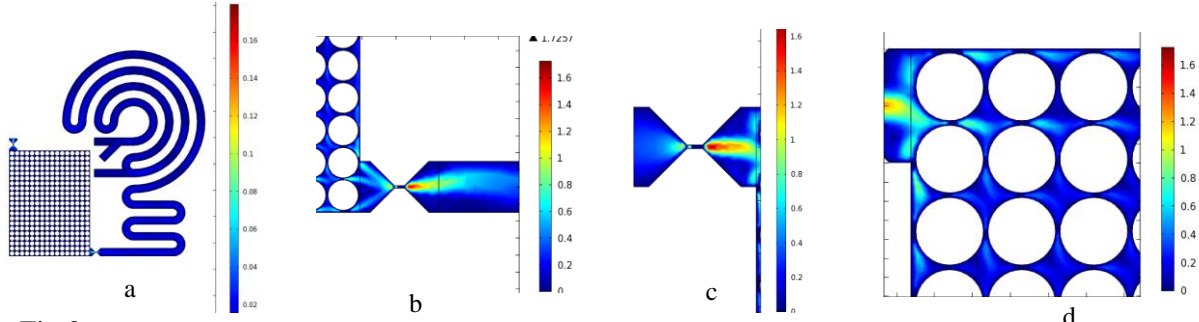


Fig 3. Flow rate variation [m / s], a) overview, b) counting channel, c) output channel d) magnified view of the selection and capture chamber

The velocity of the fluids collected from Comsol at points in the median flow circuit, due to the parabolic distribution of the laminar flow, was very low on the straight lines and much higher on the curved lines or the reduced flow section (Fig.3). The objectives of the blood sample analysis with lysis and lysis stopping substances have been achieved. Calculating the length of each circuit in relation to the corresponding values of the average speed, the travel time for circuit 1 was 2,831 s less than the characteristic value of 3 s required for the proper red cell lysis process. For circuit 2, the speed was 46,289 s. This is higher than the reference value for stopping lysis, which is 30 s.

In order to reach the final version above, we started from an initial version that went through various changes shown in the following images:

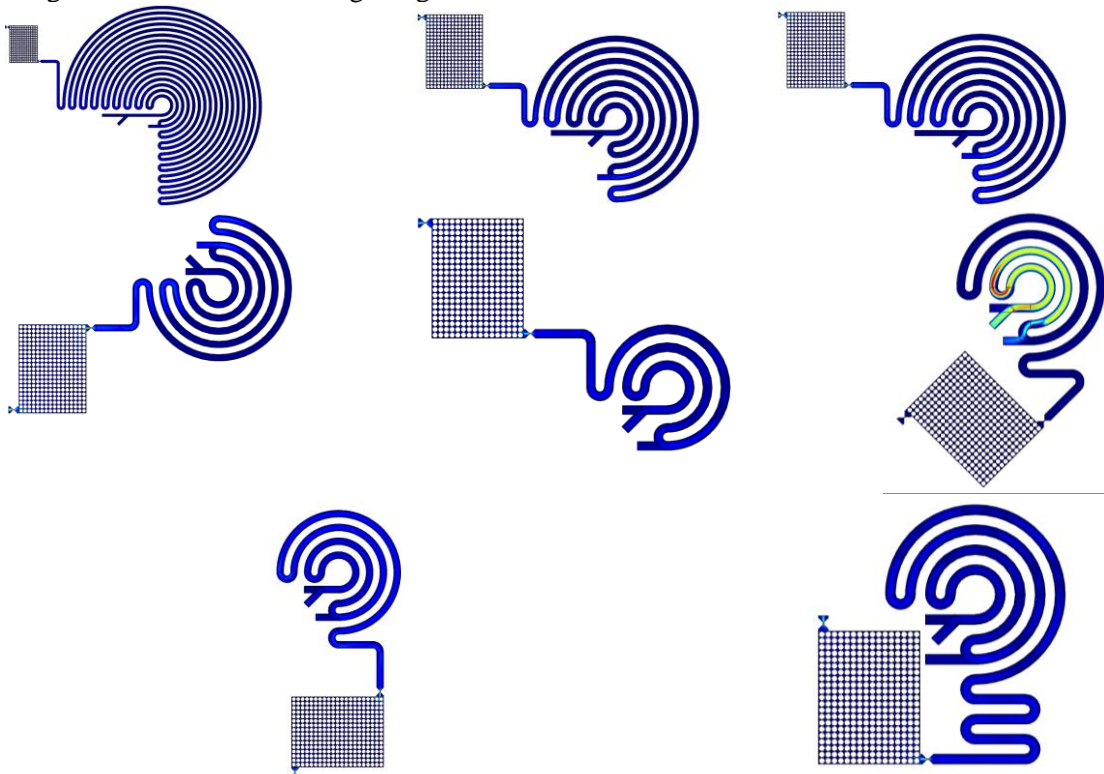


Fig. 4 Modeling models of the circular microfluidic device

6. Manufacture of microfluidic chip

Figure 5 shows the execution drawing of the microfluidic chip.

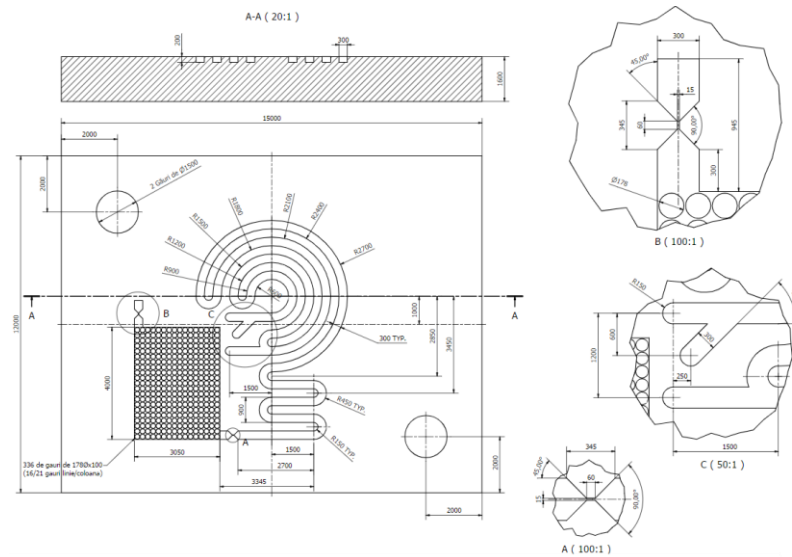
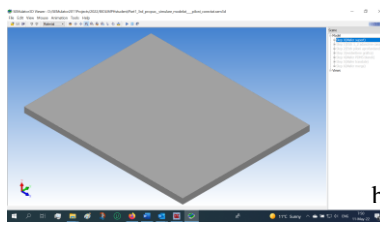
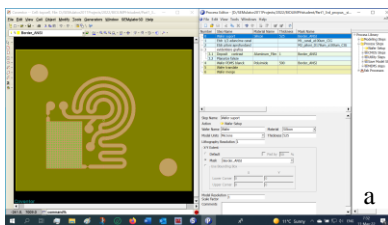


Fig. 5 Microfluidic circuit drawing

The figures below show the steps taken to make the microchip. SEMulator3D software was used to verify the correctness

- Data input for 3D modeling: on the left DXF format graphic file, on the right standard processing steps for technology flow modeling.
- Choice of chip holder 15x12mm², thickness G525 μ m
- 3D modeling result for 100 μ m depth corrosion, channel and other 100 μ m depth tank
- 3D modeling deepening pillars at a depth of 100 μ m and another 100 μ m in channel depth
- Highlighting (for graphic purposes) the contrast substance of the geometries dug by corrosion in their 525 μ m thick monosilicon support
- Casting using the mechanical mask of the PDMS following the geometries excavated in the subducted monosilicon
- Adhesive PDMS adhesion to subducted monosilicon
- Duplicate 31 chips of 15x12mm² - 4inch monosilicon wafer



d

f

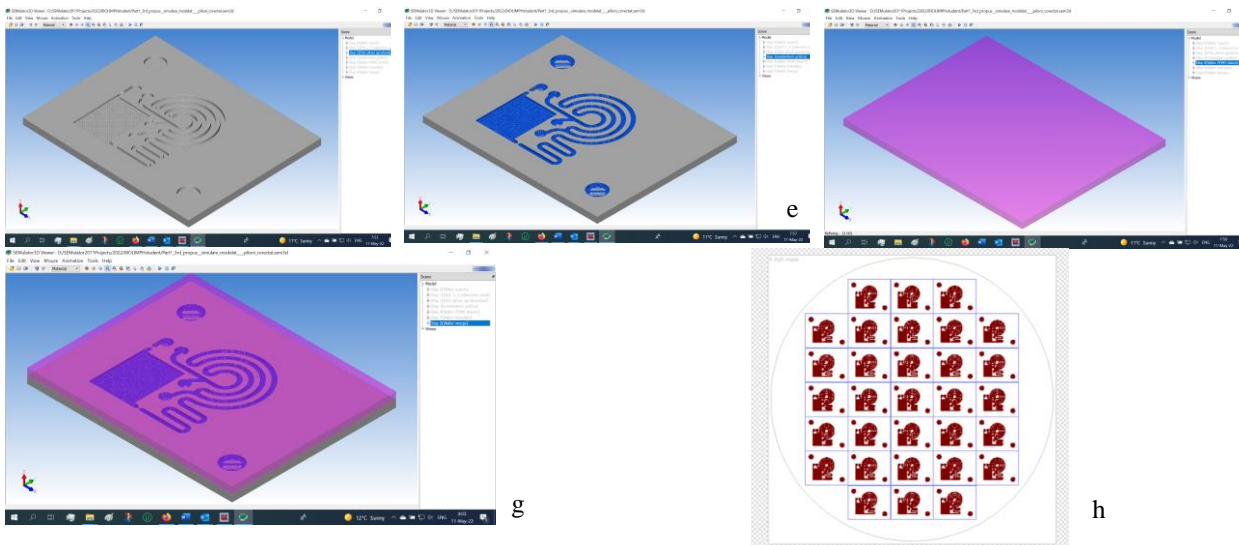


Fig. 6 Stages of microfluidic chip manufacturing in SEMulator3D software

7. Cleaning the device

Several cleaning steps are normally required during the production stage of the device, as well as before its actual use, to ensure that the chips and connectors are properly cleaned. After precise connections and experimental preparation, the last thing a microfluidics user wants to observe on its microscope is a clogged channel with debris that could have been avoided. If this happens, the options to remove contamination inside microchannels and connections are unfortunately limited. [5]

A classic and easy method of cleaning the microfluidic device is the manual one which includes the following series of steps:

- Manual application of a detergent solution for 5 minutes (removal of small particles)
- Manual application of a methyl alcohol (methanol) for 5 minutes
- Manual application of acetone for 5 minutes (for the removal of organic residues)
- Manual application of demineralized water for 5 minutes
- Drying the device with an oven or laboratory hob (Figure 7)



Fig. 7. Laboratory electric hob

Another method is to put these liquids in glass or plastic cups and place in an ultrasonic bath for a few minutes. These actions include manipulative steps that make the process tedious and time consuming. [5]

Using bags can reduce the time and the complexity of cleaning microfluidic chips and other laboratory tools (connectors, tweezers, glass slides prior to plasma bonding to PDMS). Additionally, we have reduced the amount of liquids used routinely. [5]

Figure 8 shows a sketch of the use of a bag for indirect cleaning of a chip inside an ultrasonic bath.

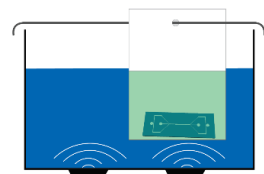


Fig. 8 Sketch of the use of a bag for indirect cleaning of a chip [5]

The tools required for this method are: ultrasonic bath, filled only with water up to the indicated filling height, cleaning liquid a tweezers, plastic bags, rod.

Using ultrasound for cleaning is a common practice in almost all laboratories around the world. Ultrasonic baths are used specially when mechanical brushing or other cleaning procedures are not possible; e.g. fragile structures or small dimensions in a microchannel which are difficult to reach. [5]



Fig.9 The result of cleaning a glass microfluidic chip [5]

Figure 9 shows the result of cleaning a glass microfluidic chip that contains a large reaction / analysis site and several inlets and channels.

Such a chip is difficult and not cheap to make; however the chip becomes unusable when the well is clogged with by-product of the reaction. Using ultrasonic cleaning inside a bag, the well can be emptied and the device reused..[5]

Figure 10 shows the cleaning of an upchurch connector can become contaminated and is difficult to clean due to the small grooves. Ultrasonic cleaning ensures rapid cleaning of the connectors. [5]

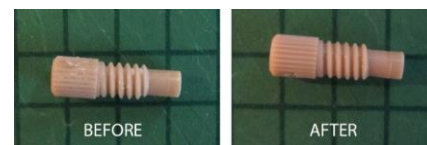


Fig. 10 Cleaning an Upchurch Connector .[5]

8. Conclusions

1. Various constructions of microfluidic circuits have been researched in order to perform blood tests with advantages that conventional technologies do not have.

2. Various concepts have been developed for the flow circuit of the microfluidic liquid and the components of the final device; Following a thorough analysis, a final version was chosen, which was verified through simulations in COMSOL Multiphysics and designed in 3D in the AUTODESK Inventor program.

3. A lab-on-a-chip (MEMS) microfluidic device was modeled for practical realization on a millimeter-sized silicon plate, using photochemical microtechnologies; the device is used for blood tests

4. This microfluidic device has major advantages, among which: it provides a fast result of this analysis; uses a very small volume of blood sample.

5. Following the analysis for transport, the distance traveled and the delivery time are reduced by 43% and 71%, respectively, with positive implications in reducing transport costs and human resources, while respecting the delivery conditions communicated and accepted by customers.

6. The outsourcing of the order delivery activity has positive effects in reducing the transport costs by approximately 20%, ensuring a greater capacity for their permanent adjustment, through regular price analysis, selection of new carriers, negotiation of new prices. Also, the delivery with external carriers eliminates the risk of syncopes in the delivery of orders, determined by the inability to use the car due to periods of parking for repairs or during the absence of the driver. Cost reductions may differ on each delivery route depending on the daily optimization taking into account route changes due to the information provided by the profile software regarding road traffic.

9. Bibliography

- [1] Jingdong Chen, Di Che, (2013) „Progress of Microfluidics for Biology and Medicine”, Nano-Micro Lett. 5(1), 66-80 (2013)
- [2]. Catherine McKenna, Efficient cleaning of a microfluidic chip, available at: https://blogs.rsc.org/chipsandtips/2016/02/08/efficient-cleaning-of-a-microfluidic-chip/?doing_wp_cron=1643008479.7458579540252685546875&fbclid=IwAR2JVEYci7OLn1Ee_vQFKGfVQCylfJtyptE6Tr6SAesqY5R1A3qo4rWszcc, accessed on date: 28.02.2022
- [3] Ghiculescu, D., Curs Ingineria Asistată a Micro și Nanotehnologiilor, available at: <https://fiir.curs.pub.ro/2019/>, accessed on date: 03.04.2022.
- [4]*** „Fabrica microfluidica pentru auto-asamblarea asistata a nanosistemelor” available at: <https://www.imt.ro/MICRONANOFAB/rez13.php> accessed on date :29.03.2022
- [5]*** ”Catherine McKenna, Efficient cleaning of a microfluidic chip”, available at: <https://blogs.rsc.org/chipsandtips/2016/02/08/efficient-cleaning-of-a-microfluidic-chip/c>, accessed on date: 03.05.2022

TOPOLOGICAL OPTIMIZATION AND GENERATIVE DESIGN OF COMPONENTS THAT ARE PART OF ELECTRIC MOTORS

JOIȚA Cristian-Gabriel¹, DAVIDOIU Alexandra¹, VĂLU Maria-Cătălina¹, ANDREI Bianca Nicoleta¹, CHIRCIOAGĂ Ioana-Bianca¹ and LĂCĂTUȘ Elena²

²Faculty of Industrial Engineering and Robotics, Specialization: I.N.P.N, D.I.P.I, Year of study: II,
e-mail: j.cristiangabriel@gmail.com

²Faculty of Industrial Engineering and Robotics, Manufacturing Engineering Department

ABSTRACT: This paper aims to use topological optimization and generative design to identify the ideal shape and dimensions for the rotor and stator of an electric motor, reducing the production cost and dimensions. After the generative design is made, the parts will be 3d Printed using FDM method.

KEY WORDS: electric motor, generative design, rotor, stator, topological optimization, 3d printing

1. Introduction

In the case of brush motors, the stationary field [stator] is generally created by permanent magnets that interact with a rotating field [rotor] that contains the motor windings. Brushless motors are the exact opposite, because the stator field is the coiled element and the rotating field is the permanent magnet. In both cases, the interaction of these fields produces a torque that rotates the rotor. As the rotor rotates, the winding current is changed or switched to produce a continuous torque. The brush motor usually uses graphite brushes that move on metal bars [the switch] that are connected to the rotor coils. As the rotor rotates, the brushes transfer current from one set of coils to another. Brushless motors are based on their switching by using a shaft position sensor that sends a signal to an external winding switching circuit (Fig. 1). [1]

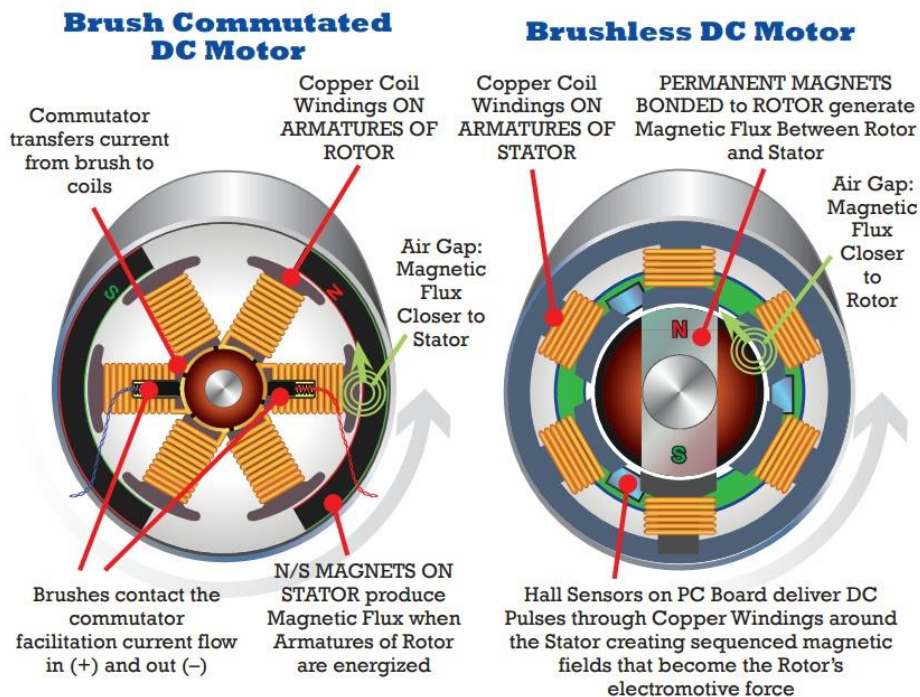


Fig. 1 Schematic diagrams of brushed and brushless motors [1]

Table 1 shows the characteristics of brushed and brushless motors. Due to the better features of the brushless motors, they were chosen to be topologically optimized.

Table 1 Motor characteristics

Characteristics	Brush motor	Brushless motor
Simplicity	They are simpler, as the motor can be powered directly from a power source.	They are more complex requiring an electronic controller.
Torque	-	Generally higher
Speed	1000-10000 rpm	Over 10,000 rpm only with certain configurations
Noise	They are generally noisier	-
Lifetime	2000-5000 hours - limited by the life of the brushes	Over 10,000 hours - bearing life limit
Cost	Generally lower but very dependent on the type of engine	-

2. Current stage

Brushless motors are often used in industrial applications (linear motors, servomotors, actuators for industrial robots, drive motors for extruders, advance drives for CNC machine tools), but also for different types of drones (flying, underwater, etc.).

The aim of this work is to optimize a brushless electric motor that is part of an overflight drone.

For medium and small drones it is effective to use brushless motors due to the fact that they are more powerful and have a long life.

Brushless motors are versatile and easy to customize due to the fact that they can be obtained by other manufacturing methods such as additive manufacturing.

Starting from the need to make electric motors as fast as possible and with minimal initial investment, the team chose to make a brushless electric motor through an additive manufacturing method that will help its construction in a shorter time, while maintaining the characteristics imposed.

The advantage of printing a 3D motor for drones is that the design of the parts can be easily modified and reprinted, depending on the need and the desired adjustments. An engine can be built in about 20 hours. Compared to other drone engine manufacturing solutions, the 3D printing method is low cost and it is important to be able to replace it as soon as possible if the aircraft is destroyed. [2]

A good example of the need for 3D printing of engines for fly drones refers to the current situation in Ukraine, where the activity must be continuously monitored with precision and access to as much information as possible, and if a drone is detected and destroyed, time and the cost of replacing the equipment will be minimal compared to other technological processes for building a new engine and eventually the whole product.

3. Topology optimization with finite element method

Starting from the idea of the current stage where we can use such types of engines in the assemblies used for the manufacture of fly drones, where we depend on the need for a long flight time, high maneuverability and small size, we decided to follow the manufacturing direction by printing 3D (FMD - Fused Deposition Modeling) of the main components that help us meet the needs mentioned above.

Given that the aim is to maintain important criteria for optimal operation, we will use the topological optimization technique with the finite element method that will generate new concepts on the imposed conditions. This technique starts from a preliminary geometry of the parts on which the conditions imposed by the functionality will be applied. The next step is to discretize the benchmark into finite elements that will help achieve a more efficient end result. The resulting parts are then analyzed by a design engineer and used to create new geometries. This topological optimization helps us to reduce the mass of the parts, keeping the imposed functionality conditions.

An electric motor on the market was chosen to have a starting point. It consists of rotor, stator, shaft, bearings, threaded rod, magnets and copper wire.

From the list of the main components that make up the brushless electric motor, the team focused on the rotor and stator parts (fig.2) to be made by 3D printing technology. The modeling of the parts was done in the Autodesk Inventor software starting from a given form and taken from open sources.

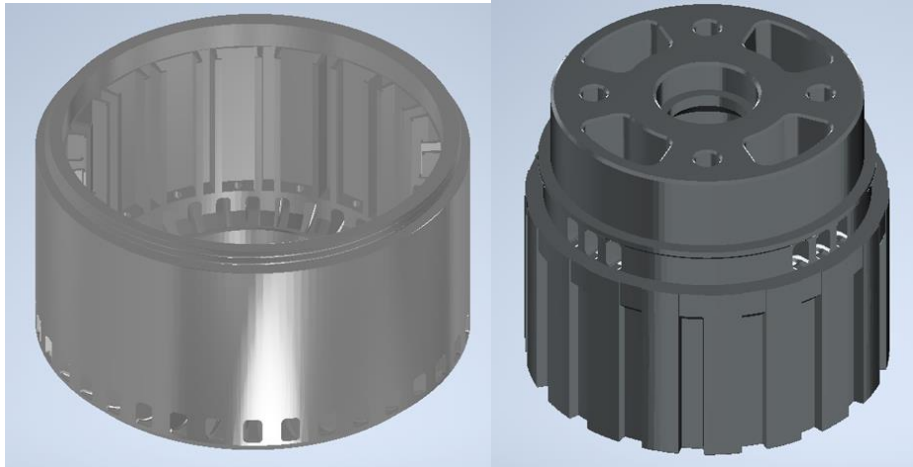


Fig. 2 –Initial model of a) Rotor and b) Stator [3]

Rotor geometry consists of slots used for the insertion of permanent magnets and vents. The rotor must be fixed to the shaft, and it must meet rigid conditions capable of withstanding the centrifugal forces required for operation. By importing the rotor geometry in a generative design software and after formulating the input parameters, 2 objects were obtained, presented in fig.3, which respect the material reduction conditions, streamlining the parameters of the final product.

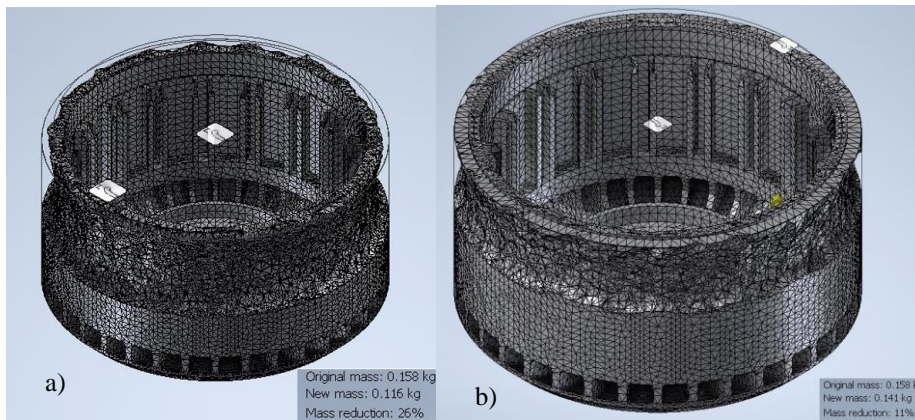


Fig 3 – Parts generated by weight reduction by a) 26% and b) 11%

Following the concepts generated, it can be seen that reducing the rotor mass is possible without this aspect affecting the efficiency of the electric motor, so the team chose to change the appearance of the rotor by introducing at least 1.5 mm channels present on its outside, which have the role of reducing the weight of the rotor.

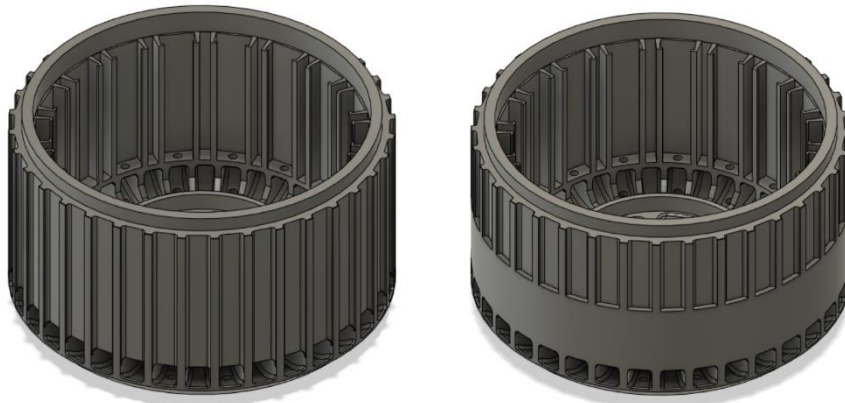


Fig. 4 – Team-generated concepts

The stator is the basis for winding the copper wire. By introducing it in the generative design software, a landmark with a mass reduced by 10% was obtained, presented in fig. 5

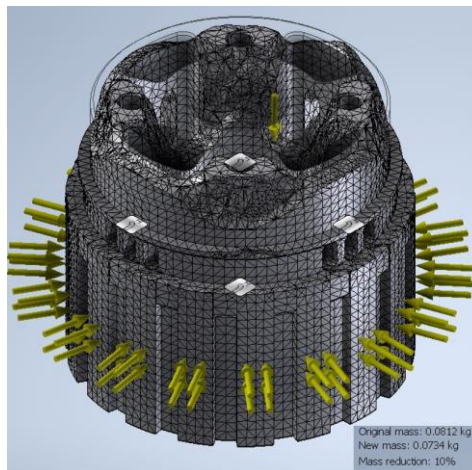


Fig. 5 Part generated for stator

The team also rethought the stator and how we could reduce its weight without affecting its efficiency. Therefore, the following two constructive solutions presented in fig. 6.

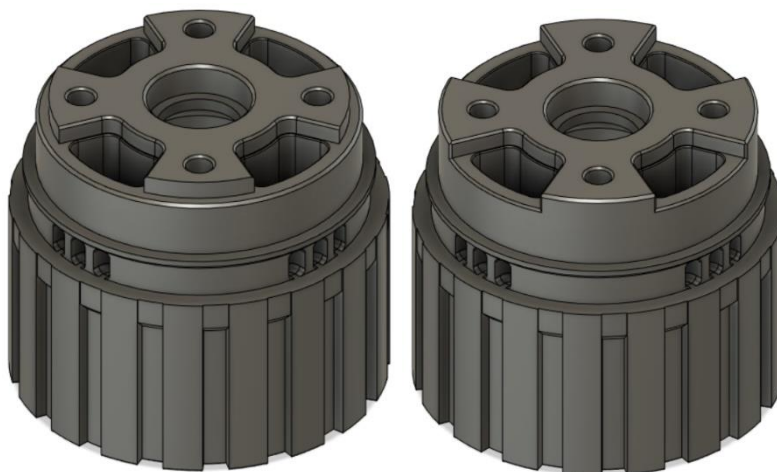


Fig.6 Concepts generated for stator

4. Materials and method of manufacture

Fused deposition modeling (FDM) is a bottom-up additive manufacturing method that involves superimposing molten material starts on a certain shape to create an object. After the first layer has been deposited, the working head rises on the working axis with the thickness of the deposited layer. The obtained objects can be independent (end-use) or be part of a certain set. Figure 7 shows a schematic representation of the operating principle of a 3D printer using this manufacturing method.

To create our parts, we use a 3D Creality Ender 3 Pro V2 printer (fig. 7) with an additional configuration with a self-calibration device BITouch, Raspberry pi 3 and Octoprint as control software.



Fig. 7 Experimental set-up

This process has the following advantages and disadvantages.

Advantages

- Flexible design
- Reduced cost
- Fast manufacturing
- Minimal waste

Disadvantage

- Limited materials
- Need for post-processing
- Limited size

Tabel 2 Material characteristics [4]

Material characteristics	ABS	PLA
Filament diameter	1.75 mm	1.75 mm
Resistance	40 MPa	65 MPa
Stiffness	5/10	7.5/10
Durability	8/10	4/10
Printability	8/10	9/10
The maximum temperature	98°C	52°C
Coefficient of thermal expansion	90µm/m-°C	68µm/m-°C
Density	1.04g/cm ³	1.24g/cm ³
Extruder temperature	235°C	190 - 220°C
Work table temperature	110°C	45 - 60°C
Work table heating	Yes	Optional
Impact resistance	Yes	-
Temperature resistance	Yes	-
Print speed	50 mm/s	70 mm/s

The materials analyzed for the parts are acrylonitrile butadiene styrene (ABS) and polylactic acid (PLA).

PLA is a thermoplastic polymer that has a fairly low transition temperature, which makes printing easier and makes it very versatile in creating different parts. This material is eco-friendly and biodegradable.

ABS has hardness and impact resistance, allowing the printing of durable parts that will have high wear resistance. ABS also has a higher transition temperature, which means that the material can withstand much higher temperatures before it starts to warp.

5. Economic analysis

A cost was made for the materials used, so an ABS (Acrylonitrile butadiene styrene) roll costs about 87 lei / piece (depending on the supplier) and has a total length of 400 m.

It has been established that 17.1 m of ABS filament are required for the manufacture of a stator and 36.4 m of filament are required for the production of the rotor. Thus, from a single roll we can make 7 rotors and 8 stators.

Also, a cost was made for a roll of PLA (Polylactic Acid) costs about 72.90 lei / piece has a total length of 400 m.

It has been established that 17.1 m of PLA filament is required to manufacture a stator, and 36.4 m of filament are required to make the rotor. Thus, from a roll, 7 rotors and 8 stators can be made.

Tabel 3. Cost

ABS (Acrylonitril butadiena stiren) – 400 m	PLA (Acid polilactic)
Stator: 17,1	Stator: 17,1
Rotor: 36,4	Rotor: 36,4
Can be made: 7 rotors and 8 stators	Can be made: 7 rotors and 8 stators
Total length: 400 m	Total length: 400 m
Length used: 391.6 m	Length used: 391.6 m
Calculation method: 7 x 36.4 = 254.8 (rotor) 8 x 17.1 = 136.8 (stator)	Calculation method: 7 x 36.4 = 254.8 (rotor) 8 x 17.1 = 136.8 (stator)
Cost / roll: 87 RON	Cost / roll: 72.90 RON
Material cost: 0.21 / m	Material cost: 0.18 / m
Energy cost: 44.0928 KWh * 0.8 lei / KWh = 35.27 lei	Energy cost: 44.0928 KWh * 0.8 lei / KWh = 35.27 lei
Labor: 21, 30 lei / h	Labor: 21, 30 lei / h
Equipment: 3D printer - 1600 lei	Equipment: 3D printer - 1600 lei
Maintenance: 0.03 lei / h	Maintenance: 0.03 lei / h
Total ABS cost: 1743.81 RON	Total cost of PLA: 1729.68 RON

6. Results and conclusions

After the realization of the concepts and the design of the parts, a part of the simulation of the production time followed, the amount of material necessary for the parts in the construction of the electric motor.

Table 4 shows the results of the simulations together with the output data of the parts that can be achieved through the additive manufacturing process. These results were obtained by importing meshes into Ultimaker Cure 5 slice-ing software, which generated the G code to be sent to the 3D printer.

Figure 8 shows the parts to be made by the additive method.

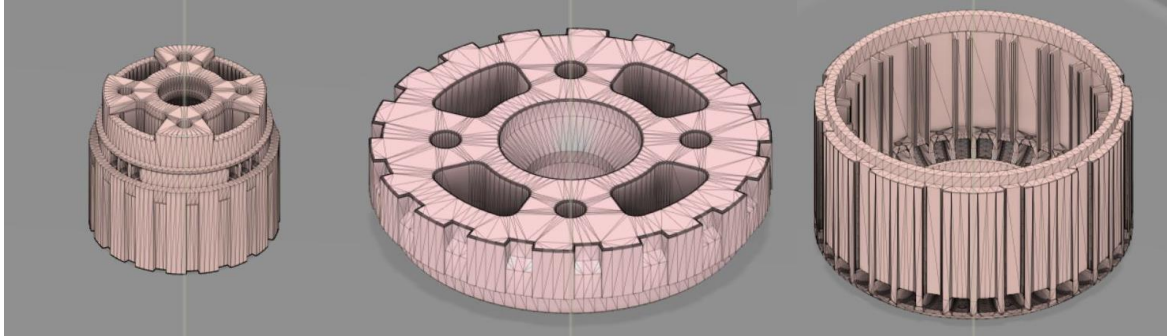


Fig. 8 Stator A (left), Stator B (middle), Rotor housing (right)

As the first production time, the calibration time was calculated, in which a measurement of the table height is performed, in 9 points, in order to make a visualization of the printing bed, fig 9. These data will be taken into account and will be adjusted. print heights so that there are no differences in height. This time will be considered as 1 minute but the calibration will be done at the table temperature of 110 ° C which will add 6 minutes to the initial time, so before each benchmark will add 7 minutes.

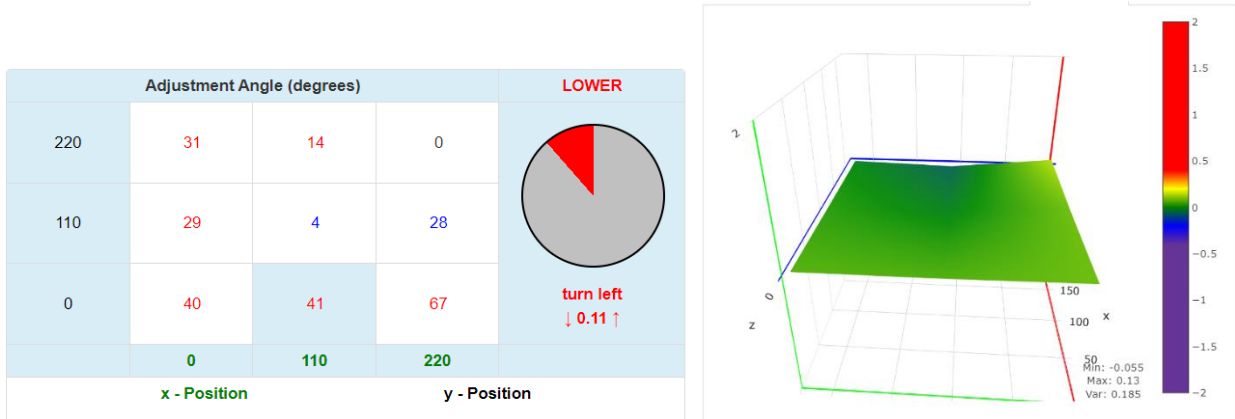


Fig. 9 Print bed calibration

Table 4 Output data

Part	Height Increase (mm)	Model fill (%)	Filing time (z: h: m)	Filament used (m)	Number of slices	Mass (g)	Support	Adhesion
Rotor Housing V1	0,12	80	1:22:23	53,12	497	129	No	Raft
Rotor housing cover	0,16	60	10:44	20,93	104	51	No	Raft
Stator A1 amount	0,16	80	16:43	30,90	271	75	No	Raft
Stator B1 amount	0,16	80	5:39	10,61	78	26	No	Raft

According to the simulation, all the landmarks that can be printed in 3D would be made in about 3 days 7 hours 29 minutes. These data show approximately 79.48 hours. The cleaning time of the printer after each print is 2 minutes per mark.

Thus the total production time can be calculated with equation (1):

$$T_p = T_{p1} + T_{p2} + T_{p3} + T_{p4} + T_{cp} * 4 + T_{cl} * 4 \quad (1)$$

$$T_p = 79,48 + 7 * 5 + 2 * 4 = 122,48 \text{ h}$$

where: T_p is the production time, $T_{p1} \dots T_{p4}$ are the individual production times, T_{cp} is the printer cleaning time, T_{cl} is the calibration time.

The actual production time is given by the relation:

$$T_{pr} = T_p * T_e \quad (2)$$

$$T_{pr} = 173,4 * 1.2 = 146,976 \text{ h}$$

where: T_{pr} is the actual production time and T_e is a risk / failure factor that may affect the production time

The amount of material used for these parts is 115.56 m of filament (281 g).

In conclusion, following the optimization and generative design, the desired landmarks were obtained through the 3D FDM printing process, resulting in a first prototype that is the basis for product development and quality improvement.

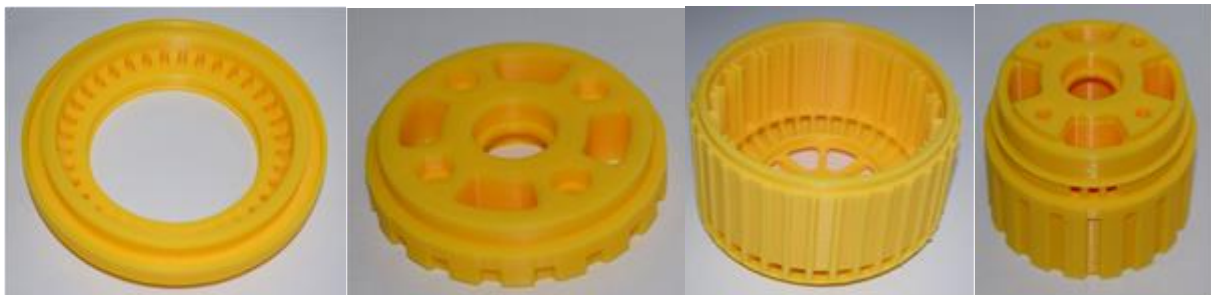


Fig. 10 Parts made
(Rotor housing cover, Stator B1 post, Housing rotor, Stator B1 post)

7. References

- [1] LYNCH T., MELA J., DC brush commutated vs. Brushless motors, PITTMAN METEK Precision Motion Control, Intern catalog.
- [2] BOCCADORO P., STRICCOLI D., GRIECO L.A., An extensive survey on the Internet of Drones, Ad Hoc Networks, Volume 122, 2021, ISSN 1570-8705
- [3] ***Modele 3D Stator/Rotor (Accesat 06.05.2022) <https://www.instructables.com/600-Watt-3d-printed-Halbach-Array-Brushless-DC-Ele/>
- [4] ***Caracterisici filament (Accesat 5.05.2022) <https://www.simplify3d.com/support/materials-guide/properties-table/?>

DETAILED DESIGN OF THE OPERATING TEMPERATURE OPTIMIZATION SYSTEM FOR ELECTRONIC DEVICES

GRĂMADĂ Victor¹, ȘERBAN Mihail-Răducu¹ and IONESCU Nicolae²

¹Faculty of Industrial Engineering and Robotics, Specialization: IEMA, Year of study: II Master,
e-mail: victorgramada@yahoo.

²Faculty of Industrial Engineering and Robotics, Manufacturing Engineering Department,
University POLITEHNICA of Bucharest

ABSTRACT: The research addresses the technical solutions chosen for the systems that make up the temperature optimization device that is the subject of the paper. The temperature monitoring and augmentation, thermal insulation and structural subassemblies work together to perform the primary function of the product. Multiple technological solutions have been considered for the design of each subassembly and the most advantageous from a technical, economic, ergonomic and environmental point of view have been selected.

KEYWORDS: electronic device; temperature; thermal insulation; sensor; microcontroller

1. Introduction

The main role of the product is to keep the temperature of the phone above the minimum optimal operating threshold [$>0^{\circ}\text{C}$]. The designed product consists of three main sub-assemblies: the heating system [Fig. 1], the structural sub-assembly and the heat-insulating case [Fig. 2]. This research is a continuation of the scientific research 3 [1] presented in the scientific communication session of 2021 in which we addressed the issues to be considered for fulfilling the main function of the product and the possible technological options to address these issues.

2. State of the art of the domain

The heating system monitors the phone's temperature and activates a set of battery-powered resistors that will operate until the minimum optimal operating temperature threshold (0°C) is exceeded. It also monitors the temperature of the electrical resistors to prevent overheating that could damage the product. When the temperature recorded by the resistor control sensor exceeds a certain value, the resistors will be deactivated.

The heat insulating cover consists of a flame retardant cotton cover that both thermally insulates the heater and the phone, as well as accommodates them and ensures the correct position of the phone in relation to the heater. Both sub-assemblies have been designed to be easily removable to allow quick intervention and repair of the product.



Fig.1. Heating system

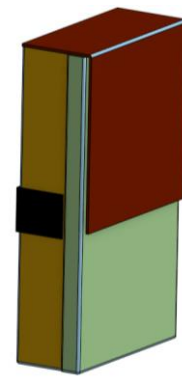


Fig.2. Heat-trapping pouch

Table 1 includes the operating parameters of the device.

Table 1. Working parameters

Item No.	Parameter	Value	Observations
1	Charging time	3.85h	At maximum charging capacity 1000mAh with 10% efficiency loss
2	Continuous functioning time	3.5h	At 0 °C
3	Start-up temperature	5°C	-
4	Overheat prevention temperature value	40 °C	-
5	Maximum temperature	35 °C	-
6	Minimum working temperature	-20°C	-

3. The problem analysed and research objectives

The objective of the research is to arrive at a final prototype design that will establish the fundamentals of the functioning of an eventual market-ready product. The problem lies in the multiple existing options for addressing each of the requirements imposed by the main purpose of the product: optimising the operating temperature of electrical devices. [1]

To achieve its primary purpose, the product must have a set of critical characteristics:

- Temperature monitoring of the electrical device;
- Heating of the electrical device once its temperature falls below the optimal threshold for operation;
- Thermal insulation of the electrical device to avoid heat loss;
- High portability;
- Use of a battery that powers the monitoring system and increases the temperature of the electrical device;

Currently, all solutions on the market that address the problem of keeping the temperature of electrical devices, specifically smart phones, within the indicated parameters are based on the principles of thermal insulation or high thermal conductivity and ventilation.

Most typical phone housings have no influence on smartphone temperature.

The best example of a case based on the principle of thermal insulation is the ClimateCase (Fig.3.) [2], which is made of 8 layers of synthetic material that insulate the phone from both high and low temperatures. This case can also be heated in the microwave or cooled in the freezer when emergency cooling or heating of the phone is needed.

A typical example of a case that works on the basis of heat dissipation and ventilation is the Mixneer case (Fig.4), [3] made of thermoplastic polyurethane. This material is cheap, durable and easily injectable, and its geometry ensures a constant airflow to the phone, thus preventing overheating.



Fig.3. ClimateCase Phonecase [2]



Fig.4. Mixneer Phonecase[3]

The product covered in this research will be the only device on the market that fulfils the role of active temperature optimisation of small electrical devices.

4. Theoretical aspects

There are two main theoretical aspects that have influenced the design process of the electrical device operating temperature optimization system:

- The Steinhart-Hart equation [4];
- Magnetic saturation of the inductor in the voltage booster [5];

The sensors chosen for monitoring the temperature of the electrical device are thermistors. Thermistors are electrical resistors whose electrical resistivity depends on their temperature. As the resistivity varies, so does the current flowing through them. The Steinhart-Hart equation is used to convert the current flowing through thermistors into degrees Kelvin:

$$\frac{1}{T} = a + b \ln R + c (\ln R)^3 \quad (1) [4]$$

where: R is the resistance of the thermistor;

T is the absolute temperature

a, b and c are Steinhart-Hart parameters and are specified by the manufacturer for each thermistor.

This equation is used in the code uploaded into the microcontroller to determine the temperature of the electrical device.

The heating elements used to regulate the temperature of the electrical device operate based on electrical resistance. In order for them to reach their maximum temperature of 55 °C, they need a power of 3W and must be connected to a voltage of 12V. The battery used in this project can output a maximum voltage of 3.7V. In order to generate the voltage required for the correct operation of the heating elements, the system must contain a voltage booster module integrated circuit. This voltage booster incorporates a metal core inductor. When current flows through the inductor coil, the metal core generates a magnetic field which increases the voltage at the current output of the coil. Magnetic materials, such as the inductor core, have a property called magnetic saturation, which is directly proportional to the strength of the magnetic field generated by the current passing through the coil. Magnetic saturation imposes an upper limit on the intensity of the magnetic field, and therefore on the current flowing through the coil. If the saturation threshold of the inductor core is exceeded, its impedance increases rapidly, causing a rise in inductor temperature, which can cause accidents or circuit destruction. This principle limits the amount of voltage rise the voltage booster can provide to increase the efficiency of the heating elements. [5]

5. The proposed solution

The system for optimising the operating temperature of electrical devices is composed of 3 sub-assemblies: the temperature monitoring and raising system, the heat-trapping pouch and the structural assembly.

The temperature monitoring and raising system is structured according to the sketch in [Fig. 5]:

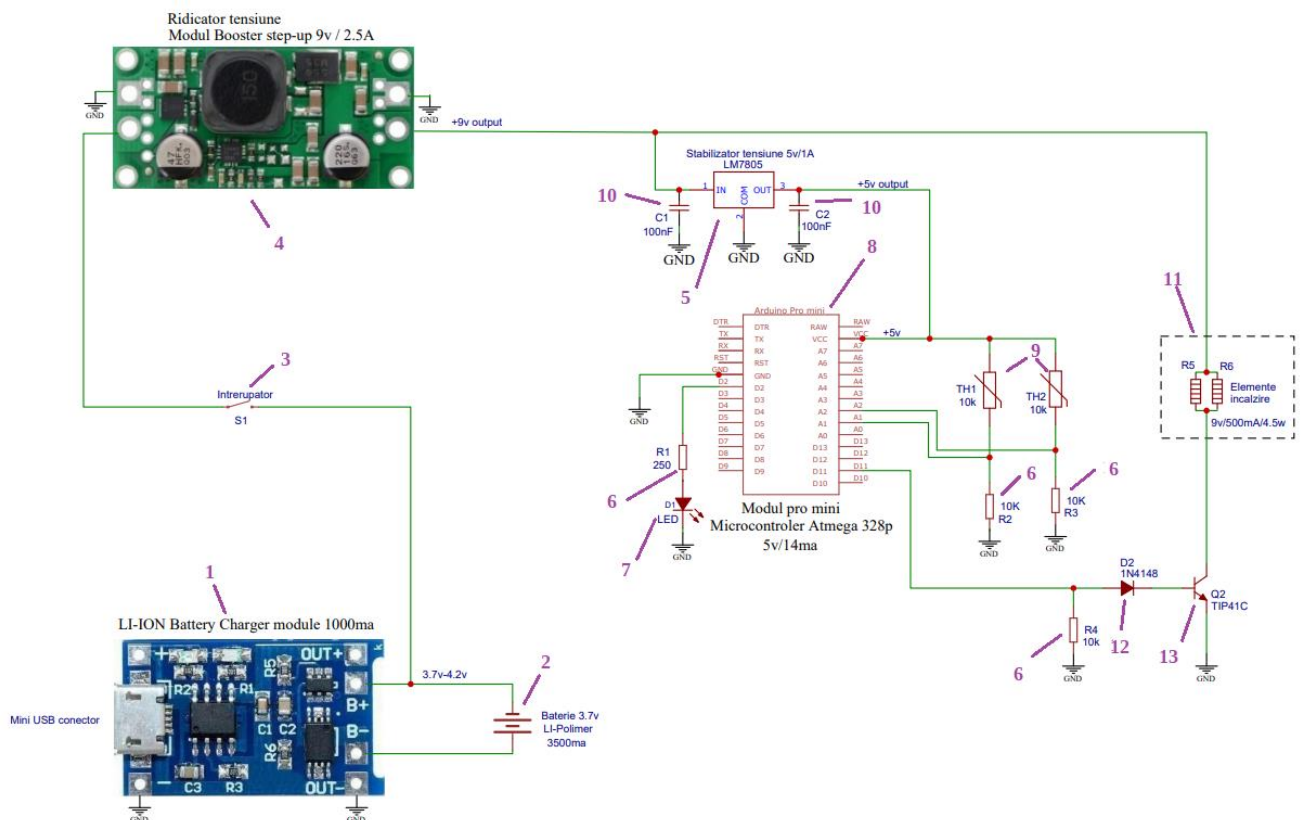


Fig.5. Electrical scheme

The main purpose of the electrical system is to heat the phone when its temperature falls below the optimal operating limit. The temperature of the phone is monitored by one of the thermistors (9) and the second thermistor monitors the temperature of the heating elements (11).

If the temperature of the heating elements becomes dangerously high, the thermistor monitoring the temperature will send a signal to the microcontroller (8) to turn off the power.

Thermistors are electrical resistors that have the property of changing their resistivity as a function of temperature. The current flowing through them changes inversely with the resistivity of the thermistor. Both thermistors are connected to the microcontroller. The microcontroller is programmed so that if the current received through the thermistors exceeds a preset value, it will send current to the transistor (13) to open the circuit branch containing the heating elements. If the current intensity from the thermistors read by the microcontroller exceeds a certain value, the microcontroller will send current to the LED branch (7) to signal the operation of the heating elements.

The microcontroller requires an operating voltage of 5V and the heaters require a maximum operating voltage of 12V. The battery (2) generates a maximum voltage of only 3.7V. For this reason it is necessary to implement a voltage booster (4) to generate the required operating parameters for the heating elements. The 12V voltage resulting from the voltage booster is too high for the microcontroller to operate. A 5V voltage stabiliser (5) will be used to bring the voltage back to the 5V value required by the microcontroller.

To facilitate charging of the battery operating on DC power from an AC power source, a battery charging module (1) used in most applications involving lithium-ion batteries is required.

The circuit breaker (3) is intended to allow the user to close and open the electrical circuit.

Capacitors (10) are designed to take up residual current fluctuations in the circuit remaining after charging from an AC source.

Diodes (12) and resistors (6) are intended to prevent reversal of circuit polarity and to protect components.

The heat-trapping pouch (Fig. 6) performs the following roles:

- thermally insulates the phone and heater against low temperatures;
- maintains the correct position of the phone in relation to the heater;
- protects the phone against mechanical shocks or abrasions;

Cotton has been chosen as the material for the heat-trapping pouch because it is the most effective thermal insulation material readily available on the market. The fabric is flame retardant due to the risks associated with housing an electrical heating system.

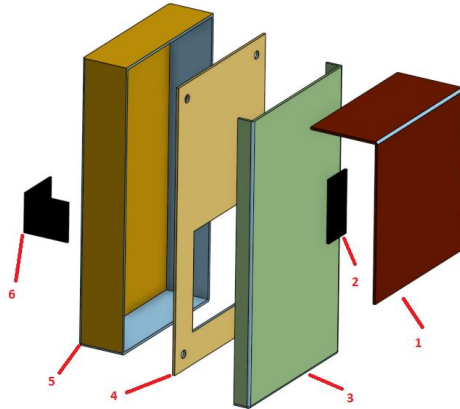


Fig.6. Heat-trapping pouch



Fig.7. Heating system housing

The structural assembly consists of the housing, the fasteners and the copper heat transfer plate. The enclosure cover [Fig. 9] and the enclosure base [Fig. 10] can be seen in the construction drawings attached to the work as well as in [Fig. 7]. The housing is manufactured by FDM additive manufacturing technology from PETG material. The material and manufacturing method were chosen due to the low cost, PETG properties of mechanical strength and high melting point compared to alternatives and low electrical conductivity of the material which does not create a short circuit hazard of the electrical system. Assembly of the cover and housing base is done with M2.5 screws and nuts to provide easy access for modifications and maintenance. The enclosure is secured in the thermal insulation cover by passing the head of the screws through the holes in the inner membrane. Afterwards, the screw heads will be covered with cotton patches to prevent scratching the electrical device. The fixing solution will be modified once the product passes the prototype stage to generate a small footprint and a pleasing appearance. The heat transfer plate will be installed in the housing next to the window to prevent direct contact between the resistors and the electrical device or user.

6. Conducting experiments and interpreting results

Initially, a design variant of the temperature monitoring and raising system was considered that would be purely electronic (Fig. 8), without being controlled using a microcontroller.

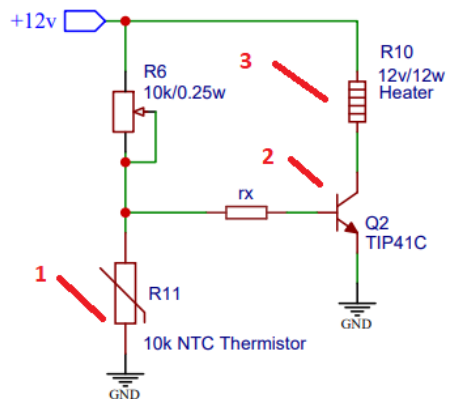


Fig.8. Tranzistor based electrical scheme

Both operating variants perform exactly the same role of monitoring the temperature of the electric device and activating the heating system under the necessary circumstances. The difference between them is that the variant with the transistor-based operating principle controls the heating of the resistors (3) by means of a transistor (2) which allows current to flow through the resistor branch only when the thermistor (1) allows a current of a specific transistor current to flow.

The microcontroller-based version was preferred because of its high versatility. If it is desired to change the operating parameters of the system, the operating code uploaded in the microcontroller can be easily modified. In the variant without microcontroller it would be necessary to change the resistivity of the variable resistor R6 and measure the current intensities after each change to calibrate the circuit.

7. Conclusions

The temperature measurement and augmentation system will operate according to the microcontroller-controlled design version due to the high degree of versatility it offers, without imposing a significant cost increase. The housing will be made by FDM manufacturing technology, using PETG material due to the design-suitable properties of the plastic material. The heat-trapping pouch will be made of flame retardant treated cotton due to its good thermal insulation properties and to avoid accidents or damage to the product.

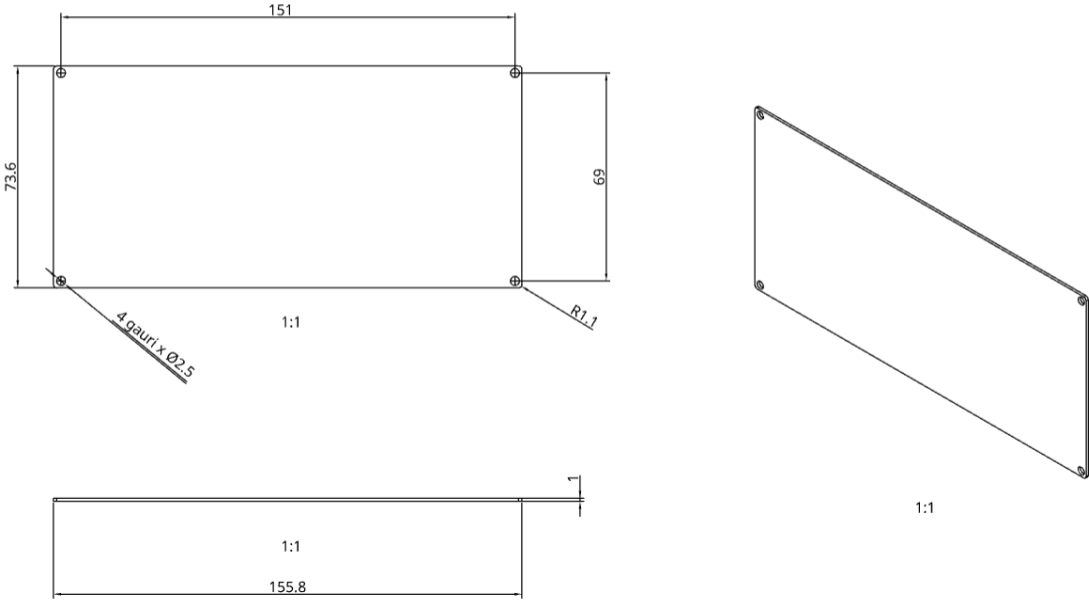


Fig. 9 Case lid drawing

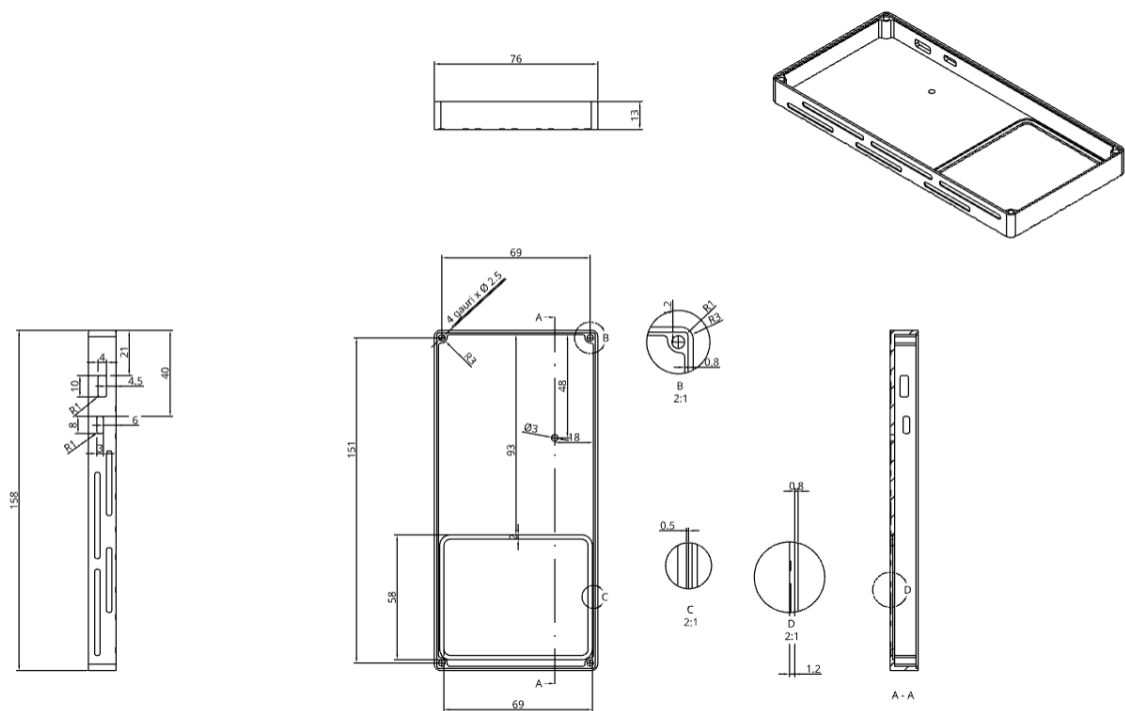


Fig. 10 Case base drawing

7. References

- [1] GRĂMADĂ Victor, ȘERBAN Mihail-Răducu, (2021), "Proiectarea detaliată a sistemului de optimizare a temperaturii de funcționare a dispozitivelor electronice"
- [2] ***, <https://climatecase.com/>, accessed on the date of 12.05.2022
- [3] ***, <https://www.ubuy.com.ro/en/product/1GC5N4Z5C-heat-dissipation-phone-case-new-breathable-hollow-cellular-hole-heat-dissipation-case-full-back-camera-lens-protection-ultra-slim-tpu-case-cover>, accessed on the date of 12.05.2022
- [4] Matus, Michael. (2013). Temperature Measurement in Dimensional Metrology – Why the Steinhart-Hart Equation works so well.
- [5] Vladimir Makarenko, Olexy Lukashev. (2021) Analysis of the Influence of Inductor Saturation on the Level of Electromagnetic Interference of DC/DC-Converters

DEVELOPMENT OF A SMART WALLET

MARIA Geni¹, CHISELEFF Alexandru-Nicolae¹, CREȚA Gheorghe-Cosmin¹, PĂUN Ionuț-Alexandru¹, PAȘAVEL Sînzian-Albert¹, POPA Bianca-Alexandra¹, SPIROIU Marius Adrian², ABAZA Bogdan Felician³ and DIJMARESCU Manuela-Roxana³

¹Faculty: Industrial Engineering and Robotics, Study program: Engineering and Management of Complex Projects, Year of study: 2, e-mail: maria.geni98@yahoo.com

²Faculty of Transports, Railway Vehicles Department, University POLITEHNICA of Bucharest

³Faculty of Industrial Engineering and Robotics, Manufacturing Engineering Department, , University POLITEHNICA of Bucharest

ABSTRACT: Today, electronic payments are used in large numbers, in some cases you do not even need physical cards to make them because you can pay directly by phone at contactless POS or online in e-commerce. However, cash does not appear to be disappearing from the sale-purchase of goods and services too soon. Therefore, there is a need for an object to help store and transport payment instruments - the wallet - the best solution to keep these objects safe. Present research work includes development regarding a product to meet the need for permanent security payment instruments and identity documents, and at the same time, to keep up with technology that is in constant development.

KEYWORDS: smart wallet, secure opening, fingerprint sensor, security

1. Introduction

The security branch is constantly evolving, with humanity using technology to ensure the highest possible security of both people and personal property. Examples that reinforce this statement are commonly found and used.

Technology is extremely important for improving security. Without cameras, detectors and alarms, businesses would not be able to identify threats and respond appropriately. For today's organizations facing current threats, it is essential to have a complete view of operations and at the same time in detail, at all times.

Having as a starting point this constant need for security that each of us has, it is proposed to develop a product that will help meet this need. Therefore, the following will be the developments made in order to obtain a product called SECURITY WALLET, a smart wallet that has a different locking system than a regular wallet and a warning system to ensure the owner more security of valuables stored in it.

2. Business strategy

Business strategy is the detailing of the complete method by which the organization achieves its objectives. It includes elements related to: the company's vision and mission, market positioning, work systems and internal processes, quality and skills of the team, how to manage financial issues. The strategy is long-term oriented and is the most important ally of the manager throughout the business cycle [1].

Following the research, the needs of potential buyers were identified and centralized, needs synthesized for the product to be developed as shown in Table 2.1.

Table 2.1 Need analysis

Need expressed	Need Characterized	
	Parameter	Associated value
To be cheap	Price	<500 lei
Easy to use	Detection matrix	450-550 DPI
To have a small size	Overall size	145 x 100 x 30 mm
To have a low weight	Weight	220 - 250 gr
Nice look	Design	Leather / Black / Brown
Long period of use (Autonomy)	Minimum	Minimum time 48h / charge

Need expressed	Need Characterized	
	Parameter	Associated value
		for use of the product at least 15 times a day
	Battery capacity	3350 mAh
Be durable	Material	Aluminum
Stop contactless	function Lock function	Lock 100%
Locate	GPS	Application (Maximum range = 1000 km)
	BUZZER	3900 ± 500Hz
Connectivity	pairing	Bluetooth
Charge quickly	Time	40-80 min
Know the location and percentage of the battery	Application	Real time
Be durable	Product durability	10,000 openings
Efficient	Number of compartments	3-10 compartments
Have a single user	Fingerprint sensor	192 * 192 pixels

Data in Table 2.1. served as estimates of the performance that the product proposed for development should meet.

The environmental elements and the interfaces of these elements with the *SECURITY WALLET* are presented in the following table:

Table 2.2. Environmental elements and their actions

Environmental elements	Actions of the environmental element
User	Helps to perform the main function
Surfaces	Ensures the storage of the wallet
Charger	Ensures the loading of the wallet
Goods / Objects stored	Helps to perform the main function
Eyes	Helps to identify the design
External environmental elements	Helps to identify materials and their protection
Physical objects	Helps to identify external material
GPS	Helps to locate the wallet
Rules and regulations	Helps to comply with norms and regulations

When defining the functions of the system, the system's relations with the environmental elements were followed, as shown in figure 2.1.

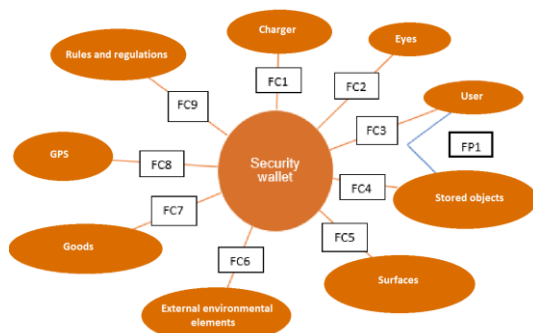


Fig. 2.1. Relationships of the system with the environmental elements

- FP1 - Ensures the protection of personal property;
- FC1 - Allows to load your wallet;
- FC2 - Be aesthetic;
- FC3 - Easy to use;
- FC4 - It adapts to stored things;
- FC5 - It adapts to different surfaces location;
- FC6 - Resist the elements of the environment outer;
- FC7 - Be resilient;
- FC8 - Allows the user to locate wallet;
- FC9 - Rules and regulations;

Following the ranking and analysis of these functions, it turned out that the first function, which ensures the user the protection of personal property is the most important, and to achieve the concepts related to the project will respect this function.

Market segmentation is a marketing term that refers to the division of customers into groups or segments with common needs [2]. Depending on the age of potential customers, we segmented the market into several sub-criteria, as shown in Table 2.3.

Table 2.3. Market segmentation

Age	16-20 years	21-45 years	> 45 years
Occupation	Pupils, students	Students, Skilled workers from different fields of industry	Unskilled workers, Skilled workers from different fields of industry, Retirees
Income	500-1500 lei	2600-6500 lei	1500- 3500 lei
Open to technology	Quite interested	Very interested	Less interested
Lesson contents	Identity card, Health card, Means of transport card, Banknotes	Identity card, Driving license, Health card, Bank cards, Banknotes, Business card, Subscription, etc.	Identity card, Health card, Pension coupons, Banknotes, Means of transport card, Driving license
Frequency of use	<5 times / day	6-10 times / day	1-3 times / day
Design / Quality	Important	Very important	Not important
The degree of necessity of the product	from time to time	Constant need to use the product	Sometimes
Availability of this product	Medium	Large	Small

According to statistics, both females and males have the same degree of interest. regarding the purchase of such a wallet because I feel the need to keep their belongings safe. Women buy their wallets more often, having a more developed sense of diversity than men, who choose the model of the wallet according to the colors of the bags or outfits they wear, while men prefer to buy a wallet less often, but with more advanced security features such as the product proposed for development.

In conclusion, we can say that the most favorable market segment for the sale of the product proposed for development is made up of potential customers in the age category 21-45 years, because they have a much higher degree of interest than the other categories, having a much greater openness to technology.

The customer profile essentially refers to a description of the type of customer the business wants. By creating a customer profile, it is easier to identify which products and services are best for him and how they can be presented effectively [3].

Following the analysis resulting from the market segmentation and the choice of the target segment, the customer profile presented in table 2.4 was developed.

Table 2.4. Target customer

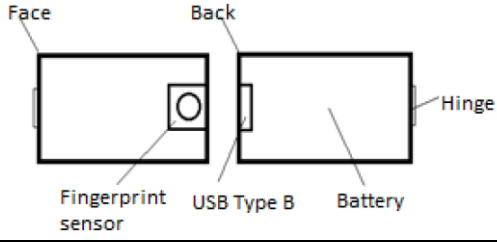
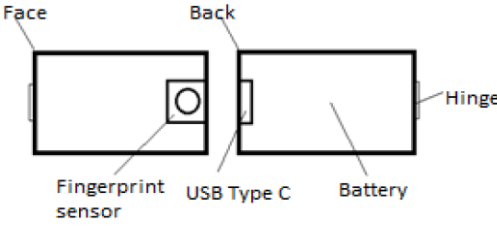
Customer profile	
Age	21-45 years
Payment method Most commonly used	Bank card
Make the most of purchases	In stores
Use wallet	Yes
Goods / Items stored in wallet	Identity card, Driving license, Health card, Bank cards, Banknotes, Service Card, Subscriptions, Etc.
Openness to technology	Very interested
The importance of the appearance of the wallet	Very important
The importance of the need for security	Very important
The purchase of a security wallet	Yes
Frequency of use	6/10 times a day
Expectations	Quality / Easy to use

3. Concurrent concepts

A product concept is the answer to a request product for specific target customers, which meets basic needs and a coherent set of other needs, where the product is defined, the differentiation fields and the benefit profile. [4]

Six technically possible solutions have been developed to fulfill the functions of the product. Below are 2 of them, the ones that best meet the requirements.

Table 3.1. Technically possible solutions

Nr.crt.	Fig.	Outline	Description
1	3.1.	 <p>Face Back Hinge Fingerprint sensor USB Type B Battery</p>	The wallet will be powered by a USB Type B charger, with energy stored in a battery. The wallet will be opened with the help of the fingerprint sensor, which stores the user's fingerprint, and then the user can store their money, cards, etc. inside the wallet. It can only be accessed by recognizing the user's fingerprint.
2	3.2.	 <p>Face Back Hinge Fingerprint sensor USB Type C Battery</p>	The wallet will be powered by a USB Type C charger, with energy stored in a battery. The wallet will be opened with the help of the fingerprint sensor, which stores the user's fingerprint, and then the user can store their money, cards, etc. inside the wallet. It can only be accessed by recognizing the user's fingerprint.

Following the analysis of the criteria (production costs of components, security of objects / goods, battery charging time, energy storage method for power supply, ease of use of the product) and analysis of concepts and their comparison, we chose for further development, concept number two, which takes into account most of the expressed needs of consumers.

4. Technical solution development

The "Security Wallet" product is a gadget that uses technology to amplify the security need that each person has. The product consists of subsystems that make it easy to use, but also efficient. Figure 4.1 shows the numerical model of the product developed with the help of CATIAV5 software, and the list of its main components can be found in table 4.1.

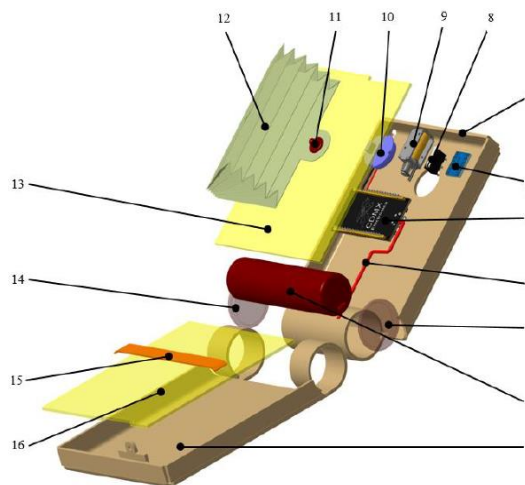


Fig. 4.1. Presentation technical solution components

Table 4.1. Component list

No. crt.	Name	No. Buc .	Specifications		Function / Role
1, 7	Housing	2	145 x 100 x 30 Material: Aluminum		Provides protection and support of goods and components
2	Battery	1	Capacity: 2600-4999mAh Interface: USB	Weight: 74.5g Size: L91 * D25	Ensures wallet autonomy
3, 14	Plug	2	26 x 4 x 30		Ensures battery protection / Fixing
4	Wires	≅10	-		Ensures connections between components
5	Motherboard	1	Max Input Voltage: 24V Model: ESP 32 GPIO pins: 11 1 pin ADC (0V to 3.3V)	Frequency of operation: 80/160 MHz Flash memory: 4MB Size: 34.2 x 25.6	Ensures wallet operation and functions
6	Logic converter	1	-		Allows the connection of two logic components even if they have different electrical potential
8	Micro-switch	1	Material: Plastic and lamella Aluminum		Shutter release solenoid
9	Solenoid	1	Voltage: 5V : 1 sec	27 x 29 x 18 mm Shock absorber height: 10mm	Secures wallet lock and unlock
10	Fingerprint sensor	1	Voltage: DC 3.3 V Module size fingerprint: 22 mm	Detection matrix: 192 x 192 pixels LED control: Yes	Ensures the protection of the goods inside the wallet and its opening
11	Staple	1	-		Ensures the catching of the fan for the cards
12	Support fans	1	Capacity: ≅ 8-10		Ensures the storage of the cards
13, 16	Plate	2	120 x 100 x 2 Aluminum		Provides support for the card fan and the elastic band
15	Elastic band	Material	5 x 110		Provides support for goods

- The prototype ensures an increased security compared to an ordinary product, both through the locking systems, which allow only the user to open it with the help of the fingerprint sensor and by locating it, in case of theft / loss;
- The user places his finger on the fingerprint sensor (10).
- After recognizing the wallet holder's fingerprint, the battery-powered solenoid (9) retracts (2), unlocking the housing hinge (1/7), allowing them to open the wallet and access the stored goods, or in the fan support card (12). , or stored on the opposite side, supported by the elastic band (15).
- When the user wants to close the wallet, it brings the two sides of the case closer (1/7), allowing the solenoid (9) to return to its original position.

5. Prototyping and testing

On the prototyping and experimentation side, the components necessary to make the product were purchased and the program for its functionality was developed.

In the first stage, the components have been tested with each other, and we are currently working on the program for the functionality of the product.

We also went on to 3D print the wallets of the wallet to have a better view of the space and the positioning of the components.

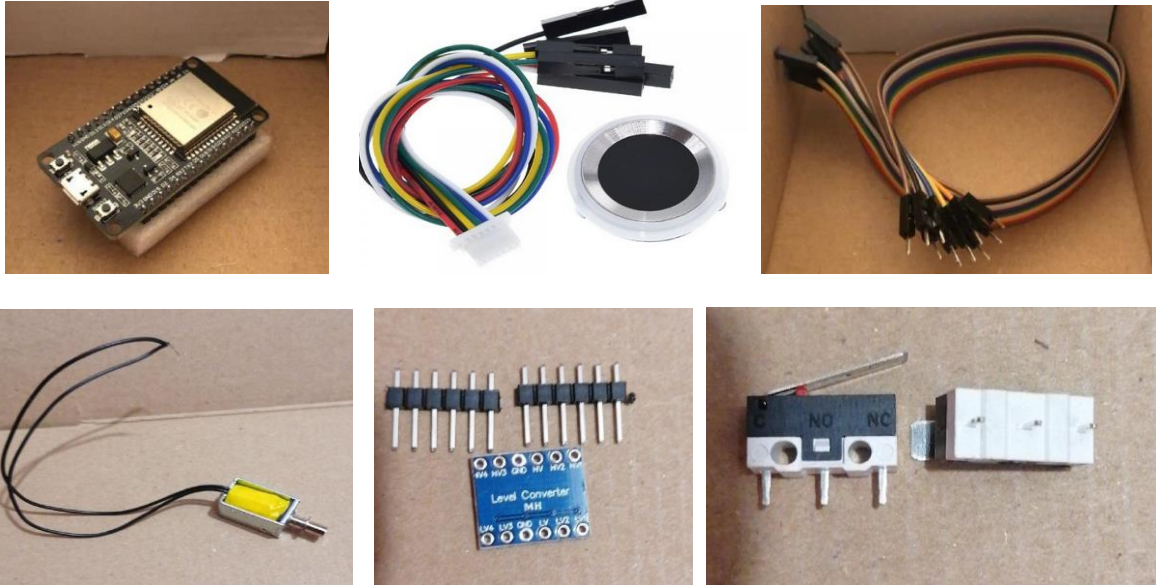


Fig.5.1. Purchased components necessary for the production of the product

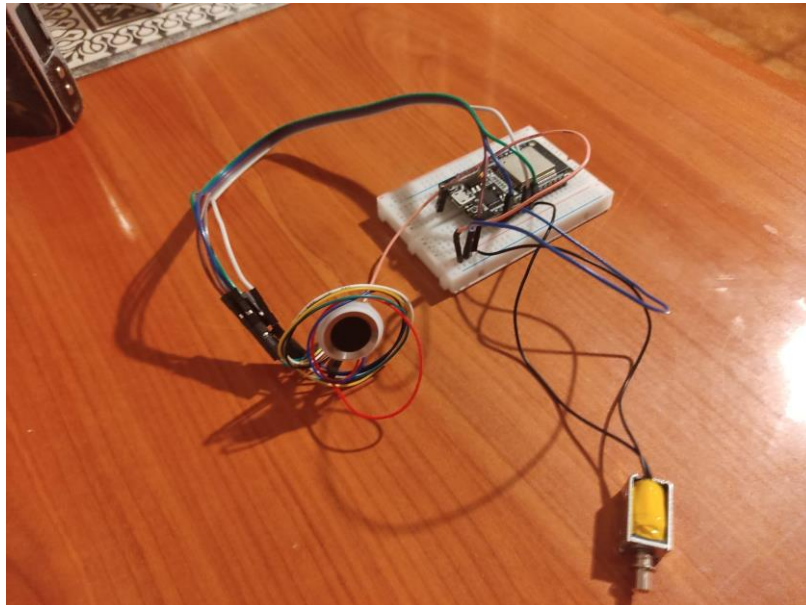


Fig.5.2. Functional realization of the product

6. Economic analysis

Following the research carried out for the acquisition and production of the necessary components, the costs necessary for the production of the product were identified (production costs, selling price, break-even point).

Table 6.1. Costs

Type of cost	Value	U.M.
Fixed costs	38161	Lei / month
Variable expenses	303	Lei / piece
Total unit cost	458	Lei / piece
Sales price	641	Lei

Analyzing the costs, we will reach the break-even point in August of the current sales year, therefore we will make a profit. These things are shown in the image below:

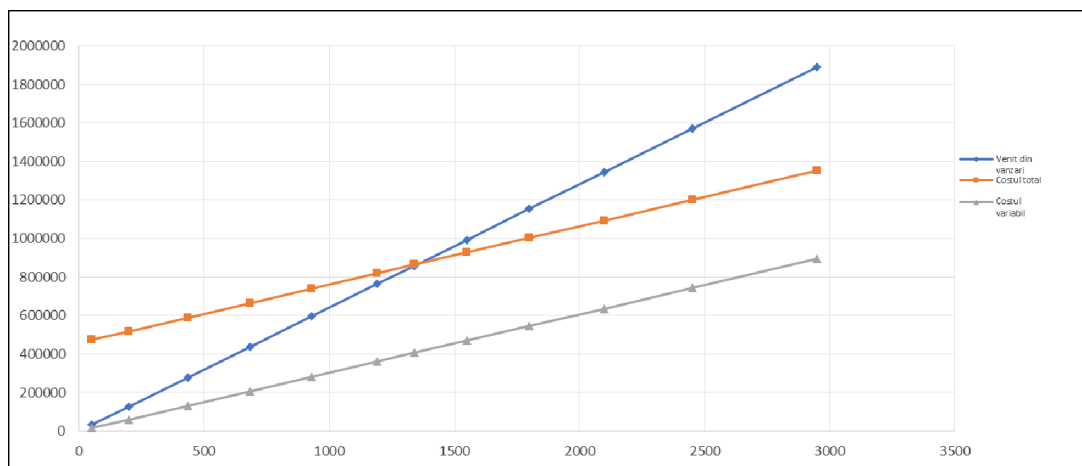


Fig. 6.1. Break even

6. Conclusions and perspectives

The research paper highlighted the developments made so far in the project that the authors are carrying out during years I and II of the master's program Engineering and Management of Complex Projects. The project focuses on the development of a smart wallet product that keeps up with technology in the field of security.

The main objective of this product was to base the research conducted in the master's program on the development of an innovative product that integrates three main subsystems - mechanical, electrical / electronic and software.

The research paper started from the presentation of the needs expressed by the respondents of the questionnaire and those resulting from studies conducted by specialists in the field of security and technology, which are carefully analyzed to obtain a good characterization of them. Analyzing the needs they have, we have identified the functions that our product should fulfill.

Following the analysis resulting from the market segmentation and the choice of the target segment, we made the profile of the target customer, according to well-established criteria.

Analyzing all these needs, we have developed six technically-possible solutions to fulfill the functions established for our product, and after analyzing the ranking of criteria and concepts and comparing them, we chose for further development the concept number two, taking into account the opinion expressed by consumers.

In order to make the prototype of the technical solution, research was carried out to find the components necessary to satisfy the functions and needs, their compatibility and their realization.

In the experimentation phase, the components were purchased, tested individually and the aim is to make a functional prototype.

The last section of the paper presents the costs related to the production of the product and the break-even point, which will be reached in August of the current sales year and a profit will be obtained.

As a final conclusion we can say that we tried to bring in tune with technology, an object that each of us uses almost daily.

Future developments will focus on the prototype of the proposed product.

7. References

- [1] ***<http://www.agoraconsulting.ro/strategie-de-business/hiddenfromyou.html?69c7286e178bf f b56d57763689e5ff2a>, accessed on 28.04.2021;
- [2] ***<https://www.business-academy.ro/cursos-planificare-si-segmentarea-pietei#>, accessed on 03.05.2021;
- [3] ***<https://antreprenoriat101.ro/profilul-clientului/>, accessed on 08.04.2021;
- [4] Abaza Felician Bogdan, Project Management 1/2 (2020-2022) - Course notes, IMPC Master, UPB;
- [5] *** [http://www.repository.utm.md/bitstream/handle/5014/2015/Conf_UTM_2016_II_pg157_159.pdf?Sequence=1 & isAllowed = y](http://www.repository.utm.md/bitstream/handle/5014/2015/Conf_UTM_2016_II_pg157_159.pdf?Sequence=1&isAllowed=y), accessed on 04.05.2021;
- [6] *** <https://laiuadrian.weebly.com/dezvoltarea-rapid259-a-tehnologiei-informa355iei-icircn-secolul-xx.html>, accessed on 15.04.2021;
- [8] *** <https://ro.eyewated.com/scanere-deget-ce-sunt-si-de-ce-castiga-in-popularitate/>, accessed on 11.02.2021;
- [9] Dijmărescu Manuela Roxana, Development projects 1/2/3 (2020-2022) - Course notes, IMPC Master, UPB;
- [10] Stanciu Camelia, Development of innovative products and services 1/2 (2020-2022) - Course notes, IMPC Master, UPB;
- [11] Spiroiu Marius, Value Analysis (2021-2022) - Course notes, IMPC Master, UPB.

Acknowledgement

The authors would like to thank to Associate prof. Camelia STANCIU from Thermotechnics, Thermal engines, Energy and Refrigeration Equipment Department, Faculty of Mechanical Engineering and Mechatronics, for the support and guidance in completing this research.

LI-ION AUTO BATTERY TEMPERATURE MONITORING DEVICE

VĂLIMĂREANU Benjamin¹, SAVCA Stelian¹, BUGHIANU George¹, VĂDUVA Rareș¹,
GRIGORE Dănuț¹, OPRAN Constantin Gheorghe² and ILIE Cristian

¹Faculty: Industrial Engineering and Robotics, Specialization: INPN/ IAAC/ IEMA, Year of study: 2,
e-mail: valimareanubeney@yahoo.com, steliandsavca1997@gmail.com,
robertbughianu@gmail.com, grigore_danutz92@yahoo.com

²Faculty of Industrial Engineering and Robotics, Manufacturing Engineering Department

ABSTRACT: This work presents research on Intelligent Monitoring of Li-Ion batteries by analyzing their behavior under the influence of temperature in order to optimally maintain their functional parameters. The strategy for implementing an integrated temperature monitoring system is presented, in particular, if the permissible critical value is exceeded. The system consists of a structure that has the role of protecting and supporting the battery and an electronic monitoring equipment. Their purpose is to bring the temperature inside the operating system to a normal level, which does not affect the parameters of the battery. It is intended to prevent the risk of explosion or ignition, given that the structure of the battery contains chemicals that promote combustion and whose temperatures can reach up to 500 ° C. An important element of the intelligent system is the heating source which has the role of maintaining the battery temperature above a lower critical temperature under special operating conditions.

1. Introduction

The system for monitoring the temperature of the Li-ion battery consists of several elements such as: cooling source (fan), heating source, elements for mounting the system, the lower part of the housing and the housing cover, which is removably assembled from the lower part to allow you to change or check the battery later. The housing is made of a plastic with very good resistance to high temperatures (over 100 degrees Celsius) to withstand and operate in extreme environments. The dimensions are made according to the dimensions of the battery, so that the space between it and the inner surfaces of the housing is large enough to allow air to pass through (> 10-30 mm). The thickness is considered to be between 3 and 4 mm, which leads to a high strength of the system. There are also openings in the housing to allow the output of positive and negative terminals and a slot for mounting the fan, as well as an opening to remove air from inside. The devices for cooling and heating the battery are of the electric type and are connected directly to the battery, no need for an external source to power them. The fan used is chosen so that the volume of air supplied by it is more than sufficient for cooling and thus for the normal operation of the battery. It is also taken into account that its voltage value does not exceed 12V, and the number of rotations and the number of decibels (dB) it generates should not exceed a maximum value.

3. Materials for making products

The components of the device are made mostly of high temperature resistant plastics and have a good resistance against shocks and vibrations given the environment in which it operates, namely the engine compartment of a vehicle. The product design diagram is shown in figure 1.

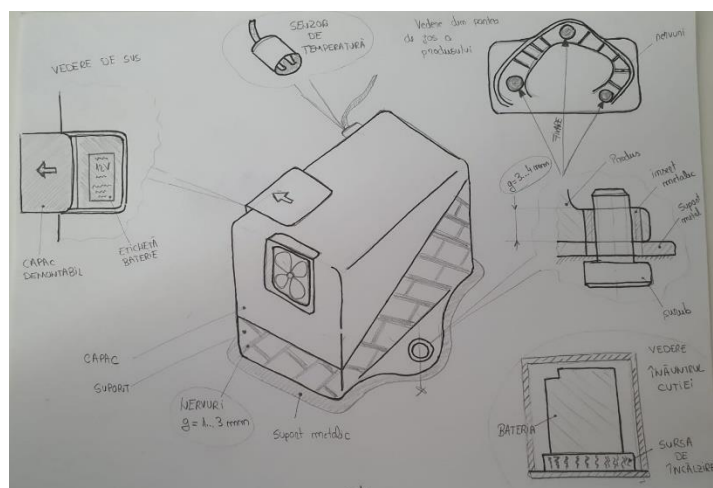


Fig.1. Product design scheme

The fixing of the casing will be done using a screw and a metal insert inserted in the plastic material, in the 3 areas it will be taken over all degrees of freedom. The thickness of the piece is about 3-4 mm to be resistant to shocks, vibrations, etc. and rib thickness 1-3 mm. The product is equipped with a simple temperature sensor that will signal when the battery temperature is critical. The removable cover (left side) is required so that the operator can see the details of the battery inscribed on its label.

The components of the device are:

1. bracket (bottom of the case)
2. cover (top of the case)
3. removable cover (side) - necessary for the operator to see the details of the battery marked on its label
4. metal inserts x3 (bottom) - required for assembling the product
5. x3 screws
6. main pipe (made of 2 components - the lower part and the upper part)
7. fan
8. temperature sensor
9. 12V battery

4. Assisted design

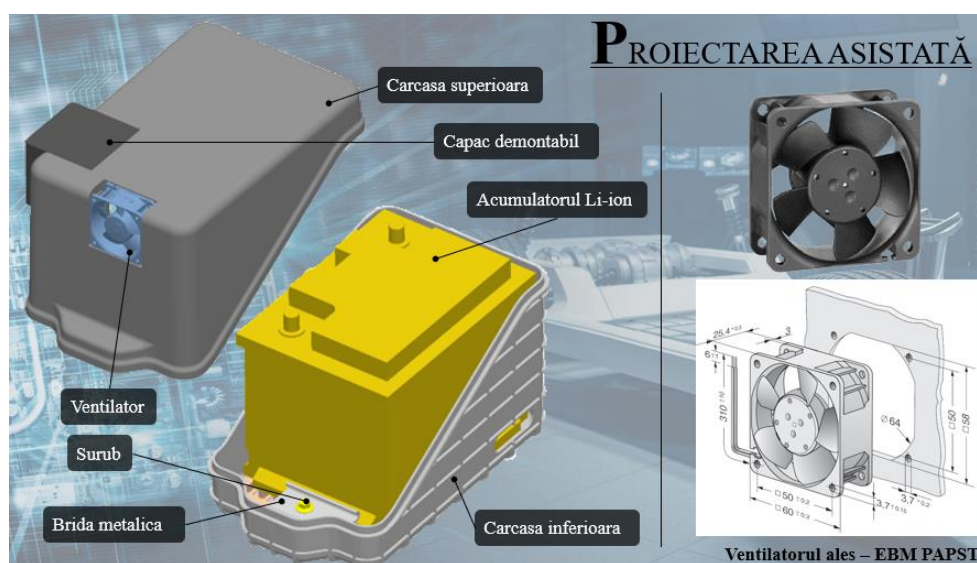


Fig. 2 - 3D design of the optimal product concept

5. Modeling - simulation

Modern engineering is so specialized and products so complex that it is difficult for a single person or team to design a product. Designers are increasingly using computers and software applications, with software being the catalyst that has revolutionized this process.

Initially, the computer was used to make drawings, a technology that later became computer-aided design (CAD) -based design. Subsequently, 3D representations of the parts that are part of the products were created. The next step was to take these models and run them on numerically controlled machines, and finally to process them on computer-aided machines. The methods used during product design involve software specific to mechanics, electronics, or design control methods and involve the ability to convert the model from one type of software to another. Standards have been developed to allow this, but sometimes the results have not been as expected, so the next step in the process is to unify the design, manufacture of components and management with the physical behavior of the product.

The process gives engineers the opportunity to be involved not only in the design and execution of the product, but also in the management of systems capable of simulating their performance, the result being the so-called virtual prototyping. Increasingly, simulation has taken the place of physical product testing, so more and more software packages specific to engineering design have included modules that allow the application of simulation techniques.

Simulation of air flow and temperature

Initial data

The own contribution is the simulation of the air flow inside the housing, the definition of the parameters necessary for the simulation, as well as the realization of short presentations containing the simulation results and their interpretation. We have made sure that the battery temperature does not exceed 70 degrees Celsius in order to operate normally.

The simulation of the air flow inside the product (housing) was done in a software that contains a special module for its realization. For this study to be correct, it is necessary to define all the necessary parameters to be able to achieve air flow, such as: initial solid temperature, ambient temperature, type of fan used, pressure inside the housing, areas through which air is evacuated from inside as well as the area through which it enters the air duct. At the same time, we considered that the housing type product should be completely sealed, without air leaks.

His own contribution to this work is the simulation of the air flow inside the housing and the interpretation of the results.

The results of the simulation are presented below.

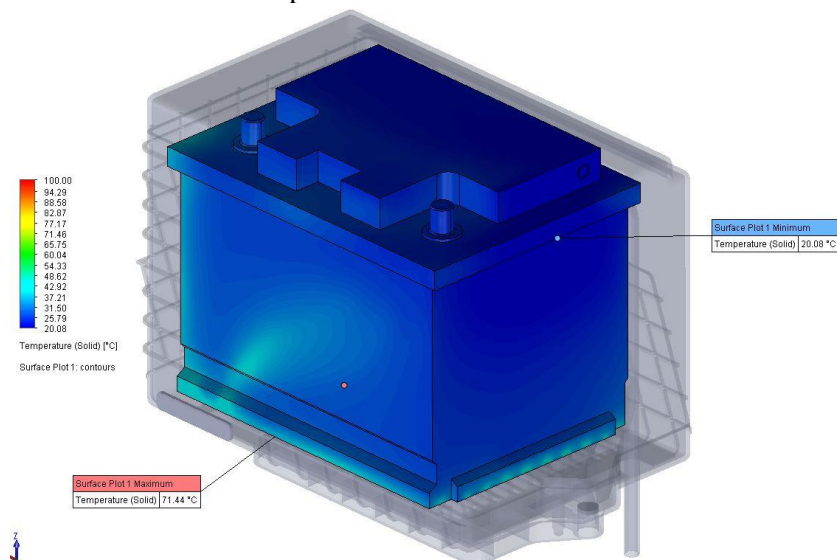


Fig. 3 - Battery temperature after simulation with fan on

A maximum temperature of approximately 71.5 °C (on the bottom surface of the battery) is observed following the simulation with the fan on and a minimum battery temperature of 20 °C, a temperature present on the surface in the immediate vicinity of the fan. The metal support on which the battery rests has a great influence on the temperature, being made of a metal, it has a much higher thermal conductivity.

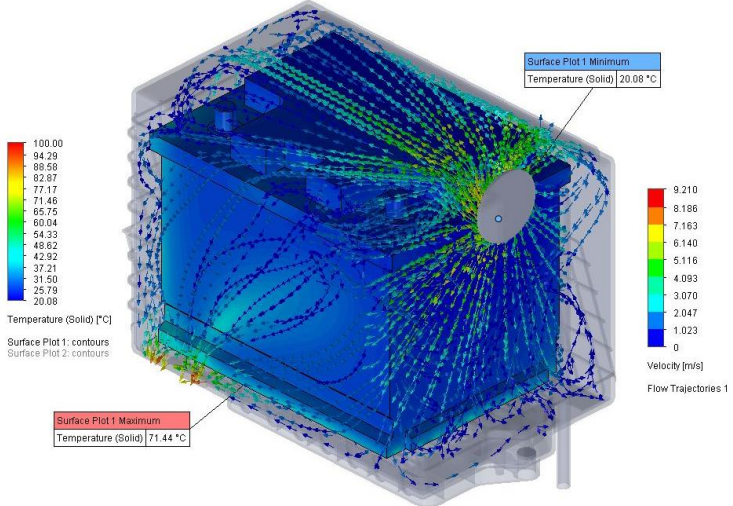


Fig. 4 - Simulation of the air flow inside the housing and the temperature of the battery with the fan on

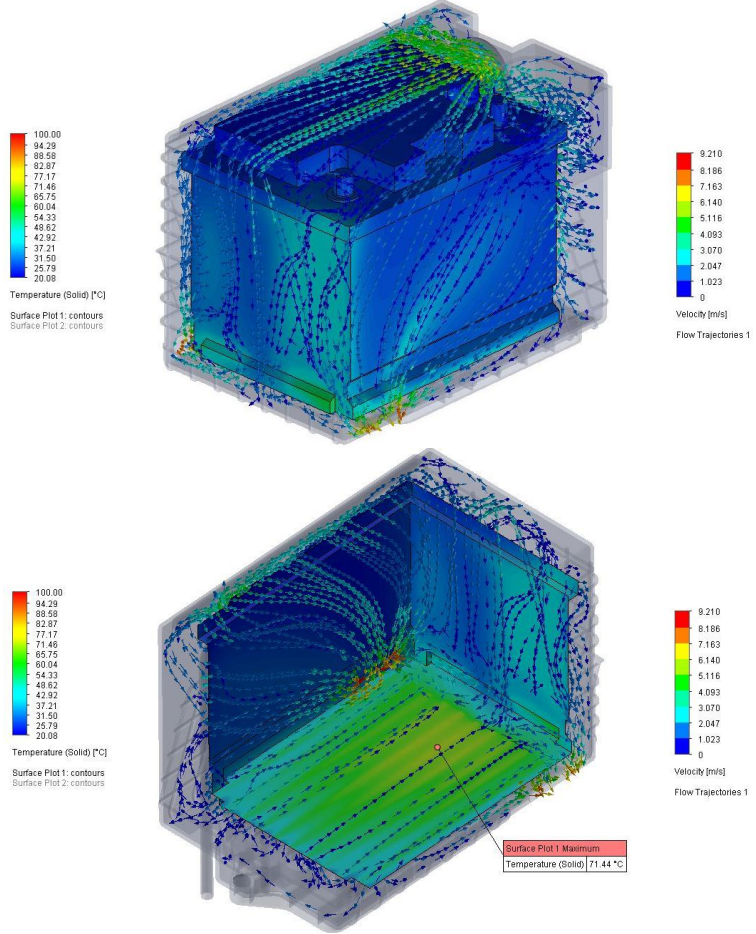


Fig. 5 - Flow directions and air velocity inside the housing (fan on)

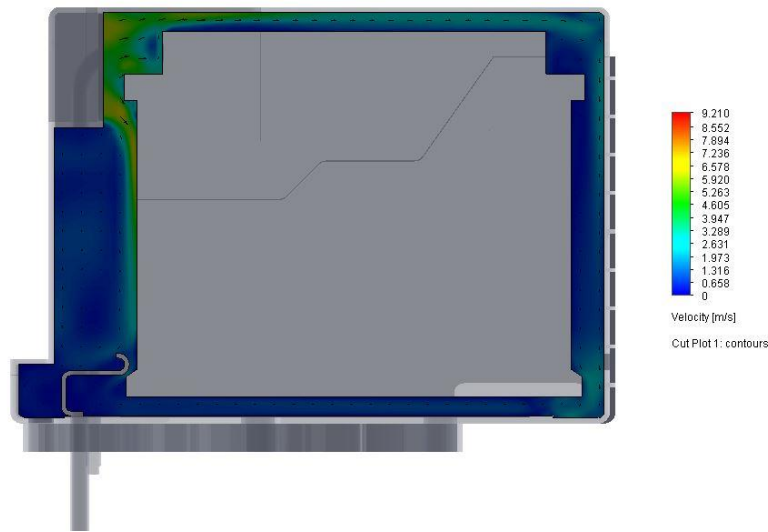


Figure 6 - Distribution of air velocity inside the housing (fan on)

The above figures show, as expected, a higher air speed in the fan area and a higher temperature of the fluid inside in the area where its speed is very low (bottom). The metal support is necessary to raise the battery to a certain height to allow the air to reach all surfaces, especially those in the lower area, where the temperature has the highest value.

The following study refers to checking the battery temperature when the fan is switched off and the airflow is generated only by the speed of the moving vehicle through an air duct, as shown in the figures below:

A very high value of the battery temperature is observed, of approximately 89°C in its lower area, a value that influences its life and possible danger of explosion. This is the main reason why I chose to use a fan, as small and efficient as possible, which does not involve high costs and which reduces the battery temperature by a considerable amount.

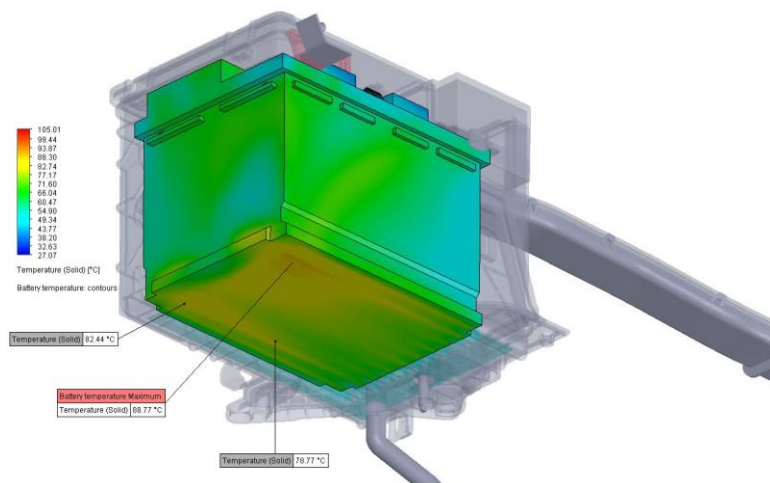


Fig. 7 - Battery temperature resulting from simulation with fan off

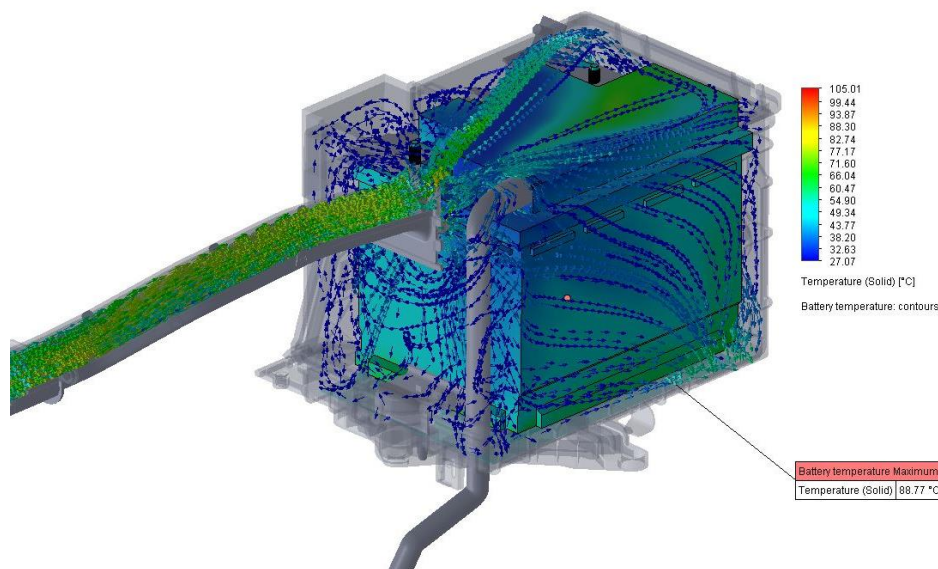


Fig. 8 - Air flow through the duct and then inside the housing (fan off)

From these simulations results the obligation to use a fan that considerably reduces the temperature of the Li-Ion battery, a temperature that resulted in approximately 71.5 °C. The volume of air supplied by the fan is the same as that which enters it, which is why the volume of air entering the duct must be equal to them.

6. Future research directions

Based on this study, a multitude of applications can be made, such as replacing the fan with a larger one that provides a much larger volume of air, increasing the height of the metal support on which the battery is placed so as to penetrate as much air as necessary for cooling, use a temperature sensor (thermocouple) at the point where it turned out to be the highest temperature, etc.

7. Bibliography

- [1] - ANKUR BHATTACHARJE, RAKESH MOHANTY, *Design of an Optimized Thermal Management System for Li-Ion Batteries under Different Discharging Conditions*, 30 October 2020
- [2] – Chen, D.; Jiang, J.; Kim, G.; Yang, C.; Pesaran, A. *Comparison of different cooling methods for lithium ion battery cells*, J. Power Sources 2016, 94, 846–854
- [3] – Daniel Cela Patrik Alerman - *Study of a 12V Li-ion Battery, Solution for Hybrid Vehicles* – Chalmers University of Technology
- [4] – D. Di Battista, M. Mauriello, R. Cipollone, *Waste heat recovery of an ORC-based power unit in a turbocharged diesel engine propelling a light duty vehicle*, Applied Energy, 152 (2015) 109-120
- [5] – E.S. Mohamed, *Development and analysis of a variable position thermostat for smart cooling system of a light duty diesel vehicles and engine emissions assessment during NEDC*, Applied Thermal Engineering, 99 (2016) 358- 372
- [6] – Feng, X.; Sun, J.; Ouyang, M.; Wang, F.; He, X.; Lu, L.; Peng, H. *Characterization of penetration induced thermal runaway propagation process within a large format lithium ion battery module*, J. Power Sources 2015, 275, 261
- [7] – Haimin Shi, Yiji Lu s.a., *Experimental study of multi-fans cooling module using different shroud structures for advanced vehicle thermal management system*, 9th International Conference on Applied Energy, ICAE2017, 21-24 August 2017, Cardiff, UK

- [8]–<https://www.hella.com/techworld/uk/Technical/Car-air-conditioning/Thermal-management-in-electric-and-hybrid-vehicles-1725/> accesat la data de 14.05.2021
- [9] – Kim, J.; Oh, J.; Lee, H. *Review on battery thermal management system for electric vehicles*, Appl. Therm. Eng. 2019, 149, 192–212
- [10] – Krüger, I.L.; Limperich, D. *Energy Consumption of Battery Cooling in Hybrid Electric Vehicles. In Proceedings of the International Refrigeration and Air Conditioning Conference*, West Lafayette, IN, USA, 16–19 July 2012
- [11] – M. Park, D. Jung, M. Kim, K. Min, *Study on the improvement in continuously variable transmission efficiency with a thermal management system*, Applied Thermal Engineering, 61 (2013) 11-19
- [12] – SCHIAVON, Stefano, MELIKOV, Arsen, *Introduction of a Cooling-Fan Efficiency Index*, UC Berkeley HVAC System, November 2009, Volume 15, number 6
- [13] – Shuai Ma, Modi Jiang, s.a, *Temperature effect and thermal impact in lithium-ion batteries: A review*, Progress in Natural Science: Materials International, 28 (2018) 653-666
- [14] – T. Wang, A. Jagarwal, J.R. Wagner, G. Fadel, *Optimization of an Automotive Radiator Fan Array Operation to Reduce Power Consumption*, IEEE-ASME Trans. Mechatron., 20 (2015) 2359-2369
- [15] – Tanabe et al. 1994; Tsuzuki et al. 1999; Melikov et al. 2002; Watanabe et al. 2005; Sun et al. 2007
- [16] – Yuksel, T.; Litster, S.; Viswanathan, V.; Michalek, J.J. *Plug-in hybrid electric vehicle LiFePO4 battery life implications of thermal management, driving conditions, and regional climate*, J. Power Sources 2017, 338, 49–64

RESEARCH ON FIXTURING SMALL PARTS IN MACHINING SYSTEMS

BARBU Ana-Maria¹, MUŞAT Miruna-Diana², FLEACĂ Cristina-Mihaela³, GHEORGHE Marian³, POLOVŢEV Nicolae Onorel, GANNAM Nasim, MANOLACHE Daniel-Silviu³

¹Faculty of Industrial Engineering and Robotics, Specialization: Industrial Economic Engineering, 4th study year, e-mail: ana_mry20@yahoo.ro

²Faculty of Industrial Engineering and Robotics, Specialization: Industrial Economic Engineering, 3rd study year

³Faculty of Industrial Engineering and Robotics, Manufacturing Engineering Department

ABSTRACT: The fixturing of small parts, within machining technological systems, requires solutions which should be determined by extensive analysis of the interacting factors. There is evidenced a series of relevant elements regarding the small displacement torsor produced by fixturing, fastening mechanisms, as well fixturing of thin-walled parts. Moreover, there are presented data and main results of an experimental research regarding the fixturing of the workpieces on magnetic table, within milling and drilling systems.

KEYWORDS: fixturing, workpiece, fixturing mechanism, error, technological system.

1. Introduction

The small parts include some constructive features – general form, wall thicknesses, sizes of the possible spaces for fixturing elements, etc. - which can influence how they are fixed within the machining technological systems. Thus, it is necessary that the type and position of fixturing elements associated with technological operations to be determined through extensive technical-economic analysis on the interacting factors – position and dimensions of possible spaces for fixturing elements, structure and dimensions of the fixturing mechanisms, the characteristics of the specific errors, time and cost associated with the clamping-releasing process.

2. General considerations

2.1. Parameters of the small displacement torsor produced by fixturing

Geometric workpiece errors, locators geometric errors, and clamping errors are factors which influence the workpiece fixturing [1]. These errors accumulate, propagate during fixturing and may be the reason why a machined characteristic is outside the tolerance range. In the modeling and analysis of the combined effect of these errors (Fig. 1), the deviation of a machined characteristic is expressed by parameters of the Small displacement torsor, SDT.

Due to the geometric errors of the part and of the fasteners, the moment M , $M = Qd$ can be created by the action of the clamping force Q [1], which generates a rotation/ angular displacement, α , of the workpiece (Fig. 2) and, accordingly, angular fixturing errors. A flat surface that nominal is parallel to a reference plane (xy), S_p , may suffer fixturing errors (Fig. 1, 2) of type: geometric, error / variation Δz , in mm, of surface position after normal direction at (xy); errors/ variations $\Delta\theta_x$ and $\Delta\theta_y$, in rad, of the angular position of the surface around the reference axes x and y , respectively. Thus, to the S_p considered surface, a SDT (S_p) torsor can be associated consisting of the small displacements Δz , $\Delta\theta_x$ and $\Delta\theta_y$, as:

$$\text{SDT } (S_p): \{ \Delta z, \Delta\theta_x, \Delta\theta_y \} \quad (1)$$

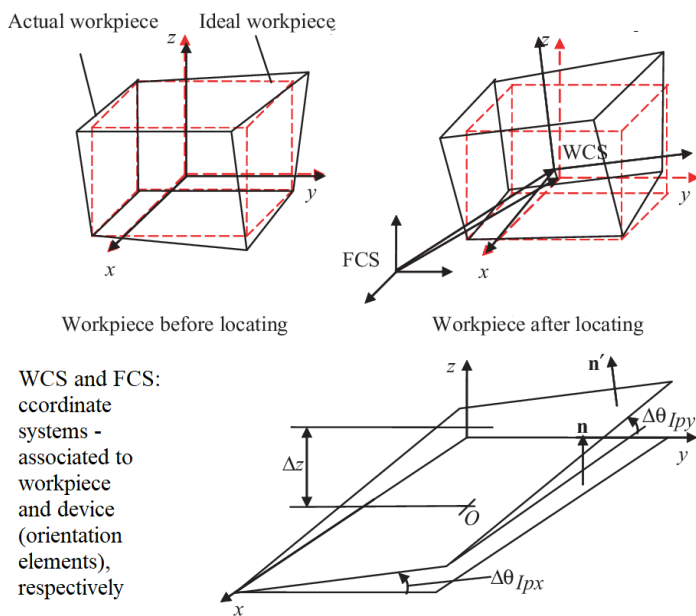


Fig. 1. Workpiece and primary plane of workpiece surface deviation (before and after locating) [1]

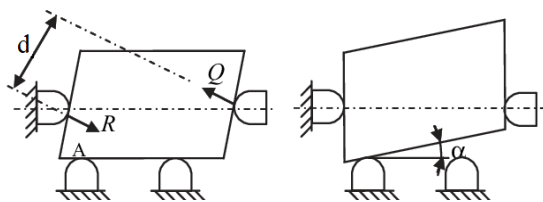


Fig. 2. Clamping error (example) [1]

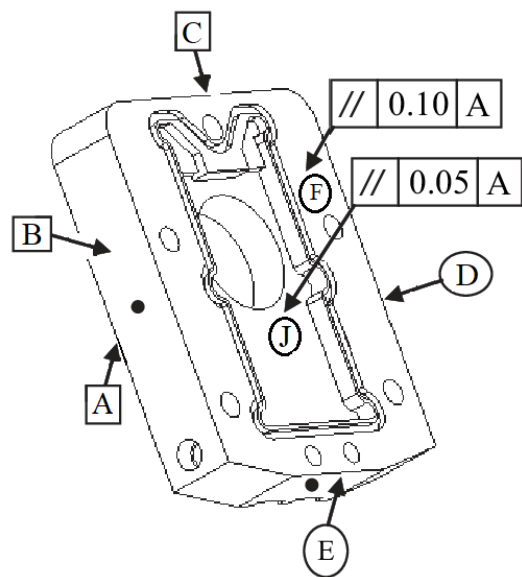


Fig. 3. Test-piece machined in the experiment (after [1])

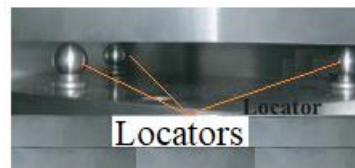


Fig. 4. Part locators from device structure (after [1])

A test-workpiece [1] (Fig. 3, 4) was oriented by contacting the A-B-C reference flat surfaces on six orientation elements type of the spherical pin, in a 3-2-1 structure and fixed on the flat surfaces D and E, respectively, by action of two fixturing elements, each with a fixturing force of 500 N (to prevent intense deformation). Thus, e.g., for the F and J surfaces of the test-piece machined by milling in the considered experiment (Fig. 3), SDT (F) and SDT (J) are:

$$\text{Prescribed SDT (F): } (0.1, 0.00125, 0.00096) \text{ and Effective SDT (F): } \{0.0541, -0.00067, -0.00067\} \quad (2)$$

$$\text{Prescribed SDT (J): } (0.05, 0.0021, 0.0013) \text{ and Effective SDT (J): } \{0.0039, -0.00067, -0.00067\} \quad (3)$$

2.2. Technological fixturing mechanisms and technological machining devices

The fixturing mechanisms in the structure of technological machining systems may be with wedge, eccentric, screw-nut, pneumatic motor, hydraulic motor and clamp strap, plunger, oscillating plate or with vacuum, magnetic, etc., and the orientation-fixing mechanisms can be with jaws, elastic bushing(s), levers, prisms, etc. [2].

For fixturing according to a predetermined direction, two variants of screw/nut-clamp mechanisms are shown in Fig. 5.

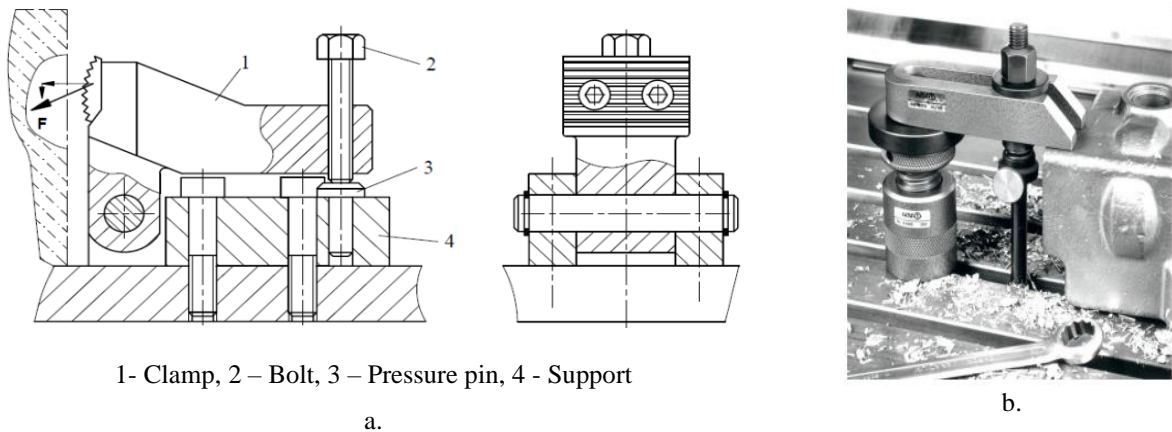


Fig. 5. Fixing mechanisms: bolt – hinged clamp (a); bolt – nut - clamp (b) [3]

For clamping small parts within automated systems, an innovative solution consists of creating hydraulic actuators and solving the problem of extreme clamping forces in a small space combined with creating the precision of these fixing forces [4]. These mechanisms operate on a relatively simple principle, respectively, the hydraulic pressure (p) is first converted to the downwards force (F) and by means of a wedge-plungers mechanism, clamping forces (F) are created (Fig. 6). The easiest way to create a hydraulic device is to use a single-acting hydraulic actuator. In the case of a double-acting hydraulic actuator, the clamping force is stronger than the return force.

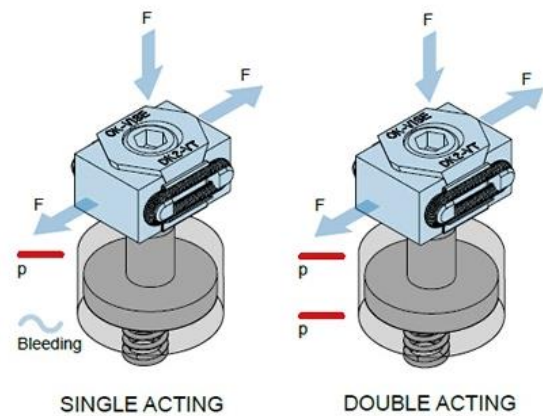


Fig. 6. Hydraulically operated fasteners in automated systems [4]

Magnetic action is a mechanized mode of action that is characterized by the fact that the acting force is achieved, e.g., with permanent magnets, which are properly oriented and insulated each - other by means of non-magnetic insulators. Magnetically operated fixtures have a number of advantages: low cost, uniformly distributed magnetic field on the surface, fixturing with no deformation, etc. [5].

Magnetically operated fixtures are built in the form of magnetic table/ plateau. A such of magnetic table that is used at CNC milling machines is shown in Fig. 7. For clamping smaller and thinner parts, the most suitable are magnetic fixtures with neodymium magnetic system [6] (Fig. 8). Neodymium ($NdFeB$) magnets are smaller and stronger than other permanent magnets.

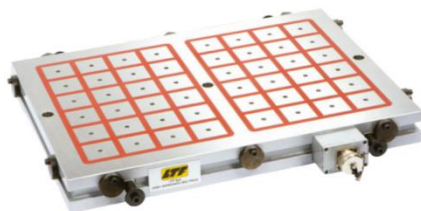


Fig. 7. Electropermanent magnetic table [7]

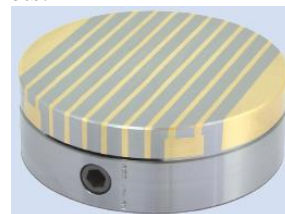


Fig. 8. Permanent magnetic chuck [6]

The fixturing force of the part is determined by the equal number of north and south poles with which is in contact. The short distances between the poles produce shorter magnetic lines of force and are therefore used for thin or small parts [8].

Vacuum fasteners are among the newest ways of fixturing workpieces in technological machining systems and have the important feature that the fixturing efficiency does not depend on the size of the fixed part. Such a fastening mechanism is a technology to fix the part by vacuum and to allow its machining from different directions, easily and quickly. Thanks to this special grip, the parts are protected against damage [9] (Fig. 9).

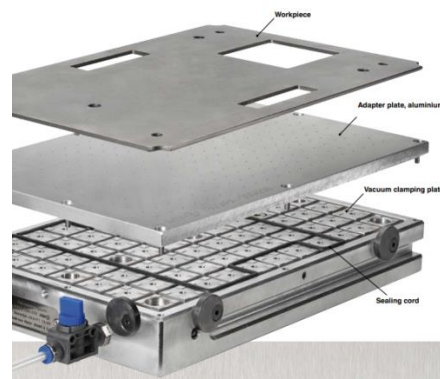


Fig. 9. Vacuum clamping system [9]

2.3. Clamping schemes of thin-walled parts

Thin-walled parts have widespread applications in the fields of aeronautics, astronauts, medicine, etc. The quality of the part (Fig. 10) is affected by several factors and the clamping scheme is a main influencing element. “Researchers mainly study from three directions: fixture design evaluation, finite element simulation, mathematical model establishment, and algorithm optimization”. In one particular case, six fixturing schemes were proposed, from which a variant was chosen based on the finite element study in the ABAQUS software [10].

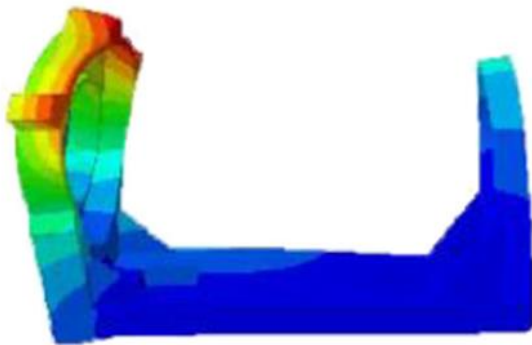


Fig. 10. Thin-walled part loaded by fixturing force, analyzed with finite element [10]

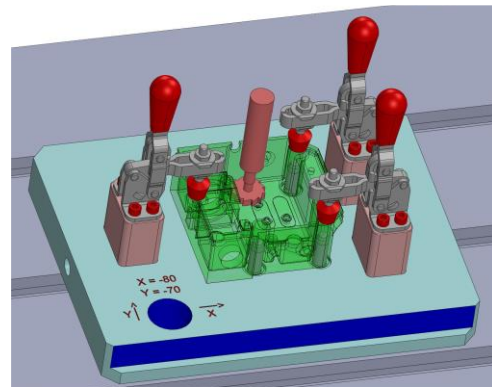


Fig. 11. Special fixture [11]

For a milling, drilling, etc. operation of a complex thin-walled workpiece, in a CNC technological system, the special fixture, that was designed, produced and used in industrial conditions, ensures the fixturing of the part in its maximum rigidity zones (Fig. 11) [11].

3. Experimental research on magnetic fixturing in machining processes

At the fixturing on the magnetic table, it is possible to apply the fixturing force after the normal direction to a main flat orientation surface, without the need to apply fixturing forces after other directions.

In the literature there are summary data on the technological conditions of use of magnetic devices in cutting operations with high cutting forces.

In relation to the above, an experiment was carried out under real machining conditions, by milling and, respectively, by drilling, in a laboratory of the Manufacturing Engineering Department, as follows.

- Test-piece: Prismatic body, made of C45 steel/ normal state, with overall sizes of 150x38x25 mm, and a flat settlement surface of 150 x 38 mm.
- Fixture: *ECLIPSE* magnetic table with permanent magnets, and overall sizes of 290x130x50 mm.

3.1. Machining by semi-finishing face milling

- Machine tool: TOS FN 32 universal milling machine.
- Fixture: *ECLIPSE* magnetic table - with settlement on the machine-tool table and fixing with bolt-clamp (2x).
- Cutting tool: Face mill, with $z = 6$ cutting tips – material P25, main angle of attack $\chi = 60^\circ$, active diameter $d = \text{Ø}70$ mm.
- Cutting parameters: cutting depth $a = 0.2, 0.4, 0.6, 0.8$ mm; cutting feed $f_z = 0.021$ and 0.027 mm/tooth; cutting speed $v = 109.95$ m/min, respectively, rotational speed $n = 500$ rpm; feed rate $F = 63$ and 80 mm/min, according to the following relationships:

$$n = 1000v/\pi d, F = nzf_z \quad (4)$$

- Lubricant coolant: without.

A series of elements regarding the unrolling of considered machining is presented in Fig. 12.

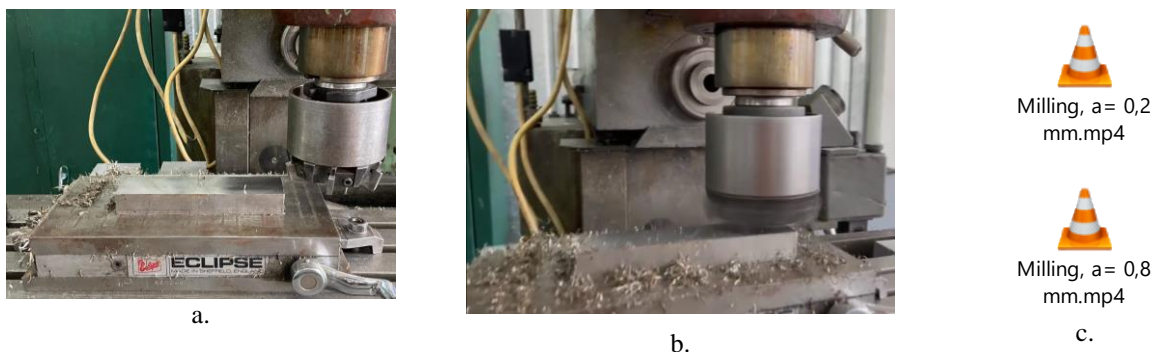


Fig. 12. Elements regarding the unrolling of machining by milling: a – preparation of the technological system; b, c - machining

3.2. Machining by drilling

- Machine tool: Drilling machine G 25.
- Fixture: *ECLIPSE* magnetic table - with settlement on the machine tool table, without fixing.
- Cutting tool: Twist drill, with diameter $d = \text{Ø}9$ mm, made of HS18-0-1 SR EN ISO 4957:2022.
- Cutting parameters: cutting feed $f = 0.1$ mm/rev, cutting speed $v = 12.7$ m/min, respectively, rotational speed $n = 450$ rot/min ($n = 1000v/\pi d$).
- Lubricant coolant: without.

A series of elements regarding the unrolling of the considered machining is presented in Fig. 13.



Fig. 13. Elements regarding the unrolling of machining by drilling (a, b)

4. Case studies

The case studies refer to the introduction of magnetic fixturing in machining operations, associated with the manufacture of a workpiece with a complex geometric shape (Fig. 14), and with thin walls (Fig. 15), respectively.

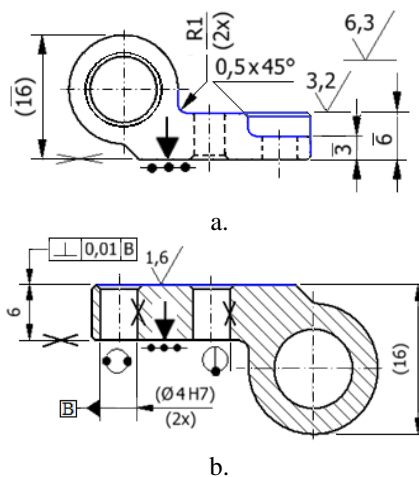


Fig. 14. Sketches of two operations including machining by milling – a, grinding – b, with magnetic fixturing of the part

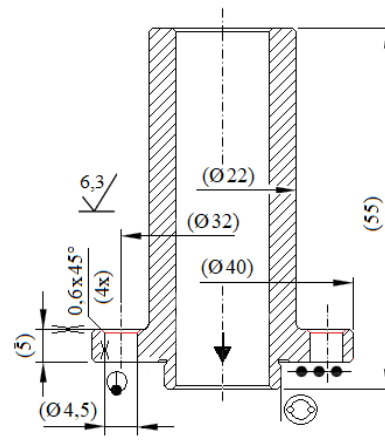


Fig. 15. Sketch of an operation including machining by countersinking, with magnetic fixturing of the part

5. Conclusions

For fixturing small parts in technological machining systems, it is necessary to analyze various fixturing schemes and mechanisms, with respect to a number of specific characteristics of the parts - general shape, wall thickness, etc.

Experimental research on the fixturing of the part on a magnetic table, in operations including milling or drilling, shows that technological conditions can be determined for the use of magnetic devices in milling, drilling, etc.

The development of theoretical and experimental research on magnetic fixturing of parts in technological operations will lead to the simplification of certain orientation-fixing systems and, consequently, to the reduction of production costs.

6. References

- [1] Asante J. N., A small displacement torsor model for tolerance analysis in a workpiece-fixture assembly, PROCEEDINGS OF THE INSTITUTION OF MECHANICAL ENGINEERS PART B-J. OF ENGINEERING MANUFACTURE, Vol. 223, Issue 8, pp 1005-1020, DOI: 10.1243/09544054JEM1337, WOS: 000268822100006, ISSN 0954-4054, eISSN 2041-1975, IDS Number 481OW, 2009.
- [2] Gheorghe M., Engineering and management of production processes 1 Course notes (in Romanian), UPB, 2020-2021.
- [3] Teodorescu-Drăghicescu F., Manufacturing equipments, Course notes (in Romanian), UPB, 2021-2022.
- [4] ***, OK-VISE Hydraulic Actuators, <https://www.ok-vise.com/en/products/automation/hydraulic-modules>, accessed on 08.04.2022.
- [5] Sanda Vasii Roşculeţ, et al., Fixtures and jigs design (in Romanian), EDP, Bucharest, 1982.
- [6] ***, Magnetic Clamping, Spreitzer, https://www.spreitzer.de/pdf_de/magnetspanntechnik.pdf, accessed on 04.05.2022.
- [7] ***, Technicas, https://www.technicasms.ro/stiri/detalii/?tx_news_pi1%5Bnews%5D=7&tx_news_pi1%5Bcontroller%5D=News&tx_news_pi1%5Baction%5D=detail&cHash=141a675767fc848499fbd33b157dd92, accessed on 03.04.2022.
- [8] Păunescu T., Magnetic Workholdings: Recent Advances and Trends, Recent, Vol.13, Braşov, 2012.
- [9] ***, AMF, <https://www.amf.de/en/products/clamping-technology/vacuum-clamping-systems.html>, accessed on 03.04.2022.
- [10] Jinhuan Su, Yan Cai1, Xiaohui Jiang, et al., Modeling of stiffness characteristic on evaluating clamping scheme of milling of thin-walled parts, Int'l J. of Advanced Manuf. Technology (Q2), Heidelberg, Vol. 113, Iss. 7-8, pp 1861-1872, DOI: 10.1007/s00170-021-06740-0, WOS: 000618170100004, 2021.
- [11] ***, Industrial documentation (in Romanian), SC Dr. Kocher, 2022, <https://www.drkocher.ro/>

RESEARCH ON THE DESIGN AND DEVELOPMENT OF A SMART KNEE ORTHOSIS

BORCAN Maria Alexandra¹, NEACȘU Angela-Miruna¹, VLAD Mihaela-Marilena¹,
ULMEANU Mihaela-Elena² and DUGĂEȘESCU Ileana²

¹Faculty: Industrial Engineering and Robotics, Study program: Economic Industrial Engineering,
Year of study: IV, e-mail: angel.miruna@yahoo.com

²Faculty of Industrial Engineering and Robotics, Manufacturing Engineering Department

ABSTRACT: The purpose of this research is to create a functional prototype for the lower limb orthosis, respectively the knee studied in the project "Bionic Orthosis for the Lower Limb", where a study of the existing needs on the market was carried out and several concepts were developed from which the optimal one was chosen. This research is about designing, manufacturing and testing a prototype orthosis and making it more useful by creating a mechatronic system that allows the patient to constantly observe his health.

The conclusion of this research is to obtain a functional prototype, who will be improved in a future research to reach an optimized version of the orthosis.

KEYWORDS: orthosis, 3D printing, mechatronic, prototype

1. Introduction

In recent years, there are more and more diseases and accidents that lead to the non-use of some limbs and to the mental state of the persons concerned. Among these diseases is diabetes, which in recent years has affected more people than in the past. Most people discover it too late, when their peripheral circulation has already been affected and they are in the stage of not being able to use a part of the limb.

The purpose of this research is to develop a product that will make life easier for people with various locomotor problems.

For the development of a bionic orthosis, various aspects regarding the market were analyzed, namely, opportunities, existing products and customers.

2. Concept model

Medical reports inform that orthoses for the lower limbs specifically for the knee, are a treatment for medical conditions such as: fracture, kneecap dislocation, damage to ligaments or cartilage, dissecting osteochondrosis. So, the orthosis for the knee must provide stability, allow some mobility, but not excessively, to align a correct position and resist external forces.

Living with a knee orthosis can take time to get used to, so doctors and engineers are constantly trying to develop and improve solutions to make patients' life easier.

After a more detailed analysis, was chosen an optimal concept for the realization of the orthosis. This is shown in Figure 1.

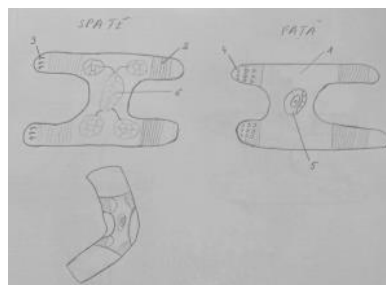


Fig.1. The chosen concept for the manufacturing of the orthosis

The lower limb bionic orthosis has the body (1) made of textile material. Adjustment of dimensions is made by elastic bands (2), by stretching them, obtaining values in the range of 30 - 85 cm. After adjusting the dimensions, both for the thigh and the calf, the orthosis is fixed using hooks (3) which are inserted into the rings (4), located over the entire range of dimensions. Depending on the doctor's recommendations, the treated area and the time of use is set through the mechanical system (5). A silicone pillows system (6) is placed on the inside of the orthosis for easy and comfortable wearing, which comes into contact with the wearer's skin, avoiding the risk of possible injury during use.

3. Modeling and 3D printing resistance structure

The schedule for wearing a knee orthosis is different for each patient, depending on the type and severity of their problem. Often patients have to go for regular physical examinations or perform therapeutic exercises and have to take off the orthosis. The orthosis also needs to be cleaned regularly.

Bearing these aspects an orthosis must be easy to use, without causing pain or scratching the skin.

Analyzing the textile material used for the orthosis, it has been established that a resistance part will be attached to the material.

To design the 3D model, anthropometric measurements of the person who will use the orthosis were used. The orthosis was designed in Inventor Software and 3D printed using HIPS material.

In figures 2 and 3 you can see the 3D model created for the orthosis.

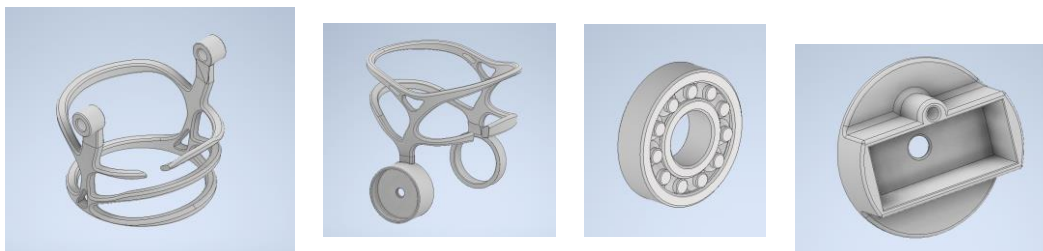


Fig. 2. 3D components models of the orthosis



Fig. 3. 3D model assembled

The orthosis for the lower limb brings to the fore a more anatomical shape with large cutups that offers better mobility to the person. Both the cutups on the surface of the orthosis and around the joint offer the patient an easier wearing, making the orthosis to have a lower weight. In order to increase the patient's mobility, the joint was realized using a bearing, assembling both parts of the orthosis with it by tightening.

Moreover, for a more detailed check of the foot dimensions in the manufacturing of the orthosis, it was also used a human body scanning application "Nettelo" presented in Figure 4.

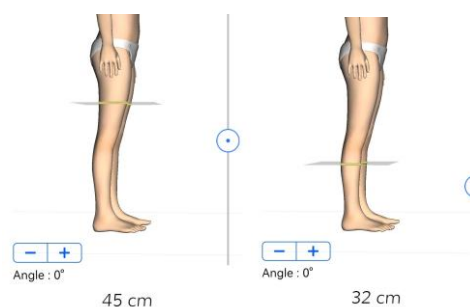


Fig. 4. Human body scan [8]

Several prototypes were printed for the orthosis and the optimal one was chosen to continue the study and to optimize the necessary elements. These are shown in figure 5.

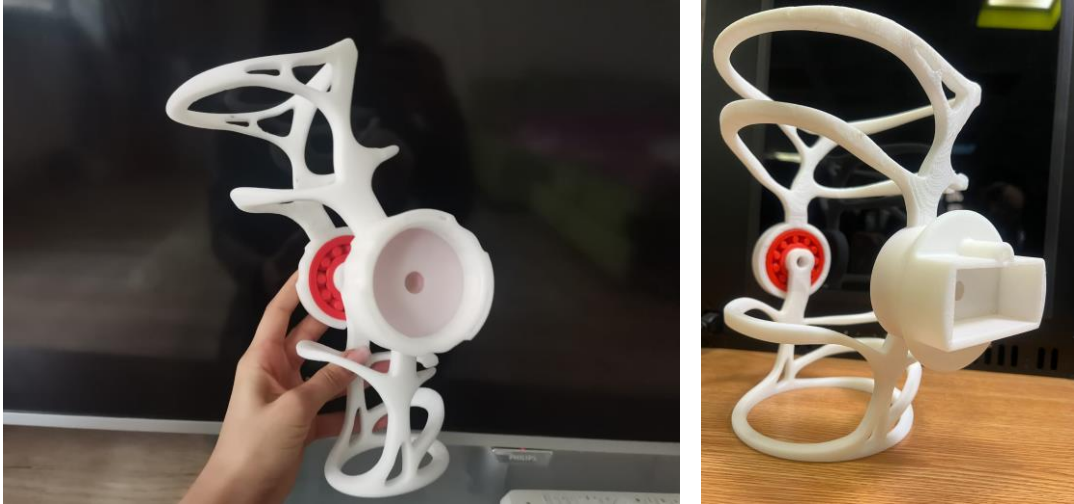


Fig. 5. Prototypes (from left to right): first functional prototype and second functional prototype

4. Materials

Choosing a material for 3D printing products has become increasingly difficult because the 3D printing market comprises a wide variety of materials. For the choice of the material used in the studied orthosis, a research was conducted on the following materials: PLA, ABS and HIPS.

PLA (Polylactic acid)

One of the most common thermoplastics in 3D printing is polylactic acid (PLA), an environmentally friendly, biodegradable polymer created from plant sugars from crops such as tapioca, corn and sugar cane.

Suitable for: applications in various fields, miniatures, cosplay, decorative pieces.

Pro arguments: low cost, easy to print, good hardness and mechanical strength, dimensional accuracy, biodegradable.

Contra arguments: can be brittle, oozing occurs, low temperature resistance, not UV resistant, degradation of prints over time.

ABS (Acrylonitrile butadiene styrene)

Acrylonitrile butadiene styrene (ABS) plastic is used in a variety of industrial applications for extrusion and injection molding, such as lego bricks. Its properties are well known, and the quality of the filament can be easily controlled during manufacture.

Suitable for: mechanisms, functional prototypes, functional parts for the automotive industry.

Pro arguments: high mechanical strength, impact resistance, water resistance, good temperature resistance, no oozing and stringing.

Contra arguments: special printing conditions, increased tendency to deformation, strong contractions, no UV resistance, unpleasant smell.

HIPS (High-impact polystyrene)

High impact polystyrene (HIPS) is a variation of styrene. HIPS has similar properties to ABS, but dissolves in limonene (a solvent derived from citrus plants). HIPS is a dissolvable backing material that is commonly used with ABS. When used as a backing material, HIPS can be dissolved in d-Limonene, leaving the print free of marks caused by backing removal. HIPS is not only excellent for supporting ABS prints, but it is also more dimensionally stable and lighter than ABS, making it an excellent choice for parts requiring lighter weight. HIPS filament is relatively new and its use is still experimental.

Suitable for: cosplay items, parts that need to be lightweight, protective housings.

Pro arguments: impact and water resistance, fine surface, lightweight material, can be used as backing material, dissolvable in d-Limonene.

Contra arguments: heated enclosure and platform, requires ventilation, high printing temperature, emits harmful particles in printing.

For a best comparison, each material characteristics are shown in Table 1 :

Table 1. Material characteristics

Features	PLA	ABS	HIPS
Strength [MPa]	32	40	65
Rigidity	5/10	7,5/10	10/10
Sustainability	4/10	8/10	7/10
Temperature of extrusion [°C]	180-220	220-240	220-230
Bed temperature [°C]	20-55	80-110	50-60
Coefficient of thermal expansion [$\mu\text{m}/\text{m}\cdot\text{°C}$]	85	68-110	80-90
Glass transition temperature [°C]	60-65	105-110	100
Price* [RON]	199,00	233,00	283,00

* Price refers to one ZORTAX 3D printer filament with 800g mass.

Because the orthosis material has to be stiff for best mobilization, but also light so as not to affect locomotor function and create discomfort for the user, HIPS material was used.

5. Mechatronic System

A mechatronic system consisting of sensors, an RGB LED and an LCD screen to help the patient use the orthosis more easily was also considered. The mechatronic system components are shown in Table 2.

Table 2. Mechatronic system components

Components name	Number of pieces
Arduino Nano Board	1
Mini Breadboard	1
RGB Led	1
Resistor 220 Ω	3
LCD display	1
Temperature sensor DHT11	1
Pulse sensor	1
The vibration module	1
Wires mom - dad	17
Wire dad - dad	1

To operate the circuit, the Arduino Nano board was placed on the mini breadboard and the other components were connected to it using mom-dad wires. The right pin of the temperature sensor was connected to the GND port of the board, the left pin to the 5V port and the middle pin to the digital port 7. The vibration module and the pulse sensor were connected in the same way, the difference being the change of ports from which they receive data. Thus, the pulse sensor was connected to analogue pin A0, and the vibration sensor was connected to digital pin 2. In the case of the RGB LED, the cathode was connected to the GND port, and the led pins for RGB colors were connected in series with a 220 Ω resistor and connected to the pulse modulated digital pins 9, 10 and 11.

A circuit was made on a normal breadbord to test the components and its operation before put it on the orthosis. This is shown in figure 6.

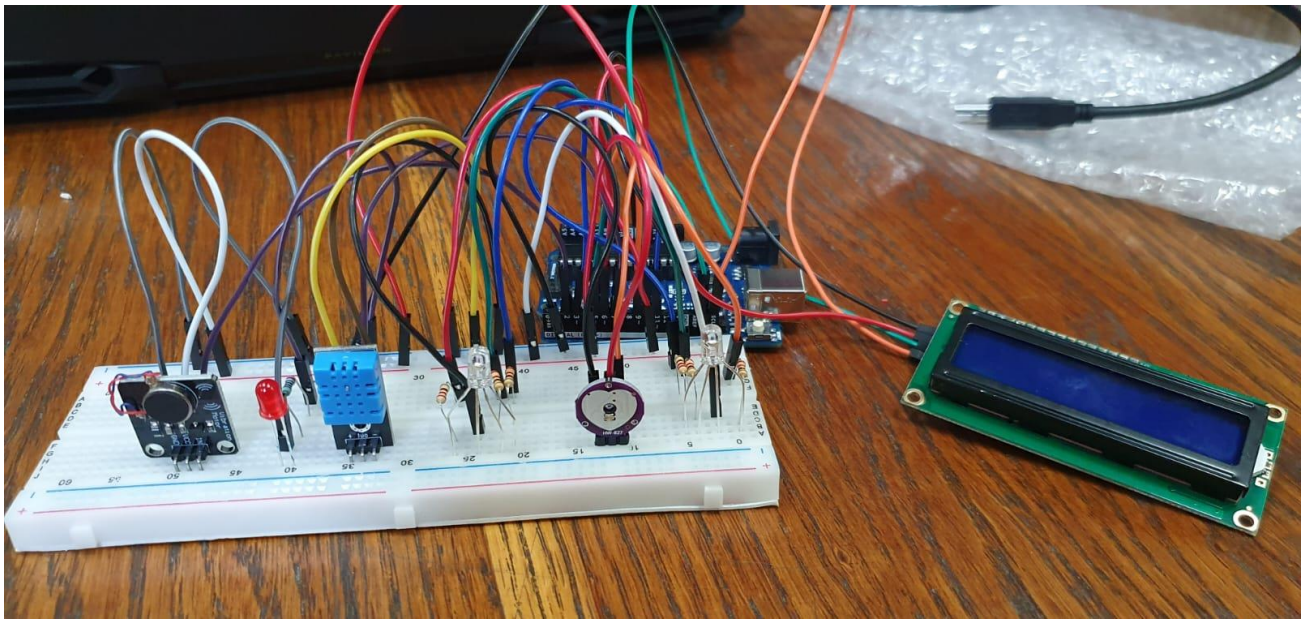


Fig. 6. The circuit for testing

The circuit principle of the operation consists in measuring the temperature and pulse of the patient, displaying them on the LCD screen and warning by light and vibration if the temperature is higher than 37°C or the pulse is not within the normal range of 400-600 heart rate. A code was also developed to operate the circuit using Arduino software. Some sequences of it are shown in figures 7 and 8.

```

if(tempC >= 37){
  digitalWrite(r,255);
  digitalWrite(g,0);
  digitalWrite(b,0);
  digitalWrite(vibratie_pin,HIGH);
  delay(1000);
}
else{
  digitalWrite(r,0);
  digitalWrite(g,0);
  digitalWrite(b,255);
  digitalWrite(vibratie_pin,LOW);
  delay(1000);
}

```

Fig. 7. Code sequence for temperature sensor [9]

```

if(val_puls < 400){
  lcd.setCursor(0,1);
  lcd.print("Puls:");
  lcd.print(val_puls);
  digitalWrite(r2,255);
  digitalWrite(g2,255);
  digitalWrite(b2,0);
  digitalWrite(vibratie_pin,HIGH);
  delay(1000);
}

```

Fig. 8. Code sequence for pulse sensor [9]

6. Conclusions

In conclusion, with the help of this research, an efficient way of measuring pulse and temperature has been developed, including warning systems for the user in case of medical problems. A textile material and a 3D-printed pattern were also combined to ensure durability. The prototype orthosis is functional and useful for the patient. This can be seen in figure 9.



Fig. 9. Wearing orthosis functional prototype

7. Bibliography

- [1]. Dugăeșescu I., Base mechatronic system, Course notes 2021-2022
- [2]. Ulmeanu M., Assisted design and additive manufacturing, Course notes 2021-2022
- [3]. Neacsu A., „Bionic Orthosis for the Lower Limb”, project at Products Development 1, 2021
- [4]. Richard Horne, Kalani Kirk Hausman, „3D Printing for dummies”, second edition, 2018
- [5].***, „Ultimate 3D Printing Materials Guide”, available at: <https://www.simplify3d.com/support/materials-guide/>, accesat la data de: 28.04.2022
- [6].***, „Materials for 3D Printing by Fused Deposition”, available at: https://www.materialseducation.org/educators/matedu-modules/docs/Materials_in_FDM.pdf, accessed on: 28.04.2022
- [7].***, Online shop, available at: <https://www.filamente3d.ro/zortrax-store>, accessed on: 28.04.2022
- [8].***, Nettel, scanning app available in Google Play
- [9].***, Arduino, available at: <https://www.arduino.cc/>, accessed on:14.04.2022
- [10].***, Optimus Digital, available at: <https://www.optimusdigital.ro/ro/>, accessed on: 21.04.2022

RESEARCH CONCERNING MACHINING SOME ALLOYS OF Co, Cr AND Ti BY MILLING AND ELECTRICAL DISCHARGE MACHINING

DINCĂ Cristian-Daniel¹, FRANCISC Petre¹ and GHICULESCU Liviu Daniel²

Faculty of Industrial Engineering and Robotics, Specialty: Manufacturing Engineering, Year of study: IV,
e-mail: cristi1999dinca@gmail.com

²Faculty of Industrial Engineering and Robotics, Manufacturing Engineering Department
University POLITEHNICA of Bucharest

ABSTRACT: The paper deals with the comparison of machining alloys based on Co, Cr and Ti, Al between mechanical processes, like milling and nonconventional thermal processes, like electrical discharge machining (EDM). The studied materials have great characteristics of resistance, corrosion, some like Co, Cr alloys are biocompatible, and some others like Ti, Al alloys have high resistance at big temperature. Generally, they are difficult to be cut, therefore EDM was used at cavity machining in comparison and combination with milling. Finally, a finite element modelling of EDM process was approached to better understand the thermal removal mechanism of these materials. Experimental data proved that CoCr alloys have higher machinability than Ti, Al alloys at both types of processes used.

KEYWORDS: alloys Co, Cr, Ti, milling, electrical discharge machining

1. Introduction

For this study it was necessary to purchase semifinished products made of CoCr alloys and Ti aluminide and to process them by milling and electrical discharge machining (EDM). It was first necessary to mill the semifinished products using a milling cutter with a diameter of $\Phi 10$ mm, in order to obtain flat surfaces. Using a cylindrical-front milling cutter with a diameter of 2 mm and, respectively, massive copper electrodes, cavities of 5x5x1,5 mm were made, and the quality of the surfaces obtained by the two processing processes was analyzed.

2. Current stage

Fields of application of Co, Cr and Ti alloys: Due to their excellent characteristics of corrosion resistance, wear resistance, high creep resistance, high temperature resistance and good biocompatibility, CoCr alloys have applications in many engineering fields such as turbomotors, nuclear, biomedical, and dentistry [1]. CoCr alloys are also widely used in other fields of medicine: stents [2], intervertebral disc replacement, knee or hip arthroplasty [3,4]. These alloys achieve their corrosion resistance by forming chromium-based oxides on the surface, and their biocompatibility then becomes extremely valuable over time [5].

High-pressure compressors use conventional titanium alloys (α and α - β) in areas where the working temperature does not exceed 500°C [6]. TiAl-based alloys are especially suitable for applications of low-pressure turbine blades and high-pressure compressor blades [7]. General Electric said that the low-pressure turbine blades in the TiAl range manufactured by Precision Castparts Corp. were used in GENx engines, which equipped Boeing 787 / Boeing 747-8 aircraft [8].

Properties of Co, Cr and Ti alloys: The main hardening mechanism of cobalt-based alloys is the formation of carbides, solid solution hardening and the formation of intermetallic compounds, acting in the same direction. The carbides disperse in the alloy matrix and precipitate at the granule boundaries, and this dispersion has a direct effect on the mechanical strength of the alloy [9].

Titanium γ (TiAl) aluminum has the highest specific stiffness compared to all other classes of alloys. At the same time, titanium aluminum alloys have high values of modulus of elasticity, compared to conventional titanium alloys and nickel-based alloys [6].

Tables 1 and 2 show the chemical composition of some CoCr alloys and titanium aluminides, respectively.

Table 1. Chemical composition of CoCr alloys used in experiments [10,11]

Alloy	Cr [%]	Mo [%]	W [%]	Nb [%]	Si [%]	Mn [%]	Fe [%]	Co [%]
P1, SYSTEM NE	21,0	6,5	6,4	-	0,8	0,65	<0,1	64,4
P2, SYSTEM SOFT	29,5	5,7	-	-	0,95	0,55	0,75	61,8
P3, LUKA CHROM	24,0	3,0	8,0	1,0	1,0	-	-	63,0

Table 2. Chemical composition of titanium alumina used in experiments [12]

Alloy	Alloy element	Ti	Al	Nb	Cr	Zr	Ta	B	α_2 phase %
Alloy 1	at %	45	44	4	-	4	1	1	2
Alloy 2	at %	43	47	7	1	-	0.5	-	25

Tables 3 and 4 show the mechanical properties of some CoCr alloys and titanium aluminides, respectively.

Table 3. Mechanical properties of CoCr alloys used in experiments [10,11]

Alloy	Tensile strength [MPa]	Young Modulus [GPa]	Elastic limit [MPa]	Breaking elongation [%]	Hardness [HV]
P1, SYSTEM NE	850	155	580	3	460
P2, SYSTEM SOFT	447	160	450	15	310
P3, LUKA CHROM	550	125	545	25	185

Table 4. Mechanical properties of titanium aluminates [12]

Alloy	Tensile strength, at 25°C, [MPa]	Tensile strength, at 760°C, [MPa]	Breaking elongation, at 25°C, [%]
Alloy 1 (1, 2, 3 samples)	620	550	3
Alloy 2 (4, 5 samples)	1100	620	2-3

Alloys based on intermetallic compounds γ (TiAl) and α_2 (Ti₃Al) have important thermo-physical and mechanical properties, such as: high melting point, above 1460°C, low density (3,9-5 g/cm³, depending on the degree alloy), high stiffness, yield strength and creep resistance at high temperatures, structural stability at high temperatures, low diffusion coefficient.

Alloys P1 and P3, which contain W, have a slightly higher thermal conductivity compared to alloy P2, as this alloying element has the highest heat transfer coefficient: 170 [W*m⁻¹*K⁻¹] [13]. According to the literature, the specific heat of CoCrMo ternary alloys (similar to alloy 2) is 452 J*K⁻¹*K⁻¹ [14].

3. Milling materials processing. Technological stages

Figures 1 and 2 show the samples of CoCr alloys according to the notation in Table 5, respectively titanium aluminide, which were subjected to milling processing according to the notation in Table 4.



Fig. 1 Samples of CoCr alloys



Fig. 2 Titanium aluminide samples

The stages of the technological milling process were:

- 1) Milling of semi-finished products using a milling cutter with a diameter of $\Phi 10$ mm, in order to obtain flat outer surfaces
- 2) 3D modeling of the part in the Autodesk Inventor 2023 design software

3) Carrying out the processing to obtain cavities of 5x5x1.5 mm (fig. 3, 4); a $\Phi 2$ mm milling cutter was used, the machining being performed on the numerically controlled machining center, Deckel Maho DMU70 (fig. 5) using the HEIDENHAIN iTNC530 CNC programming software (fig. 6). The processing regime for roughing operation for CoCr and titanium alloy parts, respectively, is shown in Table 5.

Table 5. Processing arrangements for parts of CoCr and titanium aluminide alloys

Part	Processing regime					
	v_c [m/min]	n [rot/min]	f_z [mm/dinte]	f [mm/min]	z	a_p [mm]
CoCr alloy parts	30	4774	0,008	153	4	0,3
Titanium aluminide alloy parts	25	3979	0,006	95	4	0,3



Fig. 3 CoCr alloy parts machined by milling

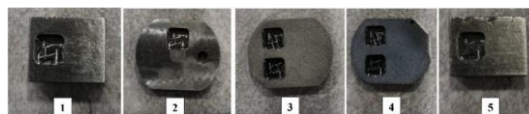


Fig. 4 TiAl alloy parts machined by milling



Fig. 5 CNC machining center, Deckel Maho DMU70



Fig. 6 HEIDENHAIN iTNC530 CNC Programs

4. Material processing by EDM. Technological stages.

1) Making copper electrodes (roughing electrode and finishing electrode), presented in fig. 7 was performed on the CNC machining center MAZAK NEXUS 350-II MY (fig. 8). The processing speed was 40 m/min for roughing turning, 50 m/min for finishing turning and 35 m/min for milling. Turning was performed with a roughing lathe knife (PWLNR 2525 M08 - WALTER) and a finishing lathe knife (SDHCR 2525 M11 - WALTER), and milling with a $\Phi 6$ mm milling cutter (MC111-06.0A4A-WJ30TF - WALTER).

2) The electrodes were checked and it was found that they fall within the tolerances included in the execution drawing (fig. 9). In order to determine the dimensions of the active part of the electrodes, respectively the size of the cross section (D_s) and the height (h_s), the relations were used [12]:

$$D_s = D_p - 2 s_L \quad [\text{mm}] \quad (1)$$

$$h_s = h_p (1 + \Theta) + c_s \quad [\text{mm}] \quad (2)$$

where: D_p - the size of the part cavity; s_L - side gap (from the ELER 01 car book); h_p - piece height [mm]; Θ - relative wear (from the ELER 01 car book) [%]; c_s - safety factor, $c_s=3-5$ mm.

The average roughness of the front surfaces is $0.230 \mu\text{m}$ and of the side surfaces is $0.325 \mu\text{m}$ when finishing milling.



Fig. 7 Roughing and finishing electrodes



Fig. 8 CNC Processing center MAZAK NEXUS 350-II MY

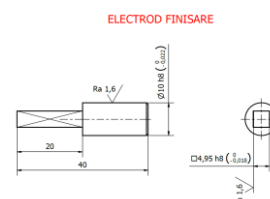


Fig. 9 Execution drawing of the finishing electrode

3) EDM was performed on the ELER 01 machine with the following regimes: roughing: controlled pulses, positive polarity at CoCr and negative at TiAl, $I=6A$ (maximum current density was observed, $J=I/S$ of $20 A/cm^2$, S-front surface), impulse time, $t_i=95 \mu s$, pause time, $t_0=24 \mu s$; finishing: negative polarity, relaxation pulses, $t_r \approx 0,8 \mu s$, given by the capacity steps, $C=10 nF$ and resistance, $R=0,74 k\Omega$. In all regimes, the pulsating regime was adopted to facilitate the flushing of the working gap: 3s processing, 2s lifting; The experimental data for roughing milling (FD) and roughing EDM (D) and finishing (F) are presented in Table 6.

Table 6. Experimental data on milling (FD) and roughing EDM (D) and finishing (F)

Material type	Processing Milling/EDM	Time [min]	t Milling/EDM [mm]	Volume Milling/EDM [mm ³]	Vw Milling/EDM [mm ³ /min]	Ra Milling/EDM [μm]
P1, NE	FD/EDM D	1,03/6,67	1,2/1,45	30/36,25	29,13/5,43	0,473/1,285
P2, SOFT	FD/EDM D	1,03/9,80	1,2/1,45	30/36,25	29,13/3,70	0,435/1,233
P3, LUKA	FD/EDM D	1,03/7,12	1,2/1,45	30/36,25	29,13/5,09	0,447/1,214
P1 TiAl	FD/EDM D	1,46/12,90	1,2/0,10	30/2,5	20,55/0,19	0,513/1,451
P2 TiAl	FD/EDM D	1,46/8,58	1,2/0,15	30/3,75	20,55/0,44	0,422/1,376
P3 TiAl	FD/EDM D	1,46/11,50	1,2/0,15	30/3,75	20,55/0,33	0,407/1,522
P4 TiAl	FD/EDM D	1,46/10,53	1,2/0,18	30/4,5	20,55/0,43	0,403/1,395
P5 TiAl	FD/EDM D	1,46/7,74	1,2/0,18	30/4,5	20,55/0,58	0,438/1,408
P1, NE	EDM F	20,97	0,05	1,25	0,06	0,483
P2, SOFT	EDM F	25,52	0,05	1,25	0,05	0,435
P3, LUKA	EDM F	15,44	0,05	1,25	0,08	0,390
P1 TiAl	EDM F	36,44	0,05	1,25	0,03	0,801
P2 TiAl	EDM F	23,20	0,05	1,25	0,05	0,693
P3 TiAl	EDM F	17,05	0,05	1,25	0,07	0,898
P4 TiAl	EDM F	36,64	0,05	1,25	0,03	0,742
P5 TiAl	EDM F	13,17	0,05	1,25	0,09	0,773

According to the results obtained for roughing by EDM, it is found that in the case of titanium aluminide parts, the processing times even in the case of small processing depths are longer, compared to those recorded in the case of processing CoCr alloy parts.

Figures 9 and 10 show the cavities made by EDM and milling, respectively.



Fig. 9 Parts of CoCr alloys processed by EDM and milling

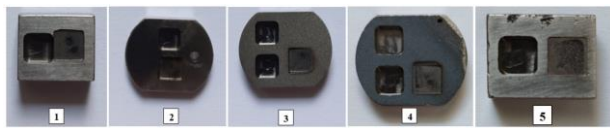


Fig. 10 Parts of TiAl alloys processed by EDM and milling

5. Control of piece

The roughness control of the cavity surfaces obtained by milling and EDM was performed with the Mahr MarSurf SD 26 roughness meter, the values obtained for roughness, being presented in table 6.

6. Finite element modeling of the EDM process

6.1 Model parameterization. Figures 11 and 12 show the parameters of the model in the Comsol Multiphysics 4.2 program for CoCr alloys, respectively, TiAl.

Name	Expression	Value	Description
rho	7800	7800	part weight
W	7000	6807.0	part weight
W1	6300	6165.0	initial crater width
W2	1.5e-5	1.5e-5	roughness
W3	0.0001	0.0001	part height
W4	0.0001	0.0001	part height
W5	0.0001	0.0001	part height
W6	0.0001	0.0001	part height
W7	0.0001	0.0001	part height
W8	0.0001	0.0001	part height
W9	0.0001	0.0001	part height
W10	0.0001	0.0001	part height
W11	0.0001	0.0001	part height
W12	0.0001	0.0001	part height
W13	0.0001	0.0001	part height
W14	0.0001	0.0001	part height
W15	0.0001	0.0001	part height
W16	0.0001	0.0001	part height
W17	0.0001	0.0001	part height
W18	0.0001	0.0001	part height
W19	0.0001	0.0001	part height
W20	0.0001	0.0001	part height
W21	0.0001	0.0001	part height
W22	0.0001	0.0001	part height
W23	0.0001	0.0001	part height
W24	0.0001	0.0001	part height
W25	0.0001	0.0001	part height
W26	0.0001	0.0001	part height
W27	0.0001	0.0001	part height
W28	0.0001	0.0001	part height
W29	0.0001	0.0001	part height
W30	0.0001	0.0001	part height
W31	0.0001	0.0001	part height
W32	0.0001	0.0001	part height
W33	0.0001	0.0001	part height
W34	0.0001	0.0001	part height
W35	0.0001	0.0001	part height
W36	0.0001	0.0001	part height
W37	0.0001	0.0001	part height
W38	0.0001	0.0001	part height
W39	0.0001	0.0001	part height
W40	0.0001	0.0001	part height
W41	0.0001	0.0001	part height
W42	0.0001	0.0001	part height
W43	0.0001	0.0001	part height
W44	0.0001	0.0001	part height
W45	0.0001	0.0001	part height
W46	0.0001	0.0001	part height
W47	0.0001	0.0001	part height
W48	0.0001	0.0001	part height
W49	0.0001	0.0001	part height
W50	0.0001	0.0001	part height

Fig. 11 Model parameters for CoCr alloys

Name	Expression	Value	Description
rho	4500	4500	part weight
W	7000	6807.0	part weight
W1	6300	6165.0	initial crater width
W2	1.5e-5	1.5e-5	roughness
W3	0.0001	0.0001	part height
W4	0.0001	0.0001	part height
W5	0.0001	0.0001	part height
W6	0.0001	0.0001	part height
W7	0.0001	0.0001	part height
W8	0.0001	0.0001	part height
W9	0.0001	0.0001	part height
W10	0.0001	0.0001	part height
W11	0.0001	0.0001	part height
W12	0.0001	0.0001	part height
W13	0.0001	0.0001	part height
W14	0.0001	0.0001	part height
W15	0.0001	0.0001	part height
W16	0.0001	0.0001	part height
W17	0.0001	0.0001	part height
W18	0.0001	0.0001	part height
W19	0.0001	0.0001	part height
W20	0.0001	0.0001	part height
W21	0.0001	0.0001	part height
W22	0.0001	0.0001	part height
W23	0.0001	0.0001	part height
W24	0.0001	0.0001	part height
W25	0.0001	0.0001	part height
W26	0.0001	0.0001	part height
W27	0.0001	0.0001	part height
W28	0.0001	0.0001	part height
W29	0.0001	0.0001	part height
W30	0.0001	0.0001	part height
W31	0.0001	0.0001	part height
W32	0.0001	0.0001	part height
W33	0.0001	0.0001	part height
W34	0.0001	0.0001	part height
W35	0.0001	0.0001	part height
W36	0.0001	0.0001	part height
W37	0.0001	0.0001	part height
W38	0.0001	0.0001	part height
W39	0.0001	0.0001	part height
W40	0.0001	0.0001	part height
W41	0.0001	0.0001	part height
W42	0.0001	0.0001	part height
W43	0.0001	0.0001	part height
W44	0.0001	0.0001	part height
W45	0.0001	0.0001	part height
W46	0.0001	0.0001	part height
W47	0.0001	0.0001	part height
W48	0.0001	0.0001	part height
W49	0.0001	0.0001	part height
W50	0.0001	0.0001	part height

Fig. 12 Model parameters for TiAl alloys

6.2 Creating the surface geometry after a single discharge: Fig. 13 shows the geometry of the surface geometry of a single discharge.

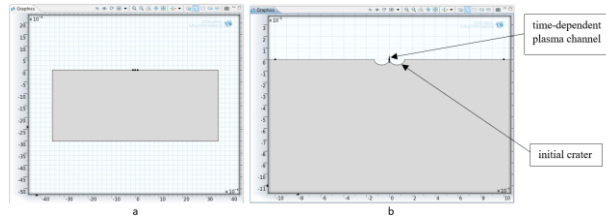


Fig. 13 Model geometry (a-part profile, b-microgeometry profile)

6.3 Introduction of material characteristics. Figures 14 and 15 show the material characteristics of the two types of materials.

Property	Name	Value	Unit	Property group
✓ Density	rho	1000 [kg/m ³]	kg/m ³	Basic
✓ Thermal conductivity	k	9.4 [W/(m*K)]	W/(m*K)	Basic
✓ Heat capacity at constant pressure	Cp	390 [J/(kg*K)]	J/(kg*K)	Basic

Fig. 14 Characteristics of CoCr alloys

Property	Name	Value	Unit	Property group
✓ Heat capacity at constant pres...	Cp	520 [J/(kg*K)]	J/(kg*K)	Basic
✓ Density	rho	4000 [kg/m ³]	kg/m ³	Basic
✓ Thermal conductivity	k	55 [W/(m*K)]	W/(m*K)	Basic

Fig. 15 Characteristics of TiAl alloys

6.4 Boundary conditions. Figures 16, 17, 18 show: heat flux, gas bubble insulation, dielectric cooling.

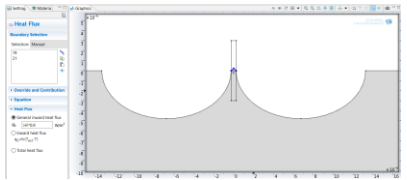


Fig. 16 Heat flux

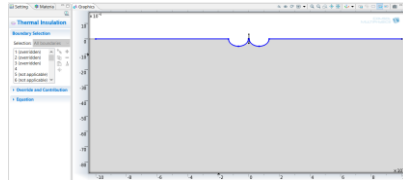


Fig. 17 Gas bubble insulation

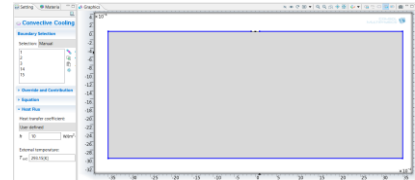


Fig. 18 Dielectric cooling

6.5 Results-temperature distribution after a single discharge on the two types of materials and discretization. Figures 19 and 20 show the temperature distributions after a single discharge on the two types of materials (in the case of CoCr alloys, the crater has a greater depth). Fig. 21 shows the discretization which has a dynamic character.

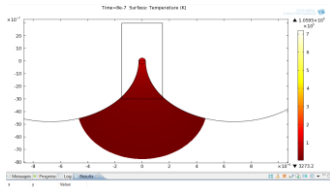


Fig. 19 Temperature distribution after a single discharge for CoCr alloys

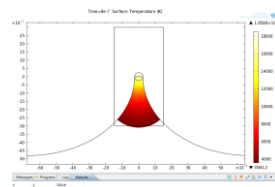


Fig. 20 Temperature distribution after a single discharge for TiAl alloys

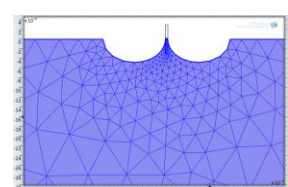


Fig. 21 Mesh

7. Conclusions

1. The experimental data obtained after processing the semi-finished products from the studied materials showed a higher machinability in both milling and EDM in the case of CoCr alloys, compared to Ti aluminides.

2. Analyzing the values obtained for the processing time and the productivity of each process used, it results that the variant that ensures a minimum time is the combination of roughing milling and finishing EDM necessary for the processing of the corners of the cavities.

3. Finite element modeling of the EDM process, respectively of a single discharge with relaxation impulse, used in finishing, shows that on the CoCr alloy a crater with a greater depth is obtained, compared to the depth obtained on the intermetallic compound, titanium aluminide, which results in the difference in productivity in the processing of the two materials.

8. Bibliography

- [1]. Vaicelyte, A.; Janssen, C.; Le Borgne, M.; Grosgeat, B. (2020), “Cobalt–Chromium Dental Alloys: Metal Exposures, Toxicological Risks, CMR Classification, and EU Regulatory Framework”, *Crystals Vol. 10*, pag. 1151
- [2]. Gherbesi, E. and Natalini, G. (2020). “The Ultimaster coronary stent system: 5-year worldwide experience”, *Future Cardiol., Vol. 16*, pag. 251–261
- [3]. Louwerens, J.K., Hockers, N., Achten, G., Sierevelt, I.N., Nolte, P.A., Van Hove, R.P. (2020). “No clinical difference between TiN-coated versus uncoated cementless CoCrMo mobile-bearing total knee arthroplasty; 10-year follow-up of a randomized controlled trial”, *Knee Surg. Sports Traumatol. Arthrosc.*, pag. 1–7
- [4]. Liu, G., Wang, X., Zhou, X., Zhang, L., Mi, J., Shan, Z., Huang, B., Chen, Z., Chen, Z. (2020). “Modulating the cobalt dose range to manipulate multisystem cooperation in bone environment: A strategy to resolve the controversies about cobalt use for orthopedic applications”, *Theranostics Vol. 10*, pag. 1074–1089
- [5]. Buser, D., Sennerby, L., De Bruyn, H. (2017). “Modern implant dentistry based on osseointegration: 50 years of progress, current trends and open questions”, *Periodontology 2000 Vol. 73*, pag. 7–21.
- [6]. Leyens, C. and Peters, M. (2003). “Titanium and titanium alloys: fundamentals and applications”, Editura on line Wiley-VCH, 532 pag., 978-3-527-60211-7
- [7]. Liu, B. and Liu, Y. (2015). “Powder metallurgy titanium aluminide alloys”-Capitol 27 în cartea “Titanium Powder Metallurgy”, ISBN 978-0-12-800054-0, Copyright © 2015 Elsevier Inc. All rights reserved, 628 pagini
- [8]. GE – Aviation: GENx, GE [Online]. <http://www.geae.com/engines/commercial/genx/>, 2007
- [9]. Mori, M. et al. (2012). “Microstructures and mechanical properties of biomedical Co-29Cr-6Mo-0.14N alloys processed by hot rolling”, *Metallurgical and Materials Transactions, Vol. A 43(9)*, pag. 3108-3119
- [10] <https://adentatec.com/>
- [11] <https://www.lukadent.de/>
- [12] Szkliniarz, W. and Szkliniarz, A. (2021) “Microstructure and Properties of TiAl-Based Alloys Melted in Graphite Crucible”, *Metals, Vol. 11*, no. 4, pag. 669-686
- [13]. <https://periodictable.com/Properties/A/ThermalConductivity.an.htm>
- [14]. Baron, S., Ahearne, E., Connolly, P., Keaveney, S., Byrne, G. (2015). “An Assessment of Medical Grade Cobalt Chromium Alloy ASTM F1537 as a "Difficult-to-Cut (DTC)" Material”, Proceedings of the Machine Tool Technologies Research Foundation Annual Meeting, San Francisco, June 30th-July 2nd, 2015
- [15]. Ghiculescu, D. Curs de tehnologii Neconvenționale, available at <https://curs.upb.ro/2021/login/index.php>, Accessed at: 1.05.2022

INFLUENCE OF HOLLOW GLASS MICROSPHERES AND MULTI WALLED CARBON NANOTUBES ON THE WATER ABSORPTION IN POLYAMIDES

ENE Elena¹, FLEACĂ Cristina-Mihaela¹, PÂRVU Gabriela-Marina², PERDUM Andrei-Ionuț³

¹Faculty of Industrial Engineering and Robotics, Specialization: IEI, Year of study: 3,
e-mail: ene_elenal23@yahoo.com

²Faculty of Industrial Engineering and Robotics, Manufacturing Engineering Department, University POLITEHNICA of Bucharest

³Doctoral School of Materials Science and Engineering, University POLITEHNICA of Bucharest

ABSTRACT: The aim of the present paper is to evaluate the influence of hollow glass bubbles (HGB) and multi-walled carbon nanotubes (MWCNT) in the polyamide 6 (PA6) matrix on water absorption. The research was carried out in the laboratory on six compositions of hybrid materials with HGB content between 30% and 10% and MWCNT between 2% and 15%. After 336 hours of immersion, it was highlighted that water absorption has increased over time, and the growth rate is a maximum of 168 hours. HGB increases water absorption while MWCNT decreases polyamide water absorption by 10%.

KEY WORDS: water absorption, polyamides, glass microbes, carbon nanotubes

1. Introduction

In today's context, pollution has become one of the global problems facing mankind, and studies and research [1] have concluded that about three-quarters of greenhouse gas emissions come from road transport, exactly from high-capacity vehicles that consume a lot of fuel. The research has also highlighted the fact that this amount of fuel consumed is related to the mass of the car [1]. Therefore, there is the issue of reducing the weight of cars, by using hybrid materials with polymeric matrix and lightweight reinforcing materials such as carbon nanotubes. One of the factors that accelerates the aging process of polymeric products is the absorption of water and other chemical compounds. Precise modelling of moisture absorption in hybrid materials based on organic polymers is required to assess the durability and to make a correct prediction of the life of the products. Chemical exposure, especially exposure to moisture, is a key degradation mechanism in polymeric systems. The process of penetration of chemicals through polymers is the consequence of two interdependent processes that take place, the dissolution in the polymer and the diffusion through the polymer [2]. Dissolution is the process of absorbing chemicals into the polymer and depends on the affinity of the polymer for the absorbing molecules, ie. the interaction energy, the volume available for absorption and the concentration of the absorbing chemical. There is a limit to the amount of absorbed chemical under a given set of conditions and this limit is solubility. Diffusion is the process of transporting the substance through material phases whose driving force is the concentration gradient of the species that diffuses between two points (areas) of the material phase. The absorbed molecules are transported by diffusion inside the polymer and the diffusion properties are characterized by the diffusion coefficients. Often, especially in thick sections, the parameter that determines the speed of the aging process is the time required for the spread of harmful species in sufficient concentrations in critical regions. One of the usual approaches in the interpretation of stationary diffusion is the application of Fick's law I in which the steady state flux of diffuser per unit area, or the diffusion flow (J) is a function of the concentration gradient with the diffusion distance [3]:

$J = -D \frac{dc}{dx}$ Fick's law I, where the diffusion coefficient (D) does not depend on the concentration, then Fick's second law can be used to determine the time dependence of the diffuser concentration in the specimen.

$$\frac{dc}{dt} = D \frac{d^2c}{dx^2} \text{ Fick's Second Law (non-stationary broadcast)}$$

The aim of this research is to evaluate the influence of glass globules (HGB) [2] and multi-walled carbon nanotubes (MWCNT) from the polyamide 6 matrix (PA6) on water absorption.

2. Materials and methods

2.1 Materials

The composition of polyamide 6-based hybrid materials reinforced with glass micro-balloons (HBG) and multi-walled carbon nanotubes (MWCNT) under study are presented in Table 1, in volumetric percentages.

Table 1. Composition of specimen used in current study, in volume percentage

Sample	HGB content (% vol.)	MWCNT content (% vol.)	PA6 content (% vol.)
1	0	0	100
2	30	0	rest
3	0	15	rest
4	10	2	rest
5	10	4	rest
6	20	4	rest
7	30	4	rest

2.2 Methods

Specimens with dimensions of approximately 40x10x4 mm cut from strips obtained by the mould injection at 260°C were used in experiment.

The protocol for determining the influence of glass microbubbles and carbon nanotubes on the water absorption of polyamides was in accordance with the ASTM D 570-98 standard for plastics and is shown in Figure 1.

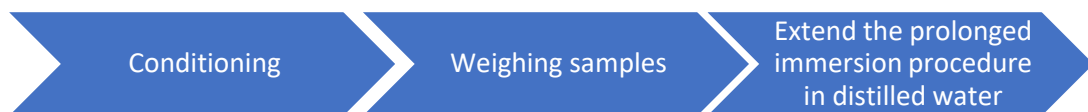


Fig. 1 Working methodology for determining the percentage of water absorbed

The labelled specimens were cleaned in the distilled water under ultrasonic field, conditioned by keeping them in the oven at 50 ± 3 ° C for 24 hours, cooled in a desiccator with calcium chloride (fig.2), then weighed to determine the initial mass at the precision analytical balance 10^{-4} g, fig.3.



Fig. 2 Conditioning samples at 50 °and drying in a desiccator, with CaCl₂ as the moisture removal agent in the enclosure

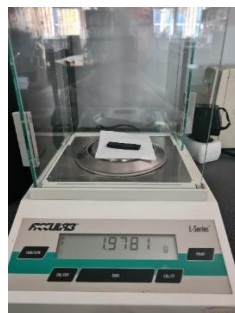


Fig.3. Weighing samples at precision analytical balance 10-4 g

The ASTM D 570 standard provides for four different immersion situations, with the current favourable case being long-term.



Long-term immersion

To determine the total water absorbed when saturated, the conditioned samples are immersed in distilled water and kept for 24 hours, then wiped with a dry cloth, weighed to the nearest 0.001 g and then reintroduced into water. Weighing shall be repeated at the end of the first week and thereafter every two weeks, until the weight gain over a period of two weeks represents, on average, less than 1% of the total weight gain, or 5 mg; when the test piece is considered to be substantially saturated.



Fig. 4. Place samples in distilled water according to the established procedure and keep at a temperature of 23 ° C in a thermostated water bath

3. Experimental results and discussions

The absorbed water concentration is calculated according to ASTM D 570 with relation:

$$c = \frac{m_t - m_c}{m_c} \times 100$$

where m_t represents the mass of the test specimen at time t , m_c - the mass of the conditioned (dry) test piece.

The obtained results are systematized in table 2 and figure 5.

Table 2. Results of water uptake during 336 h

test SAMPLE	m_c , g	m_{24} ,g	Wup 24, (%)	m_{168} ,g	Wup 168, (%)	m_{336} ,g	Wup 336, (%)
1	17,429	1,768	0,014401	18,144	0,041024	18,456	0,058925
2	16,553	17,252	0,042228	19,129	0,155621	20,422	0,233734
3	16,813	17,036	0,013264	17,381	0,033783	1,77	0,052757
4	15,479	15,788	0,019963	16,287	0,0522	16,731	0,080884
5	18,868	19,199	0,017543	19,779	0,048283	20,336	0,077804
6	1,562	15,745	0,008003	16,776	0,074008	17,854	0,143022
7	14,346	14,888	0,037781	1,631	0,136902	17,194	0,198522

Wup=water uptake

m_c = mass of the test conditioned specimen

m_{24} = mass of the conditioned specimen after 24 hours of immersion

Wup₂₄ = water absorption durring 24 hours of immersion

m_{168} = mass of the conditioned specimen after 168 hours (one week) of immersion

Wup₁₆₈ = water absorption during 168 hours of immersion

m_{336} = mass of the conditioned specimen after 336 hours of immersion

Wup₃₃₆ = water absorption during 336 hours

Usually [2,4] it is used the dependence of water absorption $C(t)$ with respect to the square root of the immersion time (fig 5) to characterize the capacity of a polymeric material to absorb moisture.. It is observed that the introduction of a quantity of 30HGB in PA6 increases the water absorption 4 times while the introduction of MWCNT decreases water absorption by 10%.

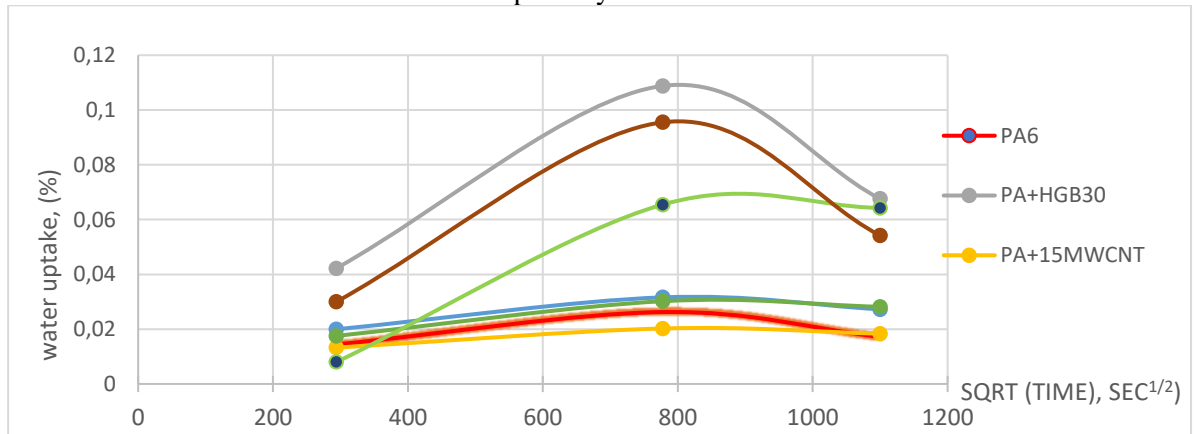


Fig. 5 Dependence of water absorption $C(t)$ on the square root of the immersion time in distilled water at 23 ° C for the seven test specimens

4. Conclusions

Following the research carried out, the following conclusions can be drawn:

- Organic polymers absorb water;
- Water absorption depends on the composition of polymeric hybrid materials
- Carbon nanotubes reduce water absorption in PA6
- Glass microbubbles promote water absorption in PA6

5. Bibliography

- [1]. Alexandra Banu, Octavian Radovici, Elemente de Stiința și Ingineria Suprafeței, Ed Printech, București, 2013
- [2]. B C Duncan and W R Broughton. (2007), “Absorption and Diffusion of Moisture In Polymeric Materials”, în: Measurement Good Practice Guide No. 102 National Physical Laboratory Teddington, Middlesex, United Kingdom, TW11 0LW ISSN 1368-6550;
- [3]. Loreto M. Valenzuela,¹ Doyle D. Knight,² and Joachim Kohn, (2016), “Developing a Suitable Model for Water Uptake for Biodegradable Polymers Using Small Training Sets”, International Journal of Biomaterials Volume 2016, doi.org/10.1155/2016/6273414,
- [4]. G. Bascheka , G. Hartwiga, *, F. Zahradnik (1999) „ Effect of water absorption in polymers at low and high temperatures”, Polymer 40 (1999) 3433–3441

Acknowledgement

The authors would like to thank to Prof. Alexandra BANU from Manufacturing Engineering Department, Faculty of Industrial Engineering and Robotics for her support and guidance in completing this research.

RESEARCH ON ANALYSIS, SIMULATION AND PROGRAMMING OF PICKING SYSTEMS

MILOIU Andrei Nicolae¹, GHEORGHE Marian² and MANOLACHE Daniel-Silviu²

¹Faculty of Industrial Engineering and Robotics, Specialization: Industrial Economic Engineering,
4th study year, e-mail: razzzer_man97@yahoo.com

³Faculty of Industrial Engineering and Robotics, Manufacturing Engineering Department

ABSTRACT: The paper presents elements regarding picking systems, with a tendency to develop and innovate. Warehouses, generally, directly affect the supply chain to meet customer orders, Thus, the picking process is described based on economic elements and outlined using a video simulation.

KEYWORDS: warehouses, analysis, simulation, picking, systems.

1. Introduction

Space and time efficiency are generally the most important criteria for warehouses management. Logistics facilities, such as distribution warehouses, directly affect the ability of the supply chain to meet customer demand. The key task of a warehouse is to fulfill customer orders on time and at the lowest cost. Therefore, it is necessary to look for organizational and technological solutions to improve the warehouse processes, such as picking up orders, ensuring the smooth, fast and precise fulfillment of orders [1]. Order pick-up processes can absorb up to 60% of the FTE (full-time equivalent employees [2]) for all activities in the warehouse and can generate approximately 55% of costs [1]. For this reason, there is a need to minimize the time of fulfillment of orders, respectively, to maximize the productivity of picking processes.

2. General considerations

2.1. Picking systems

Picking systems are classified according to different criteria - number of employees, type of picking process, order processing. Thus, there are order processing systems: manual; semi-automated; automated. In the manual system (from operator-to-product), picking operators move to locations and manually select items. A semi-automatic system (product-to-operator) moves products from storage locations to the picking station by internal means of transport, such as carousels, vertical lifting modules (elevators), SBS/ RS, mobile shelves, etc. Automatic control systems are able to fulfil orders without any human assistance (eg A-frame) [1].

In manual picking systems, manual order picking usually requires a number of operators working simultaneously. The order picking process is very laborious. System flow should potentially increase, but congestion is very common. Congestion in the manual pick-up system is related to the situation where the operator's tasks are interrupted by another operator, while all the requirements for a normal picking process are met [1]. The picking process is considered normal when the flow of orders is uninterrupted, all support systems (e.g. IT or equipment) are able to operate, and interfaces with other areas (receiving, sorting, etc.) are in operation [3]. A representation of the "operator-to-product" system is shown in Fig. 1.

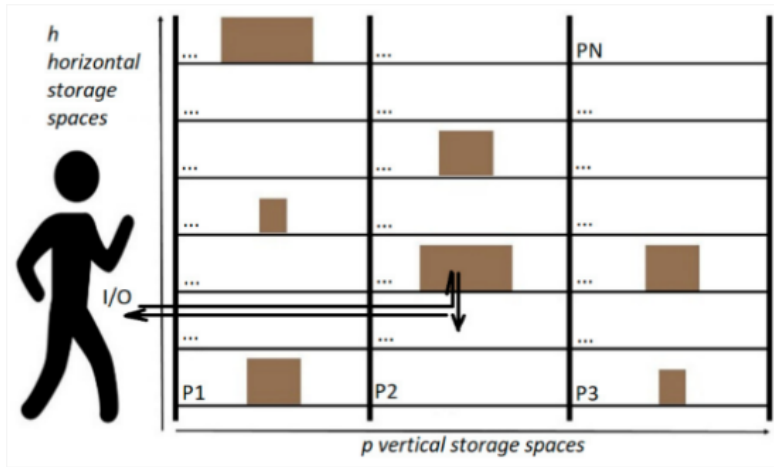


Fig. 1. Operator-to-part system [5]

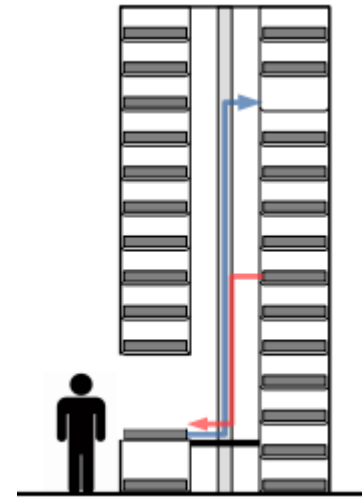


Fig. 2. VLM system [4]

VLMs are AS/ RS (systems of goods/ parts/ products) in which several trays are stored in a high rectangular prism. In these systems, the trays who containing the required parts are presented at the input/output location (I/O). Trays in a VLM are generally divided into boxes to form individual storage locations. Once a tray is in the I/O location, the operator picks up the product from the box using indicators that point the correct box. A representation of a VLM system can be seen in Fig. 2 [4].

2.2. Analytical methods regarding the efficiency of the standard manual-picking system

The pick-face blocking approach (the place in front of each shelf, where the picking is performed) is based on probability theory and combinatorial calculations. One working element is the binomial coefficient to calculate the number of possible combinations of having j from K collectivities located in front of a shelf column at the same time. By weighting the probability that an operator is located in front of a shelf column, and at some point in time and taking into account all shelf columns, the following relationship is obtained to estimate the flow decrease [3]:

$$\lambda_{\text{Decline}} = \lambda_{\text{OP}} * (K - \sum_{i=1}^c \sum_{j=2}^K \binom{K}{j} (p_i * r)^j) \quad (1)$$

where λ_{Decline} - the reduced throughput (order lines per hour), λ_{OP} - the throughput (order lines per hour) of a single picker without any congestion, c - the number of rack columns in the aisle, p_i - the pick frequency of rack column i , and r - the probability that a picker is picking, i.e. the portion of picking time with regard to the total order picking time.

A similar approach estimates additional travel time caused by in-the-aisle interferences. First, the extra time t_{add} is derived, so that, a picker K needs to walk in order to pass $(K - 1)$ other pickers, assuming that K pickers meet in a certain segment i . Note that one segment does not necessarily represent one rack column. After deriving the probability that K pickers interfere in segment i , the number of interferences I_K is calculated. In accordance with the calculations on pick-face blocking, the binomial coefficient is used and the percentage increase in travel time X_K is [3]:

$$X_K = \sum_{j=2}^K \binom{K}{j} * t_{\text{add},K} * I_K \quad (2)$$

„Experiments show that for random storage travel time typically increases as much as 2% for less crowded aisles (5:1 ratio of segments to order pickers) and the increases can be as high as 7% for very crowded aisles (3:2 ratio). For class-based storage increases are much higher, namely 5% for less crowded aisles and up to 30% for very crowded aisles. Based on these results, an important element is derivation operational guidelines. In random storage there should be at most one picker per 3 meters of pick face. For class-based storage, there should not be more than two pickers per aisle, independent of the total length of the pick face as picks often tend to concentrate on a few rack columns” [3].

3. Simulation and analysis: Case study

„In the proposed models it is assumed that the items are stored with a random storage assignment, in both systems, and that the picking orders are processed individually, with a simple order picking strategy (and no batching). Moreover, both systems are considered to be always available, and the replenishment activity, needed for refilling the storage locations with items, is assumed to be performed in an additional time with a similar strategy for both systems” [7]. „All the indirect costs are assumed to be included in the total annual cost, and the throughput of the systems are described through a picking time, which could depend on the adoption of paperless picking technologies” [6].

“Two different terms are considered into the general total cost function: the fixed cost component is related to the annual costs of facilities, equipment and devices, including the indirect costs; on the other side, the variable cost component is connected to the resources necessary yearly to perform the required items picking” [6]:

$$TC^s = C_{fix}^s + C_{var}^s \quad (3)$$

where $s = W$ for the warehouse with R3000 racks, mezzanine system, and $s = V$ for the dual bay VLM [6].

The following case study shows the application of the economic model developed in the present paper. A step-by-step procedure is used to explain which data are necessary and how to compare the VLM system to the traditional warehouse with R3000 racks.

- Input data collection and estimation

The first step for the application of the method consists in retrieving the data that are needed for the formulations. General information and useful input data about the warehouse and the pickers are reported in Table 1.

Table 1. Information about the case studied

	Type A	Type B
Type of products	Spare parts, small parts, bushings, fasteners, etc. (usually car parts)	Various products, products for bathroom installations, batteries, etc.
Number of stored items	≈ 4.000 pcs.	≈ 3.500 pcs.
V [m ³]	≈ 180 m ³ on the mezzanine floor	≈ 180 m ³ on the ground floor
Q [picks/h]	220	360
N [lines/order]	12	25
t _i ^W [s]	40.5	47
h _v [h]	1,800 h	3,600 h
k ^W	2.59	1.47
SL ^W		0.2
C _{SP} [€/(hm ²)]		100
C _{OP} [€/h]		35

The studied warehouse has an area A^W of about 30 x 10 m², with a mezzanine where two different categories of products are stocked in R3000 racks. These two groups are stocked in the two floors: type A on the mezzanine level (with a resulting k^W = 2,59) and type B on the ground floor (then, k^W = 1,47).

Direct measurement method has permitted to estimate the average picking time per order line t_1^W . The total amount of time spent by the operators in the overall picking operations has been divided by the total amount of order lines performed in a period of 20 weeks, resulting in $t_1^W = 40,5$ s for type A and $t_1^W = 47$ s for type B.

From a first analysis of the available height of the warehouse area, it could be installed a VLM system of 10 m high, with 75 m^3 as storage volume V^V . From the information provided by different technical sheets and also confirmed by previous researches, typical values of t_{pick}^s , t_{fix}^s and t_{travel}^s for this kind of system are about 28 s, 60 s and 5 s, respectively. Thus, considering the different average number of lines per order N , the average picking time t_1^V is 28 s for the items of type A and 26 s for the items of type B.

- R_Q calculation and VLM applicability evaluation

Starting from the average cycle times per line t_1^W and t_1^V , it can be estimated the throughput ratio R_Q between the traditional solution and the VLM system for both cases: $R_Q = 1.26$ for the type A and $R_Q = 1.56$ for type B. Then, based on the input data available from the previous step, for the products of type A, R_Q^* (equal to 1.30) is higher than R_Q , and consequently, the traditional warehouse with R3000 racks is preferable.

For the other group of items (B) the throughput ratio is higher, $R_Q = 1.56$. In this particular case, $R_Q^* = 1.23$ because the warehouse works for $h_y = 3,600$ h/year. Thus, the VLM system is preferable for this group of products, since $R_Q > R_Q^*$.

- Area of application and system position representation

The VLM application areas for the two analysed cases, type A and type B, are reported in Fig. 3. For the items of type A, it can be seen that there is no VLM area of application, and the position of the adopted solution, related to $V^V = 75 \text{ m}^3$, lays on the area of the warehouse with R3000 racks ($\frac{Q}{N^V * Q^V} = 0,57$). For type B, the VLM area of application is for values of Q^*/Q^V higher than about 65%, for the storage volume V^V of 75 m^3 . Here, the condition $\frac{Q}{N^V * Q^V} > \frac{Q^*}{Q^V}$ is verified, since $\frac{Q}{N^V * Q^V} = 0.866$.

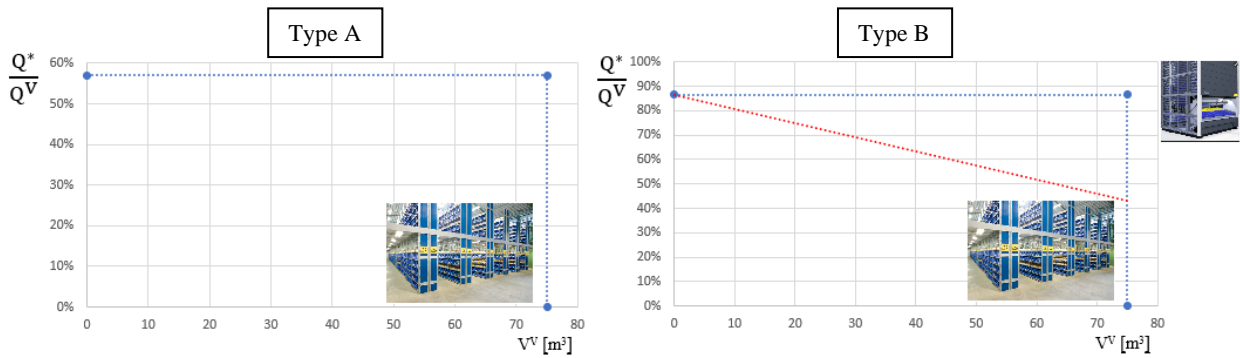


Fig. 3. „Trend of $\frac{Q^*}{Q^V}$ and VLM area of application for the analyzed cases” [6, 8, 9, 10].

- Total costs and saving calculation

For type B, the applicability of the VLM system can be demonstrated also by calculating the total cost functions of the two alternatives. For the as-is scenario of the warehouse with R3000 racks, the total cost is :

$$TC^W = C_{SP} * k^W * \frac{V}{SL^W * H} + C_{OP} * \frac{Q}{Q^W} * h_y = 23.310 + 155.925 = 179.235 \text{ €/year} \quad (4)$$

Based on the input data, the required number of VLMs to be installed N^V is :

$$N^V = \max \left(\left\lceil \frac{Q}{Q^V} \right\rceil ; \left\lceil \frac{V}{V^V} \right\rceil \right) = \max \left(\left\lceil \frac{360}{138} \right\rceil ; \left\lceil \frac{180}{75} \right\rceil \right) = 3 \quad (5)$$

and the total cost can be estimated as such:

$$TC^V = N^V * \left[\left(C_{SP} * k^V * \frac{V^V}{SL^V * H} \right) + C_{OP} * \frac{Q}{N^V * Q^V} * h_y \right] = 3 * 5.512,5 + 109.200 = 125.737,5 \text{ €/year} \quad (6)$$

The total savings obtained by installing the VLM system is approx. € 53,500/year, so approx. 29.8%. It is to be noted that the structure of the model analyzed above is taken from the reference [6].

The simulation of such an example of picking system efficiency is presented in the following video:



Simulation_SCSS.m
p4

Video no.1 - Parallel simulation of picking systems [11]

4. Conclusions

In the process of supplying and orders fulfilling in the logistics system, it is important to develop picking. Thanks to innovation, the work is easier for the operators, but the process is also more efficient: better times, more order lines/h, flow with fewer interruptions in the supply chain, more space in warehouses, more storage capacity, etc.

The trend is developing for the transition, at least, from standard systems to semi-automated picking systems, which creates the wave effect, as an improvement, in the supply chain.

5. References

- [1] Klodawski, M., Jachimowski, R., Jacyna-Golda, I. & Izdebski, M. (2018), SIMULATION ANALYSIS OF ORDER PICKING EFFICIENCY WITH CONGESTION SITUATIONS, INT'L J. OF SIMULATION MODELLING (Q2), Volume 17, Issue 3, pp 431-443, DOI: 10.2507/IJSIMM17(3)438, WOS: 000450486200005, ISSN 1726-4529, eISSN 1996-8566, 2018.
- [2] ***, Number of FTEs that perform the process "operate outbound transportation" as a percentage of FTEs that perform the process group "manage logistics and warehousing", <https://www.apqc.org/what-we-do/benchmarking/open-standards-benchmarking/measures/number-ftes-perform-process-operate-2#:~:text=This%20measure%20calculates%20the%20number,a%20warehouse%20to%20a%20customer>, accessed on 01.05.2022
- [3] Huber, C., Throughput Analysis of Manual Order Picking Systems with Congestion Consideration, Dissertation, KIT Scientific Publishing, Karlsruhe, Volume 76,ISSN: 0171-2772, ISBN: 978-3-86644-759-2, 2011.
- [4] Öz, Burak (2019), ORDER PICKING ORIENTED STORAGE ASSIGNMENT PROBLEM IN A VERTICAL LIFT MODULE SYSTEM, Master of Science in Industrial Engineering Department, Middle East Technical University, 2019.
- [5] Gajšek B., Šinko S., Kramberger T., Butlewski M., Özceylan E., Đukić G., Towards Productive and Ergonomic Order Picking: Multi-Objective Modeling Approach, J. Appl. Sci. 2021, 11, 4179.mhttps://doi.org/10.3390/app11094179,WOS: 000649896000001, eISSN: 2076-3417.
- [6] Martina C., Fabio S., Alessandro P., Vertical Lift Modules (VLMs) for small items order picking: an economic evaluation, International Journal of Production Economics, Volume 210, April 2019, pp 199-210.
- [7] Bartholdi J. J., III, Steven T. HACKMAN (2019), WAREHOUSE & DISTRIBUTION SCIENC, Release 0.98.1, The Supply Chain & Logistics Institute H. Milton Stewart School of

Industrial and Systems Engineering Georgia Institute of Technology Atlanta, GA 30332-0205 USA, 2019, <https://www.warehouse-science.com/>

[8] ***, SSI Schaffer presents its products at Motortec Automechanika 2011, <https://www.interempresas.net/Transportation/Articles/47893-SSI-Schaffer-presents-its-main-products-in-Motortec-Automechanika-2011.html>, accessed on 07.05.2022

[9] ***, SSI Schaffer, <https://www.ssi-schaefer.com/ro-ro/produse/depozitare-/small-load-carriers/ma%C5%9Fini-pentru-depozit-%C5%9Fi-sisteme-navet%C4%83/liftul-pentru-depozit-logimat--208996>, accessed on 07.05.2022

[10] ***, Microsoft Excel, Microsoft Corporation

[11] ***, Modula VLM Video, <https://www.youtube.com/watch?v=hvS7IaOeABY>, accessed on 09.05.2022

6. Notations

Symbol	Significance	Notations
Q [picks/h]	Required flow/hour $Q = \sum_{i=1}^n Q_i$	
N [lines/order]	Average number of lines on the picking order	
V [m ³]	Total storage volume $V = \sum_{i=1}^n V_i$	
H [m]	Available height	
C _{SP} [€/hm ²]	Annual cost of space per square meter	
C _{OP} [€/h]	Hourly operating cost	
h _y [h]	Number of working hours in a year	
TC ^S [€/an]	The total cost of the annual order picking system, $s \in \{W, V\}$	
C _{fix} ^S [€/an]	The fixed cost of the annual order picking system, $s \in \{W, V\}$	
C _{var} ^S [€/an]	The variable cost of the annual order picking system, $s \in \{W, V\}$	
k ^s	Cost coefficient of the order picking system space, $s \in \{W, V\}$	
SL ^s	Saturation level of the control lift system, $s \in \{W, V\}$	
Q ^s [picks/h]	Flow / hour of the control lifting system, $Q^s = 3,600/t_i^s$, $s \in \{W, V\}$	
t _i ^s [s]	Average cycle time per line, $s \in \{W, V\}$	
t _{pick} ^s [s]	Picking time, $s \in \{W, V\}$	
t _{fix} ^s [s]	Time for fixed activities, $s \in \{W, V\}$	
t _{travel} ^s [s]	Travel time, $s \in \{W, V\}$	
A ^W [m ²]	The area of the surface where the mezzanine is located	
N ^V	Number of VLMs	
V ^V [m ³]	The storage capacity as volume of a VLM	
R _Q	Systems flow ratio	
SBS/RS	Transfer-based storage and retrieval system	
VLM	Vertical Lift Module	
AS/RS	Automatic storage and recovery system	

RESEARCH ON DIVIDING SCHEMES AND DEVICES WITH NUMERICAL CONTROL

GHIȚĂ Nicoleta-Sorina¹, FĂȚU Andrei-Marian¹, DUCMAN Dorina-Denisa¹, GHEORGHE Marian², POPAN Gheorghe, GANNAM Nasim, PÂRVU Corneliu²

¹Faculty of Industrial Engineering and Robotics, Specialization: Industrial Economic Engineering, 4th study year, e-mail: nicoletaghita64@gmail.com

²Faculty of Industrial Engineering and Robotics, Manufacturing Engineering Department

ABSTRACT: Dividing/ indexing represents a necessary process in certain technological operations/ systems of machining, control or assembly. In industrial or laboratory conditions, different variants of dividing/ indexing heads or tables/plateaus are used. In this paper, there is presented a series of elements of calculus, constructive-functional and simulation regarding dividing schemes and devices, with mechanical or computer numerical control. Specific elements refer to a dividing/ indexing table from the structure of a CNC machining center with 5 axes, of which 3 are numerically controlled and 2 - manually controlled.

KEYWORDS: dividing, indexing, dividing head, dividing table, CNC.

1. Introduction

The objective of this paper is to present general elements and applications on the development of functional schemes and dividing devices with mechanical control and computer numerical control, respectively.

The research-development methodology is structured in relation to the following reference elements: general framework; functional scheme; dividing calculations; constructive-functional development of dividing devices; simulation of dividing devices.

2. General considerations

The dividing/ indexing devices are type of: dividing/ indexing head, dividing/ indexing/ rotary table or plateau, etc.

The dividing head is used to divide the circumference of the workpiece into equally spaced divisions - on gears, helical gears, screws and for irregular profile workpieces. Indexing plates are used to ensure that the workpiece is positioned with accuracy. Most dividing heads have an indexing plate permanently attached to the spindle (Fig. 1) [1].



Fig. 1. Dividing head [4]

Rotary indexers use a scale and display the angle of rotation (0 - 360°) [4]. Dividing heads can be simple, universal (Fig. 2, 3), etc.

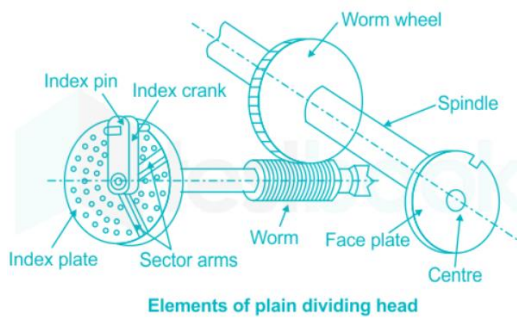


Fig. 2. Elements of a simple dividing head [5]

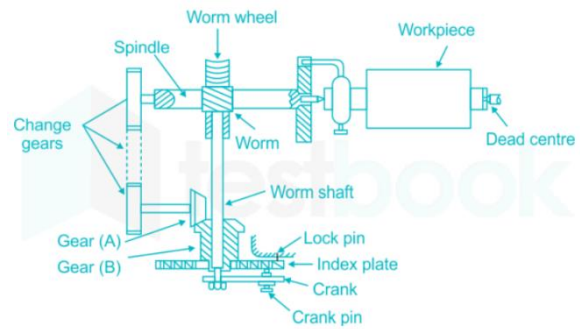


Fig. 3. Elements of a universal dividing head [5]

In a simple dividing head, an worm wheel is rigidly fixed to the spindle, while the index crank is rigidly mounted on the worm shaft, so that rotation of the index crank rotates the worm shaft (Fig. 2) [5].

The universal dividing head is used to set the horizontal, vertical or inclined working position in relation to the table of the machine - tool. Periodically, the working position is changed to a given angle for indexing the workpiece or to achieve a continuous rotary movement of the workpiece, e.g., for milling helical splines (Fig. 3) [5].

The optical dividing head is used for high-precision angular position indexing. The optical system is incorporated in the dividing head for angle reading (Fig. 4) [5].



Fig. 4. Optical divider head [5]

3. Numerical control indexing

A CNC indexing head is driven by a servo motor coupled to the drive shaft and electronically controlled. Control can be a keypad for operator or entirely type CNC (Fig. 5) [5].

A stepper motor is included in the structure of an indexing head. The stepper motor is a brushless DC motor in which the rotation is divided into a number of steps, which results from the motor construction. By default, a full 360° shaft rotation is divided into 200 steps, which means that the shaft takes a new step every 1.8° . Motors are also available in which the shaft pitch is 2; 2.5; 5, 15 or 30° . A complete rotation of the shaft is divided into several discrete segments; the stepper motor does not rotate continuously, but in steps, passing through intermediate states, which is why the operation of such a motor is accompanied by a characteristic sound or vibration (Fig. 6) [8].



Fig. 5. CNC indexing head [9]



Fig. 6. Stepper motor [10]

A closed-loop electronic indexing head uses servomotor and feedback measurements to ensure that the desired position is achieved. A common feedback sensor used in an electronic indexing head is the optical rotary encoder [2]. This consists of a light source, a photocell and a disc containing a series of slots through which the light source can shine to power the photocell. The disc is connected to the rotating shaft. The plate rotates, and the slots cause the light source to be seen by the photocell as a series of flashes, which are converted into an equivalent series of electrical pulses. By counting the pulses and calculating their frequency, the angle and rotational speed of the workpiece, determined in the basic optical encoder, can be calculated.

The angle between the disk slots, α , in $^\circ/\text{slot}$, is:

$$\alpha = \frac{360}{n_s} \quad (1)$$

where n_s is the number of slots from the disk, in slot/rev, and the angle of 360 is in $^\circ/\text{rev}$.

For a given angular rotation of the workpiece, A_g , the encoder generates a number of pulses n_p :

$$n_p = \frac{360n_s}{A_g} \quad (2)$$

The frequency of the pulses, f_p , in Hz (pulse/sec), is:

$$f_p = \frac{f_r n_s}{60p} \quad (3)$$

where: n_s - the number of slots in the encoder disk, in pulses/rev; f_r – the feed rate in mm/min (known); p – the pitch, in mm/rev (known); 60 - converts seconds to minutes (Fig. 7) [2].

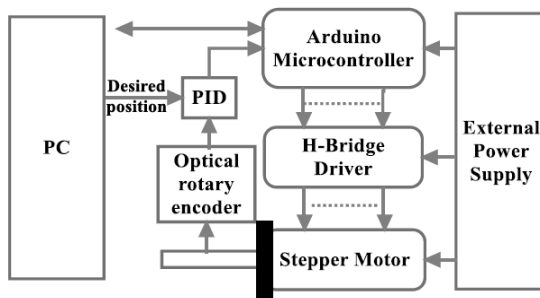


Fig. 7. Schematic diagram of an electronic indexing head [2]



Fig. 8. Indexing table [11]

The indexing table (Fig. 8) [11] is used to transport components of the production line from one point to another, stabilizing a component to perform a production task, a certain quality control or marking - through the side devices of the table. The side devices can be placed around the table and near to special stations to perform the specific operation [3].

4. Constructive-functional analysis and simulation of the dividing table from the structure of a CNC machining centre

Within Dr. Köcher SRL, an analysis has been performed in order to highlight the functionality of the dividing/ indexing table from the structure of a DMU 50 CNC Centre (Fig. 9). The core business of the company is the production of die-casting and injection moulds for plastic mass, the manufacturing of die-cast parts and other products [7].

The DMU 50 CNC Center presents a robust construction, with a simple installation concept, low space requirements, high rigidity, precision and long service life.



Fig. 9. DMU 50 CNC

The specifications of the DMU 50 CNC Centre are as follows:

- Traverse range: X = 500 mm, Y = 450 mm, Z = 400 mm;
- Rotational speed: 20 - 8 000 rpm;
- Drive capacity: 13 kW (40% DC), 9 kW (100% DC);
- Permissible tool diameter: 130 mm;
- Permissible tool height: 290 mm;
- Permissible tool mass: 6 kg;
- 3 automatic axes / X, Y, Z
- 2 angular axes, manual/ B, C;
- The B-axis is specific to the linear Y-axis and the C-axis is specific to the linear Z-axis.

In order to machine an electrode, EL1F/ Cu, on the DMU 50 CNC Center, with the semi-automatic activation of the indexing table from the structure, a series of associated elements are presented in Fig. 10 – 13.

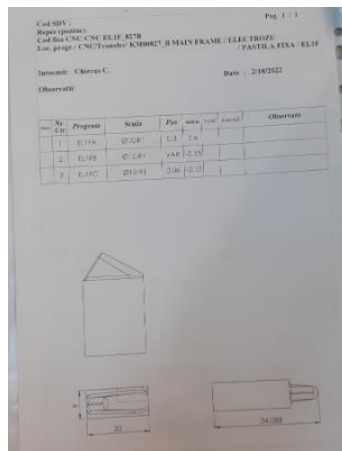


Fig. 10. The design drawing of EL1F/Cu part



Fig. 11. The semi-finished product for EL1F/Cu part

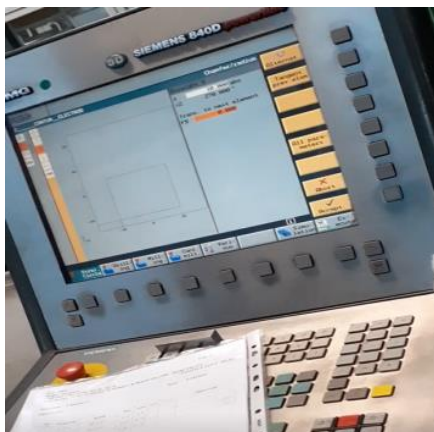


Fig. 12. Entering parameters in the machine program



Fig. 13. Sequence from the machining operation of EL1PF part

Constructive-functional elements of the dividing table of the DMU 50 CNC center structure are presented in Fig. 14, 15, 16. The main components of the dividing table are: the gear worm shaft - worm wheel, the worm gear subassembly, the hydraulic cylinder and the springs for axial locking of the dividing table. By pressing the start button, the hydraulic cylinder is actuated and, respectively, the dividing table is unlocked, etc. [7].

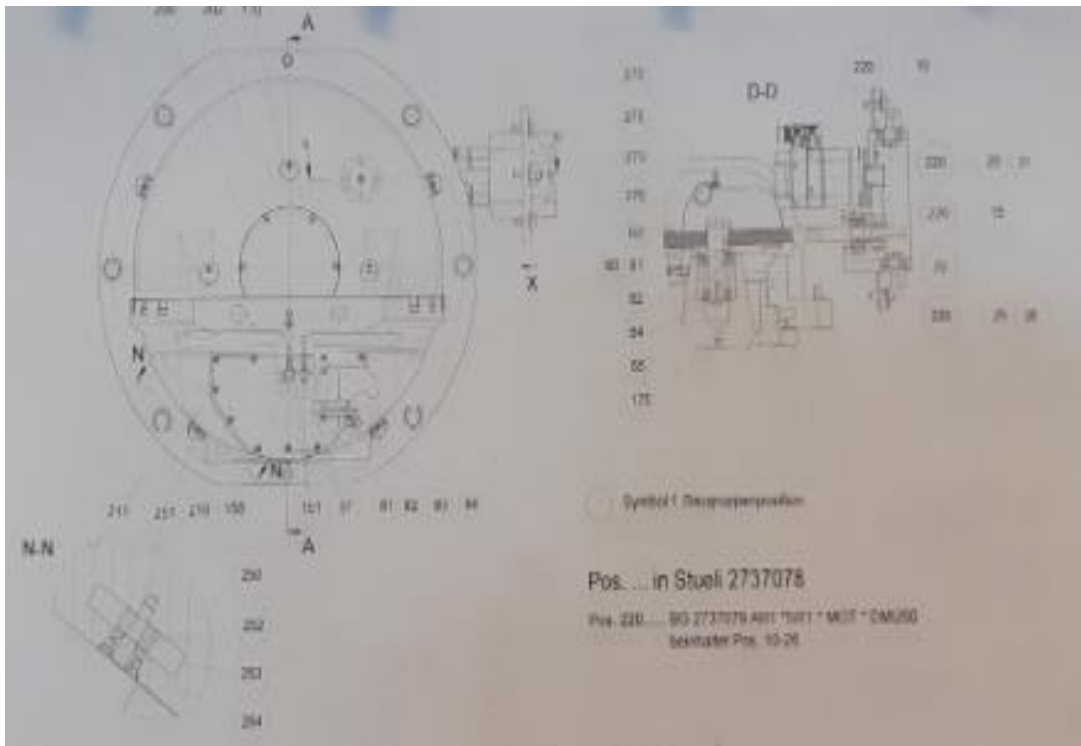


Fig. 14. Design drawing of dividing table - front projection

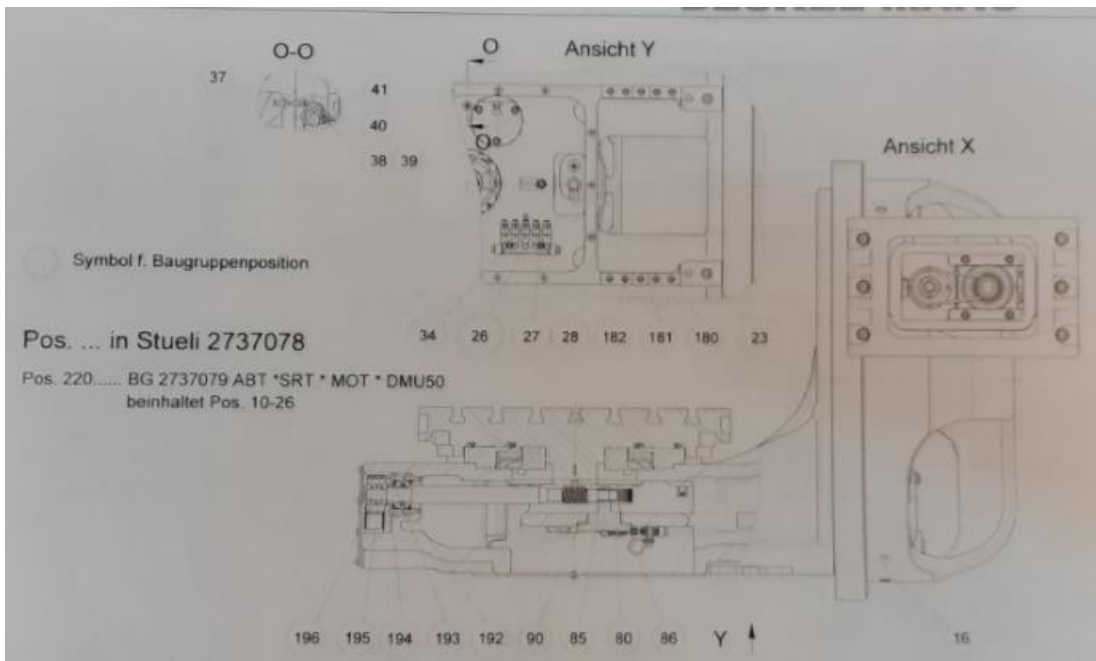


Fig. 15. Design drawing of dividing table - side projection



a.



b.

Fig. 16. Elements of the operation of a dividing table:
a - rotation C relative to the Z-axis; b - rotation B relative to the Y-axis.

5. Conclusions

From the analysis of mechanical, semi-automatic and automatic dividing schemes and devices, the superiority of the automatic dividing process is shown by a number of advantages.

By digitization, all data are kept intact for future reference. In case of emergency, data can be easily retrieved. It is faster, more reliable and more cost-effective. The processing quality is stable, the processing accuracy and repeat accuracy are at a high level, so that, the processing requirements are satisfied.

6. References

- [1] Ghiță N., Fătu A., Developments regarding modules of a dividing head with digital display, Scientific Student Session (in Romanian), May 2021, UPB.
- [2] Jha N., Amin M., DESIGN AND ANALYSIS OF MANUFACTURING COMPONENT UNDER SUSTAINABILITY CONSIDERATIONS: A CASE STUDY OF ELECTRONIC AND MECHANICAL INDEXING HEAD FOR MILLING OPERATION, IDETC/CIE, Canada, 2018, www.researchgate.com (accessed on 04.04.2022).
- [3] Karami J., Roohi A., Design and Implementation of Electronic System and Computer Control of an Indexing Table and Quality, Springer Science, site, 2007 (accessed on 17.04.2022).
- [4] ***, *Use a dividing indexing head*, <https://evolventdesign.com/blogs/history/how-to-use-a-dividing-indexing-head> (accessed on 20.04.2022).
- [5] ***, *Dividing Head or Indexing Head*, <https://testbook.com/question-answer/the-mechanism-which-serves-the-purpose-of-dividing--6008f34de10b415e9b24441c>, (accessed on 04.05.2022).
- [6] ***, *Indexarea Head-Definition*, <https://learnmechanical.com/indexing-head/> (accessed on 05.05.2022).
- [7] ***, Dr. Kocher SRL,, București, <https://www.drkocher.ro/>
- [8] ***, STEPPING MOTOR - TYPES AND EXAMPLES OF USING STEPPING (in Romanian), <https://www.tme.eu/ro/news/library-articles/page/41861/Motorul-pas-cu-pas-in-salturi-tipuri-i-exemple-de-utilizare-a-motoarelor-pas-cu-pas/> (accessed on 06.05.2022).
- [9] ***, *Convert dividing head to electronic head*, https://www.youtube.com/watch?v=oqRs6fGzQ6M&ab_channel=dzzie (accessed on 06.05.2022).
- [10] ***, *Stepper motor*, https://www.tme.eu/ro/details/pololu-1475/motoare-pas-cu-pas/pololu/stepper-motor-unipolar-bipolar-57x76mm/?brutto=1¤cy=RON&gclid=EAlaIqObChMIk8zh9dTa9wIVZ4ODbx3sZgTbEAYBiABEgLNHPD_BwE, (accessed on 04.05.2022).
- [11] Sarabjeet Singh, Nitin S. Solke, Ravi Sekhar, Design of a Novel Multi-Stacker Mechanism for Bearing Seal Pressing Station, © Research India Publications, 2015, India, www.researchgate.com (accessed on 04.05.2022)

THERMOFORMING TECHNOLOGY OF HYBRID SANDWICH STRUCTURES

DĂNICIUC Marius¹, OPRAN Constantin Gheorghe² and DRĂGHICI Cătălin²

¹Faculty of Industrial Engineering and Robotics, Specialization: Manufacturing Engineering,
Study Year: IV, e-mail: mariushdd99@gmail.com

²Faculty of Industrial Engineering and Robotics, Manufacturing Engineering Department, University
POLITEHNICA of Bucharest

ABSTRACT: The most interesting and promising ways to obtain composite material consisting of polymeric resins and fiber-glass structures are hybrid sandwich structures. The faces of the sandwich structure can be metallic materials (such as aluminum alloys or stainless-steel) and non-metallic materials (polymeric laminates with glass-fiber or carbon-fiber). For special applications in the field of aircrafts or shipbuilding, where the main priority is the strength/weight ratio, honeycomb core sandwich materials are used. In these materials, the core can be made of paper that's pre-impregnated with resin and especially of aluminum alloys or polymers reinforced with glass-fibers.

KEY WORDS: composite, hybrid, structures, fibre, automobiles

1. Introduction

Hybrid Sandwich Structures

Sandwich materials with fiberglass-reinforced thermosetting polymers are widely used for applications where the main requirement is bending. An ideal sandwich material has thin, rigid, high-strength faces, a low-density core, and a low cost price [1].

The following Table 1 [1] shows the mechanical properties of the faces of sandwich-type materials made of glass-fiber-reinforced polymers, compared to metal materials.

Hybrid structures are such that the dynamic design of lightweight structures allows the use of the most advantageous properties of materials of different degrees of origin and their incorporation into a single structure. A typical and ideal combination of desired material properties of hybrid structures is the low weight merging with good mechanical properties. The number of beneficial combinations is very large, since the constituent materials of a hybrid structure may have substantially different properties than those of the material itself [2].

The manufacturing step of a structure is usually challenging. Especially in laminated hybrid structures, where macroscopic mechanical interlocking between layers is impossible, the level of adhesion between the constituent materials may be insufficient.

Table 1. – Mechanical properties regarding Hybrid Structure Faces compared to metals [1]

Material	Resistance (Mpa)	Modulus of elasticity (Gpa)	The weight of the structure with the surface of $1m^2$ and thickness of 1mm,kg
Fiber-glass composite and: Polyester resin	769	56	1,92
Epoxy resin	1009	56	1,83
Phenolic resin	769	56	1,81
Aluminum: 2024 – T3	800	160	2,69
5052 – H34	416	160	2,69
6061 – T6	560	160	2,69
7075 – T6	1169	160	2,69
Stainless-steel: 316	961	480	7,68
17-7	3200	480	7,68

2. Current stage

Non-metallic and metallic honeycombs introduced in the unconventional technologies in the late 1960s revolutionized the performance of composite materials. The represent hybrid cellular structures, similar to natural honeycombs in Figure 1 [1], having the following characteristics:

- Extremely low specific gravity (sub $100\text{ kg}/m^3$);
- Good flexural strength and stabilized compression;
- Excellent properties in the fields of thermal and sound insulation;

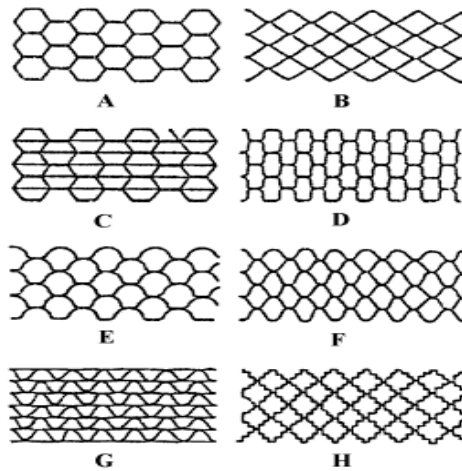


Figure 1 – Hybrid structures for metallic honeycombs [1]

A–hexagonal; B–rhombic; C–reinforced hexagonal; D–rectangular; E–flexible; F–sinusoidal shape; G – multistrat; H–rhombic wavy;

Metal honeycombs are made of aluminum foil with a thickness of 10-80 μ , while for non-metallic variants special fireproof paper is used. Metal / non-metal honeycombs with different dimensions of the base cell are obtained depending on the specific weight and strength of the required parts (4,7 ; 6,3 ; 9,5 ; 12,7 mm etc.), depending on the specific weight and strength of the required part [3].

After removing the organic solvents by passing through a tunnel kiln with a maximum temperature of 130°C, the foil is cut with a guillotine-type device, according to the dimensions of the thermoforming die, reaching stage B. The resulting sheets are placed in the thermoforming die in such a way so that the adhesive tapes of one are evenly spaced.

After superimposing 100-300 sheets, it reaches stage C. The package is placed in a press with hot platters, at a temperature of 170 – 210°C and a pressure of 150 – 300 daN/mm². This leads to the unexpanded block stage. The resulting block is then cut longitudinally using special cutters, without the use of cooling/lubricating fluids, at low machine speeds (in order to avoid the appearance of micro-welds between the component aluminum foils).

- The great advantage of this technology is that the combs can be transported in the form of compact blocks, thus achieving large space saving and also avoiding cell damage, pre-expansion and expansion operations can be performed directly by beneficiary clients [3];
- The technology of obtaining honeycombs from paper or cardboard is similar, the place of degreasing/pickling operations being taken by the impregnation of the material with flame retardant resins [3];
- Note that the thermoforming operation is conducted at lower temperatures (max. 140°C), to avoid degradation of cellulosic material [1];

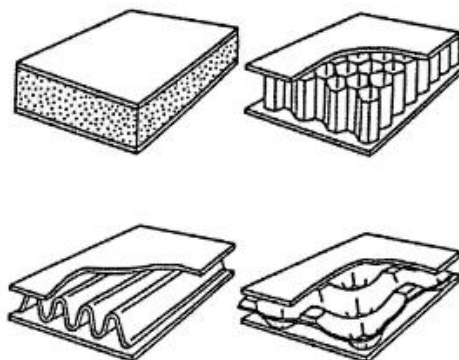


Figure 2 – Hybrid sandwich structures with non-metal faces [1]

Hybrid structures with fiber-glass and carbon/polymer foil

Widely used for automobiles, these types of structures are commonly used with fiber-glass combined with carbon and aramid fibers, but all are non-degradable and difficult to recycle; It has been found that natural plant fibers are viable alternatives to synthetic fibers to increase the economy, recycled thermoplastic resins are usually used, especially in the manufacture of body-secondary elements or other components that are not fundamental in ensuring the functionality of the vehicle. For example, Mercedes-Benz has in the past initiated the use of jute fiber reinforced plastics for the interior cladding of class E doors [4]. These will be the main aspects of the composite structures for future research.

Below is shown in Image 4 and Image 5 a model used by Alseca [5 - <https://alseca.com/>] where one of the polymer plates of the structure type carbon fiber and glass for automobiles is used.

Advantages:

- The ability to print even very thin thicknesses, which injection molding technology does not allow (due to technical limitations);

- Being able to build a mold with many cavities depending on the size of the machine table, production times can be significantly reduced compared to injection molding;

Disadvantages:

- Low production speed for plate machines, high speed for digital web machines;

- The inconsistent and uneven spread of the plastic on the sinuosity of the mold;

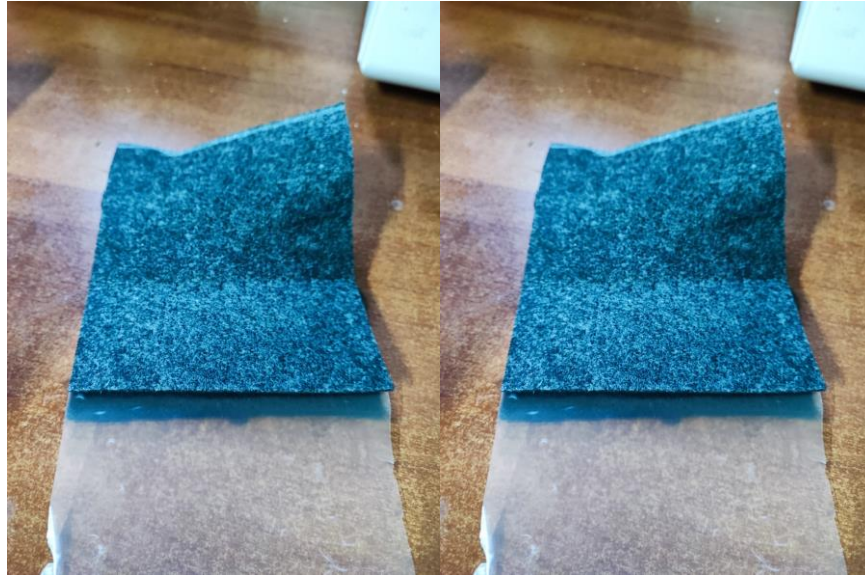


Figure 3 and Figure 4 – Hybrid structures used in structural applications

For this component to serve its purpose, a layer of polymer foil is used that will be between two films of the same structure. The polymer film will aim to bond the layers together using the thermoforming process. The foil is pushed onto the mold due to the high pressure exerted by the outside air, which also facilitates cooling.

After bonding, a thicker layer of fiber is formed which is then used for placement on the car components (bars, doors, etc.). This layer of fiber structure also benefits from the ability to absorb sound and vibration.

3. Marketing Strategy

In other words, the production process and the forming behavior of the local reinforced steel/polymer/steel area (316L/PP/316L), also known as Sandwich Hybrid Composite Materials (SMS) was investigated in detail because the traditional structures had disadvantages related to by their modulus, and slightly deformed when applied in civil engineering. The effect of simple reinforcements with plates of different sizes, shapes and geometries was studied for new development, where as local reinforcement, simple inlays made of simple solid steel and steel mesh with central edge positions were chosen instead of a polymer core laminated sandwich. Given the increased strength by moving the tested surfaces, this “wafer” method was favored thanks to its efficiency and low cost [6].

4. Conclusion

The increasing use of laminated composites and sandwich structures in various fields of engineering has required the development of various refined theories that predict the precise dynamic behavior of such structures. The main purpose of this research is to present various methods available for the analysis of “Rolled metal fiber composites and sandwich panels” and to guide researchers for future research. Many theories have been reported in the literature for vibration analysis [7].

5. Bibliography

- [1] Lupșea Adrian (2022). *Mat Compozite 2*. Preluat de pe Scribd;
Link: <https://www.scribd.com/doc/309748389/mat-compozite-2-pdf>
- [2] Sandeep S.H. ; Srinivasa Chikkol Venkateshappa, Hybrid Sandwich Panels: A Review. GM Institute of Technology, Davanegere; Publicat: August 2020;
Link: https://www.researchgate.net/publication/343954212_Hybrid_Sandwich_Panels_A_Review
- [3] Design, Manufacturing, and Characterization of Hybrid Carbon/Hemp Sandwich Panels ;
Autori : Luca Boccarusso, Fulvio Pinto, Stefano Cuomo, Dario De Fazio, Kostas Myronidis, Massimo Durante, Michele, Meo ; Journal of Materials Engineering and Performance, 3 Sept.2021;
Link : <https://link.springer.com/article/10.1007/s11665-021-06186-1>
- [4] Perspective în fabricarea de materiale si structure composite
Link: https://mec.tuiasi.ro/wp-content/uploads/2021/09/12_Perspective.pdf
- [5] <https://alseca.com/>
- [6] Autori: Olga Sokolova, Adele Carrado, Heinz Palkowski;
Production of customized high-strength hybrid sandwich structures; Octombrie 2010;
Institute of Metallurgy (IMET), Metal Forming and Processing, Clausthal University of Technology (TUC) ;
Link: <https://www.scientific.net/AMR.137.81>
- [7] Mechanical Behaviour of Sandwich Panels with Hybrid PU Foam Core;
Autori: Xudong Zhao, Li Tan, Fubin Zhang;
School of Physics and Electrical Engineering, Weinan Normal University, Weinan, China;
Faculty of Civil Engineering and Mechanics, Jiangsu University, Zhenjiang, China;
Link: <https://www.hindawi.com/journals/ace/2020/2908054/>
- [8]. OPRAN Constantin Gheorghe; 2017; Tehnologia produselor din materiale avansate, Îndrumar laborator; Editura Bren; București, România; ISBN: 978-606-610-097-8;
- [9]. OPRAN Constantin, Gheorghe; 2016; Tehnologii de injecție în matriță produse polimerice; Editura Bren; Bucuresti, România; ISBN; 978-606-610-201-8;
- [10]. OPRAN Constantin Gheorghe; 2014; Tehnologii de injecție în matrițe, Îndrumar proiectare; Editura Bren; București, România; ISBN:978-606-610-085-4;
- [11]. OPRAN Constantin Gheorghe; 2018; Tehnologii de injecție în matrițe; Curs format electronic, IMST-TCM; Universitatea POLITEHNICA din București; România;
- [12]. Constantin OPRAN; 2004; Nicolae VASILE; Virgil RACICOVSCHI; Paul PENCIOIU; Ion PAUNA; Maria CASARIU; Gheorghe MOHAN; Biostructuri polimerice degradabile în mediu natural; Editura "VASILE GOLDIS" UNIVERSITY PRESS; Arad; ISBN 973-664-041-8;
- [13]. DUMITRESCU Andrei; OPRAN Constantin; Materiale polimerice, Caracterizare, Proprietăți, Prelucrare; Oficiul de informare documentară pentru industrie, cercetare, management; București, România, 2002; ISBN973-8001-32-3

RESEARCH ON DESIGNING-SIMULATION AND 4D PRINTING OF A PRODUCT

VLAD Mihaela-Marilena¹ and DOICIN Cristian²

¹Faculty of Industrial Engineering and Robotics, Study program: Economic Industrial Engineering, Year of study: IV, e-mail: ella.mihaela8@yahoo.com

²Faculty of Industrial Engineering and Robotics, Manufacturing Engineering Department, University POLITEHNICA of Bucharest

ABSTRACT: The aim of this research was to gain knowledge about a new product concept - 4D products. 4-dimensional printing uses the same techniques like 3D printing through computer-programmed deposition of material in successive layers to create a three-dimensional object. 4D printing is mainly based on 3D printing and become a branch of additive manufacturing; objects are no longer static and they can be transformed into complex structures. Compared with the static objects created by 3D printing, 4D printing allows a 3D printed structure to change its size, shape, property, and functionality with time in response to external stimuli such as temperature, light, water, etc., which makes 3D printing alive.

KEY WORDS: 4D, printing, stimuli, simulation

1. Introduction

4D printing has become an exciting new branch of 3D printing. Unlike 3D printing, 4D printing allows shape and function to change over time in response to changing external conditions such as temperature, humidity, pH, electricity, and light.^[1] 4D printing is also known as active origami, 4D bioprinting or shape transformation system.^[2]

The main objective behind 4D printing is the self-assembling property of 3D printed objects when exposed to certain stimuli.^[1] This shape-changing phenomenon of 3D printed objects is based on the material's ability to transform over time in response to specific stimuli, and it does not require human intervention to aid the process.^[4]

A four-dimensional product (4D product) regards a physical product as a living organism capable of altering the shape and physical attributes on its own over time when exposed to stimuli.^[2]

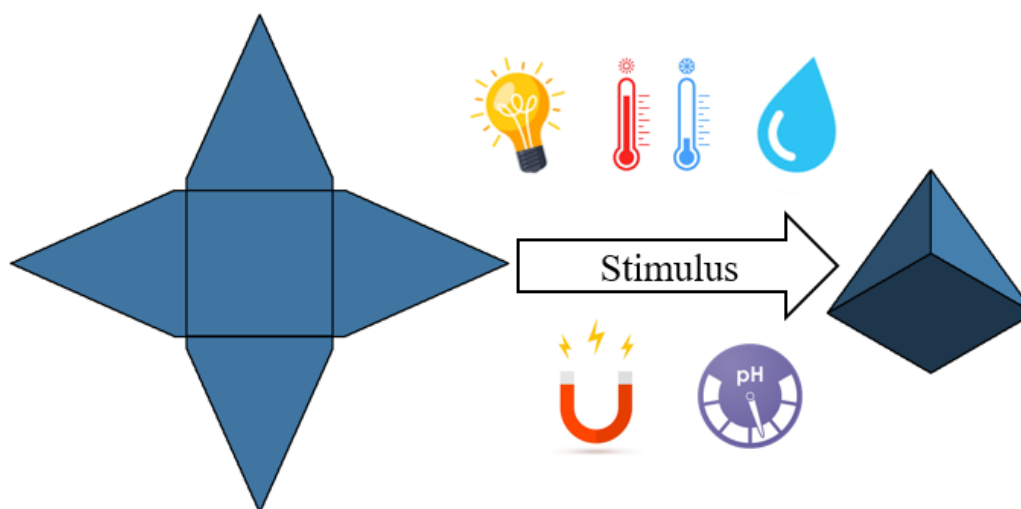


Fig 1.1 4D product

2. Current stage

4D printing marks a futuristic approach to printing technology with incredible potential. 4D printing offers the ability to design any transformable shape from a variety of materials that exhibit shape transformation characteristics under the influence of stimuli. [1]

The increasing need for flexible objects in various applications has fueled the emergence of 4D printing. Researchers are currently looking ahead of conventional 3D printing to develop a new structure by combining different materials that respond to stimuli and allowing the product to change its structure by bending, elongating and twisting along axes. [4]

The major differences between 3D printing and 4D printing are the use of materials to be printed and the printing facility. [4]

Four-dimensional (4D) printing stimulation method

The form and function of printed structures can be changed depending on one or more stimuli. There are several categories of stimuli: physical stimuli, biochemical stimuli and chemical stimuli. These stimuli are shown in the table 1. [3]

Table 1. Stimuli classification

Physical Stimuli	Biochemical stimuli	Chemical stimuli
Light	Glucose	pH
Temperature	DNA	Ion
Water/Humidity	Protein	Gas
Magnetic field	Enzyme	Redox
Electric field		

Material selection

The key to 4D printing is not so much the process, based on the familiar 3D printers, but the materials. As this is a fairly new technology, the materials available are not as varied as those used for standard 3D printing.

- ❖ SMP (shape memory polymers) – Polymers that remain rigid at room temperature and offer special properties when they reach the glass transition point. An example would be Convena's TPU SMP: a 4D filament with a composition based on TPU (thermoplastic polyurethane) that allows post-processing to modify the shape of 3D printed parts. Thanks to its special composition and Shape Memory Polymer technology, parts printed with this filament can be modified manually, allowing them to acquire another shape and maintain it over time.
- ❖ LCE (liquid crystal elastomers) – They contain liquid crystals that are sensitive to heat. By controlling their orientation, the desired shape can be programmed: under the effect of temperature, the material will relax and transform according to the dictated code.
- ❖ Hydrogels – Polymer chains consisting mainly of water, particularly used in light-curing processes. The latter is focused on the medical sector due to its biocompatibility.

In addition, some 4D printing processes can use various materials, mainly composites such as wood or carbon, which are added to SMP or hydrogels. This results in objects with rigid and movable areas. [5]

Application of 4D printing

Being a novel technology, most of the applications are currently in the research & development phase. Major end-use applications of 4D printing technology are expected to arise from healthcare, automotive, aerospace, and consumer industries. However, the potential of 4D printing is expected to impact other industries as well, such as electronics, construction, industrial, etc., in the near future.⁴¹

Medicine and surgery

In 2015, a medical team from the University of Michigan saved the lives of three babies with respiratory problems by inserting a 4D printed implant. This polycaprolactone device, designed to fit each patient, was designed to adapt its size to the child's growth and to dissolve itself when no longer necessary.

At present, the use of 4D printing in ultrasound scans allows, for example, to know more precisely the structural and functional development of the nervous system of the fetus.

In the future, vascular endoprosthesis (stents) or other 4D parts that react to body heat and expand to adapt to the patient, may be able to be printed.^[6]

Clothing and footwear

4D printing allows the manufacture of clothing that adapts to the body's shape and movement. The U.S. military is testing, for example, uniforms that change color depending on the environment, or that regulate perspiration depending on the soldier's pulse or environment temperature.

4D printed shoes will also be able to adapt to movement, impact, temperature, and atmospheric pressure.^[6]

Aeronautics and automotive

The NASA has developed an intelligent metallic fabric with 4D printing. This fabric, which is already used for astronaut suits due to its insulating nature, could also be used to protect spacecraft and antennas against the impact of meteorites. Meanwhile Airbus is testing materials that react to heat to cool its aircraft engines.

Thanks to 4D printing, intelligent airbags can be produced in the future that can anticipate any impact and reduce the risk of injury to the driver and passengers. ^[6]

3. Designing–simulation and 4D printing

To design a 4D product, it is necessary to consider the change of size and/or shape when the product is exposed to a stimulus. Thus, the product must be designed considering both the function for which it is designed and its future changes.

Designing and printing 4D products are done in a similar way to 3D. This is why the same software used for 3D products can be used. These programs are Autodesk Inventor, SolidWorks, Catia, and Cura, Z-Suite can be used to generate G-code.

Because it is a relatively new technology, 4D simulation software is not widely available and is in short supply. Because of this, it was decided to perform the simulation physically. The simulation was done using colored cardboard and a string as follows:

1. Draw the model of the product on the colored cardboard;
2. Cut out the cardboard and make the holes for the string;
3. Insert the string into the holes made;
4. Attach the ends of the string.

The modifications of the chosen models are shown in Figures 1.2-1.5. The simulation was done using simple models.

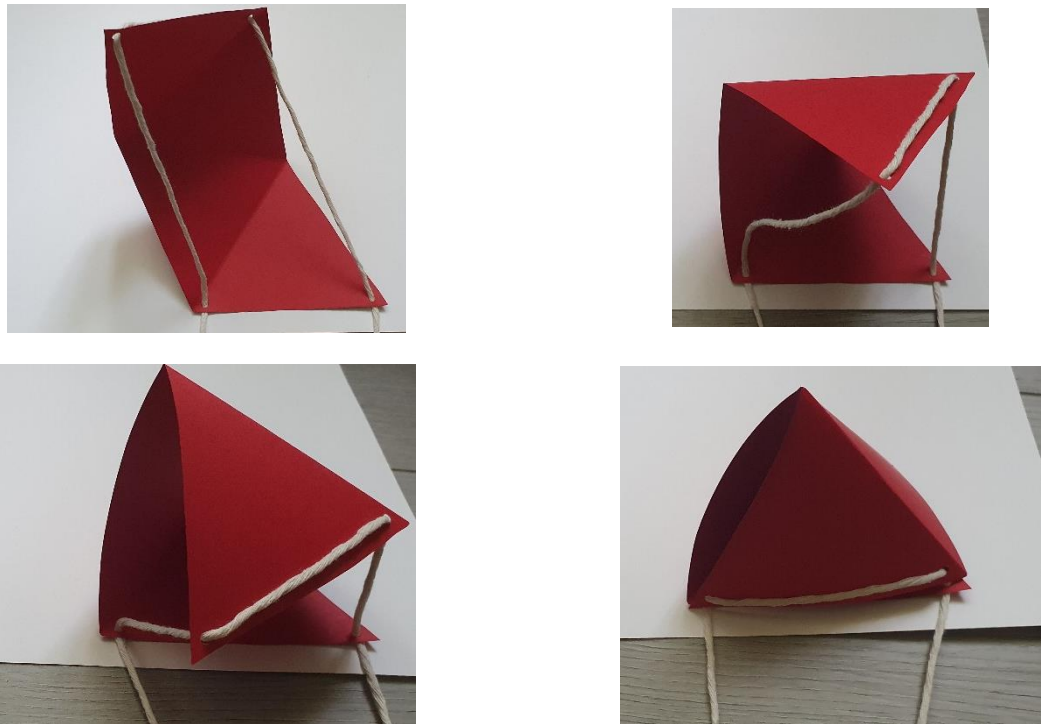


Fig1.2 Triangle based pyramid

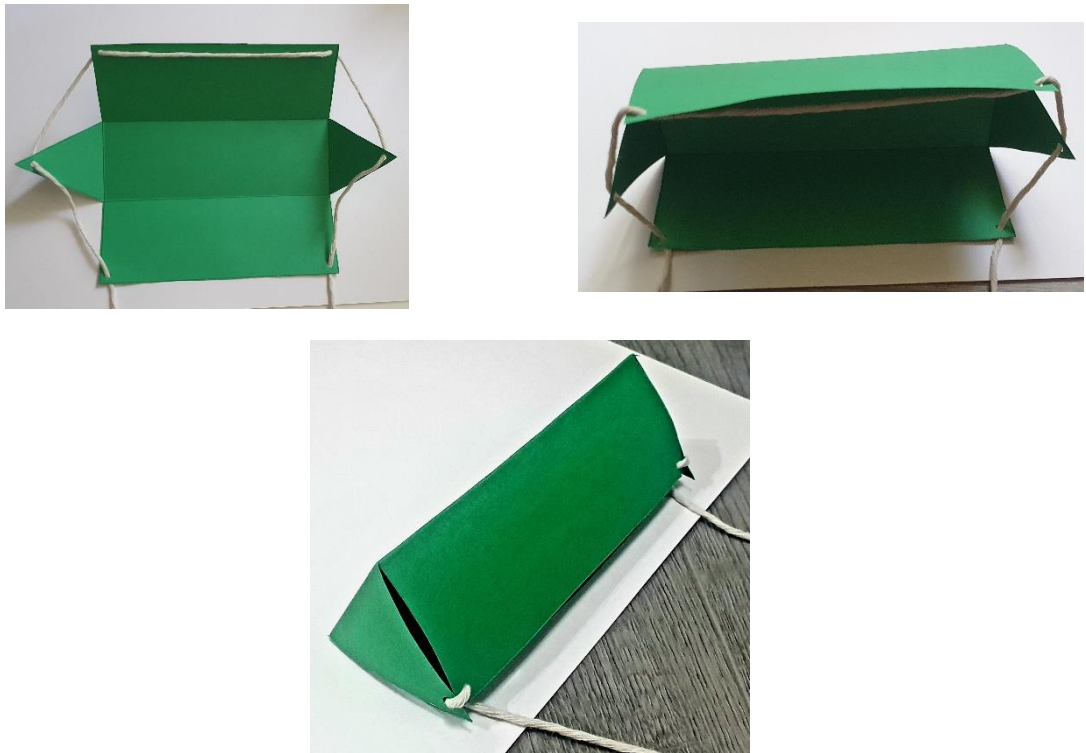


Figura 1.3 Triangular prism

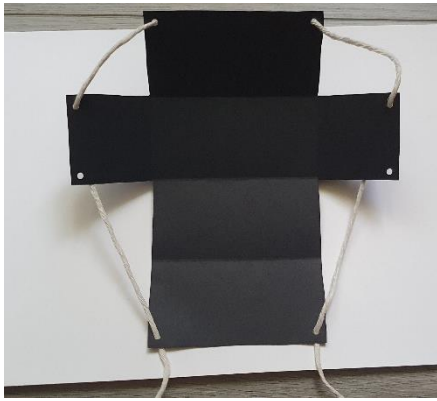


Figura 1.4 Cuboid

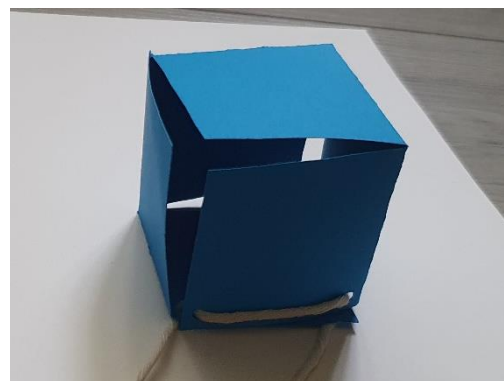
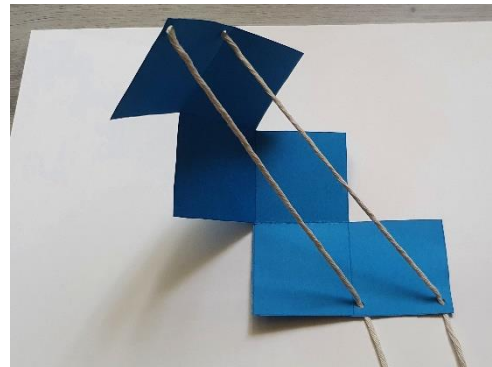
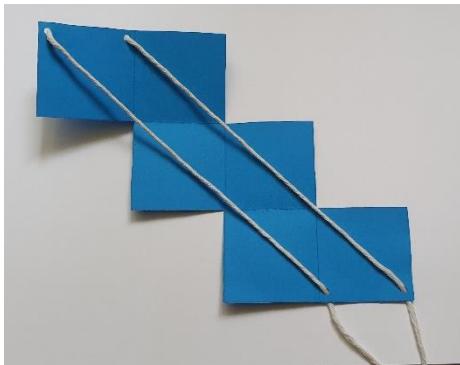


Figura 1.5 Cube

4. Conclusions

Even though it is a new technology, the potential opportunities for using 4D printing are vast. That's why there will be more research and development projects in industries such as healthcare, electronics, automotive, aerospace and defense, fashion and consumer durables, textiles, construction, and industrial machinery.

4D printing is a promising technology because of its self-assembly property.

The advantages of 4D printing are change of size, shape, property, and functionality according to current needs, the realization of complex structures, innovative design, environmentally friendly, and biocompatible.

Disadvantages of 4D printing are lack of control over intermediate deformation states, slow response of material when exposed to stimuli, lack of low-cost smart printers and materials, limited long-term reliability.

4D printing uses the same techniques as 3D printing. Because the materials used to respond to certain stimuli such as temperature, humidity, etc., it makes 3D printing come alive.

5. Bibliography

- [1]. Kishor Kumar Sadasivuni, Kalim Deshmukh și Mariam Alali Almaadeed, "3D and 4D Printing of Polymer Nanocomposite Materials" (2019), Editor ELSEVIER , ISBN: 978-0-12-816805-9
- [2]. Fouad Sabry, " Wait a Second, Did You Say 4D Printing?" (2021), ISBN: 6610000317271
- [3].*** https://www.researchgate.net/figure/Physical-chemical-and-biochemical-responsiveness-of-stimuli-responsive-polymers_fig3_346497143
- [4].*** " 4D Printing – The Technology of the Future" available at: <https://www.futurebridge.com/industry/perspectives-mobility/4d-printing-the-technology-of-the-future/>;
- [5].*** "4D printing: The Future of 3D printing" available at: https://filament2print.com/gb/blog/151_4d-printing.html
- [6].*** "4D printing: Is this the Fourth Industrial Revolution?" available at : <https://www.iberdrola.com/innovation/what-is-print-4d>
- [7].*** <https://www.instagram.com/reel/CcfKUnqLu0L/?igshid=YmMyMTA2M2Y=>

DESIGN AND IMPLEMENTATION OF AN EXPERIMENTAL PATRUPED ROBOT MODEL

SIMA Mihai¹, SIMA Gabriel¹, SAVU Tom²

¹Faculty of Industrial Engineering and Robotics, Study program: Applied Informatics in Industrial Engineering,
Academic year: 4, e-mail: mihaisima17@yahoo.com

²Faculty of Industrial Engineering and Robotics, Manufacturing Engineering Department, University
POLITEHNICA of Bucharest

ABSTRACT: The present project aims to highlight both mechanical and electronic and computer features of the design of an experimental model of a four-legged robot. On the other hand, the construction of a test bench can be a preview of the robot's operating cycle, as the operating principle is similar, both the robot and the test bench operate the robot's joints. with the help of hydraulic cylinders. An identical operating principle, in this case the hydraulic drive, also includes a set of similar components that aim to compose the hydraulic unit.

KEYWORDS: sensor , patruped foot , hydraulic system, acquisition data.

1. Introduction

The design of the test bench was necessary for the simulation and composition of the motion quadrature. precise hydraulic gear.

The monitoring and control system is composed of the following equipment:

- resistive angle sensor;
- pressure sensor;
- current sensor.

The test bench is made up of the following key components:

- acquisition and control board module;
- tilting system distributor mode;
- HAA foot cylinder.

In order to determine the necessary components and the mode of operation of the test bench, a general scheme of the mode of operation was made (Fig.1.1).

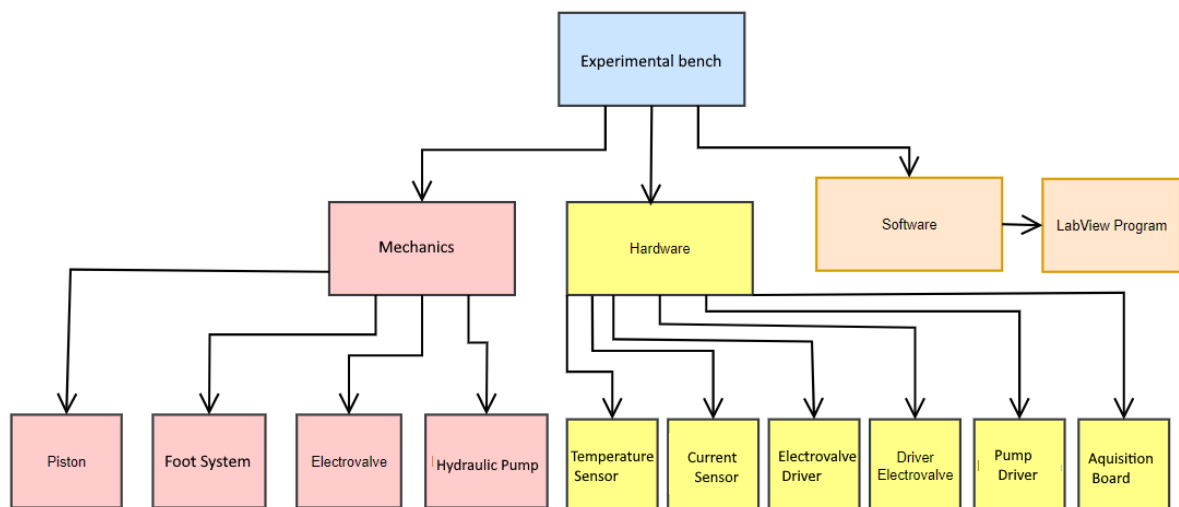


Fig. 1.1 General operating scheme

To establish the input and control parameters, the table below was made:

Table 1. Features pressure sensor

Measurable sizes	
Temperature	0-50 C
Intensity	0-20A
Pressure	0-100 bar
Tilt angle	0-200 grade
Sizes to control	
Pressure	0-100bar
Oil flow	0-20l/m

The control of the hydraulic fluid pulsation system is based on a constant feedback loop, made by the pressure sensor. when the pressure is higher than the required standard, the system will enter a fault state in which the hydraulic unit will be disconnected.

The test bench was made after the design of a preliminary connection electrical diagram, shown in Fig 1.2.

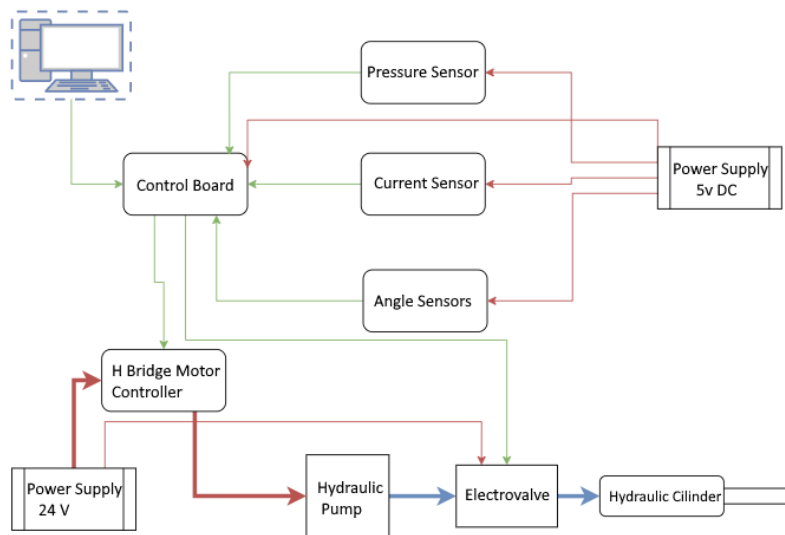


Fig.1.2. Wiring diagram test bench

Pressure sensor

The pressure sensor transmits a linear signal (Table 2) directly proportional to the degree of pressure load. It is powered by a maximum voltage of 24V DC.

Table 2. Features pressure sensor

Technical data	Values
Measuring range	0-200 bar
Output voltage	0,5 – 4,5 V
Working temperature	-40~+120°
Master	+ 5v red, GND-black, Green - signal
Protection class	IP67
Environment of use	Gas,Mineral Oil
Clamping thread	1/8" NPT
Accuracy	+/-0.5%
Response time	<1ms

MAX6675 Temperature Sensor

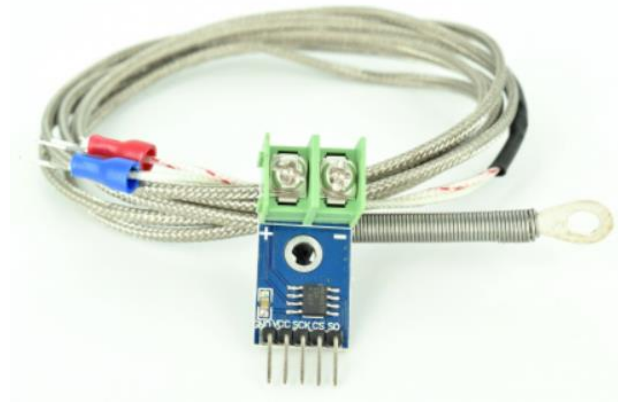


Fig.1.3. Temperature sensor MAX 6675

The technical characteristics of the temperature sensor are provided in table 3:

Table 3. Features Max6675

Supply voltage:	3V - 5V
Operating current:	50mA
Measured temperature:	2C - 1024C, with a resolution of 0.25C;
ADC resolution	12 biti
Differential input	high impedance
Thermocouple type	K
Communication	SPI
Other	Thermocouple disconnected connection detection
Dimensions:	15 x 25 mm.

This model of temperature sensor (Fig.1.3) can measure high temperatures with a very low resolution, providing high accuracy. The communication mode of the Max6675 module is via the SPI interface, so it can be easily integrated into AVR systems.

Current sensor:



Fig. 1.4 Intensity sensor

With the help of this module (Fig 1.4) which has the integrated component I INA219-B, current and voltage measurements can be performed with a high resolution up to the threshold set by the manufacturer. (Table 4). The measured values are transmitted to the microprocessor via the bus. I2C.

Table 4. Voltage Sensor Features

Technical specifications:	
Resistance	0.1ohm 1% 2W
Maxime voltage	26V DC
Maxim current:	3.2A, with a resolution of $\pm 0.8\text{mA}$
Dimensions[mm]:	25.5 x 22.3
Adresses I2C	0x40, 0x41, 0x44, 0x45, selectable by jumpers

Hall 360 Angular Sensor

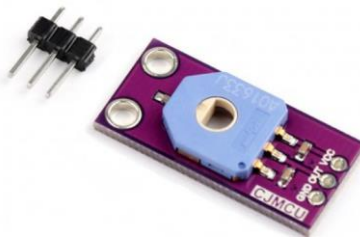


Fig 1.5. Angle sensor Hall 360

The module with angle sensor (Fig.1.5) has as principle the reading of the internal resistance of the potentiometer. Unlike a classic potentiometer, this module can transmit information over a 360-degree measurement range.

The sensor indicates the position according to the degree of rotation of the potentiometer directly proportional to the change of the internal resistance of the potentiometer. (Table 5).

Table 5. Angular sensor Features

Mechanical rotation	continuous (has no travel limit)
Electric rotation	after a 333 degree rotation, the value will restart from 0 degrees
Electrical resistance:	10k ohm
Output:	Analog

Pump drive

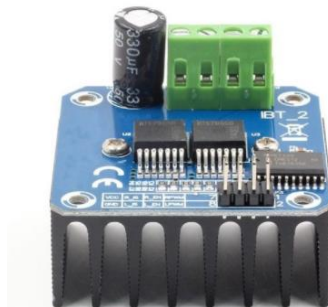


Fig 1.6 H bridge driver hydraulic

Specifications:

Table 6 Tehnical data H Bridge Driver

Technical data	
Processor	BTS7960
Input frequency	maxim 25KHz
Applications	hobby
Maximum current supported	43 A
Size	4 * 5 * 1.2 cm
Weight	65g.

The test stand was designed in Fusion 360 CAD software. In this project, parts such as the hydraulic pump, the piston, the pressure sensor and its adapter, the solenoid valve and its flow subsystem were modeled as illustrated in Fig.1.7. After modeling the parts, an assembly of the test bench was made to establish the areas where the parts will be mounted.

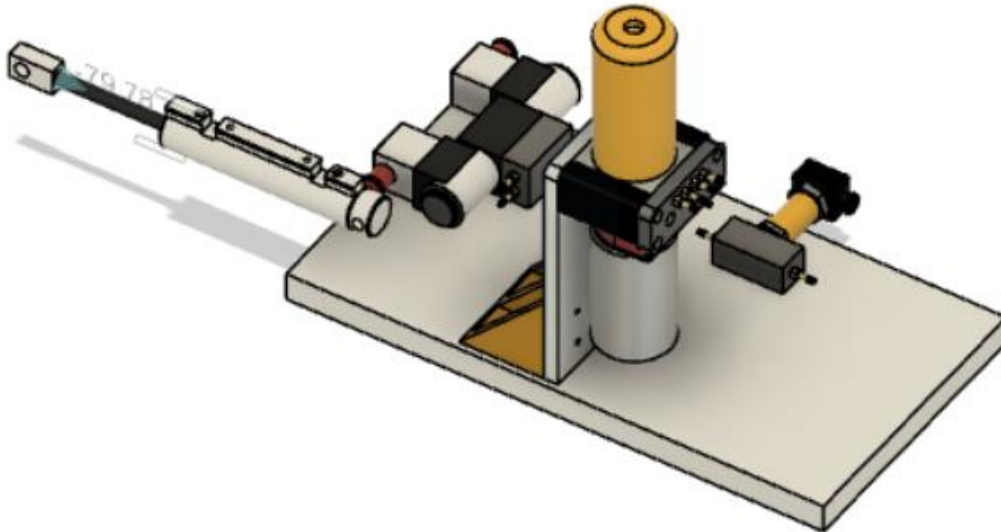


Fig 1.7. Test bench assembly

2. The current stage

The current stage of the test bench is 60% complete. At the moment, the stand is able to execute orders on a single hydraulic cylinder. Even if from an electronic and computer point of view the test bench is able to execute the movement of 2 hydraulic cylinders, from a mechanical point of view the order cannot be realized because an increased flow rate is required for the synchronous use of the 2 cylinders.

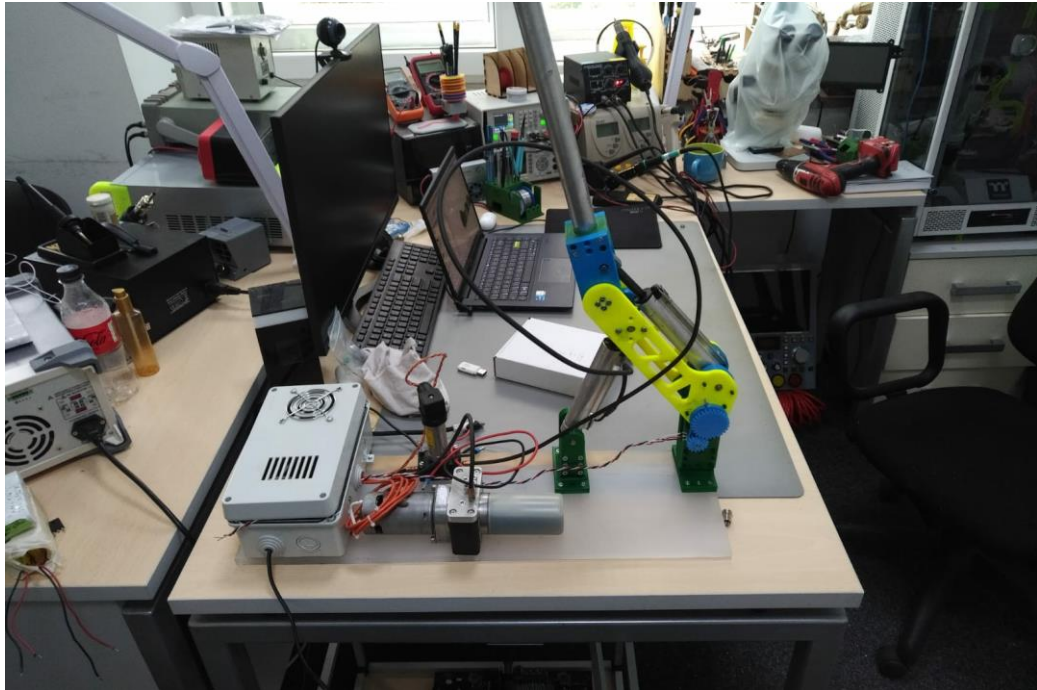


Fig 2.1. Current status of the test bench

3. Conclusions

The experimental test bench pattern has been found to be essential in the study of step algorithms. For future research on the bench, we will intervene by ensuring the flow necessary to control both hydraulic cylinders, mounting tensiometric marks for their force control and the use of linear displacement sensors.

The primary purpose of the experimental test bench is to simulate the ways of walking a leg. By performing the test bench, experimental models of stepping algorithms were tested and designed.

The only vulnerability of the test bench is the leakage of hydraulic fluid in the area of the fittings. This phenomenon is due to the non-use of standardized fittings, but their realization in diy mode.

4. References

- [1]. Sensor driver: https://ardushop.ro/ro/electronica/84-1298n-punte-h-dubla-dual-h-bridge-motor-dcsteppe.html?gclid=EAIaIQobChMIru3P7za9wIVWo9oCR1wLQULEAQYASABEgJ1RfD_BwE
- [2]. Voltage sensor: https://ardushop.ro/ro/electronica/84-1298n-punte-h-dubla-dual-h-bridge-motor-dcsteppe.html?gclid=EAIaIQobChMIru3P7za9wIVWo9oCR1wLQULEAQYASABEgJ1RfD_BwE

MONITORING AND REMOTE CONTROL, BY IOT, OF A HYDRAULIC PRESS

SPĂȚARU Andrei¹, SAVU Tom²

¹Faculty of Industrial Engineering and Robotics, Study program: Applied Informatics in Industrial Engineering, Academic year: 4, e-mail: spataru.andrei30@gmail.com

² Faculty of Industrial Engineering and Robotics, Manufacturing Engineering Department, University POLITEHNICA of Bucharest

ABSTRACT: The following paper will present the process of software development for hydraulic press monitoring and control. Also, it will present the components belonging to the system, the wiring diagram, and the operational scheme that the user will use to control the press.

KEYWORDS: LabVIEW, IoT, Hydraulic press.

1. Introduction

Hydraulics is a science that has the property of studying the laws of motion and equilibrium of various liquids. In its applications, hydraulics is used to generate, control and transmit energy by using pressurized liquids.

Pascal's principle states that when pressure is applied to a closed liquid, there is a change in pressure in the liquid. For a hydraulic press, the pressure in a liquid is applied by a piston that acts as a pump to create mechanical force. [1]

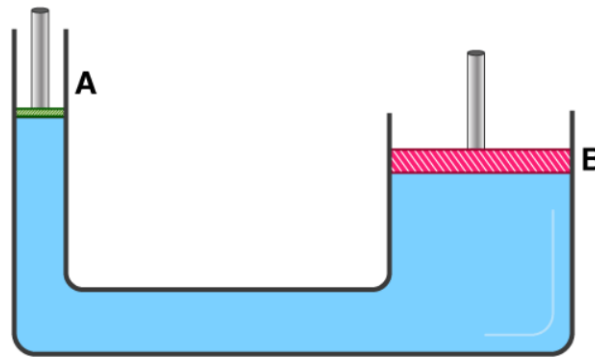


Fig 1. Illustration for Pascal's principle [2]

A hydraulic press is a mechanical device that uses the static pressure of a liquid, as defined by Pascal's principle, to shape, deform, and configure various types of metals, plastics, rubber, and wood.

The mechanism of a hydraulic press consists of a main frame, feeding system and controls.

Thus, the paper aims to create a platform easily accessible to a user who will be able to log in with a username and password, so that access is allowed only to authorized and trained people to work with a hydraulic press. [3]

Once connected, the user will be able to remotely monitor data on the hydraulic fluid pressure, the temperature of the heated press tray, but there will also be the possibility to see a live session in the press room and to control the movements of the hydraulic cylinders.

2. Description of the press

The press on which remote monitoring and control is desired is a two-cylinder workshop press for 75tf heated plate press (tons of force) from the manufacturer Hidromold Hydraulic Power Equipment model PA-75.150.R.00.



Fig 2. Descriptive image for press PA-75.150.R.00. [4]

The press assembly consists of the press chassis with the heated plate and the hydraulic cylinders, the hydraulic drive unit, the electrical connection panel and the manual control panel of the press.

The lower cylinder of the press has as specifications a pressing force of up to 30 tf. The upper cylinder has a pressing force of 75 tf. The hydraulic fluid communicates from the hydraulic pump to the hydraulic cylinders through a complex hydraulic path consisting of hydraulic distributors, pressure gauges, safety valves and hydraulic hoses.

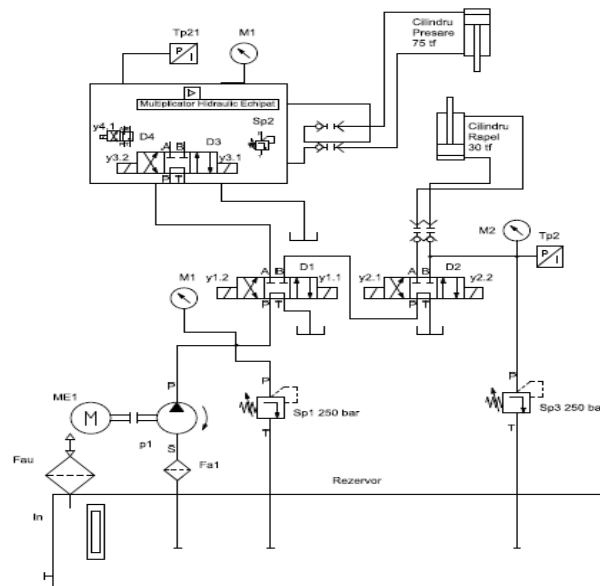


Fig 3. Schematic of the hydraulic route [4]

The electrical connection part between the electrical connection panel and the rest of the electrical components included in the system has now been completed.

The press did not work manually in the early stages of the project because the documentation of the press on the electrical part to be connected by the customer was erroneous, but also the electrical connections made by the manufacturer in the panel were made incorrectly.

So, the first step in going through the chosen project was to identify each component of the electrical connection panel and learn how it works in order to determine if the way it was connected is correct or wrong.

The following incorrect connections were discovered:

- The phases of the three-phase motor of the hydraulic pump were connected in the wrong order and caused the pump to rotate in the opposite direction, failing to send the hydraulic fluid into the system.

- The hydraulic distributors were not connected to the corresponding relays and did not open in the correct order for the press to operate.

- The PLC output wires for the analog signal that was to reach the acquisition board had common connections between the 12V power supply part and the ground part, causing the wires to heat up and the whole system to go into failure and requiring restart it.

- Reversing the connections of the pressure sensors with those for temperature.

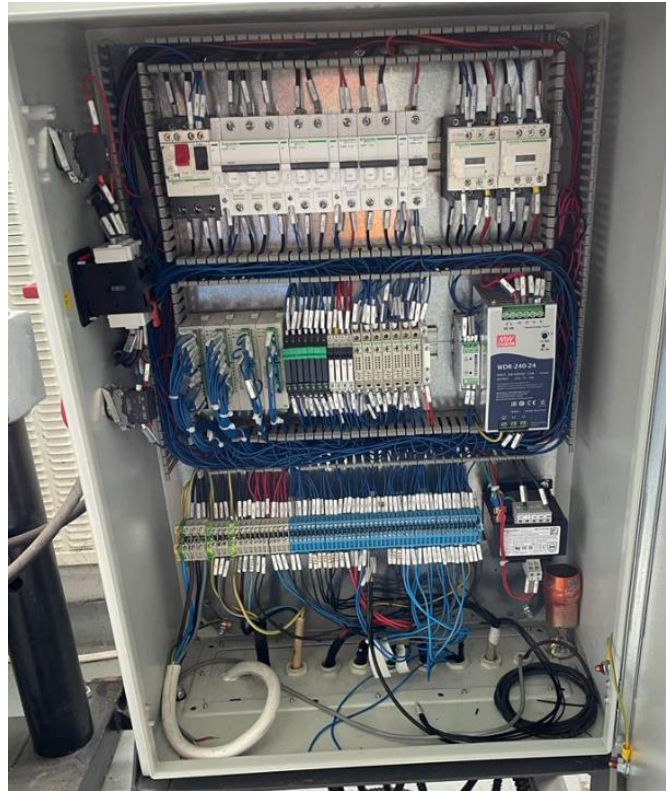


Fig 4. Electrical connection panel following rectifications

3. Development of the LabVIEW program

After the test and the correct operation of the press in the manual operation mode were ensured, I started to identify the dedicated cables for the operation of the cylinders and sensors with the help of the acquisition board.

Therefore, we have used the instructions for connecting to the purchasing board provided by the supplier.

Cablul de legatura placa achizitiei presa:	
1.	Firul cu tila 255 → pump ON / OFF command
2.	Firul cu tila 256 → heating ON / OFF control
3.	Firul cu tila 261 → upper cylinder selection command
4.	Firul cu tila 262 → lower cylinder selection command
5.	Firul cu tila 263 → cylinder advance control
6.	Firul cu tila 264 → cylinder retracted control
7.	Firul cu tila 271 → press command
8.	Firul cu tila 371 → signal 0 ÷ 10V → upper cylinder force value in [KN]
9.	Firul cu tila 372 → signal 0 ÷ 10V → lower cylinder force value in [KN]
10.	Firul cu tila 381 → signal 0 ÷ 10V → plate temperature value in [° C]
11.	Firul cu tila 152 → it will be connected to the minus of the source that feeds the acquisition board.

Fig 5. Plug-in connections. [4]

This is how the LabVIEW program for computer operation was developed.

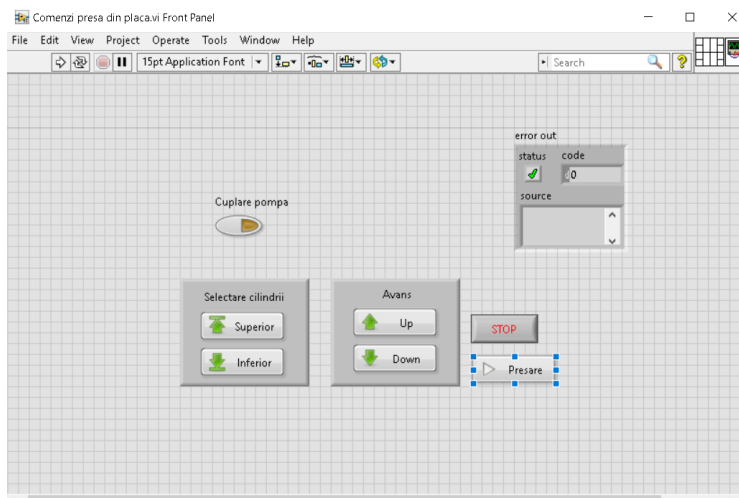


Fig 6. Application front panel.

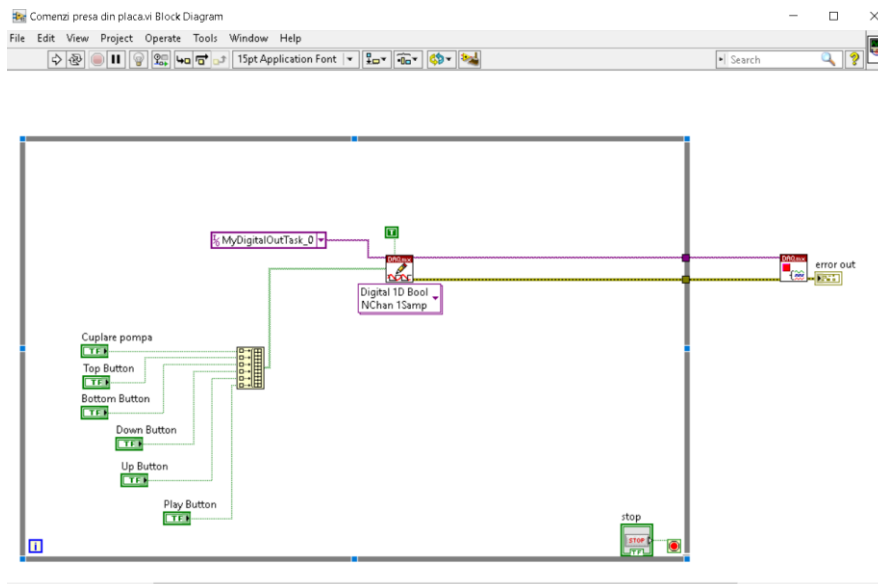


Fig 7. Block Diagram of the application.

4. Future implementations

Furthermore, the LabVIEW program will be assigned functions for displaying the pressure in the two cylinders but also for displaying the temperature in the heated plate.

A website will be created with a username and password but also with buttons that will be operated by a user to control the press.

At the same time, a web service will be available to connect the dedicated site with the press, this web service will run on a local station near the press.

5. Forecasts regarding the press

After the completion of the remote action and monitoring project, taking into account that the press is in the possession of the faculty, it will have a didactic and demonstrative role, but I think it would have a stronger impact on students and would arouse more interest if they could control the press even from their mobile devices: laptops, tablets, phones, etc. and could view the results even remotely.



Fig 8. Idea for interactive teaching material. [5]

6. References

- [1]. <https://ro.wikipedia.org/wiki/Hidraulic%C4%83>
- [2]. <https://cdn1.byjus.com/wp-content/uploads/2020/01/Pascals-Law-1.png>
- [3]. <https://www.iqsdirectory.com/articles/hydraulic-press.html>
- [4]. „Manual de operare și întreținere” – Hidromold Hydraulic Power Equipment.
- [5]. <https://i.ytimg.com/vi/yYcK4nANZz4/maxresdefault.jpg>

DESIGNING AN ALGORITHM AND MAKING AN INFORMATIC APPLICATION FOR IMPLEMENTING MQTT SPECIFIC ACTIONS

TUREAC Marius¹, SAVU Tom²

¹Faculty of Industrial Engineering and Robotics, Study program: Applied Informatics in Industrial Engineering, Academic year: IV, e-mail: marius.tureac2212@stud.fiir.upb.ro

² Faculty of Industrial Engineering and Robotics, Manufacturing Engineering Department, University POLITEHNICA of Bucharest

ABSTRACT: We are going to talk about the MQTT protocol and how it sends data (values measured by sensors in converted to bytes format) from a publisher that is an ESP32 to different topics that are stored on a server then accessed by clients which subscribe to certain topics on the server. The word topic refers to an UTF-8 string that the server uses to filter messages for each connected client. Subscribers can use the topics to control other devices from distance.

KEYWORDS: ESP32, Arduino, Server, Publish, Subscribe

1. Introduction

MQTT is a publish-subscribe network protocol which is designed for remote connections with limited network bandwidth.[1]

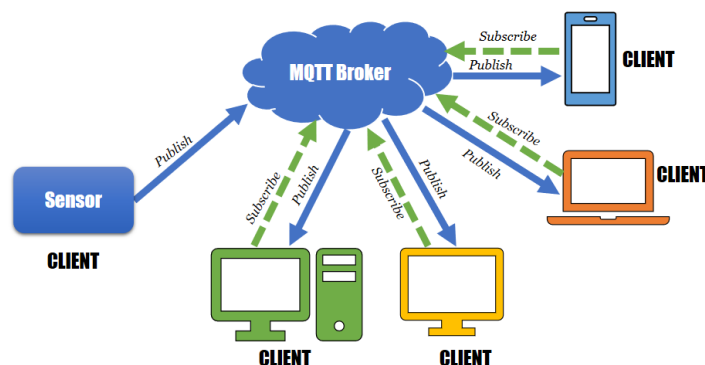


Fig. 1. MQTT diagram Publish-Subscribe [2]

The goal of this project is implementing MQTT protocol specific actions, in order to achieve this, we are going to use several MQTT specific for example:

“Connect” initializes connection with the server.

“Connack” confirms server connection.

“Publish” packet send the data measured from the sensors or data set by the user to the server.

“Puback” packet confirms that the data has been sent to the server.

“Subscribe” packet subscribes to a topic in which first client published data, the second client receiving data.

“Suback” packet confirms that the data sent from the server was received.

“Unsubscribe” packet unsubscribes from the topic that was subscribed and stops receiving data.

“Unsuback” packet confirms that the client unsubscribed.[3]

2. Current state

In this project for data publish to the server we used a ESP32 development board which acts as a client and the software ArduinoIDE to compile the program and uploading it to the board. The ESP32 board having integrated wifi module we connected it to the local wifi for tests then we changed the IP and PORT on which the server runs to publish data.

```
const char* ssid = "*****";
const char* password = "*****";
const char* mqtt_server = "141.85.192.24";
const char* mqtt_port = "1883";
const char* mqtt_server1 = "192.168.0.94";
void setup_wifi() {
  delay(10);
  Serial.println();
  Serial.print("Connecting to ");
  Serial.println(ssid);
  WiFi.begin(ssid, password);
  while (WiFi.status() != WL_CONNECTED) {
    delay(500);
    Serial.print(".");
  }
  Serial.println("");
  Serial.println("WiFi connected");
  Serial.println("IP address: ");
  Serial.println(WiFi.localIP());
}
```

Fig. 2. Development board configuration used to connect to the internet and server

After configuring the board for internet connection and server connection we configured the temperature, humidity and atmospheric pressure sensors to read the measured data.

```
#define DHTPIN 18
#define DHTTYPE DHT22
#include <Adafruit_BMP280.h>
temperatură=dht.readTemperature();
umid=dht.readHumidity();
atmpres = (bmp280.readPressure()/100);
```

Fig. 3. Define sensor pins connected to the board and read measured data

To publish the measured data to the server we use the client.publish function, this function sends the values in byte format to the server. Every measured value is stored in a specific topic for example, temperature is stored in the topic : „Temperatura”,humidity in the topic „Umiditate”,atmospheric pressure in the topic : „Presiune Atmosferica”.

```
char tempString[8];
dtostrf(temperature, 1, 2, tempString);
client.publish("Temperatura", tempString);
char humString[8];
dtostrf(humid, 1, 2, humString);
client.publish("Umiditate", humString);
char pressString[8];
dtostrf(atmpres, 1, 2, pressString);
client.publish("Presiune Atmosferica", pressString);
```

Fig. 4. Publish measured data to server

For the server and subscriber we use LabView with which we can program through interface.

We open a TCP/IP connection on the „1883” port and wait for a connection between the client (publisher) and server.

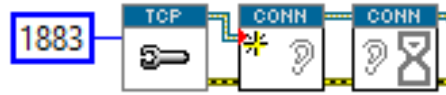


Fig. 5. Opening TCP connection server-client

If there is a connection we start the MQTT server which allows access of data writing in the topics and in a window in the front panel it shows the number of existing connections to the server.

The subscriber connects to the server IP with TCP Connect function and if it returns a valid connection we can subscribe to a topic.

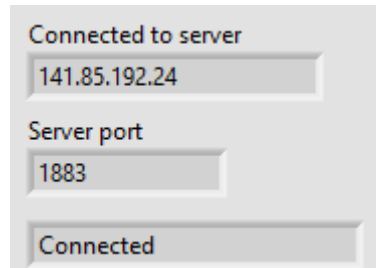


Fig. 6. Subscriber connected to server

To command a device we connected an Arduino UNO board to Labview, selected the communication port to „COM 5” and the bitrate to „9600”.

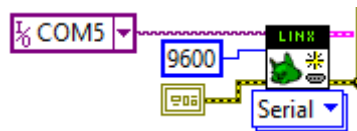


Fig. 7. Labview configuration with the arduino board

After we made the connection between the board and software, we need to login because not all subscribers have access to all the topics , as we see in the login window we have three subscribers „Admin” , „Subscriber 1” and „Subscriber 2”. Admin can subscribe to all topics, Subscriber 1 can subscribe only to Temperature and Humidity and Subscriber 2 can only subscribe to Atmospheric Pressure.

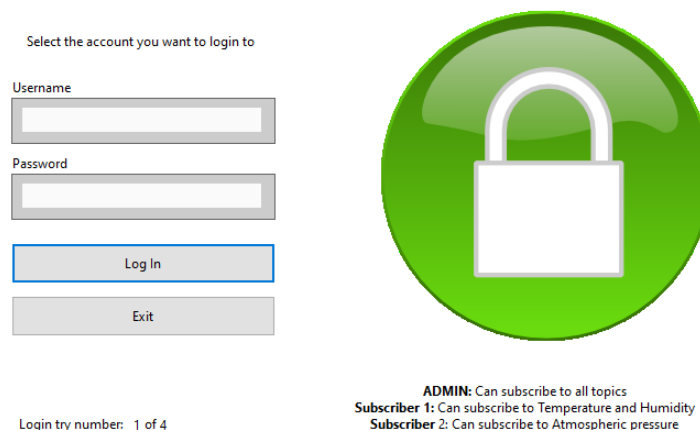


Fig. 8. Login window

Following the authentication process we have access to all topics because we logged in with Admin credentials.



Fig. 9. Subscribe/Unsubscribe interface in LabView

Now, subscribing to a topic , the client (subscriber) receives the data from server (byte value) and converts them to numeric (float) values.

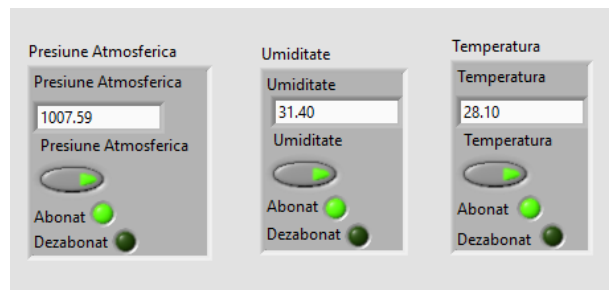


Fig. 10. Subscribed client to topic interface

To control the devices we use for example temperature, this having a limit of 30 degrees Celsius , if its above 30, a fan starts the cooling process.



Fig. 11. Temperature < 30 degrees Celsius LabView

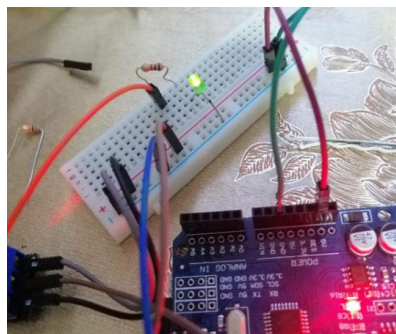


Fig. 12. Temperature < 30 degrees Celsius Arduino LED

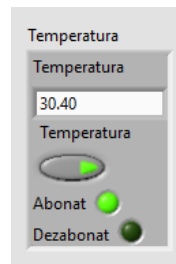


Fig. 13. Temperature > 30 degrees Celsius LabView



Fig. 14. Temperature > 30 degrees Celsius Fan

3. Conclusion

Original contributions to this project:

1. Physical connection of sensors on the ESP32 board, fan connection on arduino Uno board.
2. MQTT server connection from LabView of ESP32 board through ArduinoIDE.
3. Making the VI-s.
4. Making the experimental stand.

4. Bibliography

- [1]. What is MQTT protocol , [What is MQTT Protocol and How MQTT works? Applications \(microcontrollerslab.com\)](http://microcontrollerslab.com)
- [2]. Using MQTT with Mosquitto [Getting Started with MQTT using Mosquitto - Embedded Laboratory.](http://embedded-laboratory.com)
- [3]. Understanding MQTT protocol packets [Understanding the MQTT Protocol Packet Structure \(steves-internet-guide.com\)](http://steves-internet-guide.com)

MONITORING AND REMOTE CONTROL, BY IOT, OF A PNEUMATIC PRESS

ANTON Andrei-Sebastian¹, SAVU Tom², DUGĂEȘESCU Ileana³

¹Faculty of Industrial Engineering and Robotics, Study program: Applied Informatics in Industrial Engineering, Academic year: 4., e-mail: ant_seby@yahoo.com

²Faculty of Industrial Engineering and Robotics, Manufacturing Engineering Department, University POLITEHNICA of Bucharest

ABSTRACT: This paper will focus on the development of software specially created for remote monitoring and control of a pneumatic press. At the same time, in the following chapters will be presented, both the components necessary for the development and the software behind the commands sent by a user.

KEYWORDS: LabVIEW, IoT, pneumatic press

1. Introduction

Pneumatics is used to pressurize the gas and give it different uses of energy. Therefore, it is interesting, because through this process different uses can be achieved, such as mechanical movements, energy implementation for large and small machines, etc. The pneumatic press uses compressed air as a medium to be able to combine it with other fluids. In addition, it is considered the least polluting compared to other gases and chemicals that cause great damage to the environment. Therefore, compressed air does no harm to humans, much less to nature. Hence the importance of its use in industrial processes. Consequently, it is a resource that is very easy to obtain and does not require any process to obtain the raw material. "Monitoring and remote control, by IoT, of a pneumatic press" is the title of the topic I chose to research for the diploma project. As the title suggests, a pneumatic press can be ordered and monitored by a remote user. A chapter of the licensing work will consist of the creation of a website (connected non-stop to the media acquisition board) through which a user will be able to control the actions of the press. Also, two pressure and temperature sensors will be added, which will transmit real-time data to the user.

2. The current stage

The current state of this application is at the level of testing and optimizing the use and functionality of the user. After the hardware components were connected and the software application was developed, the use of the remote press was made possible by accessing the created site. The site was also created from an html code created on w3schools and further introduced in the LabVIEW development application. User orders are first received by LabVIEW software and forwarded to the press.

Moving on, it will be described the principle of operation of the press and the site, which was created for users.

Figure 1 shows the connections for the Arduino UNO acquisition board, meaning two analog pins for the temperature sensor and the pressure transmitter and four digital pins for solenoid valves and microswitches.

Figure 2 shows the detailed wiring diagram of the connections for an optimal operation of the application.

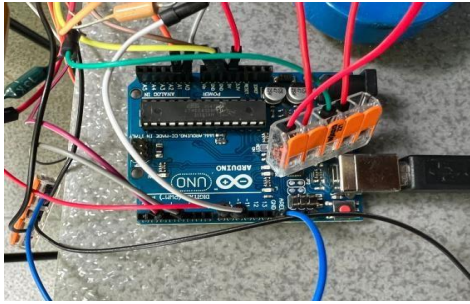


Fig 1. Connections to the Arduino UNO acquisition board

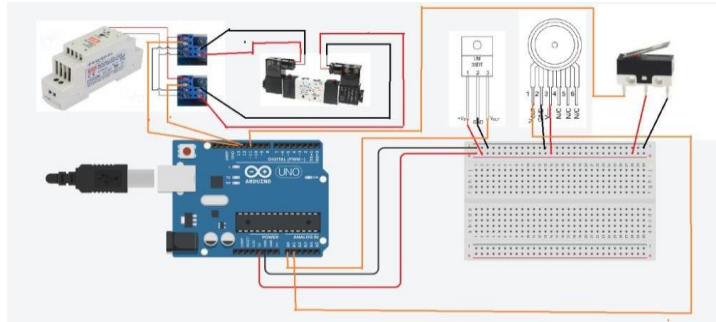


Fig 2. Detailed wiring diagram

• Wiring diagram legend

- Power supply +
- Power supply -
- Signal transfer/frequency

In order to receive and send orders to the pneumatic press it was necessary to connect a computer. Being connected to the acquisition board, it sends commands to the relays and these further to the solenoid valves, which deal with the movement of the pneumatic cylinder.

At the same time, the temperature and pressure sensor send information to the computer so that it can be displayed to the user.

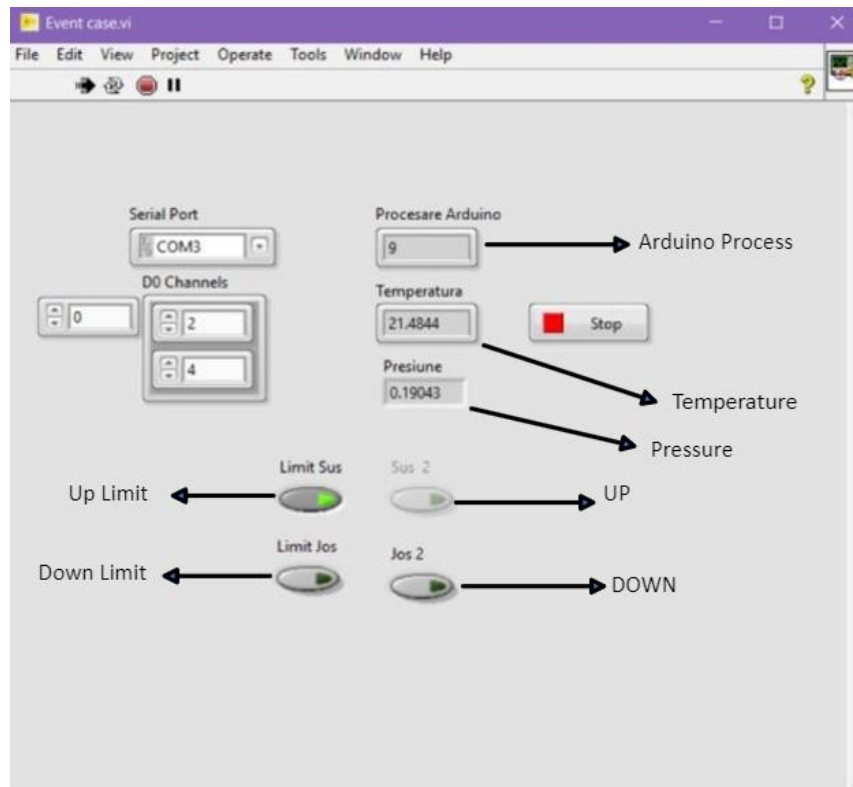


Fig 3. Program LabVIEW

Figure 3 shows the LabVIEW manual press control program. First the USB port of the Arduino board will be inserted and then when it will run, the values of temperature and pressure will be displayed on the screen. The two buttons "Sus 2" and "Jos 2" represent the commands given by a user to the press, at the same time the operation of the two buttons "Up Limit" and "Down Limit" represents the end of the stroke for each given order.

After testing and verifying the manual control program, it was necessary to develop the remote control website.

Figure 4 shows the first page of the site created, Authentication.

Fig. 4. Platform login portal

The first time it was necessary to create a login portal because several users could connect simultaneously and automatically the press would go into error and no more commands could be sent.

Fig. 5. User verification portal

Once the user has been found, the image above shows the user's instructions to proceed to the web page for remote control.

Figure 6 shows the remote control web page for any user.

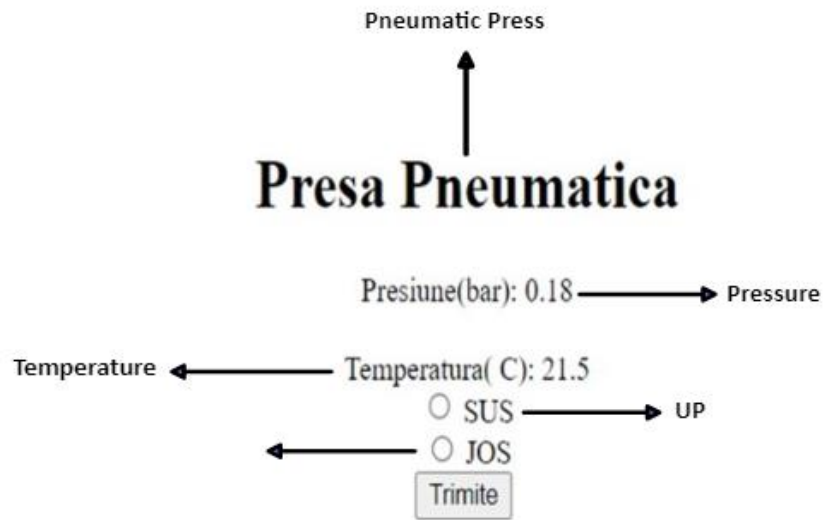


Fig. 6. Remote drive portal

3. Experimental stand

Figure 7 shows the experimental stand and its components.

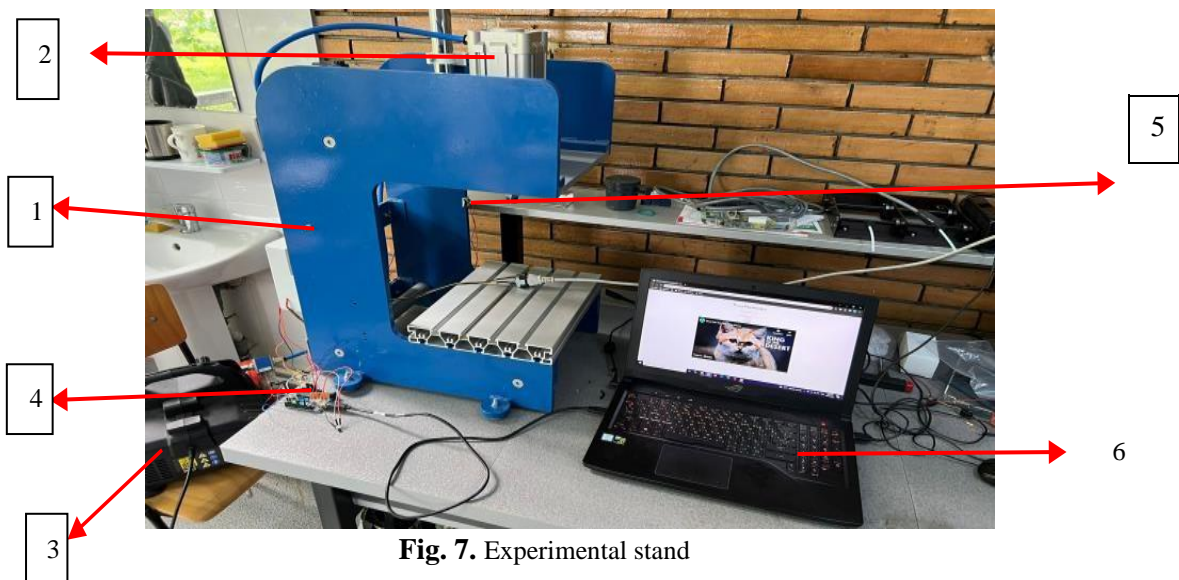


Fig. 7. Experimental stand

Component list:

1. Frame
2. Pneumatic cylinder + solenoid valve
3. Compressor

4. Arduino UNO purchasing board
5. Microswitches
6. Computer

The rearrangement of this experimental stand was possible because the press existed in physical format and I only had to make the connections between the hardware and software components.

4. Conclusions

In the industry, pneumatic presses are usually, manually controlled because certain factors can occur that can disrupt functionality. Due to the fact that the industry is constantly developing and the principle of having a "workforce" in a factory is declining, the systematization and remote monitoring of all possible devices will be pursued.

5. Bibliography

- [1]. <https://internavytec.ro/produs/presa-pneumatica/>
- [2]. https://ro.wikipedia.org/wiki/Sistem_de_ac%C8%9Bionare_pneumatic%C4%83.
- [3]. <https://www.depanero.ro/internet-of-things%E2%80%93ce-inseamna-si-ce-impact-poate-aveaasupra-noastr%C4%83>
- [4]. <https://ro.wikipedia.org/wiki/Arduino>
- [5]. <https://www.w3schools.com/html/>
- [6]. Velicu, Șt., Cristescu, C., Gândilă, S., Velicu, A., Mihai, L. Mașini pentru prelucrări prin deformare. Laborator, ISBN 978-606-521-494-1

DESIGN OF AN ALGORITHM AND DEVELOPMENT OF AN ONLINE APPLICATION FOR MANAGING THE STRUCTURE OF PRODUCTS

PINTILIE Dănuț – Sebastian¹, GHEORGHITĂ Vlad²

¹Faculty Industrial Engineering and Robotics, Specialization: IAIL, Year of study: IV, e-mail: pntiliedanutsebastian@gmail.com

²Faculty Industrial Engineering and Robotics, TCM Department

ABSTRACT: The main concern of those involved in the manufacturing industry is to make products as correctly and quickly as possible and to use resources efficiently. Product management systems are the tool through which these requirements are met. These systems are so important because they provide the ability to manage and track all the information, applications and processes that define a product from the design phase until it is ready for market.

KEY WORDS: product, management, processes, web services, database.

1. Introduction

Product data management (PDM) systems typically manage product-related information such as geometry, engineering drawings, product specifications, CNC programs, analysis results, component tables, engineering change orders and more. PDM can also be seen as an integration tool that connects many different areas of product development, which ensures that the right information is available to the right person, at the right time and in the right form, across the enterprise. In this way, PDM improves communication and cooperation between different groups within the organisation, as well as between the organisation and customers. [1]

This paper focuses on the development of a PDM web application. A web application is software that performs a specific function using a web browser as a "client". Through the browser the client connects to processing functions that are located on a server. The typical structure of a web application is a 3-tier structure:

- Presentation Layer - The interface of the client, usually implemented using a browser-sensitive programming language, such as JavaScript or jQuery, combined with a markup language, such as HTML.
- Logical level - is the level where customer requests are received, processed and fulfilled. This layer differentiates a web application from a website. Client requests are transmitted via the HTTP communication protocol and are processed using algorithms in a dynamic development language such as PHP, ASP, ASP.NET and others.
- Data management layer - is represented by the database engine, such as MySQL, Oracle, etc., for managing data persistence and querying through appropriate tools, receiving and fulfilling DB read/write requests from the application logic [2]

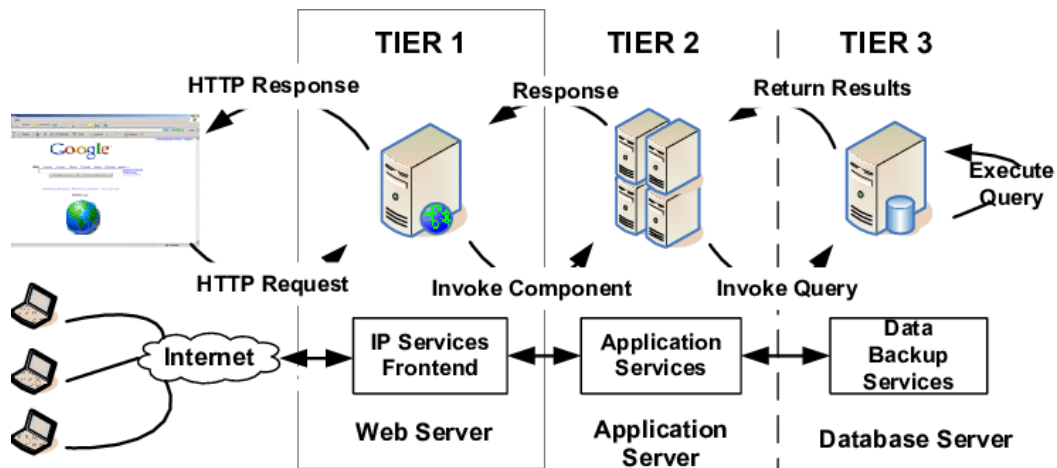


Figure 1. Typical structure of a web application [3]

The application in this paper aims to provide the possibility to manage the structure of products, in terms of their composition (BOM), the processes that products and their components undergo to reach their final state and the resources that are required to obtain the finished product. In order to fulfil these functionalities, we have structured the application on 3 levels, according to the typical structure. For the client interface we used the JavaScript programming language, together with the HTML markup language and the CSS formatting standard. For easier development of the interface we also used the Alpine.js framework which helps in easier development of dynamic elements in the web page, and for formatting elements we used the Tailwind CSS framework. The logic functions in the second level were realized using the LabVIEW (Laboratory Visual Instrumentation Engineering Workbench) programming environment. This is a well-known program for graphical instrumentation and coding (the graphical language is called "G") and is generally used for data acquisition, industrial automation or as control instrumentation. In this case, we used the Web Service module to be able to retrieve customer requests and process them further. Commands to the third level, the database represented in the MS Access application (MS Office package), were carried out using the Database functions in the Connectivity package of LabVIEW. These functions facilitate the connection to the database and the performance of database queries.[4]

2. Current status

At this moment, the application offers the possibility to query the database in order to display products to the user, add products to the database, define and display the composition and process structure of a product. These functionalities are accessible to the user through the web interface of the application. This interface has been built using HTML, JavaScript, CSS and the Tailwind CSS and Alpine.JS frameworks.

The form is divided into 3 sections: the general product information input area, the component input area and the process input area. The component and process input areas are initially defined with a single component or process definition area. To add more such zones, two functions have been defined in the JavaScript language, "adaugaComponenta()" and "adaugaProces()".

```

<template x-if="isFormOpen">
  <div class="absolute top-1/2 -translate-y-1/2 left-1/2 -translate-x-1/2 shadow-2xl z-50 @click.away="closeForm" @keydown.escape="closeForm">
    <form class="border-2 border-black action="http://127.0.0.1:8001/ Aplicatie_web/adaugare" method="post">
      <div>
        <div class="grid grid-cols-12 gap-6 bg-white">
          <div class="col-span-12 p-2 flex flex-col gap-3 border border-gray-400">...
          </div>
          <div class="col-span-12 p-2 border border-gray-400"> <!--Zona definire componente-->
            <h1 class="font-bold italic"> TABEL DE COMPONENTE</h1>
            <div id="componente">...
            </div>
            <div class="mt-2">
              <span class="italic cursor-pointer hover:bg-slate-200 p-2 onclick="adaugaComponenta()">+Adauga inca o componenta</span>
            </div>
          </div>
          <div class="col-span-12 p-2 border border-gray-400"> <!--Zona definire procese-->
            <h1 class="font-bold italic"> ETAPE OBTINERE</h1>
            <div id="procese">...
            </div>
            <div class="mt-2">
              <span class="italic cursor-pointer hover:bg-slate-200 p-2 onclick="adaugaProces()">+Adauga inca un proces</span>
            </div>
          </div>
          <input type="submit" class="col-span-12 px-6 py-2 block rounded-md text-lg font-semibold text-indigo-100 bg-indigo-600 cursor-pointer" value="TR
        </div>
      </form>
    </div>
  </template>

```

Figure 2. Definition of the form component

```

var b = 1;

function adaugaComponenta(){
  var n = parseInt(document.getElementById("nrcrt").innerHTML) + b;
  var i = document.createElement("div");
  i.className = document.getElementById('rand').className;
  var inputDenumire = document.createElement("input");
  inputDenumire.setAttribute("type", "text");
  inputDenumire.setAttribute("id", "denumireComponenta"+n);
  inputDenumire.setAttribute("name", "denumireComponenta"+n);
  inputDenumire.className = "w-full h-full";
  var inputCantitate = document.createElement("input");
  inputCantitate.setAttribute("type", "number");
  inputCantitate.setAttribute("id", "cantitateComponenta"+n);
  inputCantitate.setAttribute("name", "cantitateComponenta"+n);
  inputCantitate.className = "w-full h-full";
  var inputDisponibilitate = document.createElement("input");
  inputDisponibilitate.setAttribute("type", "text");
  inputDisponibilitate.setAttribute("id", "disponibilitateComponenta"+n);
  inputDisponibilitate.setAttribute("name", "disponibilitateComponenta"+n);
  inputDisponibilitate.className = "w-full h-full";
  var id = document.createElement("div");
  var den = document.createElement("div");
  var cant = document.createElement("div");
  var disp = document.createElement("div");
  id.className = document.getElementById("nrcrt").className;
  den.className = document.getElementById('d').className;
  cant.className = document.getElementById('cantitate').className;
  disp.className = document.getElementById('disponibilitate').className;
  id.innerHTML = n;
  den.appendChild(inputDenumire);
  cant.appendChild(inputCantitate);
  disp.appendChild(inputDisponibilitate);
  i.appendChild(id);
  i.appendChild(den);
  i.appendChild(cant);
  i.appendChild(disp);
  document.getElementById('componente').appendChild(i);
  b++;
}

```

Figure 3. Defining the function "adaugaComponenta()"

This function creates, using the function "document.createElement", the „div” type element that defines the row for entering data. The same function is used to create the "input" add fields, which are assigned the

same attributes as the field originally defined with the help of ".setAttribute" function. With the function ".appendChild" the elements of type "input" are added to the element "row".

For the display and registration of the products I have developed algorithms in the LabVIEW programming environment, which I will present below.

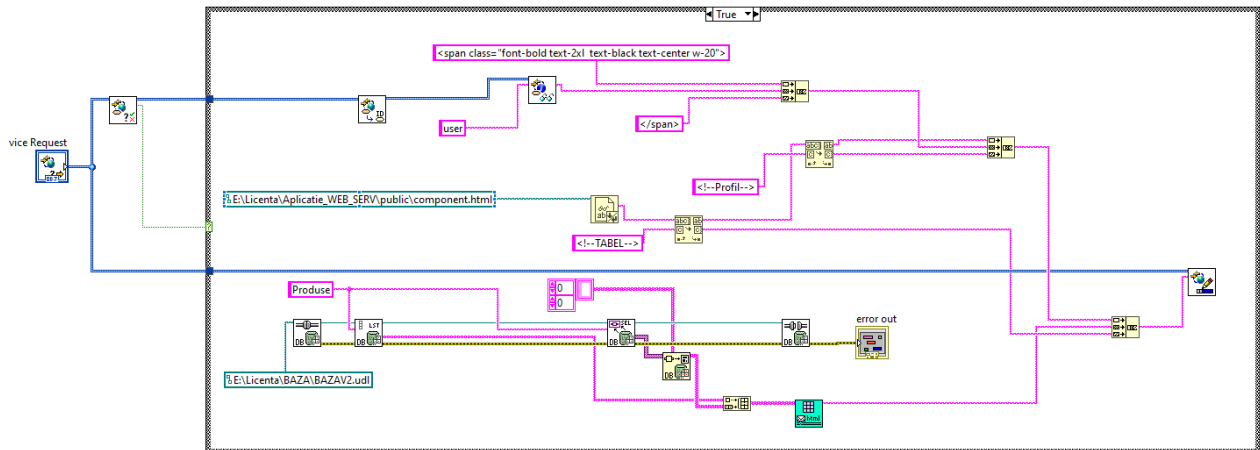


Figure 4. Algorithm for displaying products

The product display algorithm is accessible when the user has successfully passed the login page. This check is done with the function "Check If Session Exist.vi" if not, the user is redirected to the login page, if yes, the algorithm accesses the HTML file that it will process. In the section dedicated to the profile the name of the user will be added using the function "Read Session Variable.vi". At the same time, the algorithm accesses the database, from which it extracts the data from the "Produce" table, as well as its column names. The table thus formed is processed by the "Array2HTML" subprogram.

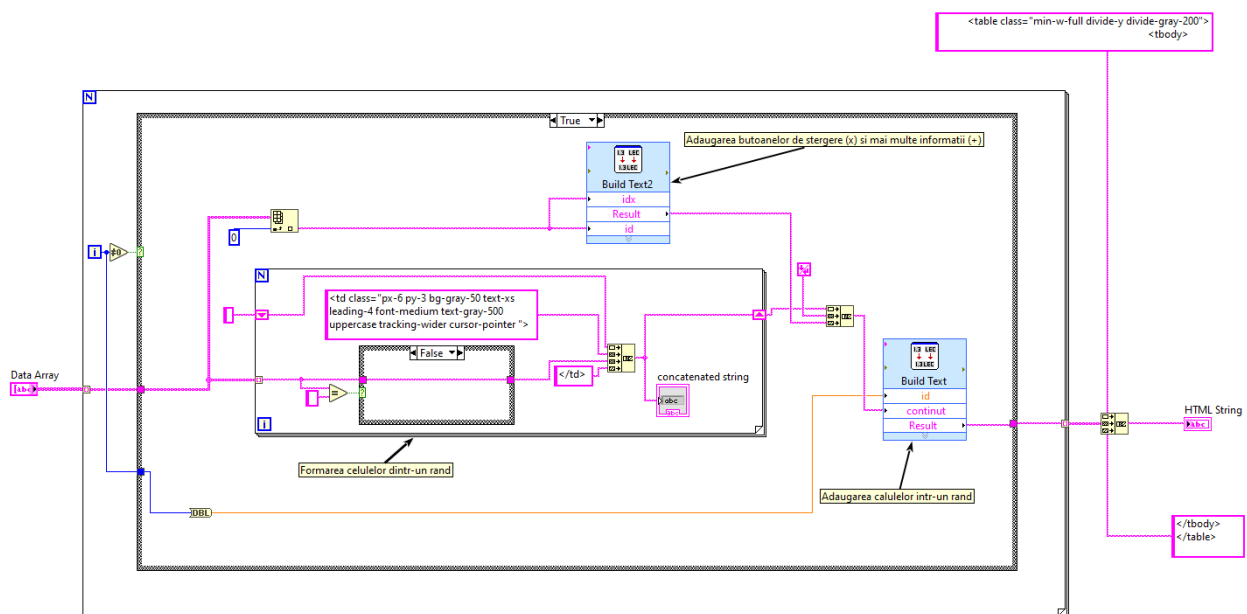


Figure 5. Subprogram for transforming an Array table in LabVIEW into an HTML table

In this algorithm, in order to access the table rows, the table is passed through a repetitive "For" structure. Then the first row is formatted to represent the head of the table. The rows are passed through another "for" structure to access the cells on each row. The data in these cells is added in html components of type "td". The array formed by the data of type "td" at the output of the second "for" is added in an html component of type "tr". The array formed at the output of the first "for" is added to an html component of type "table", and the text thus formed is sent to the main program. The main algorithm takes the text and inserts it, in the table section, into the text that is sent as a response via the "Write response.vi" function.

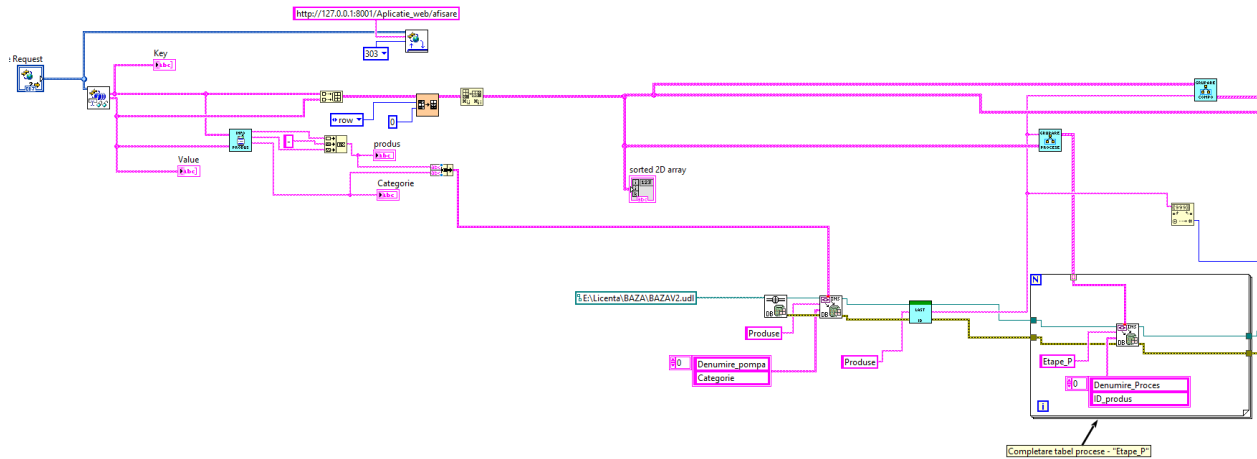


Figure 6. Data adding algorithm

The add product algorithm is called when the user submits the completed form with the required data. These are accessed using the "Read all form data.vi" function. The data is then grouped into arrays of clusters so that it can be added to the database. In order to be able to add the data to the tables, these arrays are traversed using a "for" structure, which is used to insert each data cluster into the corresponding table.

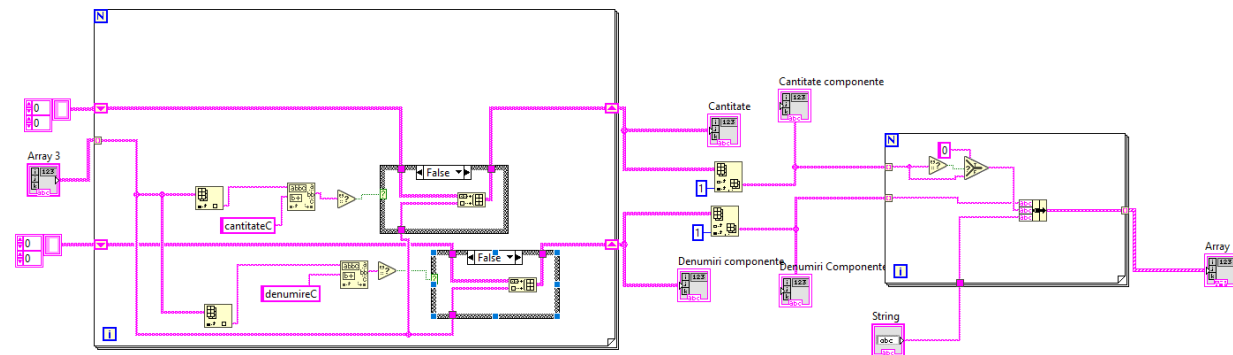


Figure 7. Subprogram for grouping component data

The grouping subprogram has as input data the array of all data in the form and the product id that is entered in the database. The algorithm selects only those data related to components, processes or resources, as needed, then the values of these data are grouped into clusters to be entered into the database.

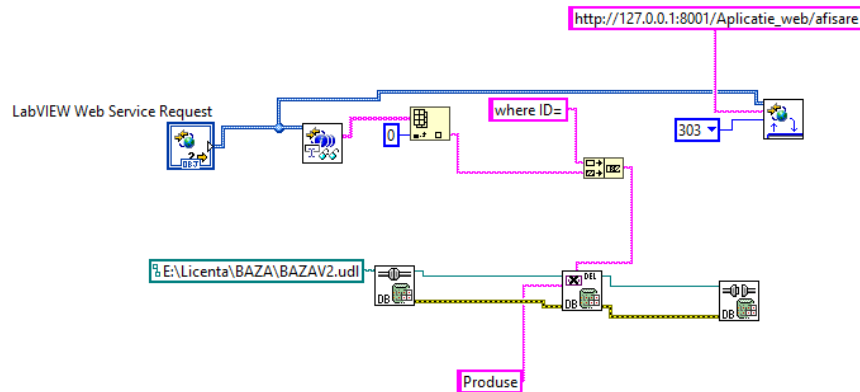


Figure 8. Algorithm for data removal

For deleting data from the database, when the delete form calls the function, the algorithm identifies the items by product id and passes the condition to the delete function. At the end of the operation the user is redirected to the main page of the application using the "Set HTTP Redirect.vi" function.

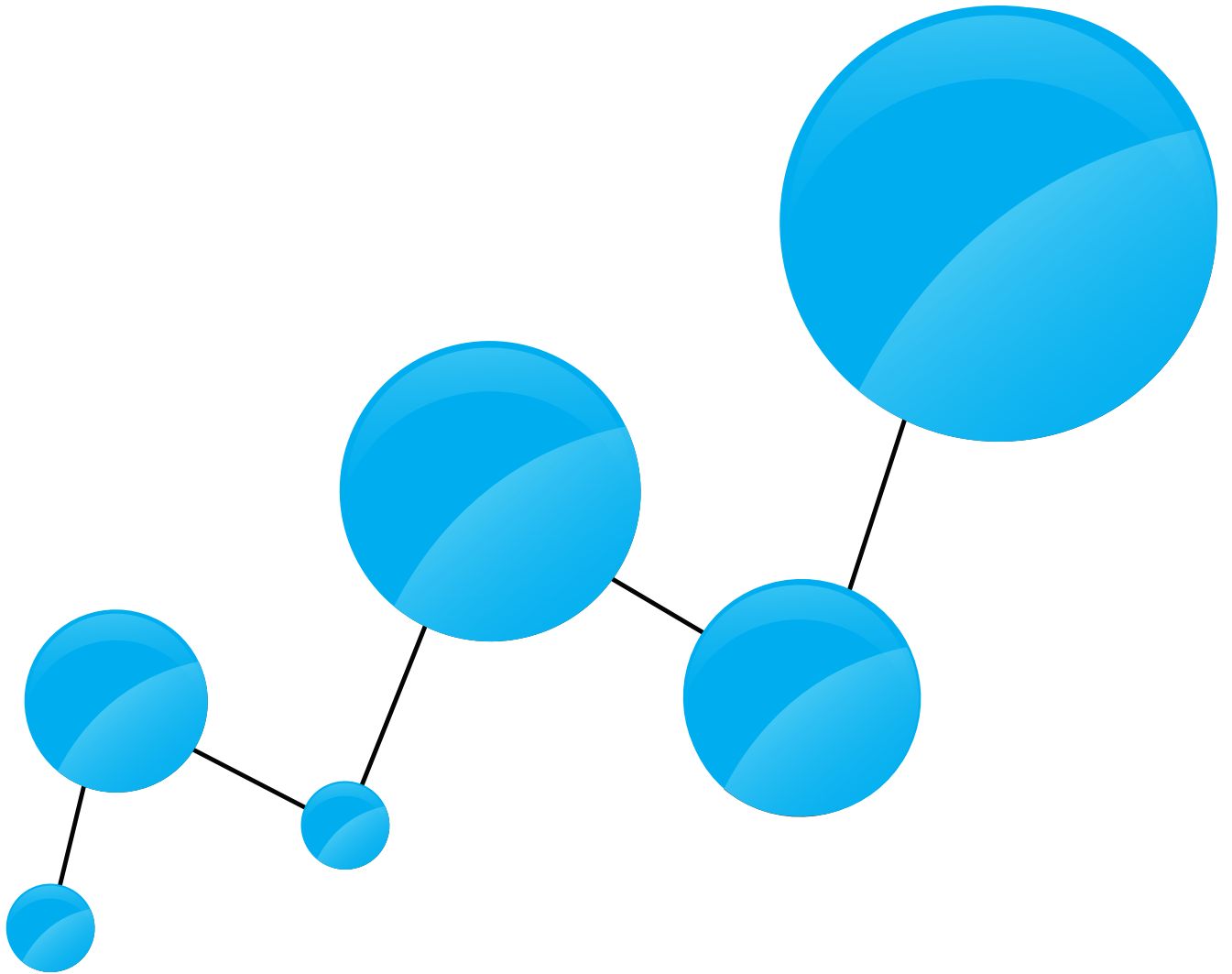
3. Conclusions and further developments

I believe that product management systems are an essential component in streamlining and automating production, processing and other processes. The importance of these systems is that they bring together information from all areas of product development.

In order to make the application as useful and powerful as possible, functionality to update product data within the application will be implemented in the coming period, as well as functionality to determine the availability of components and resources. Another option that can be added to this application is related to the possibility of accessing and uploading component working drawings, product overview drawings and appliance datasheets.

4. Bibliography

- [1] X. W. Xu and T. Liu, "A web-enabled PDM system in a collaborative design environment," *Robotics and Computer-Integrated Manufacturing*, vol. 19, no. 4, pp. 315-328, Aug. 2003, doi: 10.1016/S0736-5845(02)00082-0.
- [2] L. Alboaie and S.-C. Buraga, "Web services : basic concepts and implementations," 2006.
- [3] T. Kgil and T. Mudge, "FlashCache: A NAND flash memory file cache for low power web servers," *CASES 2006: International Conference on Compilers, Architecture and Synthesis for Embedded Systems*, pp. 103-112, 2006, doi: 10.1145/1176760.1176774.
- [4] John Essick, *Hands-On Introduction to LabVIEW for Scientists and Engineers*. Oxford University Press, 2018.



www.fir.pub.ro

ISSN 2601-5471

ISSN-L 2601-5471